UNIVERSITÉ DU QUÉBEC

THÈSE PRÉSENTÉE À

L'UNIVERSITÉ DU QUÉBEC À CHICOUTIMI

COMME EXIGENCE PARTIELLE

DU DOCTORAT EN RESSOURCES MINÉRALES

PAR

ROBERT THÉRIAULT

INFLUENCE DE L'ASSIMILATION DE ROCHES SÉDIMENTAIRES ENCAISSANTES SUR L'ORIGINE DES GISEMENTS DE CU-NI-ÉGP DE L'INTRUSION DE PARTRIDGE RIVER, COMPLEXE DE DULUTH, MINNESOTA.

DÉCEMBRE 1999

Bibliothèque
Paul-Émile-Boulet

UQAC
Université du Québec
à Chicoutimi

Mise en garde/Advice

Afin de rendre accessible au plus grand nombre le résultat des travaux de recherche menés par ses étudiants gradués et dans l'esprit des règles qui régissent le dépôt et la diffusion des mémoires et thèses produits dans cette Institution, **l'Université du Québec à Chicoutimi (UQAC)** est fière de rendre accessible une version complète et gratuite de cette œuvre.

Motivated by a desire to make the results of its graduate students' research accessible to all, and in accordance with the rules governing the acceptation and diffusion of dissertations and theses in this Institution, the **Université du Québec à Chicoutimi (UQAC)** is proud to make a complete version of this work available at no cost to the reader.

L'auteur conserve néanmoins la propriété du droit d'auteur qui protège ce mémoire ou cette thèse. Ni le mémoire ou la thèse ni des extraits substantiels de ceux-ci ne peuvent être imprimés ou autrement reproduits sans son autorisation.

The author retains ownership of the copyright of this dissertation or thesis. Neither the dissertation or thesis, nor substantial extracts from it, may be printed or otherwise reproduced without the author's permission.

RÉSUMÉ

L'intrusion de Partridge River est située le long de la marge nord-ouest du complexe de Duluth, Minnesota, et repose sur des roches sédimentaires de la Formation de Virginia. Un total de quatre gisements non exploités de Cu–Ni–éléments du groupe du platine (ÉGP) se retrouvent près de la base de l'intrusion, soit ceux de Dunka Road, Babbitt, Wetlegs et Wyman Creek. L'origine de la minéralisation est principalement liée à la contamination du magma hôte suite à l'assimilation de roches argileuses sulfurées de la Formation de Virginia.

La minéralisation en sulfures est en grande partie de type disséminé (1-5% de sulfures), avec localement quelques zones de sulfures massifs à semi-massifs. Les zones minéralisées sont caractérisées par la présence de nombreuses enclaves partiellement assimilées de roches encaissantes appartenant à la Formation de Virginia. Une étude détaillée du gisement de Dunka Road a mené à l'identification et la caractérisation de cinq différents types de minéralisation en sulfures, soit: 1) sulfures disséminés dans la norite hôte; 2) sulfures disséminés dans la troctolite hôte; 3) horizons de sulfures disséminés enrichis en ÉGP; 4) lentilles de sulfures massifs à pyrrhotite; et 5) sulfures disséminés enrichis en cuivre.

Les sulfures disséminés dans la norite se retrouvent soit à proximité d'enclaves de roches sédimentaires encaissantes ou près de la base de l'intrusion. Ils se sont formés à des taux élevés d'assimilation (ex. 20-75%) sous des conditions de faibles facteurs *R* (ex. 50-400), comme en témoigne les valeurs moyennes élevées de $\delta^{34}S$ (11,2‰) et de S/Se (9700) déterminées pour le gisement de Dunka Road, les teneurs appauvries en ÉGP et autres métaux, les valeurs élevées de Cu/Pd, Ni/Pd et Cu/Pt, et les proportions élevées de pyrrhotite et de minéraux arsénifères. Les sulfures disséminés dans la troctolite forment la plus grande partie de la minéralisation, et se retrouvent à une certaine distance (ex. 50-300 m) du contact basal. Ils sont associés à des taux d'assimilation faibles à modérés (ex. 5-20%) et à des valeurs modérées du facteur *R* (ex. 700-3000), tel qu'indiqué par les valeurs moyennes intermédiaires de $\delta^{34}S$ (7,8‰) et de S/Se (4600), et les teneurs modérées en ÉGP et autres métaux. Les horizons de sulfures disséminés enrichis en ÉGP (jusqu'à 2,9 ppm Pd+Pt) se retrouvent généralement à 150-250 m de la base de l'intrusion directement sous des niveaux de roches ultramafiques. Ils se sont formés à des valeurs élevées du facteur *R* (ex. 3000-15 000) à partir d'un magma parent non contaminé, tel que le laisse suggérer les faibles valeurs moyennes de $\delta^{34}S$ (2,1‰) et de S/Se (2600) qui rappellent celles du manteau, les teneurs élevées en ÉGP, les faibles valeurs de Cu/Pd, Ni/Pd et Cu/Pt, et la faible proportion de pyrrhotite par rapport aux sulfures à métaux de base. Les sulfures

massifs enrichis en pyrrhotite, et les sulfures disséminés enrichis en cuivre (chalcopyrite et cubanite) avec lesquels ils sont associés, se retrouvent sous forme de lentilles horizontales le long de la base de l'intrusion, ou plus rarement sous forme de veines subverticales recoupant les roches mafiques minéralisées. Ils ont des valeurs moyennes relativement élevées de $\delta^{34}S$ (10,2‰) et de S/Se (8000) qui témoignent d'une importante contamination du magma parent.

Il est interprété que les cinq différents types de minéralisation en sulfures décrits ci-dessus résultent de l'action combinée de trois principaux processus, qui ont opéré de façon progressive à partir de la mise en place du magma jusqu'à la cristallisation complète des sulfures. Ces processus sont: 1) l'assimilation de roches sédimentaires encaissantes; 2) l'interaction entre le liquide sulfuré et le magma silicaté (facteur *R*); et 3) la cristallisation fractionnée du liquide sulfuré. Une augmentation générale du taux d'assimilation est observée vers la base de l'intrusion, associée à une diminution du facteur *R* et de la teneur en métaux des sulfures. Ceci résulte de l'introduction d'un produit de fusion partielle granitique enrichi en soufre dérivé des roches sédimentaires encaissantes, qui étant moins chaud que le magma mafique environnant, a mené à la précipitation hâtive du liquide sulfuré à l'intérieur des roches hôtes noritiques. Le liquide sulfuré a cristallisé près de sa source (*i.e.* roches encaissantes et enclaves) de telle sorte qu'il a eu moins de temps pour interagir avec le magma, ce qui explique les faibles valeurs du facteur *R* associées à ce type de minéralisation. Les sulfures disséminés dans la troctolite se sont formés à partir d'un magma moins contaminé et donc plus chaud que le magma noritique, favorisant une interaction prolongée entre le liquide sulfuré et le magma hôte troctolitique et expliquant par le fait même les plus grandes valeurs du facteur *R* obtenues par rapport aux sulfures dans la norite. Les sulfures disséminés enrichis en ÉGP se sont quant à eux formés suite à une nouvelle injection de magma non contaminé directement au-dessus de la séquence de roches basales minéralisées. Le liquide sulfuré présent dans ce magma a atteint des facteurs *R* très élevés suite à son interaction prolongée avec le magma en turbulence. Le liquide sulfuré a éventuellement percolé dans les roches sous-jacentes et a cristallisé pour former les horizons de sulfures disséminés enrichis en ÉGP. Finalement, aux endroits où une importante quantité de liquide sulfuré s'est accumulé (*i.e.* zones minéralisées de Local Boy et de Tiger Boy du gisement de Babbitt; gisement de Dunka Road), sa cristallisation fractionnée a mené à la formation d'une solution solide de monosulfure enrichie en fer et d'un liquide sulfuré résiduel enrichi en cuivre. Avec une baisse de température, le liquide sulfuré fractionné a migré vers la bordure du sulfure massif pour éventuellement cristalliser en chalcopyrite et en cubanite, alors que la solution solide de monosulfure s'est exsolvée en pyrrhotite et en pentlandite.

REMERCIEMENTS

La réalisation de cette thèse n'aurait pu être possible sans le support et la collaboration de nombreuses personnes et organismes. Je suis particulièrement reconnaissant envers ma directrice de thèse Sarah-Jane Barnes pour son aide, sa très grande disponibilité et ses nombreux conseils et encouragements, lesquels m'ont permis de mener à terme ce projet. Sincères remerciements également à Mark Severson et Steven Hauck du Natural Resources Research Institute du Minnesota pour leur collaboration significative dans toutes les phases de ce projet, et pour leur hospitalité lors de mon séjour à Duluth. Des remerciements sont envoyés à Penny Morton et John Green de l'Université du Minnesota à Duluth pour leur support logistique et leur aide et expertise sur le terrain, respectivement. Je remercie également John McGoran de PolyMet Mining Corporation (anciennement Fleck Resources Limited) pour avoir autorisé la publication des résultats, Richard Ruhanen du Minnesota Department of Natural Resources pour m'avoir donné la permission de faire l'échantillonnage des carottes de forage, Roger Eckstrand de la Commission Géologique du Canada pour m'avoir autorisé l'utilisation de données non publiées, Richard Lechasseur et Bernard Lapointe de l'Université du Québec à Chicoutimi pour leur aide avec le travail analytique, et Gilles St-Jean (Centre Géoscientifique d'Ottawa-Carleton) et Ed Ripley (Université de l'Indiana) pour avoir effectué les analyses des isotopes du soufre et pour leurs commentaires judicieux en ce qui a trait à l'interprétation des résultats. Daniel Bandyayera, Pierre Doucet, Rock Flamand, Jean Lafrance, Marc Legault, Hassan Nabil, Luc Théberge et Christine Vaillancourt ont été au cours des années des collègues de travail

très agréables. Le support des membres de ma famille et de mes amis fut également des plus apprécié. La réalisation de ce projet n'aurait pu être possible sans le support financier du Fonds pour la Formation de Chercheurs et l'Aide à la Recherche, et du Conseil de Recherches en Sciences Naturelles et en Génie du Canada. Pour terminer, j'aimerais exprimer ma reconnaissance la plus profonde envers ma fiancée Lucie (et son compagnon Gizmo), qui a su m'apporter encouragements et joie de vivre lors de la réalisation de ce travail.

TABLE DES MATIÈRES

page

TABLE DES MATIÈRES

page

LISTE DES TABLEAUX

page

LISTE DES FIGURES

page

Article #1: Revue canadienne des sciences de la Terre

Article #2: The Canadian Mineralogist

LISTE DES FIGURES

page

LISTE DES FIGURES

page

LISTE DES FIGURES

page

Article #3: Economic Geology (suite)

INTRODUCTION

Le complexe de Duluth est une intrusion mafique composite d'âge protérozoïque (1100 Ma) associée à la province de basaltes de plateau de Keweenawan, lesquels furent mis en place à l'intérieur du rift médio-continental du centre nord des États-Unis (article #1, figure 1). De nombreux gisements de sulfures de Cu-Ni-ÉGP sont regroupés le long de la bordure nord-ouest du complexe au Minnesota. Ceux-ci contiennent des ressources de l'ordre de 4,4 milliards de tonnes de minerais à 0,66% Cu et 0,20% Ni (Listerud et Meineke, 1977), ce qui en font les plus gros gisements non exploités de Ni-Cu au monde (Naldrett, 1989). Les gisements se retrouvent principalement dans les parties inférieures des intrusions de Partridge River et de South Kawishiwi, où les roches hôtes troctolitiques sont en contact avec des roches argileuses sulfurées de la Formation de Virginia.

La minéralisation en sulfures est en grande partie de type disséminé (1-5% de sulfures), avec localement quelques zones de sulfures semi-massifs à massifs. De nombreux xénolites de roches encaissantes appartenant à la Formation de Virginia se retrouvent dans les zones minéralisées, constituant jusqu'à 25% de la séquence. Les modèles suivants ont été proposés pour expliquer l'origine de la minéralisation: 1) une ségrégation des sulfures à partir d'un magma mafique suite à sa contamination par assimilation des roches sédimentaires encaissantes (Mainwaring et Naldrett, 1977; Ripley, 1981, 1986; Grant et Molling, 1981; Rao, 1981; Rao et Ripley, 1983; Foose et Weiblen, 1986); 2) une remobilisation tardive des métaux sous l'action de fluides hydrothermaux (Mogessie et al., 1991; Ripley et al., 1993); et 3) une ségrégation des sulfures à partir d'un magma mafique originairement enrichi en fer

(Martineau, 1989; Grant et Chalokwu, 1992).

Cette étude a été entreprise afin d'évaluer l'influence du processus d'assimilation de roches sédimentaires encaissantes sur l'origine des minéralisations en sulfures du complexe de Duluth (premier modèle cité ci-dessus). L'hypothèse de travail avancée au départ est que l'assimilation de roches sédimentaires sulfurées aurait fourni une quantité appréciable de soufre d'origine sédimentaire au magma mafique, menant à la formation des volumineux gisements de sulfures magmatiques. Suite à une consultation des travaux effectués antérieurement sur les différents gisements de Cu-Ni-ÉGP du complexe de Duluth, le gisement de Dunka Road de l'intrusion de Partridge River a été choisi comme site d'étude pour les raisons suivantes: 1) à l'inverse du gisement de Babbitt, celui-ci montre très peu d'évidence de déformation structurale tardive et ne contient que de très faibles quantités de minéraux hydratés, suggérant une activité hydrothermale post-magmatique restreinte; 2) plus de 120 trous de forage avaient été effectués sur le gisement en date de l'année 1990 (Severson et Hauck, 1990), de telle sorte qu'il est très bien documenté et cartographié; et 3) il contient de nombreuses enclaves de roches sédimentaires, lesquelles montrent des signes de fusion partielle et une association spatiale évidente avec la minéralisation.

Les travaux de terrain ont été effectués au cours de l'été 1993 ainsi que lors d'une brève visite en 1994, et consistaient en l'échantillonnage de carottes de forage provenant du gisement de Dunka Road et des roches sédimentaires encaissantes, ainsi que d'une visite sur le terrain dans la région de l'intrusion de Partridge River. Un total de 81 échantillons ont été prélevés pour fins d'analyse.

Les principales observations de terrain ainsi que les résultats des travaux de pétrographie et de géochimie des roches totales et des sulfures ont été compilés en 1995. Ils se retrouvent dans le premier article, publié en 1997 dans la Revue canadienne des sciences de la Terre en collaboration avec Sarah-Jane Barnes et Mark Severson. Une très importante observation soulevée dans cet article est que le gisement contient jusqu'à cinq différents types de minéralisation en sulfures, soit trois types de minéralisation disséminée formant l'ensemble du gisement, ainsi que quelques occurrences de veines de sulfures massifs à pyrrhotite associées à des sulfures disséminés enrichis en cuivre. Les nombreuses études effectuées précédemment sur les différents gisements du complexe de Duluth n'avaient pas fait état de ces différences significatives à l'intérieur d'un même gisement, préférant regrouper tous les types de minéralisation en les décrivant de façon générale et uniforme. Cela explique à mon avis l'absence de consensus et la confusion existant quant à l'origine de la minéralisation. Ce premier article traite des trois principaux types de minéralisation disséminée rencontrés dans le gisement de Dunka Road, soit: 1) sulfures disséminés dans la norite hôte; 2) sulfures disséminés dans la troctolite hôte; et 3) horizons de sulfures disséminés enrichis en ÉGP. Les sulfures disséminés dans la norite sont généralement appauvris en métaux, et se retrouvent soit dans les zones adjacentes aux enclaves ou près de la base de l'intrusion. Les sulfures disséminés dans la troctolite contiennent des teneurs modérés en Cu, Ni et ÉGP. Ils forment le plus gros du gisement, et apparaissent à une certaine distance du contact basal et des enclaves. Quant aux horizons de sulfures disséminés enrichis en ÉGP et métaux de base, ils se retrouvent en moyenne à 200 m de la

base de l'intrusion directement sous des niveaux de roches ultramafiques. Il est ainsi démontré que les principaux types de minéralisation de sulfures disséminés ont des différences marquées en ce qui a trait à leur position stratigraphique, la composition de la roche hôte, et la minéralogie et la géochimie des sulfures. Ces différences reflètent le taux variable de contamination du magma mafique suite à l'assimilation d'un produit de fusion partielle enrichi en soufre et en silice dérivé des roches sédimentaires encaissantes. De plus, les résultats de modélisation ont permis de démontrer que le taux de contamination a directement influencé le degré d'interaction entre le liquide sulfuré et le magma silicaté, soit le facteur *R*, et que chaque type de minéralisation disséminée résulte donc d'une interaction entre ces deux processus. Ainsi, les sulfures disséminés dans la norite hôte se sont formés à partir d'un magma fortement contaminé (taux moyen de 33%) sous des conditions de faibles facteurs *R* (moyenne de 150). Les sulfures disséminés dans la troctolite hôte se sont quant à eux formés à de faibles taux de contamination (moyenne de 13%) sous des conditions de facteurs *R* modérés (moyenne de 1300). Finalement, les sulfures disséminés enrichis en ÉGP ont été modélisés en utilisant des facteurs *R* élevés (moyenne de 8000) à partir d'un magma parental non contaminé.

Afin d'étudier de façon plus approfondie le modèle de contamination par assimilation de roches sédimentaires encaissantes dans le gisement de Dunka Road, la composition isotopique du soufre ($\delta^{34}S$) et le rapport S/Se des différents types de minéralisation en sulfures ont été déterminés pour plusieurs échantillons. De plus, la composition et l'origine des veines de sulfures massifs à pyrrhotite et des sulfures disséminés enrichis en cuivre

retrouvés à proximité de ces veines ont été examinées plus en détail. Les résultats de ces études se retrouvent dans le deuxième article, publié en 1998 dans la revue The Canadian Mineralogist en collaboration avec Sarah-Jane Barnes. Il est démontré en premier lieu que les valeurs isotopiques du soufre et du rapport S/Se supportent le modèle d'assimilation développé dans le premier article. Ainsi, les sulfures disséminés dans la norite hôte ont des valeurs élevées de $\delta^{34}S$ et S/Se démontrant que le magma parental a subit une importante contamination, les sulfures disséminés dans la troctolite hôte ont des valeurs intermédiaires de $\delta^{34}S$ et S/Se, alors que les sulfures disséminés enrichis en ÉGP ont des valeurs relativement faibles de $\delta^{34}S$ et S/Se similaire à celle du manteau, ce qui suggère une absence de contamination. Ces résultats viennent confirmer qu'une importante proportion du soufre contenu dans le gisement est d'origine sédimentaire, provenant des niveaux d'argillites sulfurés de la Formation de Virginia. De plus, une étude approfondie de la minéralogie des sulfures a également permis d'associer certaines phases sulfurés et arsénifères au processus d'assimilation de roches sédimentaires encaissantes. Dans la deuxième partie de l'article, une analyse de la composition géochimique des veines de sulfures massifs à pyrrhotite et des sulfures disséminés enrichis en cuivre a permis de démontrer que les veines de sulfures massifs se sont formées par cristallisation fractionnée d'un liquide sulfuré, et représentent l'accumulation d'une solution solide de monosulfure (*mss*), alors que les sulfures enrichis en cuivre représentent un liquide sulfuré fractionnée. Finalement, les relations observées en ce qui a trait à la position stratigraphique, le taux de contamination et la valeur du facteur *R* des différents types de minéralisation ont été

développées dans un modèle géodynamique qui tient compte de l'action séquentielle de trois principaux processus, soit: 1) l'assimilation de roches sédimentaires encaissantes; 2) l'interaction entre le liquide sulfuré et le magma silicaté (facteur *R*); et 3) la cristallisation fractionné du liquide sulfuré. Il est démontré qu'en se rapprochant d'une source de contamination (roches encaissantes ou enclaves), les roches magmatiques montrent des évidences indiquant une augmentation progressive du taux de contamination, dû à l'incorporation et au mélange d'un produit de fusion partielle de composition granitique dérivé des roches sédimentaires. L'addition importante de silice favorise la formation de l'orthopyroxène au dépend de l'olivine, expliquant ainsi la présence de roches noritiques à proximité des roches encaissantes ou des enclaves. De plus, l'addition d'un produit de fusion de composition felsique a pour effet de réduire la température du magma hybride et donc de la rapprocher de celle du solidus, réduisant par le fait même le degré d'interaction entre le liquide sulfuré et le magma silicaté, soit le facteur *R*. À l'inverse, les roches magmatiques retrouvées à une certaine distance des roches encaissantes ou des zones à enclaves montrent peu d'évidence de contamination, et sont constituées essentiellement de roches troctolitiques. La température de ce magma était plus élevé que celle du magma noritique contaminé, ce qui favorisa la formation de roches minéralisées ayant un facteur *R* plus élevé, donc plus riches en métaux de base et ÉGP.

Le modèle développé dans le second article a été appliqué pour les trois autres gisements de Cu-Ni-ÉGP de l'intrusion de Partridge River, soit ceux de Babbitt, Wetlegs et Wyman Creek. Les résultats sont présentés dans le troisième article, soumis récemment à la

revue Economic Geology et rédigé en collaboration avec Sarah-Jane Barnes et Mark Severson. La composition géochimique de plus de 700 échantillons tirée de la littérature (Annexe 4) a été modélisé et interprété à l'aide de diagrammes de rapports de métaux (Cu/Pd *versus* Pd; Ni/Pd *versus* Cu/Ir), permettant de comparer les trois gisements avec celui de Dunka Road. De ce nombre, un total de 22 échantillons ont été prélevés en 1997 dans le cadre de cette étude, provenant de nouveaux horizons de sulfures disséminés enrichis en ÉGP situés à l'intérieur des gisements de Wyman Creek et de Babbitt (Severson et Hauck, 1997). Cette étude géochimique a permis de déterminer que les différents types de minéralisation en sulfures retrouvés dans le gisement de Dunka Road étaient également présents dans les gisements environnants, et que ces derniers s'étaient aussi formés suite à l'action progressive de trois principaux processus, tel que discuté précédemment. Ainsi, pour les quatre gisements de l'intrusion de Partridge River, les horizons de sulfures disséminés enrichis en ÉGP se retrouvent à une certaine distance des roches encaissantes et des enclaves et ne montrent pas de signe apparent de contamination, alors que les sulfures appauvris en métaux sont associés à des roches relativement contaminées se retrouvant près de la base de l'intrusion ou des enclaves. Tout comme à Dunka Road, des veines et amas de sulfures massifs associés à des sulfures disséminés enrichis en cuivre sont également présents dans les autres gisements, plus particulièrement dans les zones de Local Boy et de Tiger Boy du gisement de Babbitt (Severson et Barnes, 1991). Finalement, un modèle génétique pour l'ensemble des minéralisations en sulfures de l'intrusion de Partridge River est proposé et discuté, tenant compte des évidences observées sur le terrain, de la

minéralogie et de la géochimie des sulfures, et des résultats de la modélisation.

Références

Foose, M. et Weiblen, P. 1986. The physical and petrologic setting and textural and compositional characteristics of sulfides from the South Kawishiwi Intrusion, Duluth Complex, Minnesota, U.S.A. *Dans* Geology and metallogeny of copper deposits. G.H. Friedrich, A.D. Genkin, A.J. Naldrett, J.D. Ridge, R.H. Sillitoe et F.M. Vokes (éditeurs), Springer-Verlag, Heidelberg, p. 8-24.

Grant, N.K. et Chalokwu, C.I. 1992. Petrology of the Partridge River intrusion, Duluth Complex, Minnesota: II. Geochemistry and strontium isotope systematics in drill core DDH-221. Journal of Petrology, vol. 33, p. 1007-1038.

Grant, N.K. et Molling, P.A. 1981. A strontium isotope and trace element profile through the Partridge River Troctolite, Duluth Complex, Minnesota. Contributions to Mineralogy and Petrology, vol. 77, p. 296-305.

Listerud, W.H. et Meineke, D.G. 1977. Mineral resources of a portion of the Duluth Complex and adjacent rocks in St. Louis and Lake Counties, northeastern Minnesota: Minnesota Department of Natural Resources, Division of Minerals, Report 93, 74 p.

Mainwaring, P.R. et Naldrett, A.J. 1977. Country-rock assimilation and the genesis of Cu-Ni sulfides in the Water Hen Intrusion, Duluth Complex, Minnesota. Economic Geology, vol. 72, p. 1269-1284.

Martineau, M.P., 1989. Empirically derived controls on Cu-Ni mineralization: a comparison between fertile and barren gabbros in the Duluth Complex, Minnesota, U.S.A. *Dans* Magmatic sulphides: the Zimbabwe volume. M.D. Prendergast et M.J. Jones (éditeurs). Institute of Mining and Metallogeny, p. 117-137.

Mogessie, A., Stumpfl, E.F. et Weiblen, P.W. 1991. The role of fluids in the formation of platinum-group minerals, Duluth Complex, Minnesota: mineralogic, textural, and chemical evidence. Economic Geology, vol. 86, p. 1506-1518.

Naldrett, A.J. 1989. Ores associated with flood basalts, *Dans* Whitney, J.A. et Naldrett, A.J. (éditeurs), Ore deposition associated with magmas: Society of Economic Geologists, Reviews in Economic Geology, v. 4, p. 103-118.

Rao, B.V. 1981. Petrogenesis of sulfides in the Dunka Road Cu-Ni deposit, Duluth Complex, Minnesota, with special reference to the role of contamination by country rock. Thèse de doctorat, Université de l'Indiana, 304 p.

Rao, B.V. et Ripley, E.M. 1983. Petrochemical studies of the Dunka Road Cu-Ni deposit, Duluth Complex, Minnesota. Economic Geology, vol. 78, p. 1222-1238.

Ripley, E.M. 1981. Sulfur isotopic studies of the Dunka Road Cu-Ni deposit, Duluth Complex, Minnesota. Economic Geology, vol. 76, p. 610-620.

Ripley, E.M. 1986. Application of stable isotopic studies to problems of magmatic sulfide ore genesis with special reference to the Duluth Complex, Minnesota. *Dans* Geology and metallogeny of copper deposits. G.H. Friedrich, A.D. Genkin, A.J. Naldrett, J.D. Ridge, R.H. Sillitoe et F.M. Vokes (éditeurs), Springer-Verlag, Heidelberg, p. 8-24.

Ripley, E.M., Butler, B.K., Taib, N.I. et Lee, I. 1993. Hydrothermal alteration in the Babbitt Cu-Ni deposit, Duluth Complex: mineralogy and hydrogen isotope systematics. Economic Geology, vol. 88, p. 679-696.

Severson, M.J. et Barnes, R.J. 1991. Geology, mineralization, and geostatistics of the Minnamax/Babbitt Cu-Ni deposit (Local Boy area), Minnesota. Part II: Mineralization and geostatistics: Natural Resources Research Institute, Duluth, Minnesota, Technical Report 91-13b, 216 p.

Severson, M.J. et Hauck, S.A. 1990. Geology, geochemistry, and stratigraphy of a portion of the Partridge River intrusion: Natural Resources Research Institute, Duluth, Minnesota, Technical Report 89-11, 236 p.

Severson, M.J. et Hauck, S.A. 1997. Igneous stratigraphy and mineralization in the basal portion of the Partridge River Intrusion, Duluth Complex, Allen Quadrangle, Minnesota: Natural Resources Research Institute, Duluth, Minnesota, Technical Report 97-19, 102 p.

Revue canadienne des sciences de la Terre
Vol. 34, pp. 375-389 (1997)

The influence of country-rock assimilation and silicate to sulfide ratios (*R* factor) on the genesis of the Dunka Road Cu-Ni-platinum-group element deposit, Duluth Complex, Minnesota.

Robert D. Thériault, Sarah-Jane Barnes

Département des Sciences Appliquées, Université du Québec à Chicoutimi,

Chicoutimi, Québec, G7H 2B1, Canada

and Mark J. Severson

Natural Resources Research Institute, Duluth, MN 55811, U.S.A.

Abstract

The Dunka Road deposit is one of several Cu-Ni-platinum group element (PGE) sulfide occurrences found along the northwestern margin of the Duluth Complex, where the host troctolitic rocks are in contact with metasedimentary rocks of the Animikie Group. Magma contamination through assimilation of sulfidic argillaceous country rocks is generally recognized as having played a key role in the genesis of the mineralization. Three main types of disseminated sulfide mineralization have been identified within the Dunka Road deposit: 1) norite-hosted sulfides; 2) troctolite-hosted sulfides; and 3) PGE-rich sulfide horizons. The

norite-hosted sulfides are found either adjacent to country-rock xenoliths or near the basal contact. The troctolite-hosted sulfides form the bulk of the deposit, and occur throughout the lower 250 m of the intrusion. The PGE-rich sulfide horizons are typically localized directly beneath ultramafic layers. The composition of the different types of sulfide occurrences is modelled using Cu/Pd ratios. It is shown that each type results from the interplay of two main parameters, namely the degree of magma contamination and the silicate magma to sulfide melt ratio (*R* factor). The norite-hosted sulfides formed at low *R* factors and high degrees of contamination, as expressed by their PGE-depleted nature, low Se/S ratios, and elevated content in pyrrhotite and arsenide minerals. The troctolite-hosted sulfides formed at moderate *R* factors and small degrees of contamination, as shown by their moderate PGE content and mantle-like Se/S ratios. Finally, the PGE-rich sulfide horizons are modelled using elevated *R* factors from an uncontaminated parental magma, which is substantiated by their elevated noble metal content and Se/S ratios, and low pyrrhotite to precious metal sulfide ratio.

Résumé

Le gîte de Dunka Road est un parmi plusieurs gîtes de sulfures de Ni-Cu-éléments du groupe du platine (ÉGP) trouvés le long de la bordure nord-ouest du Complexe de Duluth, où les roches hôtes troctolitiques sont en contact avec les roches métasédimentaires du Groupe d'Animikie. Il est généralement reconnu que la contamination du magma par l'assimilation de roches argileuses sulfurées encaissantes a joué un rôle capital dans la genèse de la minéralisation. Trois types principaux de minéralisation de sulfures disséminés ont été

identifiés dans le gîte de Dunka Road : *(i)* sulfures dans la norite hôte, *(ii)* sulfures dans la troctolite hôte et *(iii)* horizons de sulfures enrichis en ÉGP. Les sulfures dans la norite hôte apparaissent soit dans les zones adjacentes aux xénolites encaissants ou près du contact basal. Les sulfures dans la troctolite hôte forment le plus gros du gisement, et ils apparaissent dans les 250 m inférieurs de l'intrusion. La localisation typique des horizons de sulfures enrichis en ÉGP se trouve directement sous les couches ultramafiques. Les rapports Cu/Pd ont été utilisés pour élaborer un modèle de la composition des différents types de minéralisation de sulfures. Il est démontré que chaque type résulte de l'interaction de deux paramètres dominants, à savoir le degré de contamination du magma et le rapport du magma silicaté au liquide sulfuré (facteur *R*). Les sulfures dans la norite hôte ont été formés sous des conditions de faibles facteurs *R* et de fortes contaminations, comme en témoignent la teneur appauvrie en ÉGP, les faibles rapports Se/S et les concentrations élevées de la pyrrhotite et des minéraux arsénieux. Les sulfures dans la troctolite hôte ont été formés sous des conditions de facteurs *R* modérés et de faibles contaminations, comme le révèlent leur teneur modéré en ÉGP et les rapports Se/S analogues à ceux du manteau. Finalement, les horizons de sulfures enrichis en ÉGP sont modélisés en utilisant des facteurs *R* élevés et un magma parental non contaminé, ce qui est appuyé par leur forte teneur en éléments nobles et les rapports Se/S élevés, et par le rapport faible de la pyrrhotite sur les sulfures de métaux précieux.

Introduction

Most of the studies pertaining to the Cu-Ni-platinum-group element (PGE) sulfide deposits of the Duluth Complex have emphasized the importance of country-rock assimilation in the genesis of the mineralization (e.g., Mainwaring and Naldrett 1977; Ripley 1981; Rao and Ripley 1983; Tyson and Chang 1984; Foose and Weiblen 1986; Ripley and Al-Jassar 1987). Sulfur isotopic data and Se/S ratios suggest that most of the sulfur in the intrusion was derived from sulfidic argillites of the underlying Virginia Formation (Mainwaring and Naldrett 1977; Ripley 1981, 1986, 1990a).

While an external source for the sulfur is generally accepted, the relative importance of magmatic and hydrothermal processes in the localization of the PGE has been the subject of much debate, and remains to be resolved. Several workers have stressed the involvement of late-stage fluids in remobilizing the PGE (Ripley 1990b; Mogessie et al. 1991; Mogessie and Stumpfl 1992; Ripley et al. 1993), based on the common occurrence of platinum-group minerals (PGM) in highly altered silicate rocks, and on the abundance of secondary sulfides such as bornite, vallerite, and violarite. However, these studies have been carried out largely in the vicinity of the Babbitt deposit, an area showing strong evidence of hydrothermal activity related to pre- and syn-Complex structures (Hauck et al. 1995). Previous work done on the Dunka Road deposit highlights the significance of country-rock assimilation, and relates the origin of the Cu-Ni-PGE mineralization to primary magmatic processes with only minimal hydrothermal effects, as indicated by the general lack of alteration throughout (Ripley 1981; Rao and Ripley 1983; Severson and Hauck 1990; Geerts 1994).

This study was initiated to describe the various types of sulfide mineralization making up the Dunka Road deposit, and to explain their mode of formation. A quantitative model is developed, which relates the composition of the sulfides to a magmatic process (i.e., *R* factor; Campbell and Naldrett 1979) in conjunction with the assimilation of sedimentary country rocks, without the need for much hydrothermal remobilization.

Geological setting

The Duluth Complex is a Middle Proterozoic (1100 Ma) composite mafic intrusion associated with the Keweenawan flood-basalt province of the Midcontinent rift of North America (Van Schmus and Hinze 1985). The complex is exposed along an arcuate belt extending for more than 220 km along the northwestern margin of Lake Superior in Minnesota (Fig. 1). It was emplaced near an unconformity between plateau lavas of the North Shore Volcanic Group and older Proterozoic (1700 Ma) basement rocks of the Animikie Group exposed to the northwest. In general, rocks forming the Duluth Complex may be subdivided into an upper anorthositic series underlain by a more mafic troctolitic series (Taylor 1964; Weiblen and Morey 1980), both of which are now assumed to be coeval based on indistinguishable U-Pb age dates (1098.6 ±0.5 to 1099.1± 0.3 Ma) recently obtained by Paces and Miller (1993).

A number of individual mafic layered intrusions have been recognized within the troctolitic series, including the Partridge River and South Kawishiwi intrusions (Severson 1994; Severson and Hauck 1990), which host most of the Cu-Ni-PGE sulfide mineralization.

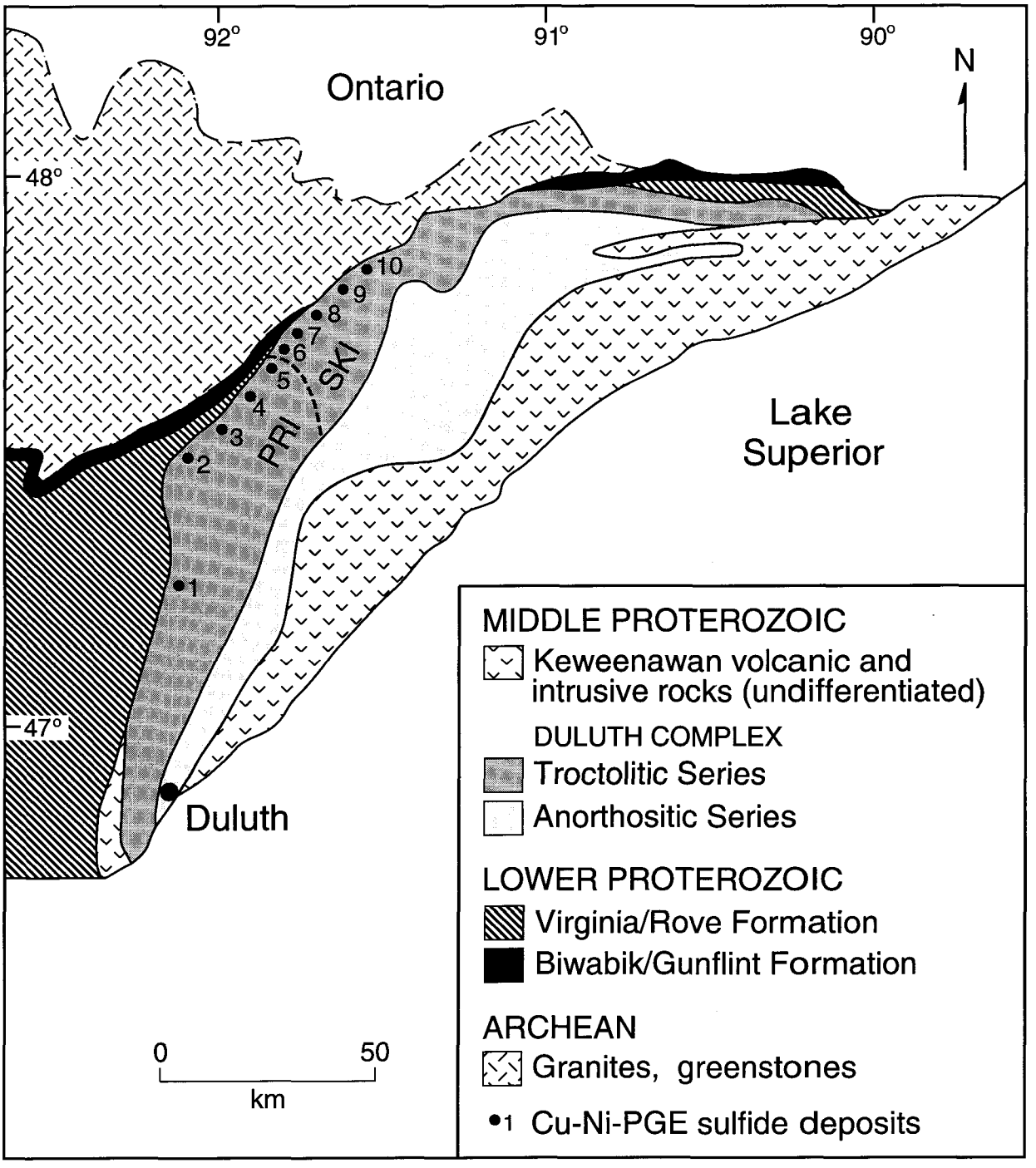

FIG. 1. Geological map showing the emplacement of the Duluth Complex within the Keweenawan flood-basalt province of North America (modified after Naldrett 1989). PRI, Partridge River intrusion; SKI, South Kawishiwi intrusion; Black circles, Cu-Ni-PGE sulfide deposits (1, Water Hen; 2, Wyman Creek; 3, Wetlegs; 4, Dunka Road; 5, Babbitt; 6, Serpentine; 7, Dunka Pit; 8, Birch Lake; 9, Maturi; 10, Spruce Road).

The deposits occur predominantly along the northwestern margin of the complex, particularly where the host troctolitic rocks are in contact with Proterozoic metasedimentary rocks of the Animikie Group, namely the Virginia and Biwabik formations (Fig. 1). The latter consists of cherty and slaty iron formation (Morey 1992), whereas the overlying Virginia Formation comprises mainly sulfidic argillite, siltstone, and greywacke (Lucente and Morey 1983). The origin of the Cu-Ni-PGE mineralization has generally been linked to the assimilation of the sulfur-bearing argillaceous rocks (e.g., Mainwaring and Naldrett 1977; Ripley 1981; Rao and Ripley 1983; Tyson and Chang 1984; Thériault et al. 1995).

Geology of the Dunka Road deposit

The Dunka Road Cu-Ni-PGE deposit occurs along the base of the Partridge River intrusion, where the host mafic rocks are in direct contact with sulfidic argillites of the Virginia Formation. The deposit extends laterally for approximately 4 km, with most of the mineralization being confined to the lower 250 m of the intrusion (Fig. 2). The extent of the mineralization at depth along the basal contact is still unknown, although geophysical work by Chandler and Ferderer (1989) has shown that the intrusive contact is roughly coplanar with the Animikie Group strata, and that the deposit could thus exist for a considerable distance downdip.

Based on drill-hole interpretation (Severson and Hauck 1990), the igneous stratigraphy of the Partridge River intrusion in the Dunka Road area has been subdivided into several correlatable correlatable cyclic units. Figure 2 shows a longitudinal southwest–northeast-

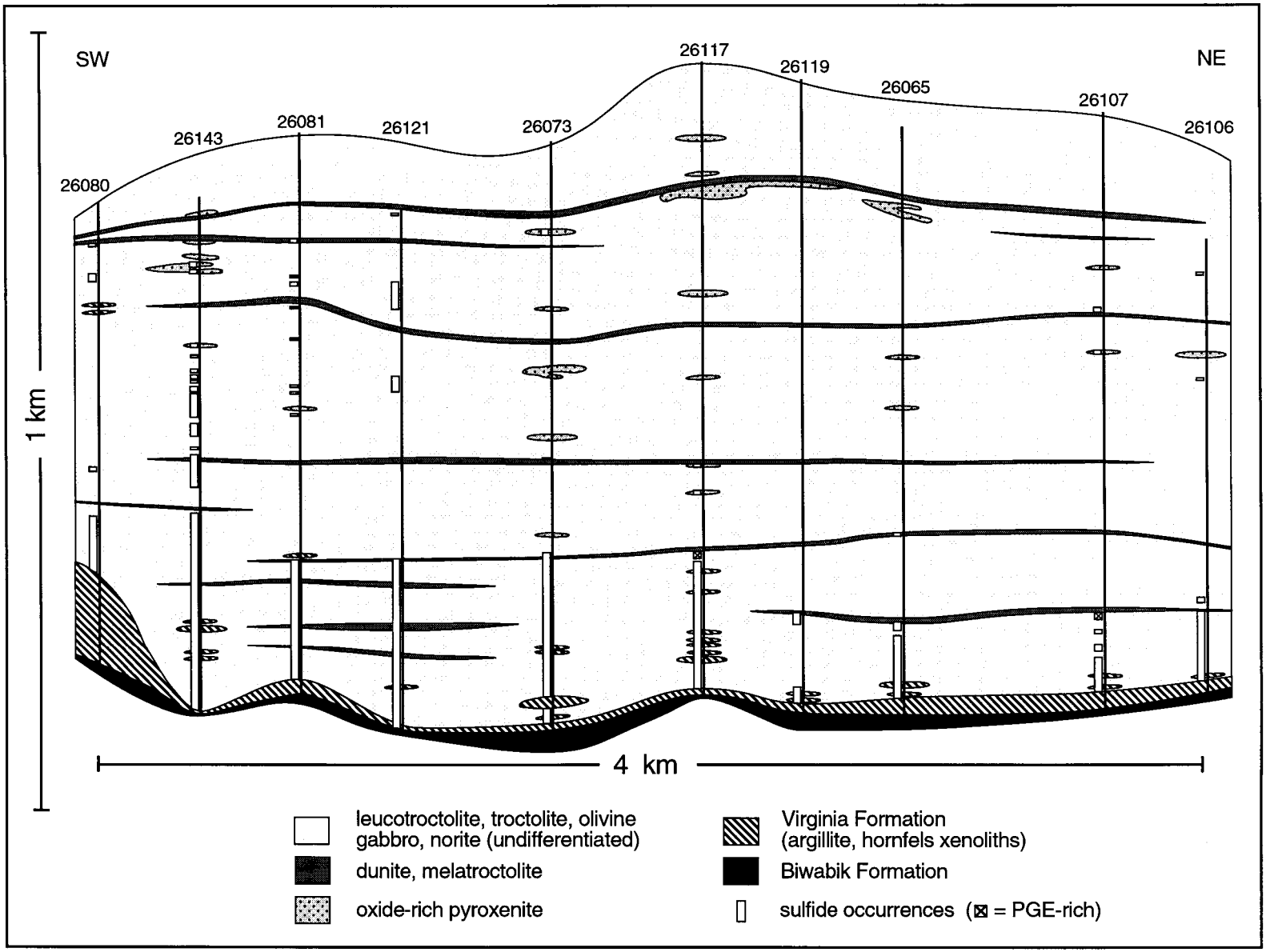

Fig. 2. Longitudinal cross section of the Dunka Road deposit based on the interpretation of 10 drill holes.

trending cross section of the Dunka Road deposit, approximately 1.5 km to the southeast and parallel to the surface contact. Each cyclic unit consists of a thin ultramafic layer (<10 m) of melatroctolite to dunite overlain by a much thicker sequence of dominantly leucotroctolite and olivine gabbro, with minor troctolite and norite. The cyclic repetition of layers is best explained in terms of periodic replenishment of new magma to the chamber. This is supported by the presence of cryptic regressions within the ultramafic layers, as expressed by an increase in whole-rock Mg number, and a decrease in initial $^{87}Sr/^{86}Sr$ ratio of plagioclase (Grant and Chalokwu 1992, Fig. 7).

As depicted in Figure 2, most of the sulfide mineralization occurs near the basal contact of the intrusion (i.e., Unit I of Severson and Hauck 1990). Whereas the upper cyclic units have a fairly coherent internal stratigraphy and generally contain little sulfides, mineralized rocks of the basal part of the intrusion are, in contrast, highly heterogeneous in terms of their texture, mineralogy, and geochemistry. Also typical of the basal mineralized rocks is the presence of hornfels xenoliths derived from the underlying Virginia Formation. These may locally form up to 25 vol.% of the rock sequence. Norite is also very common, typically occurring in proximity to country-rock xenoliths as well as directly along the basal contact.

The variability in composition and texture of the basal rocks hosting the Dunka Road deposit is interpreted to result from contamination of the parental magma upon mixing with derivatives from the underlying Virginia Formation. Evidence of partial melting is indicated by the occurrence of granitic selvages along the margin of country-rock xenoliths (Fig. 3). Mixing between the felsic partial melt and the resident magma is inferred to have led to local

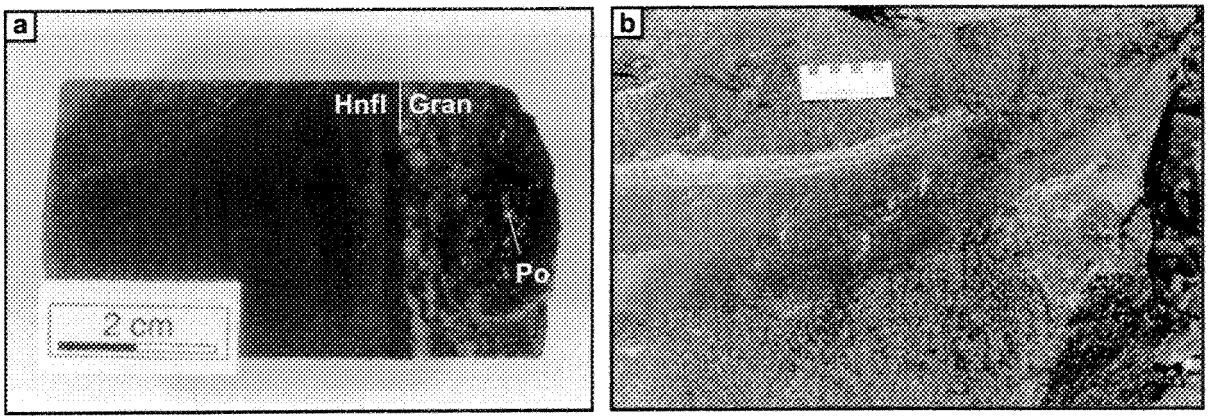

Fig. 3. (a) Granitic selvage along the margin of a hornfels xenolith from the Dunka Road deposit. Note the presence of pyrrhotite within the hybrid norite. (b) Granitic selvage rimming the upper margin of a hornfels xenolith from the Dunka Pit deposit. Scale is in centimeters.

enrichment in silica and alkalis early in the crystallization history of the basal mineralized rocks, as indicated by the general increase in orthopyroxene at the expense of olivine, and the increase in biotite content. An increase in the sodium content of plagioclase has also been attributed to be the result of mixing with a granitic partial melt (Tyson and Chang 1984).

Dehydration reactions in the Virginia Formation related to heating by the intrusion are interpreted to have led to early dissolution in the magma of a sulfur-bearing hydrous fluid (Rao and Ripley 1983; Tyson and Chang 1984; Ripley and Alawi 1988). The release of sulfur results from the conversion of pyrite into pyrrhotite (Ripley 1981). Contamination of the magma by sulfur-bearing fluids is manifested by the generally high positive $\delta^{34}S$ values of the sulfides in the mineralized rocks, values which are similar to those obtained from the underlying Virginia Formation (Ripley 1981). Tyson and Chang (1984) further argue that the sulfur-bearing fluids may have acted as a transport mechanism for iron, thus explaining the observed increase in the iron content of olivine in the basal mineralized sequence.

Mineralization

The Dunka Road Cu-Ni-PGE sulfide deposit has estimated resources of 1450 Mt, grading 0.397 wt.% Cu, 0.094 wt.% Ni, 445 ppb Pd, 118 ppb Pt, and 61 ppb Au (Wright Engineers Limited 1991). The bulk of the mineralization (i.e., >95 vol.%) consists of disseminated sulfides making up no more than 5 vol.% of the rock. The sulfides are typically interstitial to the silicates, and consist of intergrowths of pyrrhotite, chalcopyrite, pentlandite, and cubanite, with minor mackinawite, sphalerite, and bornite. Small amounts of the arsenide minerals

maucherite, niccolite, and cobaltite-gersdorffite, as well as a few grains of the platinum-group mineral froodite ($PdBi_2$), are observed in association with the sulfides.

Three different types of disseminated sulfide mineralization have been recognized within the Dunka Road deposit: 1) norite-hosted sulfides; 2) troctolite-hosted sulfides; and 3) PGE-rich sulfide horizons. In all three cases, the analyzed sulfide composition is interpreted to be representative of the original sulfide melt without any significant fractional crystallization or hydrothermal remobilization of the sulfides. The rather homogeneous composition and texture of each type of mineralization and lack of alteration support such an interpretation.

The norite-hosted sulfides are found either in proximity to country-rock xenoliths or within approximately 30 m of the basal contact of the intrusion. The troctolite-hosted sulfides occur within plagioclase-olivine cumulate rocks, namely leucotroctolite and olivine gabbro. They are found throughout the lower 250 m of the intrusion, and make up the greater part of the ore deposit. Two different occurrences of PGE-rich sulfide horizons have been recognized within the lower mineralized sequence. These horizons measure approximately 3 m in thickness and occur directly beneath ultramafic layers, their respective location being shown in Figure 2. In both cases, the sulfides are hosted by leucotroctolite.

The remainder of the mineralization forming the Dunka Road deposit (i.e., <5 vol.%) consists of isolated occurrences of massive pyrrhotite, either in the form of narrow veinlets reaching 1 to 2 cm in width or as massive aggregates along the margin of country-rock xenoliths. Associated with the pyrrhotite veinlets are minor disseminated Cu-rich sulfides (i.e., chalcopyrite and cubanite). The latter are interpreted to be the result of the fractional crystalli-

zation of a monosulfide solid solution (MSS) from the original sulfide melt, as described in Barnes et al. (1988).

In the following section, the three types of disseminated sulfide mineralization will be compared in terms of *(i)* the major and trace element geochemistry of the silicate host, *(ii)* the modal abundance and composition of the sulfide minerals, *(iii)* the metal geochemistry of the sulfides, and *(iv)* the Se/S ratio of the sulfides. In each case, emphasis will be put on describing the consequences of country-rock assimilation observed in the mineralized rocks. Owing to their minor occurrence and more complex origin, the massive pyrrhotite and associated Cu-rich ore will not be discussed any further.

Silicate host geochemistry

Whole-rock samples from the three types of disseminated sulfide mineralization, as well as other pertinent rock types (i.e., sulfidic argillite, hornfels xenolith, granitic selvage, basalt, and diabase dike) were analyzed for major and trace elements (Table 1). Major elements (except Na), S, Ni, and Cu were determined by X-ray fluorescence spectrometry at Analabs-Caleb Brett in England. All other analyses were carried out at the Université du Québec à Chicoutimi. The PGE and Re were determined by instrumental neutron-activation analysis (INAA) after preconcentrating the metals into a nickel sulfide bead following the method of Robert et al. (1971). The remaining trace elements (including Au) and Na were determined directly by INAA using the method of Bédard and Barnes (1990).

Table 1. Major and trace element composition of the 3 types of disseminated mineralization and other pertinent rock types.

Sample #	DC-49	DC-54	DC-52	DC-27	DC-60	DC-63	DC-66	DC-72	DC-53	DC-79	DC-55	DC-56	DC-61	DC-58	DC-64	DC-62
Rock type	NOR	NOR	NOR	NOR	NOR	NOR	NOR	NOR	TROC	TROC	TROC	TROC	TROC	TROC	PGE	PGE
SiO_2(wt%)	49,27	46,03	54,38	42,89	38,99	40,21	43,05	31,93	48,24	45,31	46,06	45,08	44,37	44,83	45,02	43,65
TiO_2	2,87	1,39	1,02	6,81	7,13	2,85	2,04	7,75	2,29	0,65	1,71	1,26	0,25	1,28	0,59	1,46
Al_2O_3	15,53	20,17	18,14	6,51	13,81	11,82	13,98	6,37	16,46	19,73	16,23	16,89	19,45	18,42	19,43	14,19
FeO(sil)	14,91	13,83	8,51	23,29	18,89	16,78	16,51	27,40	12,55	10,11	12,84	13,28	9,12	10,03	9,95	14,56
MnO	0,18	0,12	0,08	0,25	0,22	0,22	0,17	0,29	0,18	0,10	0,17	0,15	0,10	0,13	0,13	0,18
MgO	5,35	8,63	5,44	11,88	7,16	9,03	5,85	10,62	6,42	9,02	7,32	8,23	8,50	7,22	8,59	11,41
CaO	7,03	2,01	2,12	4,10	6,66	6,67	7,21	3,33	8,58	8,02	8,09	8,25	8,75	8,92	9,35	7,41
Na_2O	2,84	1,55	2,85	0,79	2,15	1,93	1,96	0,91	3,19	2,16	2,82	2,71	2,57	2,86	2,41	2,20
K_2O	0,48	0,75	3,98	0,17	0,48	0,55	0,66	0,30	1,05	0,49	0,82	0,55	0,35	0,58	0,43	0,59
P_2O_5	0,54	0,02	0,07	0,51	0,13	0,07	0,26	0,11	0,31	0,08	0,23	0,12	0,04	0,07	0,10	0,19
S	0,20	0,31	0,66	0,77	1,57	2,45	4,32	4,65	0,15	1,12	1,11	1,44	1,50	2,00	0,59	1,69
Fe(sul)	0,32	0,48	1,12	1,22	2,38	4,02	6,76	7,69	0,22	1,14	1,54	1,87	1,82	2,38	0,60	1,54
LOI	1,13	5,86	2,19	1,29	0,94	1,06	1,15	1,06	0,78	1,32	0,47	0,78	0,86	0,14	0,56	0,36
TOTAL	100,70	101,23	100,62	100,64	100,92	97,96	104,79	102,89	100,49	100,19	99,88	101,36	98,60	100,13	98,26	101,03
Os(ppb)	<0,5	0,7	<0,9	<0,6	<1,3	1,2	2,2	1,3	<0,8	1,3	0,9	1,6	2,5	1,9	4,1	3,2
Ir	0,10	0,22	0,25	0,28	1,20	0,92	4,28	1,46	0,57	3,04	1,01	2,79	3,76	3,08	8,62	10,50
Ru	<5,0	<5,0	4,9	<2,6	<5,0	<5,0	20,3	<5,0	<5,0	10,1	6,9	12,9	16,2	10,3	31,5	34,2
Rh	<0,21	0,46	0,53	0,74	3,96	2,65	18,81	4,72	1,24	14,99	4,17	11,80	14,99	15,89	47,63	65,65
Pt	2,5	6,9	3,7	12,8	50,2	15,6	35,1	5,4	10,2	163,9	42,1	111,7	124,3	160,7	299,1	559,7
Pd	5,4	8,1	11,1	22,7	104,7	62,8	463,7	120,1	39,0	583,3	174,3	402,1	501,3	712,2	1630,4	2250,6
Au	<3,2	2,3	<3,2	10,9	18,5	18,4	45,1	44,5	<2,1	66,7	32,2	47,6	58,9	144,0	88,7	421,4
Re	0,22	1,24	0,93	0,86	2,70	4,92	26,82	2,82	0,46	8,82	3,57	6,06	6,03	8,79	4,06	5,13
Ni(ppm)	151	265	186	348	1140	824	2283	1138	230	2246	1073	1909	2051	2439	1684	3742
Cu	373	622	293	1296	3000	2210	6395	3699	514	7120	3652	5550	7129	10228	3382	12249
Co	52,4	62,3	39,7	113,7	126,6	180,1	309,8	289,7	55,2	120,4	89,0	170,4	113,2	113,2	82,6	150,0
As	1,96	2,77	6,28	12,89	3,42	6,76	15,49	37,55	2,23	4,68	1,58	3,52	<0,38	0,71	0,56	1,49
Se	<2,0	<1,7	<1,1	1,9	3,2	3,2	5,9	9,6	<1,3	3,5	2,4	3,2	4,3	4,6	1,9	8,2
Sb	1,59	0,80	1,35	0,89	0,57	0,57	0,71	0,58	1,03	0,60	1,51	2,86	0,56	2,65	0,39	0,44
Cs(ppm)	0,6	2,8	2,6	<0,4	0,5	1,2	1,5	0,8	1,7	2,1	1,5	0,4	<0,3	<0,3	0,3	0,7
Rb	7	31	86	<6	12	16	21	16	34	19	21	9	<6	7	3	13
Ba	199	198	673	30	164	146	276	83	276	117	204	162	81	143	76	152
Th	0,84	0,48	4,66	0,44	1,40	0,89	2,56	1,32	3,82	1,11	2,21	1,28	0,18	0,69	0,66	1,46
U	1,29	0,26	2,07	0,16	0,44	0,12	0,75	0,30	1,04	0,26	0,63	0,33	<0,21	0,22	0,19	0,39
Ta	1,18	0,71	<0,29	2,54	1,26	0,66	0,89	1,58	0,88	0,22	0,72	0,25	<0,11	0,17	0,28	0,40
La	19,27	14,07	31,54	10,50	8,67	8,49	19,40	8,50	21,12	7,38	15,64	9,37	2,87	5,64	6,00	11,47
Ce	44,54	22,60	60,12	25,44	21,06	17,71	44,34	19,28	48,43	16,75	35,61	21,82	6,46	13,50	13,26	27,43
Nd	24,25	7,54	21,27	12,42	11,48	10,91	25,84	7,79	25,28	8,37	19,03	8,32	1,06	7,01	6,71	14,06
Hf	2,28	0,96	2,50	1,78	2,54	1,28	5,95	2,55	4,33	1,36	3,31	2,22	0,27	1,12	1,33	2,69
Sm	5,96	1,17	3,91	3,89	3,08	2,42	6,21	2,33	5,91	1,75	4,37	2,48	0,59	1,78	1,76	3,60
Tb	0,92	<0,17	0,62	0,87	0,56	0,43	1,12	0,32	1,08	0,26	0,82	0,38	<0,09	0,33	0,19	0,57
Cu/Pd	68819	77076	26302	57168	28651	35174	13791	30794	13166	12206	20957	13801	14222	14361	2074	5443
Mg #	0,39	0,53	0,53	0,48	0,40	0,49	0,39	0,41	0,48	0,61	0,50	0,52	0,62	0,56	0,61	0,58
$Se/Sx10^6$	-----	-----	-----	244	175	131	136	206	-----	314	218	223	284	228	320	485

Table 1 (continued).

Sample #	DC-35	DC-37	DC-38	DC-1	DC-3	DC-5	DC-6	DC-7	DC-8	DC-9	DC-70	DC-26	DC-69	DC-81	DC-78	DC-80
Rock type	DIKE	KEW	KEW	ARG	ARG	ARG	ARG	ARG	ARG	ARG	ARG	HNFL	HNFL	HNFL	HNFL	GRAN
SiO_2(wt%)	47,01	49,10	48,87	63,58	62,04	61,85	69,66	66,73	60,08	59,92	56,17	46,94	38,05	46,74	44,11	60,61
TiO_2	0,96	0,82	0,95	0,71	0,63	0,76	0,55	0,69	0,80	0,79	0,72	0,10	0,58	1,62	1,70	0,75
Al_2O_3	16,98	17,16	16,90	15,44	13,38	15,51	12,81	12,62	17,00	17,17	15,82	29,04	25,61	22,06	26,63	17,24
FeO(sil)	9,29	8,37	8,96	7,57	5,17	5,35	6,14	5,86	5,03	8,11	0,56	8,20	9,48	14,49	12,42	6,15
MnO	0,29	0,14	0,15	0,06	0,08	0,05	0,05	0,06	0,05	0,06	0,03	0,06	0,05	0,11	0,07	0,05
MgO	8,36	8,28	8,55	3,34	2,66	3,19	2,53	2,52	3,20	3,71	2,56	10,94	8,94	10,13	9,12	3,41
CaO	9,88	10,60	10,80	0,75	3,37	0,66	0,99	2,09	0,55	0,54	1,11	0,45	0,20	0,42	0,07	0,87
Na_2O	2,45	2,37	2,51	3,16	2,83	1,98	4,13	2,23	2,04	2,67	1,75	0,23	0,18	0,97	0,18	4,73
K_2O	0,23	0,36	0,36	2,36	2,01	3,18	1,17	2,27	3,62	3,08	3,24	0,58	0,61	0,65	0,64	4,29
P_2O_5	0,09	0,07	0,10	0,18	0,16	0,17	0,12	0,17	0,19	0,15	0,13	<0,01	<0,01	0,02	0,02	0,11
S	<0,01	<0,01	<0,01	0,02	0,31	0,53	<0,01	0,09	1,08	0,03	4,45	0,70	5,90	0,40	1,56	0,15
Fe(sul)	0,00	0,00	0,00	0,03	0,54	0,92	0,00	0,16	1,88	0,05	7,75	1,20	10,09	0,66	2,65	0,22
LOI	6,00	2,68	1,57	1,97	5,40	5,64	2,49	3,68	4,49	4,37	5,86	1,29	1,80	2,86	1,83	1,22
TOTAL	101,57	99,98	99,75	99,18	98,59	99,81	100,65	99,18	100,01	100,66	100,18	99,78	101,73	101,20	101,11	99,88
Os(ppb)	<0,5	<0,5	<1,1	<0,6	0,9	<1,2	<0,6	<0,6	<0,7	<0,5	<1,5	0,7	1,2	0,6	0,7	<0,6
Ir	0,03	0,19	0,21	0,14	0,07	<0,07	0,02	0,04	0,10	0,09	0,06	0,33	0,82	0,26	0,22	0,08
Ru	<3,4	<1,4	<5,0	<3,3	<5,0	<9,8	<5,4	<3,4	<5,3	<3,5	<5,0	<2,9	7,5	<2,6	1,7	<2,5
Rh	<0,13	0,35	0,35	0,17	0,23	<0,37	0,26	<0,31	<0,20	0,13	0,12	0,57	1,17	0,31	0,43	0,07
Pt	<3,4	10,1	7,0	3,1	<3,2	6,5	8,2	<4,2	3,5	3,9	<4,7	6,0	13,1	7,4	9,0	2,6
Pd	3,3	9,2	10,7	1,8	2,4	4,9	2,7	3,3	2,6	<3,2	3,5	2,9	36,1	8,3	5,3	4,0
Au	<1,7	<1,7	<1,2	5,4	<5,9	2,8	2,4	<1,6	<3,5	<1,6	<2,8	3,1	28,2	7,2	12,2	6,5
Re	0,15	0,09	0,41	0,07	0,67	0,68	<0,09	0,34	2,06	0,20	0,10	1,35	5,81	0,80	1,48	0,34
Ni(ppm)	181	221	218	67	61	89	41	48	85	78	144	150	1035	291	355	123
Cu	74	97	117	39	43	73	30	46	58	59	170	422	1335	420	732	646
Co	57,2	58,9	62,3	38,7	33,9	25,5	43,3	31,5	28,2	34,8	33,3	165,8	227,0	82,9	69,1	24,6
As	0,57	<0,20	0,21	7,16	13,04	25,75	4,53	8,96	27,32	3,83	9,40	14,43	95,93	38,41	5,99	5,99
Se	<1,0	<0,8	<0,8	<1,3	<1,1	<2,4	<2,3	<2,2	<2,3	<2,5	1,6	6,0	1,9	2,0	<2,6	<1,4
Sb	0,51	0,65	1,37	1,83	4,56	5,09	1,33	2,47	5,98	1,83	5,38	1,06	0,35	1,07	0,20	1,91
Cs(ppm)	1,8	<0,6	0,4	7,2	5,6	9,7	2,4	6,0	10,4	8,4	10,8	5,6	3,7	3,2	6,2	5,1
Rb	3	<11	<6	89	51	131	38	77	136	125	142	53	39	43	40	133
Ba	65	79	84	600	351	479	228	471	598	546	477	24	23	18	102	539
Th	0,54	0,22	0,38	10,64	6,83	9,70	6,12	7,77	11,17	10,16	10,47	<0,15	0,21	0,49	1,12	15,15
U	<0,24	<0,16	<0,16	4,05	3,92	9,38	2,01	3,87	8,14	3,93	23,25	<0,19	0,12	0,14	0,25	5,30
Ta	0,21	0,23	0,39	1,31	0,96	1,03	1,07	1,02	0,92	0,74	0,55	4,96	0,11	0,64	0,90	0,62
La	7,52	4,55	5,42	43,53	25,81	25,34	23,02	23,67	25,07	25,13	43,01	0,43	0,62	1,83	6,35	33,97
Ce	16,24	13,41	15,10	90,78	57,80	52,68	48,38	50,07	52,33	55,96	73,49	<0,83	<1,7	3,58	12,73	71,77
Nd	8,30	5,88	5,81	33,27	31,41	14,16	19,71	18,89	15,24	19,50	36,21	3,29	1,89	1,12	3,22	32,14
Hf	1,36	0,81	0,95	3,38	2,54	4,18	2,27	5,02	4,44	4,59	3,91	<0,38	0,28	0,81	1,32	3,51
Sm	2,30	1,93	2,45	7,82	6,96	5,96	4,05	4,63	5,23	5,59	9,12	0,09	0,14	0,37	1,04	6,42
Tb	0,47	0,30	0,44	0,99	1,26	0,97	0,79	0,60	0,86	0,76	1,29	<0,13	<0,05	<0,04	0,08	0,77
Cu/Pd	22561	10532	10914	21910	17992	14807	11029	13814	22568	-----	48023	146021	37032	50725	138899	159901
Mg #	0,62	0,64	0,63	0,44	0,48	0,52	0,42	0,43	0,53	0,45	0,89	0,70	0,63	0,55	0,57	0,50
$Se/Sx10^6$	-----	-----	-----	-----	-----	-----	-----	-----	-----	-----	35	859	32	488	-----	-----

NOTES: NOR= norite-hosted mineralization; TROC= troctolite-hosted mineralization; PGE= PGE-rich sulfide horizons; KEW= Keweenawan flood basalt; DIKE= Duluth diabase dike; ARG= argillite; HNFL= hornfels xenoliths; GRAN= granitic selvage; FeO(sil)= total FeO in silicate minerals; Fe(sul)= iron in sulfide minerals; LOI= loss on ignition; Mg # = mole fraction MgO/MgO + FeO(sil)

Geochemical results show that the mineralized norites are typically enriched in TiO_2, FeO, and Ta relative to the mineralized troctolites (Table 1) owing to the abundance of ilmenite (3-20 vol.%). The elevated ilmenite content of the norites implies a decrease in the oxygen fugacity of the host magma (Ishihara 1977), brought about by its interaction with hydrocarbonderived from the argillaceous country rocks (Hollister 1980). The other main characteristic of the norites is their relatively low noble metal content, especially in the PGE. They are, however, quite enriched in As relative to the mineralized troctolites, which correlates with the elevated As content of the adjacent metasedimentary rocks.

Apart from their different metal content, the mineralized troctolites and the PGE-rich sulfide horizons are quite similar in terms of their major and trace element geochemistry, which is not surprising, considering that they are both hosted in plagioclase-olivine cumulates (i.e., leucotroctolite ± olivine gabbro).

To better compare their trace element geochemistry, samples from the three types of disseminated mineralization were plotted on a mantle-normalized spider diagram (Fig. 4*a*). Apart from the elevated Ti and Ta content of the norites discussed above, the average pattern of each type of mineralization is rather similar. However, when the most trace element enriched samples of each ore type are compared, one can see a systematic increase in trace element abundance from a relatively depleted PGE-rich horizon to a more enriched norite. This is especially apparent for the highly incompatible elements such as Cs, Rb, Ba, Th, U, and K, which are expected to be most easily mobilized by a felsic partial melt derived from the argillaceous country rocks.

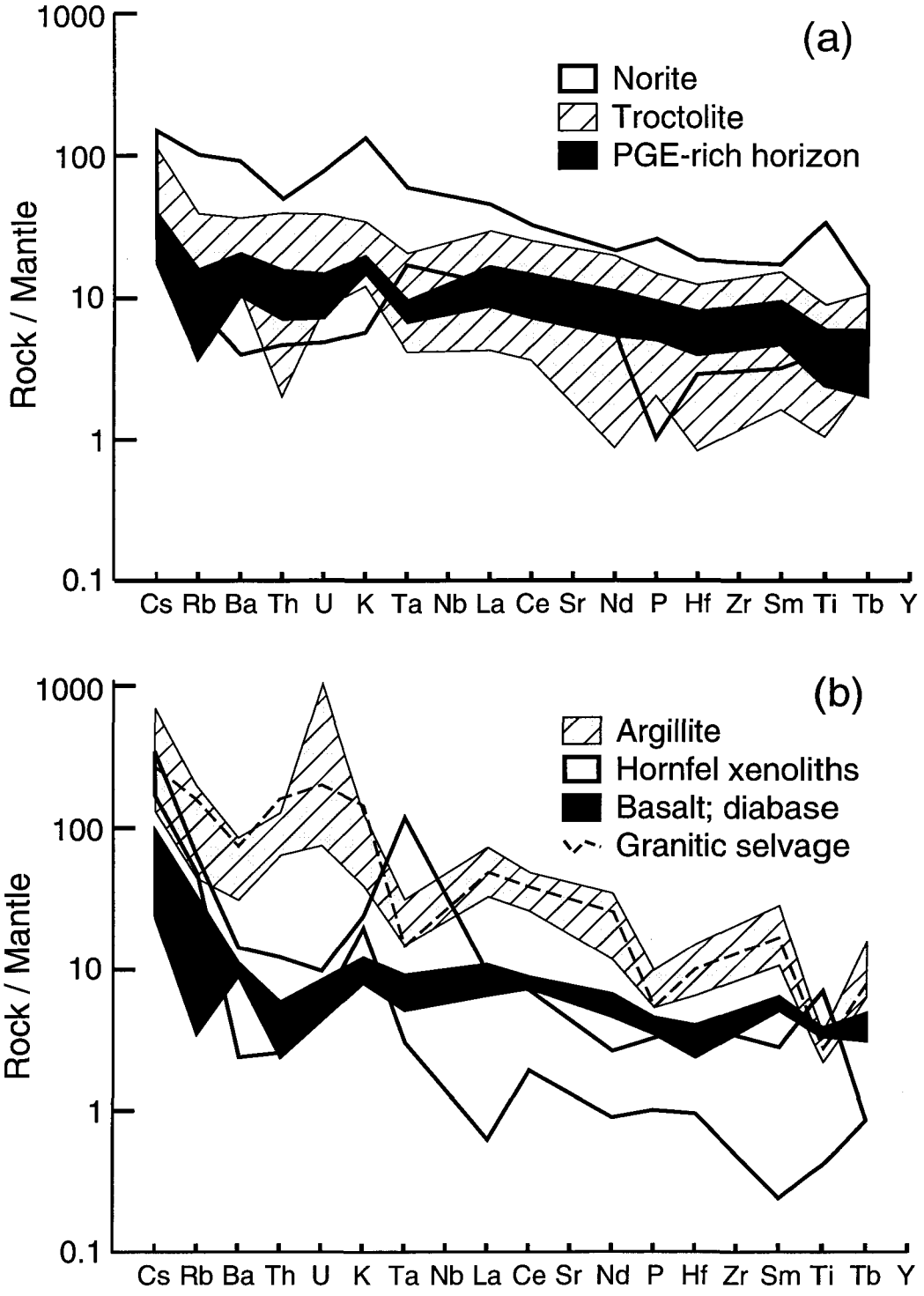

FIG. 4. Mantle-normalized spider diagram showing the range in trace element composition for *(a)* the three types of disseminated sulfide mineralization; and *(b)* the argillite and associated granitic selvage, hornfels xenoliths, and potential parental rocks. Normalization factors are from Wood (1979).

Figure 4*b* shows the mantle-normalized patterns of the argillite and its derived granitic selvage, residual hornfels xenoliths, and likely representatives of the parental magma composition (i.e., basalt and diabase dike). As expected, the argillite and associated granite are quite enriched in highly incompatible elements, and their pattern mimics that of the most trace element enriched norite. Hornfels xenoliths are clearly residues of the extraction of a granitic melt from the argillite, as most trace elements show an antithetic relationship. Basalt and diabase dike contain relatively low trace element abundances and correlate well with samples from the PGE-rich horizons.

Samples were also plotted on the ternary system forsterite-anorthite-silica as a means of evaluating the effect of country-rock assimilation on the major element composition of the different types of disseminated sulfide mineralization (Fig. 5). Results show that all norite samples except one lie in the silica-oversaturated part of the diagram, further attesting to their hybridization through contamination by a granitic partial melt. Moreover, most norite samples are displaced towards the composition point of enstatite relative to the parental rocks, reflecting the accumulation of orthopyroxene. Neglecting this cumulate effect, norite samples would plot more or less along a mixing line between the parental rock composition and the argillite. The fact that the composition of the granitic selvage also lies along this particular mixing line suggests that the partial melt may have interacted with the mafic parental magma.

Samples from the mineralized troctolites and the PGE-rich horizons fall near the parental basalt composition slightly towards the anorthite-forsterite join, indicating that they are truly plagioclase-olivine cumulates. Considering this accumulation process, it could be argued that

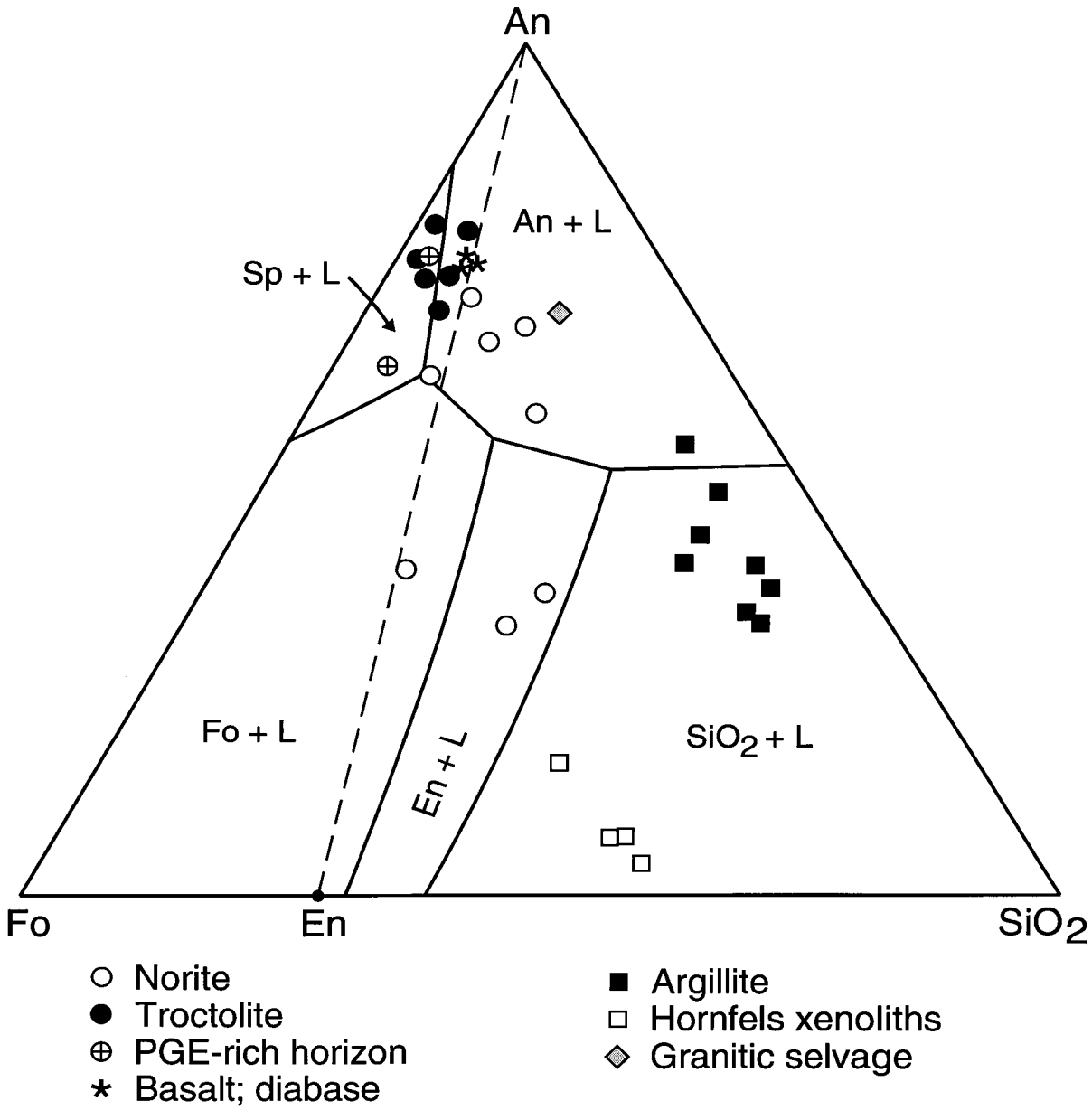

FIG. 5. Position of mineralized samples and related rocks within the forsterite-anorthite-silica ternary system. The broken line separates silica-saturated from silica-oversaturated rocks. Diagram modified after Anderson (1915).

the troctolite samples lying nearest to the parental rock composition crystallized from a hybridized magma that would fall in the silica-oversaturated field and along the hypothetical mixing line indicative of magma contamination.

Sulfide mineralogy

The variable degree of magma contamination that affected each type of disseminated sulfide mineralization, demonstrated above by the distinct geochemistry and normative composition of their respective silicate host, is also displayed when comparing the mineralogy and the composition of their sulfide assemblage.

The norite-hosted sulfides typically consist of interstitial grains of pyrrhotite intergrown with ilmenite, with lesser amounts of chalcopyrite, cubanite, and pentlandite, and trace quantities of mackinawite and bornite. The sulfide mineralogy reflects that of the assimilated sulfidic argillite (i.e., pyrrhotite bearing), with only a small contribution of metals being provided by the mafic magma. Arsenide minerals (i.e., maucherite, niccolite, and cobaltite-gersdorffite) are also commonly observed in the norites, frequently occurring within semi-massive, pyrrhotite-rich lenses bordering hornfels xenoliths. Textural relationships strongly suggest that the arsenides are primary phases that crystallized directly from the sulfide melt.

The troctolite-hosted sulfides comprise interstitial grains of intergrown pyrrhotite, pentlandite, chalcopyrite, and cubanite, with trace amounts of mackinawite and bornite. A general decrease in the pyrrhotite content at the expense of the precious metal sulfides is

observed relative to the norite-hosted mineralization. Furthermore, unlike the norites, only a few grains of maucherite were observed in the troctolites.

Although the sulfide mineralogy of the PGE-rich horizons and troctolite-hosted mineralization are identical, they differ markedly in terms of their respective modal proportions. The PGE-rich sulfide horizons are typically composed of interstitial grains of intergrown chalcopyrite, cubanite, and pentlandite. Pyrrhotite is much less common, usually amounting to no more than 20 vol.% of the sulfide assemblage. Arsenide minerals were not observed in any of the two samples from the PGE-rich sulfide horizons.

The normative sulfide mineralogy of each type of disseminated mineralization was determined from the calculated composition of the sulfide fraction (Table 2). Results clearly support the petrographic observations, and show that the proportion of precious metal sulfides (i.e., chalcopyrite, cubanite, and pentlandite) decreases with increasing degree of assimilation owing to the metal-depleted nature of the contaminant relative to the mafic magma.

The average mineral compositions of the different sulfides, arsenides, and the PGM froodite were determined by x-ray emission spectrometry using the electron probe microanalyzer at the Université du Québec à Chicoutimi (Table 3). Both monoclinic and hexagonal pyrrhotite are found, the former variety being identified only in samples of the norite-hosted mineralization. This association is likely due to the greater availability of locally derived sedimentary sulfur. The compositions of chalcopyrite, cubanite, pentlandite, and mackinawite are approximately stoichiometric and show very little variation among the different types of mineralization.

Table 2. Metal composition of the sulfide fraction, normative sulfide mineralogy, and results of the modelling of the disseminated sulfide mineralization.

Sample #	DC-49	DC-54	DC-52	DC-27	DC-60	DC-63	DC-66	DC-72	DC-53	DC-79	DC-55	DC-56	DC-61	DC-58	DC-64	DC-62	AVG	AVG	AVG
Rock type	NOR	NOR	NOR	NOR	NOR	NOR	NOR	NOR	TROC	TROC	TROC	TROC	TROC	TROC	PGE	PGE	NOR	TROC	PGE
Sulphides(wt%)	0,56	0,90	1,84	2,15	4,36	6,99	11,54	12,60	0,42	3,21	3,11	4,01	4,31	5,63	1,71	4,78	-----	-----	-----
S(wt%)	36,08	35,99	36,39	36,07	36,05	36,18	36,12	36,25	35,94	35,28	35,86	35,68	35,59	35,56	35,34	35,14	36,14	35,65	35,24
Fe	57,64	55,54	61,99	57,24	54,66	59,39	56,55	59,98	53,19	35,88	49,69	46,25	43,15	42,32	35,82	31,99	57,87	45,08	33,91
Cu	4,93	6,11	1,07	5,61	6,66	3,12	5,26	2,80	9,93	22,12	11,48	13,50	16,68	18,01	19,67	25,26	4,45	15,29	22,47
Ni	0,93	1,97	0,48	0,70	2,39	1,07	1,82	0,73	0,73	6,45	2,82	4,23	4,40	3,98	8,92	7,36	1,26	3,77	8,14
Os(ppb)	<96	81	<49	<29	<30	18	18	10	<186	42	30	40	59	33	245	67	29	40	156
Ir	18	26	14	13	28	14	36	11	137	96	33	69	89	55	516	218	20	80	367
Ru	<893	<556	<272	<121	<115	<72	170	<40	<1190	317	222	319	385	183	1884	711	59	285	1297
Rh	<38	53	29	35	91	39	157	37	297	472	135	292	356	282	2853	1365	58	306	2109
Pt	455	805	205	597	1154	230	293	42	2444	5161	1360	2767	2949	2857	17918	11636	472	2923	14777
Pd	978	937	614	1062	2404	928	3877	936	9354	18375	5630	9965	11893	12662	97669	46790	1467	11313	72230
Au	<571	267	<174	511	425	272	377	347	<500	2101	1040	1179	1397	2560	5313	8761	329	1656	7037
Re	40	144	51	40	62	73	224	22	110	278	115	150	143	156	243	107	82	159	175
As	354	322	346	604	79	100	130	293	534	147	51	87	<9	13	34	31	278	139	32
Co	3173	3358	288	2997	2104	2158	2287	1862	1288	2234	1269	2977	1525	1123	2021	2073	2278	1736	2047
Sb	287	93	74	42	13	8	6	5	247	19	49	71	13	47	23	9	66	74	16
Se	<204	<106	<60	88	63	48	49	75	<310	111	78	79	103	81	113	171	58	90	142
TOTAL(%)	100	100	100	100	100	100	100	100	100	100	100	100	100	100	100	100	100	100	100
Cp+Cb	14,1	17,5	3,1	16,0	19,0	8,9	15,0	8,0	28,4	63,2	32,8	38,6	47,7	51,4	56,2	72,2	12,7	43,7	64,2
Pn	3,0	6,4	1,6	2,3	7,7	3,5	5,9	2,3	2,4	20,8	9,1	13,7	14,2	12,8	28,8	23,7	4,1	12,2	26,3
Po	82,9	76,2	95,4	81,7	73,3	87,6	79,1	89,6	69,3	16,0	58,1	47,8	38,1	35,7	15,0	4,1	83,2	44,2	9,6
Contam.(%)	-----	65	20	55	25	30	5	30	5	15	20	10	15	15	0	0	33	13	0
R-factor	-----	100	50	150	300	125	400	100	1000	2000	700	1200	1500	1500	11000	5000	153	1317	8000

NOTES: Composition of the sulfide fraction calculated assuming that the main sulfide minerals (pyrrhotite (Po), chalcopyrite (Cp), cubanite (Cb), and pentlandite (Pn)) have compositions similar to those determined by electron probe (see Table 3), and allowing 200 ppm Ni and 150 ppm Cu in the silicate component of the rock. Details of the calculations in Barnes and Francis (1995). Contam.(%)= proportion of granitic material in hybrid magma based on Cu/Pd ratio and Pd content.

Table 3. Average mineral composition of sulfide, arsenide, and platinum-group minerals.

	Po(hex)	Po(mon)	Cp	Cb	Pn	Mk	Ma	Ma[a]	Nc	C-G	Fr	D.L.
S(wt%)	36,50	38,41	34,67	35,65	33,17	36,24	0,18	1,59	0,16	21,17	n.d.	0,10
Fe	62,82	59,93	30,01	41,06	33,86	56,54	1,35	3,18	0,93	9,22	0,71	0,14
Ni	0,01	0,24	0,02	0,01	30,72	5,97	49,37	34,80	40,24	4,96	0,21	0,03
Cu	0,02	0,05	35,12	23,45	0,00	0,06	0,07	0,00	0,00	4,44	0,58	0,03
Co	0,00	0,00	0,00	0,00	1,45	0,00	1,13	2,35	0,55	19,10	n.d.	0,03
As	n.d.	n.d.	n.d.	n.d.	n.d.	n.d.	48,38	37,24	55,02	38,07	n.d.	0,17
Sb	n.d.	n.d.	n.d.	n.d.	n.d.	n.d.	0,14	10,22	0,87	1,16	0,07	0,08
Pd	n.d.	n.d.	n.d.	n.d.	n.d.	n.d.	0,38	6,77	0,06	0,97	19,40	0,12
Pt	n.d.	n.d.	n.d.	n.d.	n.d.	n.d.	0,08	0,08	0,08	0,06	1,80	0,05
Rh	n.d.	n.d.	n.d.	n.d.	n.d.	n.d.	0,00	0,00	0,00	0,63	0,05	0,16
Ag	n.d.	n.d.	n.d.	n.d.	n.d.	n.d.	0,00	4,39	0,00	0,00	2,79	1,13
Bi	n.d.	n.d.	n.d.	n.d.	n.d.	n.d.	n.d.	n.d.	n.d.	n.d.	78,79	0,26
Total	99,35	98,63	99,82	100,18	99,20	98,80	101,08	100,62	97,90	99,79	104,39	
n	14	10	19	12	25	7	16	3	5	7	7	
S(at%)	50,28	52,63	49,79	50,17	47,26	50,34	0,37	3,48	0,33	35,94	-----	
Fe	49,69	47,15	24,75	33,17	27,70	45,09	1,56	3,99	1,14	8,98	2,05	
Ni	0,01	0,18	0,01	0,01	23,91	4,53	54,54	41,61	47,00	4,60	0,56	
Cu	0,01	0,04	25,45	16,65	-----	0,04	0,07	-----	-----	3,81	1,46	
Co	-----	-----	-----	-----	1,13	0,00	1,25	2,80	0,65	17,64	-----	
As	-----	-----	-----	-----	-----	-----	41,87	34,88	50,33	27,66	-----	
Sb	-----	-----	-----	-----	-----	-----	0,08	5,89	0,49	0,52	0,10	
Pd	-----	-----	-----	-----	-----	-----	0,23	4,46	0,04	0,50	29,35	
Pt	-----	-----	-----	-----	-----	-----	0,03	0,03	0,03	0,02	1,49	
Rh	-----	-----	-----	-----	-----	-----	-----	-----	-----	0,33	0,07	
Ag	-----	-----	-----	-----	-----	-----	-----	2.86	-----	-----	4,17	
Bi	-----	-----	-----	-----	-----	-----	-----	-----	-----	-----	60,70	
X	0,99	0,90	1,01	0,99	1,12	0,99	1,30	1,19	0,93	-----	2,07	

NOTES: Po= pyrrhotite (hexagonal; monoclinic); Cp= chalcopyrite; Cb= cubanite; Pn= pentlandite; Mk= mackinawite; Ma= maucherite; Ma[a]= Sb-Pd enriched maucherite; Nc= niccolite; C-G= cobaltite-gersdorffite; Fr= froodite; n= number of analyses; n.d.= not determined; *X*= M/S for sulfides, Ni/As for arsenides, Bi/Pd for froodite; D.L. = detection limit = 3σ (50% error); wavelength dispersive (WDS) electron probe analyses made at 20 kv, 7 nA, 5μm beam diameter, and 100 s counting interval. S, Fe, and As analyzed by EDS for 50 s.

Mineral analyses of maucherite, niccolite, and cobaltite-gersdorffite yielded significant concentrations of Pd, Pt, Rh, and Sb (Table 3). Ripley and Chryssoulis (1994) obtained relatively low values for Pd (<750 ppm), Rh (<300 ppm), Ir (< 100 ppm) and Pt (<37 ppm) in maucherites from the Babbitt deposit. However, Cabri and Laflamme (1976) reported up to 1.84 wt.% Pd in maucherite and 1.95 wt.% Pd in cobaltite-gersdorffite from the Sudbury deposit, whereas niccolite with 4-12 wt.% Pd was described by Watkinson and Ohnenstetter (1992) from the Two Duck Lake intrusion. Experimental work by Gervilla et al. (1994) on the system Pd-Ni-As at 790° and 450°C reveals that arsenide minerals may be important collectors of Pd. The common occurrence of arsenides in the norite-hosted mineralization may be related to the derivation of As from the surrounding country rocks. Elevated concentrations of As were found in unmetamorphosed argillites of the Virginia Formation (Table 1).

A few grains of the PGM froodite were observed in a norite sample, occurring along the margins of pentlandite in Cu-rich disseminated sulfides associated with a pyrrhotite-rich veinlet. The source of Bi may also be from the argillites, considering that niccolite and cobaltite-gersdorffite were also found in the same sample.

Sulfide geochemistry

To systematically compare the average metal composition of each type of disseminated sulfide mineralization, whole-rock metal contents were recalculated to 100% sulfides (Table 2).

Several key features can be drawn from the recalculated data that demonstrate the variable degree of magma contamination that affected each of the three types of disseminated sulfide mineralization. First, the norite-hosted sulfides show an enrichment in S and Fe and depletion in Cu and Ni relative to the other types of mineralization, which reflects the abundance of pyrrhotite in the sulfide assemblage and suggests significant assimilation of the sulfur-bearing contaminant. On the other hand, sulfides from the PGE-rich horizons contain relatively low amounts of S and Fe associated with elevated Cu and Ni contents, values that concord with the composition of the observed sulfide phases (see mineral analyses of chalcopyrite, cubanite, and pentlandite in Table 3). Hence the proportion of pyrrhotite in the sulfide assemblage may be used as a guide in evaluating the relative extent of magma contamination. As in the case of Cu and Ni, the PGE, Au, Re and Se content of the sulfides decreases systematically from the PGE-rich horizons to the troctolites, and reaches a minimum in the norites, illustrating the relative input of noble metals supplied by the parental magma. The abundance of As and Sb in the norite-hosted sulfides and to a lesser extent in the troctolite-hosted sulfides, and strong depletion in the PGE-rich sulfides, is in accordance with the amount of arsenides observed in these rocks, and further supports their interpreted sedimentary-derived origin.

Mantle-normalized metal patterns of the different types of disseminated sulfide mineralization (Fig. 6) illustrate the metal-enriched nature of the PGE-rich horizons, particularly in the platinum-group elements Rh, Pt, and Pd. The following average enrichment factors are observed in the PGE-rich horizons relative to the norite-hosted sulfides: Cu(5),

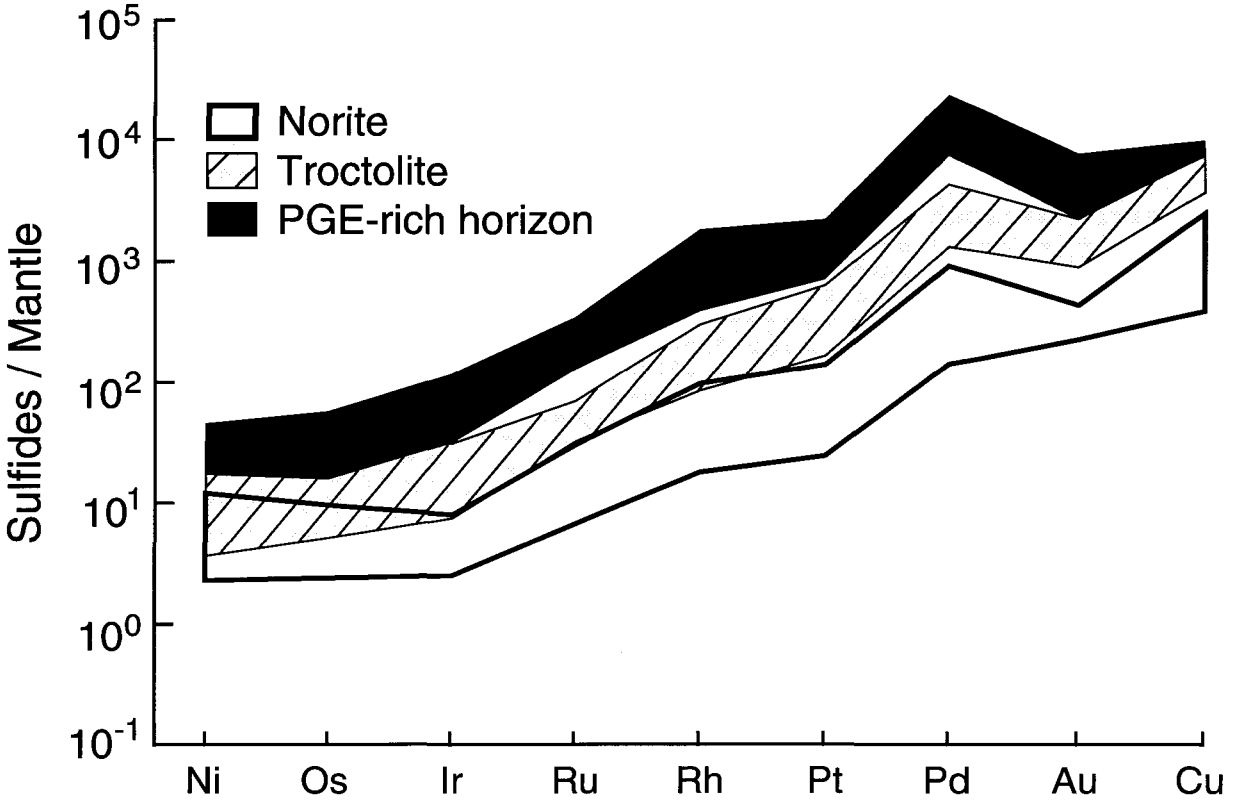

FIG. 6. Mantle-normalized metal patterns showing the range in composition of the three different types of disseminated sulfide mineralization. Normalization factors are from Barnes et al. (1988).

Os(5), Ni(6), Ir(18), Au(21), Ru(22), Pt(31), Rh(36), and Pd(49). The higher enrichment factors of the Pd-group PGE (i.e., Rh, Pt, and Pd; Barnes et al. 1985) are likely indicative of the higher partition coefficient of these metals into the sulfide melt. Recent experimental work (e.g., Francis 1990; Peach et al. 1990) and numerical modelling (e.g., Lesher and Campbell 1993; Barnes and Francis 1995) have shown that the partition coefficient of Cu into sulfides (i.e., ~1000-2000) appears to be significantly greater than that of Ni (i.e., ~200-800). The fact that Cu and Ni have similar enrichment factors in the PGE-rich horizons relative to the norite-hosted sulfides may imply that Cu has been preferentially supplied to the norite via assimilation. Such interpretation is further supported by the very elevated Cu/Ni ratio of the granitic selvage.

Se/S ratios

Se/S ratios have commonly been employed to identify the source of sulfur in magmatic sulfide deposits, especially where country-rock assimilation is believed to have been important in the genesis of the mineralization (e.g., Paktunc 1989; Eckstrand et al. 1989; Ripley 1990a). The convenience of using Se/S ratios is that sedimentary crustal rocks are generally depleted in selenium relative to mantle-derived rocks (Eckstrand and Hulbert 1987). As shown in Figure 7, whole-rock Se/S ratios increase rather systematically from the mineralized norites to the PGE-rich horizons, accompanied by a concomitant increase in the Pd+Pt content of the sulfides. All norite samples (except DC-27) have Se/S ratios below that of estimated mantle rocks (i.e., $230x10^{-6} - 350x10^{-6}$), and they also plot closest to the argillite

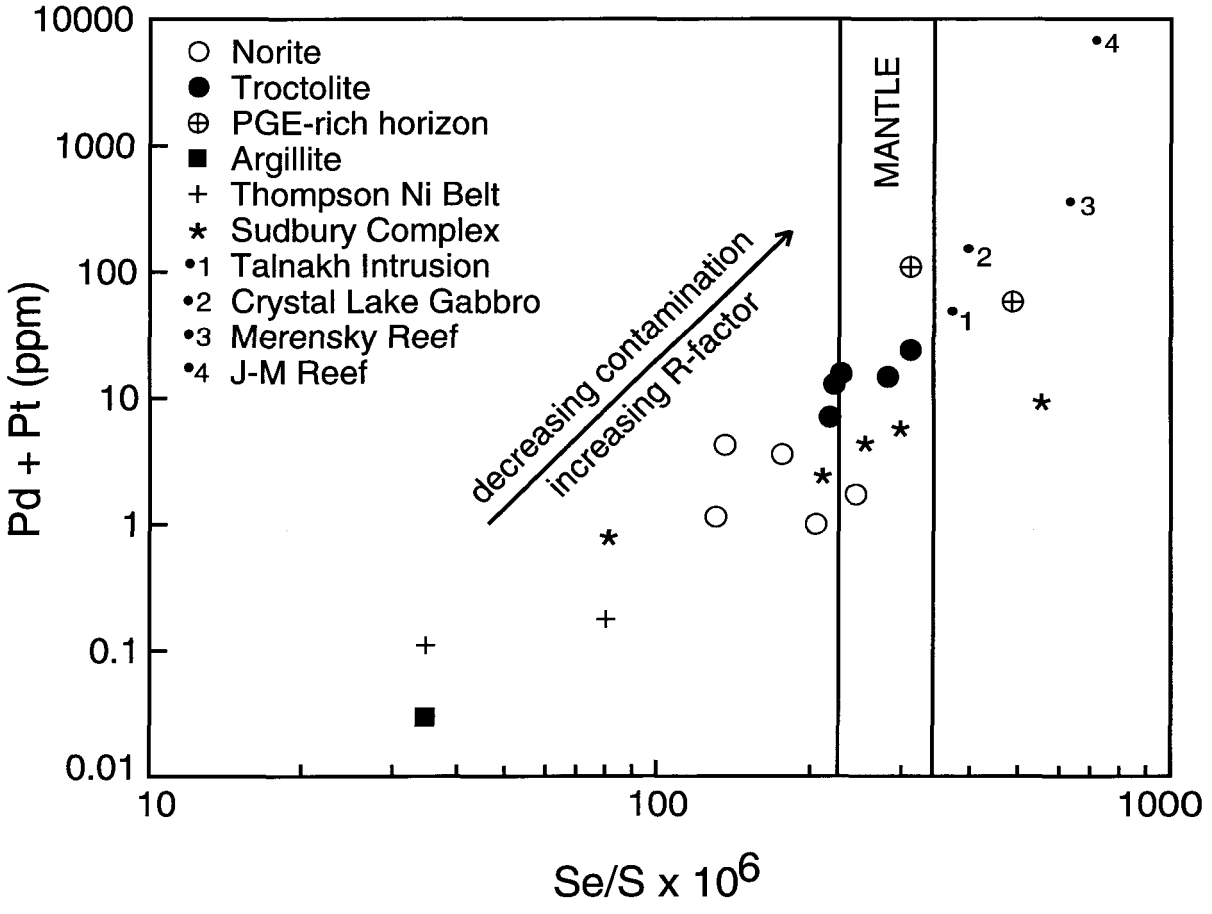

FIG. 7. Whole-rock Se/S ratio vs. Pd + Pt in sulfide fraction for the three types of disseminated sulfide mineralization of the Dunka Road deposit, argillite of the Virginia Formation, and various other magmatic sulfide deposits. Data of other deposits are taken from Naldrett (1981) and O.R. Eckstrand (unpublished data). Range in Se/S ratio of the mantle is taken from Eckstrand and Hulbert (1987).

sample (i.e., $35x10^{-6}$) relative to the other mineralized rocks. Similar Se/S ratios (i.e., $2x10^{-6}$–$118x10^{-6}$; mean= $43x10^{-6}$) were obtained for argillite samples from the equivalent Rove Formation in the vicinity of the Crystal Lake Gabbro (Eckstrand and Cogulu 1986).

Most mineralized troctolite samples fall within the range of mantle rocks, whereas one of the two samples from the PGE-rich horizons has a very elevated Se/S ratio of $485x10^{-6}$ that exceeds the estimated upper limit of the mantle. The enrichment in Se observed in sample DC-62 is most likely attributable to a high silicate magma to sulfide melt ratio (*R* factor) prior to sulfide crystallization, considering the elevated partition coefficient of Se into sulfide melt (i.e., 1770) as deduced from natural basaltic material (Peach et al. 1990). The very high Se/S ratios determined for various PGE-dominated deposits (Fig. 7; O.R. Eckstrand, unpublished data, 1988) are also associated with very large *R* factors typical of reef-type deposits. Hence the positive correlation observed between Se/S ratios and Pd+Pt content for the entire Dunka Road deposit is interpreted to result from the action of two main processes, namely country-rock assimilation and the silicate magma to sulfide melt ratio. Both appear to be closely interrelated, as will be shown in the following section.

Modelling the composition of the sulfides

The composition of the sulfides was modelled using the equilibrium fractionation equation developed by Campbell and Naldrett (1979):

[1] $C_C/C_L = D(R+1)/(R+D)$

where C_C is the concentration of the metal in the sulfide, C_L is the concentration of the metal in the silicate magma, D is the partition coefficient of the metal between the sulfide melt and the silicate magma, and R is the ratio of silicate magma to sulfide melt (R factor).

The Cu/Pd versus Pd diagram of Barnes et al. (1993) is used to better illustrate the results of the modelling (Fig. 8). The diagram is subdivided into three separate fields: *(i)* "depleted", for rocks that have Cu/Pd ratios greater than mantle and are thus depleted in Pd relative to Cu; *(ii)* "undepleted", which represents the range of mantle rocks; and *(iii)* "enriched", for PGE-rich rocks having a low Cu/Pd ratio indicative of Pd enrichment relative to Cu.

As shown in the diagram, the proposed parental magma composition has a high Cu/Pd ratio, i.e., 12 800, which plots outside the expected range for mantle rocks. This indicates that the basaltic magma has likely segregated sulfides at depth, becoming depleted in Pd relative to Cu in light of the much higher partition coefficient of the former into the sulfide melt (Peach et al., 1990). The metal content of the hypothetical initial magma prior to sulfide segregation may be estimated from the following equilibrium fractionation equation:

[2] $C_F/C_L = 1/[1 + X(D\text{-}1)/100]$

where C_F/C_L (depletion factor) is the concentration of the metal in the fractionated magma (i.e., basalt) divided by the concentration of the metal in the initial magma, D is the partition coefficient of the metal between the sulfide melt and the silicate magma, and X is the amount of segregated sulfides in weight percent. Assuming partition coefficients for Cu and Pd of 2,000 and 100,000, respectively (Barnes et al. 1993; Barnes and Francis 1995), calculations

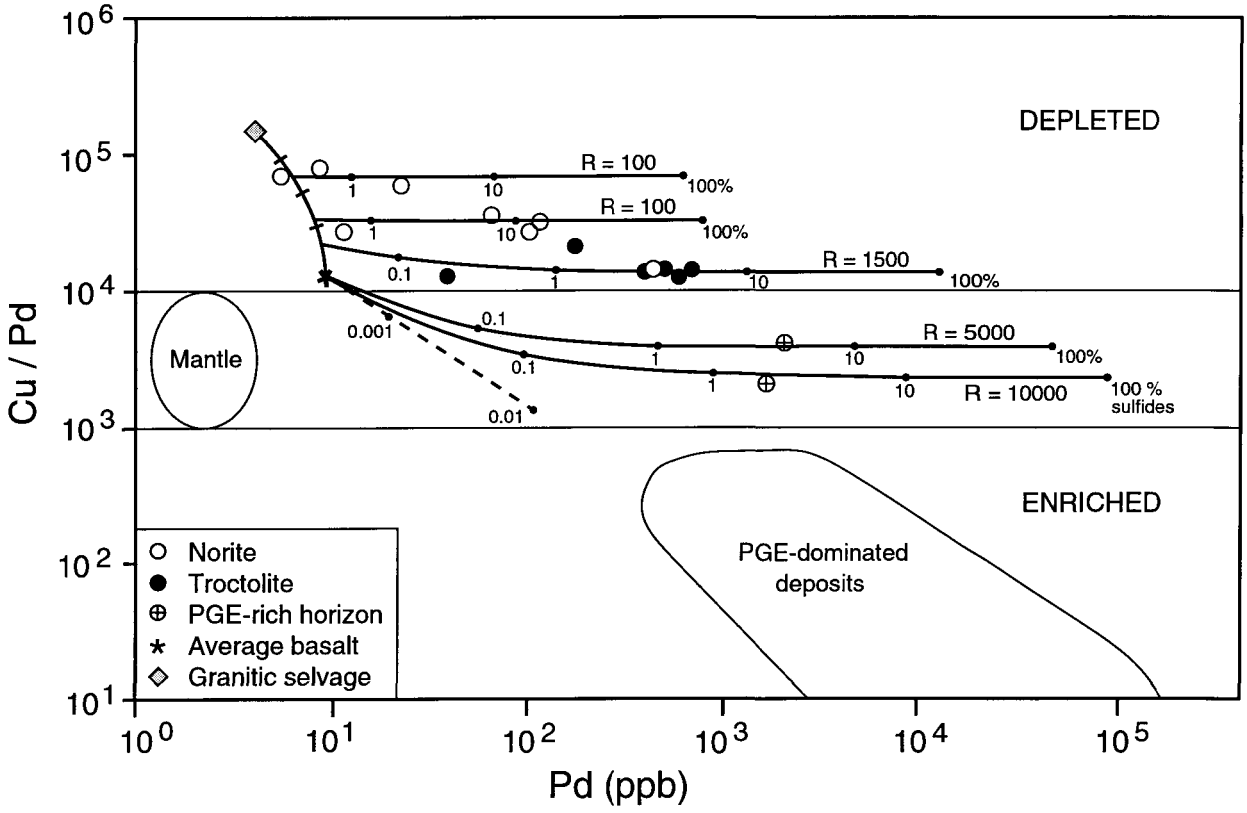

FIG. 8. Plot of Cu/Pd vs. Pd, showing the composition of the three types of disseminated sulfide mineralization and the results of the modelling. Fields of mantle rocks and PGE-dominated deposits (e.g., PGE reefs from the Bushveld, Stillwater, and Penikat intrusions) are taken from Barnes et al. (1993).

show that 0.0005–0.01 wt.% sulfide may have been removed from the magma at depth (see broken curve in Fig. 8), perhaps within an auxiliary magma chamber. A similar conclusion was reached by Saini-Eidukat (1991), who calculated that up to 0.1 wt.% sulfide may have segregated from the magma during its ascent.

The contaminant, represented by the granitic selvage (i.e., DC-80), has a very high Cu/Pd ratio, which reflects the very low Pd content of the argillite. Magma compositions from which the different types of disseminated sulfides segregated are interpreted to lie along a mixing line between the contaminant and the composition of the assumed parental magma (Fig. 8). Hence, in the modelling, each selected daughter magma represents the outset of a tie line linking its composition to that of sulfides in equilibrium with this magma. An infinite number of tie lines may be generated from the same daughter magma composition by simply changing the *R* factor value. As shown on the diagram, increases in *R* factor yield compositions having lower Cu/Pd ratio and higher Pd contents due to the higher partition coefficient of Pd into sulfides relative to Cu. Hence the grade of the mineralization is influenced by both the metal content of the daughter magma and the volume of silicate magma with which the sulfide melt interacted (respectively C_L and *R* in [1]). Finally, the dots along each tie line indicate the Cu/Pd ratio and Pd content of rocks that would contain 0.1, 1, 10, and 100% sulfides.

An important constraint on the modelling is that the computed amount of sulfide, given by the position of each sample along a particular tie line, must agree with the actual observations. Hence the weight fraction sulfide was calculated for each sample (Table 2) based on the composition of the main sulfide minerals given in Table 3.

Results indicate that most of the mineralized norite samples may be modelled using a very low *R* factor of 100 and a daughter magma that has undergone 25–65% contamination by the granitic material (Fig. 8). For simplicity, only two tie lines are shown on the diagram. However, all norite samples (except DC-49) were modelled individually, yielding *R* factors between 50 and 400 (mean= 153) and degrees of contamination varying between 5 and 65% (mean= 33%) (Table 2). The composition of all mineralized troctolite samples was modelled using moderate *R* factors of 700 to 2,000 (mean= 1317) and low degrees of contamination ranging from 5 to 20% (mean= 13%) (Table 2). The tie line generated at *R*= 1500 and 15% contamination (Fig. 8) models the composition of troctolite samples DC-58 and DC-61. Finally, elevated *R* factors of 5000 and 11 000 from an uncontaminated parental magma were used to model the composition of the two samples from the PGE-rich sulfide horizons (Table 2).

An important point to outline regarding these results is that the variations observed in the computed *R* factor and degree of contamination are in accordance with the geochemical and mineralogical attributes characterizing each type of disseminated mineralization. Therefore, the approach adopted to model the composition of the sulfide-bearing rocks, combined with the use of the Cu/Pd ratio diagram, is very useful in interpreting the origin of the mineralization in the Dunka Road deposit.

Conclusions

Based on the results of the modelling and on the evidence given by the geochemistry and mineralogy of the rocks, the following interpretations are favoured to explain the origin of the different types of disseminated sulfide mineralization observed in the Dunka Road deposit.

(1) The norite-hosted sulfide mineralization formed from a magma that was contaminated by the assimilation of a granitic partial melt and a sulfur-bearing hydrous fluid, both derived from sulfidic argillites of the underlying Virginia Formation. This is expressed by the relatively elevated orthopyroxene, ilmenite, biotite, pyrrhotite, and arsenide content of the norites, as well as their low Se/S ratios. The sulfide melt interacted with a very low volume of silicate magma, as indicated by the low *R* factors given by the modelling. This suggests that the sulfides segregated very close to the source of sulfur, which is confirmed by the proximity of the norites to country-rock xenoliths and to the basal contact. The PGE-depleted nature of the norite-hosted sulfides results from a combination of low *R* factors and a relative absence of PGE in the contaminant. It is also possible that certain mineralized norite samples, particularly those associated with high degrees of contamination and that are the most depleted in Pd (i.e., high Cu/Pd ratio), originate from a daughter magma that had previously segregated sulfides elsewhere in the deposit (e.g., within overlying PGE-rich horizons), thereby depleting the magma in PGE and increasing its Cu/Pd ratio.

(2) The troctolite-hosted disseminated sulfide mineralization, which makes up the bulk of the deposit and occurs throughout most of the lower 250 m of the intrusion, formed at moderate *R* factors and small degrees of contamination. This is particularly reflected by the

moderate PGE enrichment of the sulfides (i.e., Cu/Pd ratios near mantle values), pyrrhotite to precious metal sulfide ratios, Se/S ratios, and biotite and ilmenite contents. Relative to the norites, the troctolite-hosted sulfides segregated further from the source of the contaminant such that the sulfide melt was able to interact with a larger volume of magma, hence collecting a larger quantity of PGE and other precious metals.

(3) Finally, the PGE-rich sulfide horizons formed at high *R* factors from an uncontaminated magma. The low abundance of incompatible trace elements, low pyrrhotite to precious metal sulfide ratios, and high Se/S ratios preclude the incorporation of a granitic partial melt. The occurrence of the mineralization along stratiform horizons found directly under ultramafic layers is best explained by the downward percolation of a sulfide melt upon mixing between evolved and primitive magmas following a magma replenishment event. Sulfide droplets achieved a high *R* factor through their swirling within the convecting magma, becoming preferentially enriched in the highly chalcophile PGE. Variations of this model have been proposed to explain the formation of PGE reefs within the Bushveld and Stillwater complexes (e.g., Irvine 1975; Campbell et al. 1983; Irvine et al. 1983). As shown by their position on the Cu/Pd versus Pd diagram (Fig. 8), these PGE reefs must have formed at extremely high *R* factors, likely in the range of 10 000 to 1 000 000.

Several oxide-bearing ultramafic layers containing high concentrations of PGE (i.e., up to 9943 ppm Pd+Pt) have been identified within the Birch Lake deposit of the South Kawishiwi intrusion (Fig. 1) (Sabelin and Iwasaki 1986; Geerts 1994). PGE-rich horizons are thus not limited to the Dunka Road deposit, and may have been overlooked elsewhere in the Duluth

Complex in light of their typically low sulfide content and the scarcity of available PGE analyses.

Acknowledgements

We would like to thank Steven Hauck of the Minnesota Natural Resources Research Institute for his invaluable cooperation in all phases of this study; Penny Morton of the University of Minnesota, Duluth for her logistic support; John Green of the University of Minnesota, Duluth for his time and expertise in the field; John McGoran of Fleck Resources Limited for his permission to sample and publish this work; Richard Ruhanen of the Minnesota Department of Natural Resources for providing drill-core samples; Roger Eckstrand of the Geological Survey of Canada for providing some of the Se/S data; and Richard Lechasseur and Bernard Lapointe for their assistance with the analytical work. This project was funded by a Fonds pour la formation de chercheurs et l'aide à la recherche research grant to R.D. Thériault and by a Natural Sciences and Engineering Research Council of Canada operating grant to S.-J. Barnes.

References

Andersen, O. 1915. The system anorthite-forsterite-silica. American Journal of Science, **39**: 407-454.

Barnes, S.-J., and Francis, D. 1995. The distribution of platinum-group elements, nickel, copper, and gold in the Muskox layered intrusion, Northwest Territories, Canada. Economic Geology, **90**: 135-154.

Barnes, S.-J., Naldrett, A.J., and Gorton, M.P. 1985. The origin of the fractionation of platinum-group elements in terrestrial magmas. Chemical Geology, **53**: 303-323. Barnes, S.-J., Boyd, R., Korneliussen, A., Nilsson, L.P., Often, M., Pedersen, R.B., and Robins, B. 1988. The use of mantle normalization and metal ratios in discriminating between the effects of partial melting, crystal fractionation and sulphide segregation on platinum-group elements, gold, nickel and copper: examples from Norway. *In* Geo-platinum 87. *Edited by* H.M. Prichard, P.J. Potts, J.F.W. Bowles, and S. Cribb. Elsevier, pp. 113-143.

Barnes, S.-J., Couture, J.-F., Sawyer, E.W., and Bouchaib, C. 1993. Nickel-copper occurrences in the Belleterre-Angliers Belt of the Pontiac Subprovince and the use of Cu-Pd ratios in interpreting platinum-group element distributions. Economic Geology, **88**: 1402-1418.

Bédard, L.P., and Barnes, S.-J. 1990. Instrumental neutron activation analysis by collecting only one spectrum: Results for international geochemical reference samples. Geostandards Newsletters, **14**: 479-484.

Cabri, L.J., and Laflamme, J.H.G. 1976. The mineralogy of the platinum group elements from some copper-nickel deposits of the Sudbury area, Ontario. Economic Geology, **71**: 1159-1195.

Campbell, I.H., and Naldrett, A.J. 1979. The influence of silicate:sulfide ratios on the geochemistry of magmatic sulfides. Economic Geology, **74**: 1503-1505.

Campbell, I.H., Naldrett, A.J., and Barnes, S.J. 1983. A model for the origin of the platinum-rich sulfide horizons in the Bushveld and Stillwater Complexes. Journal of Petrology, **24**: 133-165.

Chandler, V.W., and Ferderer, R.J. 1989. Copper-nickel mineralization of the Duluth Complex, Minnesota: a gravity and magnetic perspective. Economic Geology, **84**: 1690-1696.

Eckstrand, O.R., and Cogulu, E. 1986. Se/S evidence relating to genesis of sulphides in the Crystal Lake Gabbro, Thunder Bay, Ontario. Program with Abstracts, Geological Association of Canada - Mineralogical Association of Canada Annual Meeting, p. 66.

Eckstrand, O.R., and Hulbert, L.J. 1987. Selenium and the source of sulphur in magmatic nickel and platinum deposits. Program with Abstracts, Geological Association of Canada-Mineralogical Association of Canada Annual Meeting, p.40.

Eckstrand, O.R., Grinenko, L.N., Krouse, H.R., Paktunc, A.D., Schwann, P.L., and Scoates, R.F.J. 1989. Preliminary data on sulphur isotopes and Se/S ratios, and the source of sulphur in magmatic sulphides from the Fox River Sill, Molson Dykes and Thompson nickel deposits, northern Manitoba. *In* Current research, part C, Geological Survey of Canada, Paper 89-1C, pp. 235-242.

Foose, M., and Weiblen, P. 1986. The physical and petrologic setting and textural and compositional characteristics of sulfides from the South Kawishiwi Intrusion, Duluth Complex, Minnesota, U.S.A. *In* Geology and metallogeny of copper deposits. *Edited by* G.H. Friedrich, A.D. Genkin, A.J. Naldrett, J.D. Ridge, R.H. Sillitoe, and F.M. Vokes. Springer-Verlag, Heidelberg, pp. 8-24.

Francis, R.D. 1990. Sulfide globules in mid-ocean ridge basalts (MORB), and the effect of oxygen abundance in Fe-S-O liquids on the ability of those liquids to partition metals from MORB and komatiite magmas. Chemical Geology, **85**: 199-213.

Geerts, S.D. 1994. Petrography and geochemistry of a platinum group element-bearing mineralized horizon in the Dunka Road prospect (Keweenawan), Duluth Complex, northeastern Minnesota. M.Sc. thesis, University of Minnesota, Duluth, Minn.

Gervilla, F., Makovicky, E., Makovicky, M., and Rose-Hansen, J. 1994. The system Pd-Ni-As at 790° and 450°C. Economic Geology, **89**: 1630-1639.

Grant, N.K., and Chalokwu, C.I. 1992. Petrology of the Partridge River intrusion, Duluth Complex, Minnesota: II. Geochemistry and strontium isotope systematics in drill core DDH-221. Journal of Petrology, **33**: 1007-1038.

Hauck, S., Severson, M., Zanko, L., Barnes, S.-J., Morton, P., Aiminas, H., Foord, E.E., and Dahlberg, E.H. 1995. A review of sulfide, platinum group element and oxide mineralization along the western contact of the Duluth Complex: as related to structural development. *In* Basement Tectonics 10. *Edited by* R.W. Ojakangas, A.B. Dickas, and J.C. Green. Kluwer Academic Publishers, pp. 47-54.

Hollister, V.F. 1980. Origin of graphite in the Duluth Complex. Economic Geology, **75**: 764-766.

Irvine, T.N. 1975. Crystallization sequences of the Muskox intrusion and other layered intrusions: II. Origin of chromitite layers and similar deposits of other magmatic ores. Geochimica et Cosmochimica Acta, **39**: 991-1020.

Irvine, T.N., Keith, D.W., and Todd, S.G. 1983. The J-M platinum palladium reef: II. Origin by double-diffusive convective magma mixing and implications for the Bushveld Complex. Economic Geology, **78**: 1287-1334.

Ishihara, S. 1977. The magnetite-series and ilmenite-series granitic rocks. Mining Geology, **27**: 293-305.

Lesher, C.M., and Campbell, I.H. 1993. Geochemical and fluid dynamic modeling of compositional variations in Archean komatiite-hosted nickel sulfide ores in Western Australia. Economic Geology, **88**: 804-816.

Lucente, M.E., and Morey, G.B. 1983. Stratigraphy and sedimentology of the Lower Proterozoic Virginia Formation, Northern Minnesota. Minnesota Geological Survey, Report of Investigation 28.

Mainwaring, P.R., and Naldrett, A.J. 1977. Country-rock assimilation and the genesis of Cu-Ni sulfides in the Water Hen Intrusion, Duluth Complex, Minnesota. Economic Geology, **72**: 1269-1284.

Mogessie, A., and Stumpfl, E.F. 1992. Platinum-group element and stable isotope geochemistry of PGM-bearing troctolitic rocks of the Duluth Complex, Minnesota. Australian Journal of Earth Sciences, **39**: 315-325.

Mogessie, A., Stumpfl, E.F., and Weiblen, P.W. 1991. The role of fluids in the formation of platinum-group minerals, Duluth Complex, Minnesota: mineralogic, textural, and chemical evidence. Economic Geology, **86**: 1506-1518.

Morey, G.B. 1992. Chemical composition of the Eastern Biwabik Iron-Formation (Early Proterozoic), Mesabi Range, Minnesota. Economic Geology, **87**: 1649-1658.

Naldrett, A.J. 1981. Platinum-group element deposits. *In* Platinum-group elements: mineralogy, geology, recovery. *Edited* by L.J. Cabri. CIM Special Volume 23, pp. 197-231.

Naldrett, A.J. 1989. Ores associated with flood basalts. *In* Ore deposition associated with magmas. *Edited by* J.A. Whitney and A.J. Naldrett. Society of Economic Geologists, Reviews in Economic Geology, vol. 4, pp. 103-118.

Paces, J.B., and Miller, J.D., Jr. 1993. Precise U-Pb ages of Duluth Complex and related mafic intrusions, northeastern Minnesota: New insights for physical, petrogenetic, paleomagnetic and tectono-magmatic processes associated with 1.1 Ga Midcontinent rifting. Journal of Geophysical Research, **98**B: 13997-14013.

Paktunc, A.D. 1989. Petrology of the St. Stephen intrusion and the genesis of related nickel-copper sulfide deposits. Economic Geology, **84**: 817-840.

Peach, C.L., Mathez, E.A., and Keays, R.R. 1990. Sulfide melt-silicate melt distribution coefficients for noble metals and other chalcophile elements as deduced from MORB: implications for partial melting. Geochimica et Cosmochimica Acta, **54**, 3379-3389.

Rao, B.V., and Ripley, E.M. 1983. Petrochemical studies of the Dunka Road Cu-Ni deposit, Duluth Complex, Minnesota. Economic Geology, **78**: 1222-1238.

Ripley, E.M. 1981. Sulfur isotopic studies of the Dunka Road Cu-Ni deposit, Duluth Complex, Minnesota. Economic Geology, **76**: 610-620.

Ripley, E.M. 1986. Application of stable isotopic studies to problems of magmatic sulfide ore genesis with special reference to the Duluth Complex, Minnesota. *In* Geology and metallogeny of copper deposits. *Edited by* G.H. Friedrich, A.D. Genkin, A.J. Naldrett, J.D. Ridge, R.H. Sillitoe, and F.M. Vokes. Springer-Verlag, Heidelberg, pp. 8-24.

Ripley, E.M. 1990a. Se/S ratios of the Virginia Formation and Cu-Ni sulfide mineralization in the Babbitt area, Duluth Complex, Minnesota. Economic Geology, **85**: 1935-1940.

Ripley, E.M. 1990b. Platinum-group element geochemistry of Cu-Ni mineralization in the basal zone of the Babbitt deposit, Duluth Complex, Minnesota. Economic Geology, **85**: 830-841.

Ripley, E.M., and Alawi, J.A. 1988. Petrogenesis of pelitic xenoliths at the Babbitt Cu-Ni deposit, Duluth Complex, Minnesota, U.S.A. Lithos, **21**: 143-159.

Ripley, E.M., and Al-Jassar, T.J. 1987. Sulfur and oxygen isotope studies of melt-country rock interaction, Babbitt Cu-Ni deposit, Duluth Complex, Minnesota. Economic Geology, **82**: 87-107.

Ripley, E.M., and Chryssoulis, S.L. 1994. Ion microprobe analyses of platinum group elements in sulfide and arsenide minerals from the Babbitt Cu-Ni deposit, Duluth Complex, Minnesota. Economic Geology, **80**: 201-210.

Ripley, E.M., Butler, B.K., Taib, N.I., and Lee, I. 1993. Hydrothermal alteration in the Babbitt Cu-Ni deposit, Duluth Complex: mineralogy and hydrogen isotope systematics. Economic Geology, **88**: 679-696.

Robert, R.V.B., Van Wyk, E., and Palemer, R. 1971. Concentration of the noble metals by fire assay technique using nickel sulphide as the collector. National Institute Metallurgy Report, **1371**: 1-14.

Sabelin, T., and Iwasaki, I. 1986. Evaluation of platinum group metal occurrence in Duval 15 drill core from the Duluth Complex. Internal Report, Minerals Resources Research Center, Minneapolis, Minnesota.

Saini-Eidukat, B. 1991. Platinum group elements in anorthositic rocks of the Duluth Complex, Minnesota: petrogenetic and economic implications. Ph.D. thesis, University of Minnesota, Minneapolis, Minn.

Severson, M.J. 1994. Igneous stratigraphy of the South Kawishiwi intrusion, Duluth Complex, Minnesota. Natural Resources Research Institute, Duluth, Minnesota, Technical Report 93-34.

Severson, M.J., and Hauck, S.A. 1990. Geology, geochemistry, and stratigraphy of a portion of the Partridge River intrusion. Natural Resources Research Institute, Duluth, Minnesota, Technical Report 89-11.

Taylor, R.B. 1964. Geology of the Duluth Complex near Duluth, Minnesota. Minnesota Geological Survey Bulletin 44.

Thériault, R.D., Barnes, S.-J., and Severson, M.J. 1995. The role of assimilation in the genesis of the Dunka Road Cu-Ni-PGE deposit, Duluth Complex, Minnesota. Proceedings and Abstracts, IGCP Project 336, Petrology and metallogeny of intraplate mafic and ultramafic magmatism, Duluth, Minnesota, pp. 191-192.

Tyson, R.M., and Chang, L.L.Y. 1984. The petrology and sulfide mineralization of the Partridge River Troctolite, Duluth Complex, Minnesota. The Canadian Mineralogist, **22**: 23-38.

Van Schmus, W.R., and Hinze, W.J. 1985. The Midcontinent Rift. Annual Review of Earth and Planetary Sciences, **13**: 345-383.

Watkinson, D.H., and Ohnenstetter, D. 1992. Hydrothermal origin of platinum-group mineralization in the Two Duck Lake intrusion, Coldwell Complex, northwestern Ontario. Canadian Mineralogist, **30**: 121-136.

Weiblen, P.W., and Morey, G.B. 1980. A summary of the stratigraphy, petrology, and structure of the Duluth Complex. American Journal of Science, **280A**: 88-133.

Wood, D.A. 1979. A variably veined suboceanic upper mantle - Genetic significance for mid-ocean ridge basalts from geochemical evidence. Geology, **7**: 499-503.

Wright Engineers Limited. 1991. Dunka Road Project: Preliminary Project Review for NERCO Minerals Co., Project 2046.

The Canadian Mineralogist
Vol. 36, pp. 869-886 (1998)

Compositional variations in Cu-Ni-PGE sulfides of the Dunka Road deposit, Duluth Complex, Minnesota: The importance of combined assimilation and magmatic processes.

Robert D. Thériault and Sarah-Jane Barnes

Département des Sciences Appliquées, Université du Québec à Chicoutimi,

Chicoutimi, Québec, G7H 2B1

Abstract

The Dunka Road deposit is one of ten occurrences of Cu-Ni sulfides bearing platinum-group elements (PGE) on the northwestern margin of the Duluth Complex, in Minnesota. Mineralization has been linked to contamination of the host troctolitic magma through assimilation of argillaceous rocks from the Virginia Formation. On the basis of texture and composition, the sulfide mineralization is divided into five types: 1) norite-hosted disseminated sulfides; 2) troctolite-hosted disseminated sulfides; 3) PGE-rich disseminated sulfide horizons; 4) pyrrhotite-rich massive sulfides; and 5) chalcopyrite-rich disseminated sulfides. The norite-hosted sulfides exhibit features suggestive of the magma's substantial contamination, such as high proportions of pyrrhotite and arsenide minerals, and high mean values of S/Se (9,700) and $\delta^{34}S$ (11.2‰). They are also generally metal poor, implying that the sulfides interacted with a relatively low volume of silicate melt (*i.e.* low *R* factor). The

troctolite-hosted sulfides formed at moderate degrees of contamination, as indicated by their intermediate mean values of S/Se (4,600) and $\delta^{34}S$ (7.8‰). The PGE-rich sulfide horizons show little sign of contamination, and have mantle-like mean values of S/Se (2,600) and $\delta^{34}S$ (2.1‰). Their very high PGE contents suggest that they formed at elevated *R* factors. The pyrrhotite-rich massive sulfides and associated chalcopyrite-rich disseminated sulfides have relatively high mean values of S/Se (8,000) and $\delta^{34}S$ (10.2‰), indicative of significant contamination. The former are interpreted to represent a cumulate of monosulfide solid-solution (*mss*), whereas the chalcopyrite-rich sulfides represent the fractionated sulfide liquid. A general increase in the degree of contamination is observed toward the base of the intrusion, associated with a decrease in *R* factor and metal concentration of the sulfides. This likely results from the introduction of partial melt from the metasedimentary country-rocks, which was cooler than the mafic magma and led to the early crystallization of the sulfide liquid.

Keywords: sulfide deposits, assimilation, sulfur isotopes, S/Se ratios, *R* factor, *mss* fractionation, troctolite, platinum-group elements, nickel, copper, arsenides, Dunka Road deposit, Duluth Complex, Minnesota.

Sommaire

Le gisement de Dunka Road fait partie d'un groupe de dix gisements de sulfures de Cu - Ni enrichis en éléments du groupe du platine (EGP) regroupés le long de la bordure nord-ouest du complexe de Duluth, au Minnesota. La minéralisation serait liée à une contamination du magma-hôte troctolitique due à une assimilation de roches argileuses de la formation de Virginia. D'après leur texture et leur composition, les sulfures sont divisés en cinq types: 1) sulfures disséminés dans la norite comme hôte; 2) sulfures disséminés dans la troctolite comme hôte; 3) horizons de sulfures disséminés enrichis en EGP; 4) sulfures massifs enrichis en pyrrhotite; et 5) sulfures disséminés enrichis en chalcopyrite. Les caractéristiques des sulfures dans la norite, par exemple les proportions élevées de pyrrhotite et de minéraux arsénifères, et des valeurs moyennes élevées de S/Se (9 700) et $\delta^{34}S$ (11.2‰), font penser que le magma a subi une importante contamination. De plus, ces sulfures sont généralement appauvris en métaux, ce qui implique qu'ils ont réagi avec un faible volume de magma silicaté (*i.e.* faible facteur *R*). Les sulfures dans la troctolite se sont formés à des niveaux moyens de contamination, tel qu'indiqué par leurs valeurs moyennes intermédiaires de S/Se (4 600) et $\delta^{34}S$ (7.8‰). Les horizons de sulfures enrichis en EGP montrent très peu de signes de contamination, et ont des valeurs moyennes de S/Se (2 600) et $\delta^{34}S$ (2.1‰) qui rappellent celles du manteau. Leur très forte teneur en EGP témoigne de facteurs *R* élevés. Les sulfures massifs enrichis en pyrrhotite, et les sulfures disséminés enrichis en chalcopyrite avec lesquels ils sont associés, ont des valeurs moyennes relativement élevées de S/Se (8 000) et $\delta^{34}S$ (10.2‰), indications d'une importante contamination. Les sulfures massifs résulteraient d'une accumulation d'une solution solide de monosulfure (*mss*), alors que les sulfures enrichis en chalcopyrite représentent un liquide sulfuré fractionné. Une augmentation générale du degré

de contamination est observée vers la base de l'intrusion, associée à une diminution du facteur *R* et de la concentration en métaux des sulfures. Ceci résulte possiblement de l'introduction d'un produit de fusion partielle dérivé des roches métasédimentaires encaissantes, moins chaud que le magma mafique, qui aurait ainsi mené à la cristallisation hâtive du liquide sulfuré.

Mots-clés: gisements de sulfures, assimilation, isotopes de soufre, rapports S/Se, facteur *R*, fractionnement de *mss*, troctolite, complexe de Duluth, éléments du groupe du platine, nickel, cuivre, arséniures, gisement de Dunka Road, complexe de Duluth, Minnesota.

Introduction

Most studies of the Duluth Complex have focussed on the Cu-Ni-PGE sulfide deposits that occur along the base of troctolitic intrusions (Thériault *et al.* 1997, and references therein). Country-rock assimilation is widely recognized as having played a significant role in the genesis of the mineralization. Evidence of assimilation is based on stable isotopes (Mainwaring & Naldrett 1977, Ripley 1981, 1986, Rao & Ripley 1983, Ripley & Al-Jassar 1987, Ripley *et al.* 1993, Lee & Ripley 1995), Se/S ratios (Ripley 1990a, Thériault *et al.* 1997), major- and trace-element geochemistry (Tyson & Chang 1984, Ripley & Alawi 1988, Severson & Hauck 1990) and silicate mineralogy (Foose & Weiblen 1986, Geerts 1991).

Although the categories of sulfide occurrences in the Duluth Complex have previously been defined (*e.g.* Foose & Weiblen 1986, Martineau 1989), no systematic description and classification of the different types of mineralization forming a deposit have ever been attempted. This situation may explain the general lack of agreement concerning the mechanisms of concentration involved in ore formation. In particular, models involving both magmatic and hydrothermal processes have been proposed to explain the localization of platinum-group elements (PGE) in the Duluth Complex.

In this paper, we describe the mode of occurrence of five types of sulfide mineralization observed near the base of the Duluth Complex in the Dunka Road area. We show that compositional variation among the types of mineralization result from the sequential action of three processes, namely country-rock assimilation, interaction between the sulfide liquid and the silicate melt (R factor), and fractional crystallization of the sulfide liquid.

Geological setting

The Duluth Complex consists of an arcuate mass of mafic intrusions of Middle Proterozoic age (1100 Ma) associated with the Keweenawan flood basalt province of the Midcontinent Rift of North America (Van Schmus & Hinze 1985). The complex extends for more than 225 km along the northwestern margin of Lake Superior, from Duluth, Minnesota, to the Canadian border (Fig. 1). It was emplaced as a succession of distinct mafic intrusions along an unconformity between volcanic rocks of the North Shore Volcanic Group and older Proterozoic (1800-2300 Ma; Hemming *et al.* 1995) basement rocks of the Animikie Group. In general, rocks forming the Duluth Complex consist of an upper anorthositic series underlain by a more mafic troctolitic series (Taylor 1964, Weiblen & Morey 1980). Recent U-Pb ages (1098.6±0.5 to 1099.3±0.3 Ma) obtained by Paces & Miller (1993) suggest that both intrusive series are essentially coeval.

Significant Cu-Ni-PGE sulfide mineralization has been observed in the basal portions of two of the troctolitic intrusions, namely the Partridge River and South Kawishiwi intrusions (Severson & Hauck 1990, Severson, 1994). These are the host to more than 6 billion tonnes of mineralization grading 0.66% Cu and 0.2% Ni (Listerud & Meineke 1977, Ripley 1990b). The sulfide-bearing troctolitic intrusions occur along the northwestern margin of the complex, where they intrude Proterozoic metasedimentary rocks of the Virginia and Biwabik formations (Fig. 1). The latter is a cherty and slaty banded-iron formation (Morey 1992), whereas the overlying Virginia Formation consists mainly of argillite, siltstone, and greywacke. The argillaceous horizons commonly contain finely disseminated pyrite,

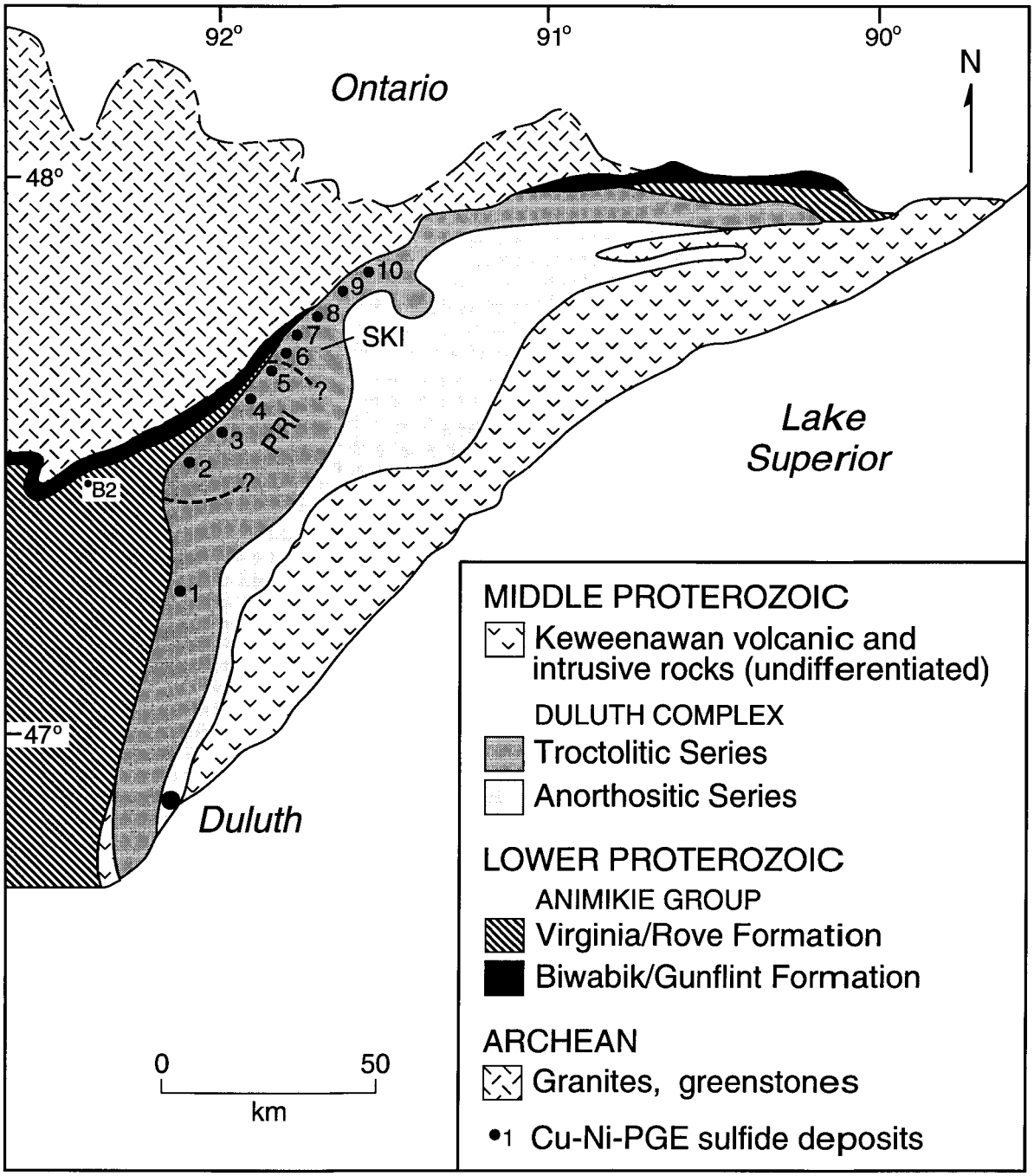

FIG. 1. Geological map showing the emplacement of the Duluth Complex and associated sulfide mineralization within the Keweenawan flood basalt province of central North America (modified after Naldrett 1989). PRI: Partridge River intrusion, SKI: South Kawishiwi intrusion. Black circles represent Cu-Ni-PGE sulfide deposits (1: Water Hen; 2: Wyman Creek; 3: Wetlegs; 4: Dunka Road; 5: Babbitt; 6: Serpentine; 7: Dunka Pit; 8: Birch Lake; 9: Maturi; 10: Spruce Road); B2: drill hole from the Mesabi deep-drilling project.

especially in proximity to the Biwabik Formation (Lucente & Morey 1983).

Analytical methods

Rock samples for this work were taken from drill core provided by the Minnesota Department of Natural Resources, Hibbing, Minnesota. Mineralized samples of the Dunka Road deposit were collected from drill holes #26107, 26117 and 26143 (Fig. 2, Table 1), whereas argillite samples of the Virginia Formation were taken from hole #B2 (Fig. 1, Table 1), which is located approximately 40 km to the southwest of the Dunka Road deposit and well beyond the metamorphic aureole of the complex.

A total of 28 whole-rock samples were analyzed for S, Ni and Cu by X-ray fluorescence spectrometry at Analabs-Caleb Brett in England. Concentrations of the trace elements Co, As, Sb, Se and Au were determined by instrumental neutron-activation analysis (INAA) at the Université du Québec à Chicoutimi using the method of Bédard & Barnes (1990). Samples with a low level of Se were further analyzed for this element by atomic absorption at Chemex Laboratories in Vancouver. Concentrations of the PGE and Re were determined by INAA in Chicoutimi, after preconcentrating the metals into a Ni-sulfide bead following the method of Robert *et al.* (1971).

The ratio of sulfur isotopes was determined on 24 whole-rock samples by mass spectrometry at the Ottawa-Carleton Geoscience Centre in Ottawa. An additional four measurements were obtained from mineral separates at Indiana University.

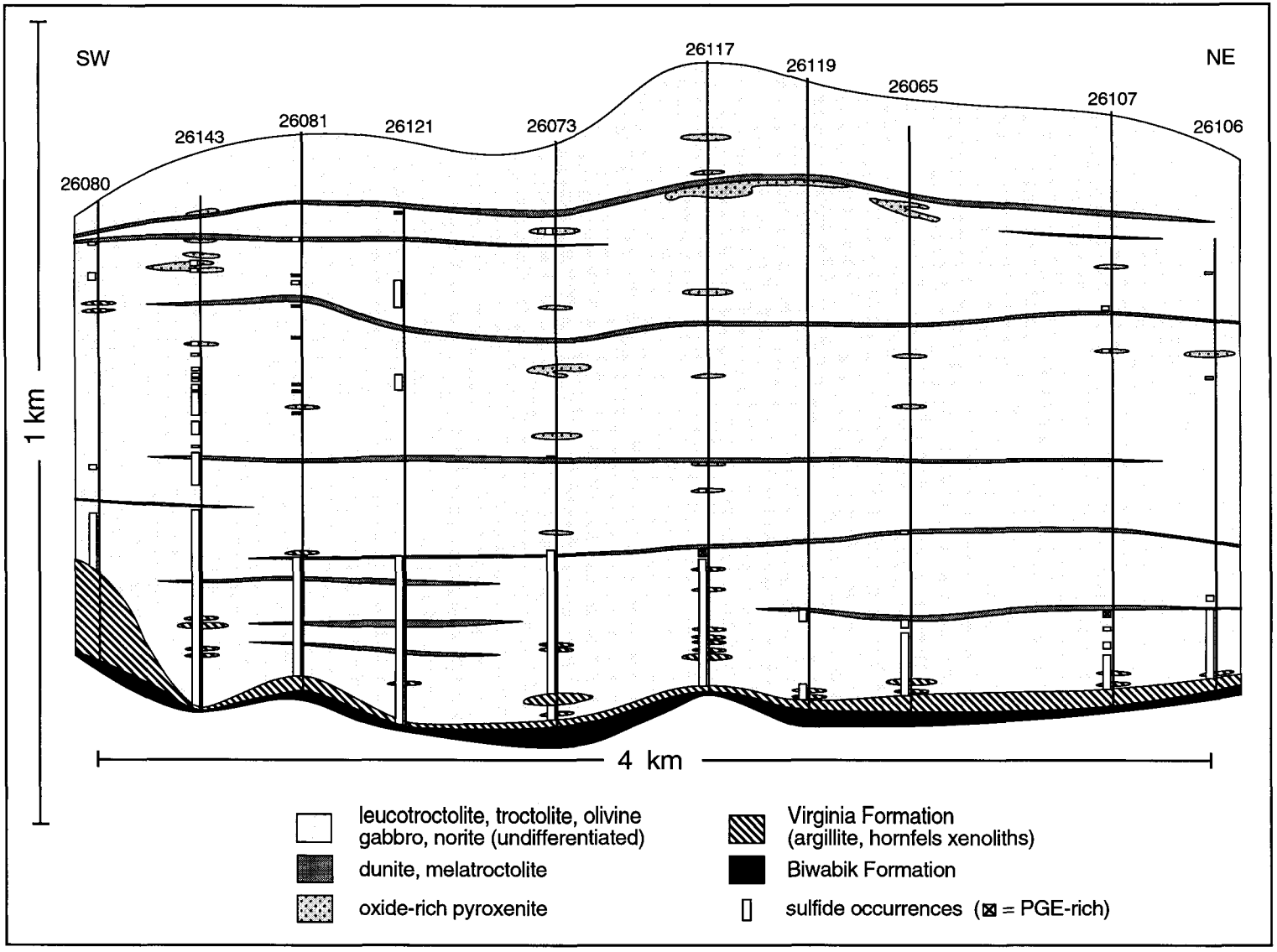

FIG. 2. Longitudinal cross-section of the Dunka Road Cu-Ni-PGE deposit, based on drill-hole interpretation (modified after Severson & Hauck 1990).

TABLE 1. WHOLE-ROCK METAL CONCENTRATIONS AND SULFUR ISOTOPE VALUES OF THE FIVE TYPES OF SULFIDE MINERALIZATION, THE BEDDED PYRRHOTITE UNIT AND UNMETAMORPHOSED ARGILLITE OF THE VIRGINIA FORMATION

Sample number	Rock type	Drill hole number	Depth (m)	S (%)	Os (ppb)	Ir (ppb)	Ru (ppb)	Rh (ppb)	Pt (ppb)	Pd (ppb)	Au (ppb)	Re (ppb)	Ni (ppm)	Cu (ppm)	Co (ppm)	As (ppm)	Sb (ppm)	Se (ppm)	$\delta^{34}S$ (‰)	S/Se
DC-27	NOR	26117	708,3	0,77	<0,6	0,28	<5,0	0,74	13	23	11	0,86	348	1300	114	12,9	0,89	0,6	14,5	13000
DC-49	NOR	26117	727,5	0,20	<0,5	0,10	<5,0	<0,21	2,5	5,4	<3,2	0,22	151	373	52	1,96	1,59	<0,2	8,2	>10000
DC-52	NOR	outcrop	-----	0,66	<0,9	0,25	<5,0	0,53	3,7	11	<3,2	0,93	186	293	40	6,28	1,35	0,6	13,7	11000
DC-54	NOR	outcrop	-----	0,31	<0,8	0,22	<5,0	0,46	6,9	8,1	2,3	1,24	265	622	62	2,77	0,80	0,6	12,5	5200
DC-60	NOR	26117	683,4	1,57	<1,3	1,20	<5,0	3,96	50	100	19	2,70	1140	3000	127	3,42	0,57	1,0	10,4	16000
DC-63	NOR	26143	252,3	2,45	<1,2	0,92	<5,0	2,65	16	63	18	4,92	824	2210	180	6,76	0,57	2,2	7,1	11000
DC-66	NOR	26107	721,7	4,32	2,2	4,28	20	18,8	35	460	45	26,8	2280	6400	310	15,5	0,71	5,9	9,8	7300
DC-72	NOR	26117	703,5	4,65	1,3	1,46	<5,0	4,72	5,4	120	45	2,82	1140	3700	290	37,6	0,58	9,6	13,6	4800
DC-53	TROC	26117	741,2	0,15	<0,8	0,57	<5,0	1,24	10	39	<2,1	0,46	230	514	55	2,23	1,03	0,2	6,7	7500
DC-55	TROC	26117	753,9	1,11	<0,9	1,01	6,9	4,17	42	170	32	3,57	1070	3650	89	1,58	1,51	2,4	9,0	4600
DC-56	TROC	26107	702,8	1,44	1,3	2,79	13	11,8	110	400	48	6,06	1910	5550	170	3,52	2,86	3,2	9,2	4500
DC-58	TROC	26107	682,5	2,00	1,4	3,08	10	15,9	160	710	140	8,79	2440	10200	113	0,71	2,65	4,6	6,6	4400
DC-61	TROC	26117	627,8	1,50	2,5	3,76	10	15,0	120	500	59	6,03	2050	7130	113	<0,38	0,56	4,3	7,5	3500
DC-79	TROC	26107	718,0	1,12	1,3	3,04	10	15,0	160	580	67	8,82	2250	7120	120	4,68	0,60	3,5	7,6	3200
DC-62	PGE	26107	627,5	1,69	3,5	10,5	34	65,6	560	2300	420	5,13	3740	12200	150	1,49	0,44	8,2	1,6	2100
DC-64	PGE	26117	609,2	0,59	4,1	8,62	31	47,6	300	1600	89	4,06	1680	3380	83	0,56	0,39	1,9	2,5	3100
DC-73	MS	26143	284,0	19,6	1,2	38,2	27	95,7	8,5	470	29	115	10700	12200	1100	40,5	0,37	25	8,4	7900
DC-75	MS	26117	716,5	31,2	3,8	2,28	<9,3	9,70	23	880	130	8,00	6840	11400	1240	387	0,84	13	16,0	24000
DC-76	MS	26143	328,9	34,9	4,6	27,1	40	96,0	35	1600	40	73	18700	5420	1050	102	2,58	43	12,0	8100
DC-65	CP	26143	288,2	2,17	<2,0	0,37	<5,0	2,37	370	600	270	0,79	1470	15700	109	14,8	1,38	8,2	11,0	2700
DC-67	CP	26143	329,0	3,42	<3,0	1,99	5,3	5,83	840	970	280	3,96	1570	14000	138	13,5	1,93	9,0	11,9	3800
DC-1	ARG	B2	135,9	0,02	<0,6	0,14	<5,0	0,17	3,1	1,8	5,4	0,07	67	39	39	7,16	1,83	<0,2	5,3	>1000
DC-3	ARG	B2	390,3	0,31	<0,9	0,07	<5,0	0,23	<3,2	2,4	<5,9	0,67	61	43	34	13,0	4,56	0,2	8,6	16000
DC-5	ARG	B2	464,8	0,53	<1,2	<0,07	<9,8	<0,37	6,5	4,9	2,8	0,68	89	73	26	25,8	5,09	<0,2	7,2	>27000
DC-7	ARG	B2	479,7	0,09	<0,6	0,04	<5,0	<0,31	<4,2	3,3	<1,6	0,34	48	46	32	8,96	2,47	<0,2	4,5	>4500
DC-8	ARG	B2	443,2	1,08	<0,7	0,10	<5,3	<0,20	3,5	2,6	<3,5	2,06	85	58	28	27,3	5,98	0,2	5,1	54000
DC-9	ARG	B2	245,3	0,03	<0,5	0,09	<5,0	0,13	3,9	<3,2	<1,6	0,20	78	59	35	3,83	1,83	<0,2	4,7	>1500
DC-70	BPU	outcrop	-----	4,45	<1,5	0,06	<5,0	0,12	<4,7	3,5	<2,8	0,10	144	170	33	9,40	5,38	1,4	15,8	29000
		R.S.D. (%)		10	20	5	20	5	10	10	20	-----	7	6	2	4	5	15	0,2[1]	

NOTES: MS: massive sulfides; CP: chalcopyrite-rich sulfides; NOR: norite-hosted sulfides; TROC: troctolite-hosted sulfides; PGE: PGE-rich sulfides; ARG: unmetamorphosed argillite of the Virginia Formation; BPU: bedded pyrrhotite unit of the Virginia Formation;$\delta^{34}S$: sulfur isotope values; R.S.D.: Precision expressed as relative standard deviation (CANMET standards); [1]: precision at 2σ error (IAEA-S1 and IAEA-S2 standards)

Geology of the Dunka Road deposit

The Dunka Road Cu-Ni-PGE deposit occurs within the basal part of the Partridge River intrusion, where the host mafic rocks are in contact with sulfide-bearing argillites of the underlying Virginia Formation (Fig. 1). As shown from a drill-hole-interpreted cross-section (Fig. 2), the igneous stratigraphy has been subdivided into correlatable cyclic units (Severson & Hauck 1990, Thériault *et al.* 1997). Each cyclic unit consists of a thin ultramafic layer of melatroctolite to dunite overlain by a much thicker sequence dominantly consisting of leucotroctolite and olivine gabbro, with minor troctolite and norite.

In contrast to rocks of the upper cyclic units, which are generally well layered and contain very sparse sulfide, rocks of the basal part of the intrusion (lower 250 m) are mineralized and very heterogeneous in terms of texture and composition. Variations in grain size and modal mineralogy are considerable throughout this zone, and leucotroctolite, olivine gabbro and norite commonly occur together on a local scale.

Hornfels xenoliths derived from the underlying Virginia Formation comprise up to 25% of the volume of the basal sequence (Fig. 3A). Norite typically occurs in proximity of country-rock xenoliths or directly at the base of the intrusion. The norite was interpreted as having crystallized from a hybrid magma, produced through mixing between the parental basic magma and a granitic partial melt derived from the surrounding argillite (Thériault *et al.* 1997). Evidence of partial melting is indicated by the occurrence of granitic selvages along the margin of country-rock xenoliths (Fig. 3A). Furthermore, on the basis of trace-element

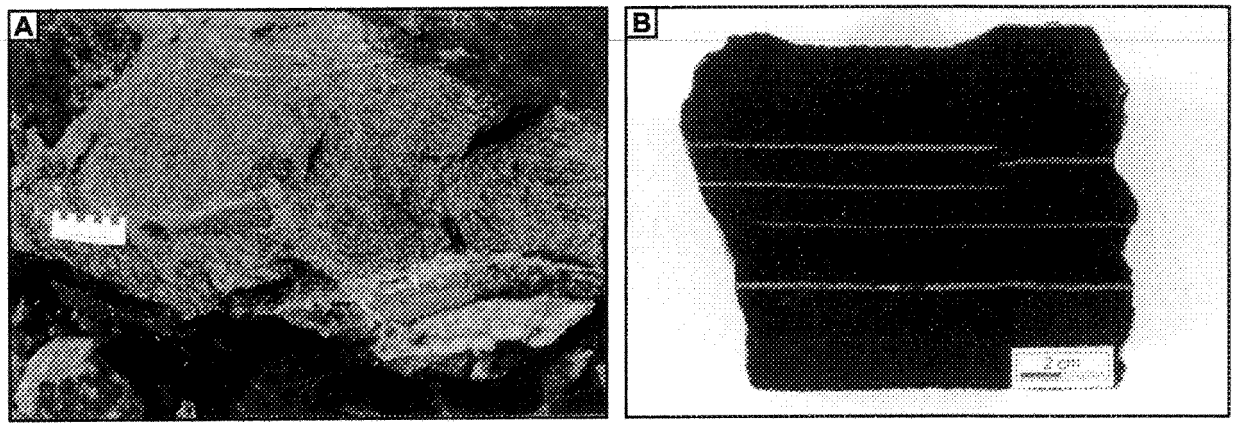

Fig. 3. A. Country-rock xenoliths hosted in heterogeneous norite and olivine gabbro near the base of the Dunka Pit deposit. Note the presence of granitic selvages along the margins of the xenoliths. B. Bedded pyrrhotite unit of the Virginia Formation showing thin laminations of pyrrhotite within hornfelsed argillite. Sample taken adjacent to the Dunka Pit deposit (DC-70, Tables 1, 2). Scale in centimeters for both photographs.

geochemistry (Tyson & Chang 1984) and sulfur isotopes (Ripley 1981, Ripley & Alawi 1988), heat from the intrusion is interpreted to have led to the early transfer of a sulfur-bearing hydrous fluid from the footwall rocks into the basic magma. Hence, the highly heterogeneous and mineralized character of the basal rocks hosting the Dunka Road deposit appears to be related to a process of magma contamination through mixing with derivatives from the underlying Virginia Formation. An important contribution of sulfur seems to have come from what has been termed the bedded pyrrhotite unit (Severson & Hauck 1990), a 10- to 15-m-thick argillite horizon located approximately 25 m above the base of the Virginia Formation and containing 10-20% banded pyrrhotite (Fig. 3B). As shown from the drill-hole-interpreted cross-section of the deposit (Fig. 2), it is more than likely that this unit has been completely assimilated by the intruding magma on the basis of the reduced thickness (10-20 m) of the Virginia Formation in the Dunka Road area.

Nature of the mineralization at the Dunka Road deposit

The Dunka Road Cu-Ni-PGE sulfide deposit has estimated resources of 1450 million tonnes grading 0.397 wt.% Cu, 0.094 wt.% Ni, 445 ppb Pd, 118 ppb Pt, and 61 ppb Au (Wright Engineers Ltd. 1991).

The bulk of the mineralization (>95 vol.%) consists of disseminated sulfides, which comprise no more than 5 vol.% of the rock. The disseminated sulfides are typically interstitial to the silicates, and generally consist of pyrrhotite, chalcopyrite, pentlandite, and cubanite, with minor quantities of mackinawite, sphalerite, and bornite. Small amounts of the arsenides

maucherite, niccolite, and cobaltite-gersdorffite, as well as the platinum-group mineral (PGM) froodite ($PdBi_2$), were observed locally with the sulfide minerals. Less than 5 vol.% of the mineralization consists of zones of massive sulfide dominated by pyrrhotite, with lesser pentlandite, chalcopyrite, cubanite, mackinawite, maucherite, and niccolite.

This study led to the identification of five types of sulfide mineralization within the Dunka Road deposit. These are: 1) norite-hosted disseminated sulfides, 2) troctolite-hosted disseminated sulfides, 3) PGE-rich disseminated sulfide horizons, 4) pyrrhotite-rich massive sulfides, and 5) chalcopyrite-rich disseminated sulfides surrounding lenses of massive sulfide.

Norite-hosted disseminated sulfides

The norite-hosted disseminated sulfides are typically found adjacent to country-rock xenoliths or within approximately 30 m of the basal contact of the intrusion. The mineralization consists mainly of pyrrhotite and ilmenite, with lesser chalcopyrite, cubanite, and pentlandite (Fig. 4A). Maucherite, niccolite and cobaltite-gersdorffite are also commonly observed, occurring as isolated grains enclosed within sulfides. This relationship suggests that the arsenides are primary magmatic phases crystallized from the sulfide liquid.

Troctolite-hosted disseminated sulfides

The troctolite-hosted disseminated sulfide mineralization occurs throughout the lower 250 m of the intrusion, and forms more than half of the deposit. The sulfides are mainly in leucotroctolite, distributed interstitially among the silicate minerals. They consist mainly of

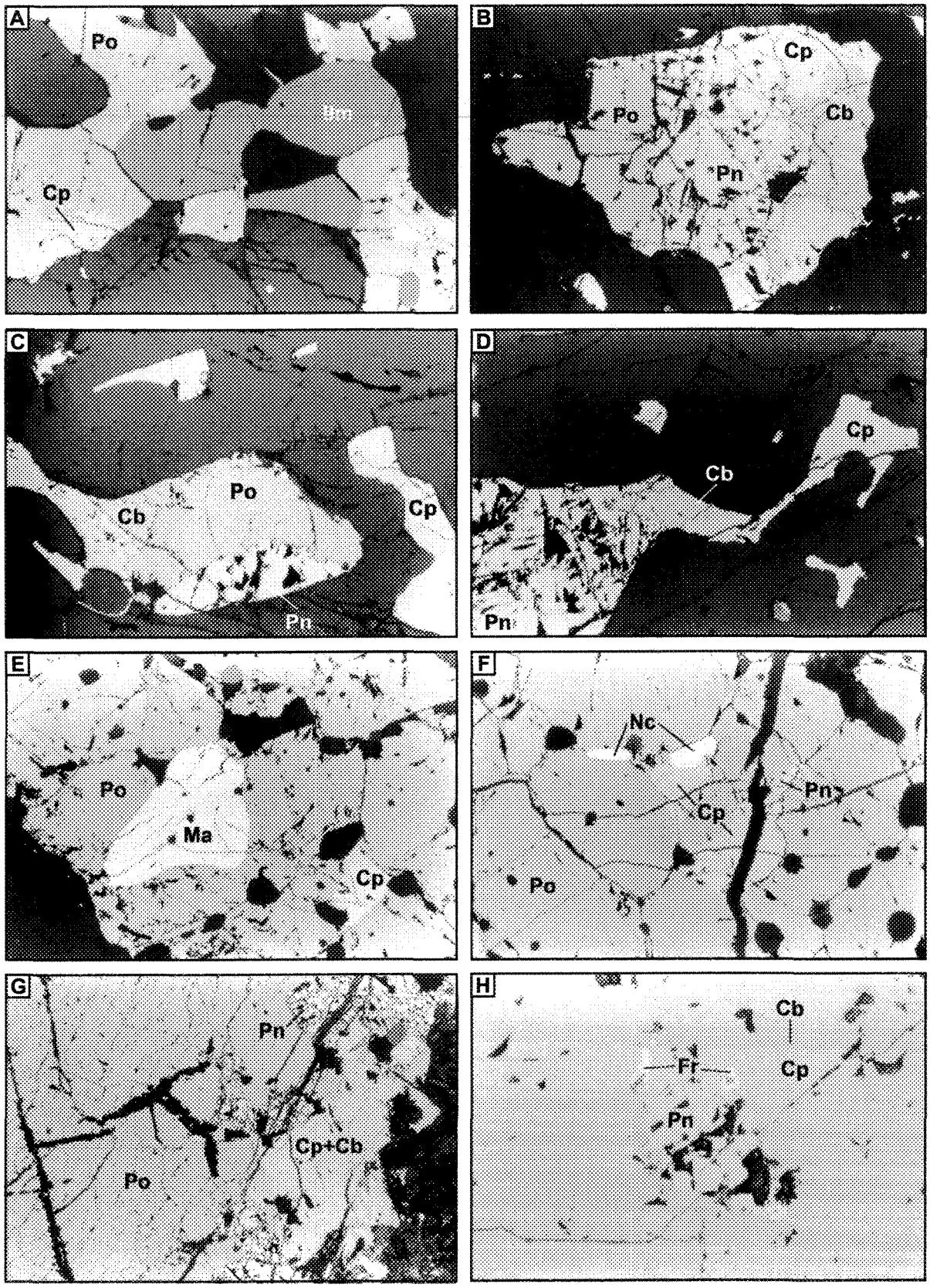
A
Po
Cp
B
Cp
Po
Cb
Pn
C
Cb
Po
Cp
Pn
D
Cp
Cb
Pn
E
Po
Ma
Cp
F
Nc
Pn
Cp
Po
G
Pn
Cp+Cb
Po
H
Cb
Fr
Cp
Pn

Fig. 4. A. Typical norite-hosted disseminated sulfide mineralization showing the close association of pyrrhotite (Po) and ilmenite (Ilm), with minor chalcopyrite (Cp) and cubanite (Cb). Field of view is 1.25 mm in width. B. Troctolite-hosted disseminated sulfide mineralization consisting of pyrrhotite (Po), pentlandite (Pn), chalcopyrite (Cp) and cubanite (Cb). Field of view is 1.25 mm in width. C. Troctolite-hosted mineralization illustrating the interstitial nature of the sulfides relative to the silicate minerals. Field of view is 1.25 mm in width. D. Interstitial sulfides from a PGE-rich horizon, consisting of pentlandite (Pn), cubanite (Cb) and chalcopyrite (Cp). Note the absence of pyrrhotite. Field of view is 1.25 mm in width. E. Grain of maucherite (Ma) with minor chalcopyrite (Cp) within a pyrrhotite (Po)-rich massive sulfide pod at the margin of a country-rock xenolith. Field of view is 1.25 mm in width. F. Subhedral crystals of niccolite (Nc) within the above pyrrhotite (Po)-rich massive sulfide pod. Pentlandite (Pn) and chalcopyrite (Cp) complete the sulfide assemblage. Field of view is 1.25 mm in width. G. Zoned massive sulfide lens consisting of a pyrrhotite (Po)-rich core, an inner rim of pentlandite (Pn) and a marginal intergrowth of chalcopyrite (Cp) and cubanite (Cb). Field of view is 5 mm in width. H. Subhedral crystals of froodite (Fr) at the margin of pentlandite (Pn), within Cu-rich disseminated sulfides composed of intergrown chalcopyrite (Cp) and cubanite (Cb). Field of view is 0.3 mm in width.

pyrrhotite, pentlandite, chalcopyrite, and cubanite, with trace amounts of mackinawite and bornite (Figs. 4B, C). The ratio of pyrrhotite to Cu- and Ni-rich sulfide phases is lower here than in the norite-hosted sulfides. Furthermore, only minor amounts of maucherite were observed.

PGE-rich disseminated sulfide horizons

Two horizons of disseminated sulfides distinctly enriched in the PGE, 10 m thick on average, were sampled from the upper portion of the mineralized zone. They occur 100 to 200 m above the basal contact (Fig. 2), and are hosted in leucotroctolite. The horizons typically underlie layers of melatroctolite to dunite. They were first identified by Geerts (1991), who related their origin to a magmatic process rather than to secondary enrichment by a hydrothermal fluid.

The PGE-rich disseminated sulfide horizons contain up to 2.8 ppm Pt + Pd (Table 1), and consist mainly of interstitial grains of chalcopyrite, cubanite, pentlandite, and lesser pyrrhotite (Fig. 4D). Unlike the norite- and troctolite-hosted sulfide mineralization, arsenide minerals were not observed in the PGE-rich horizons.

Pyrrhotite-rich massive sulfides

The pyrrhotite-rich massive sulfides occur as lenses in the basal sequence, and, less commonly, as pods of massive sulfide bordering country-rock xenoliths. The massive sulfide pods (1-3 cm wide) are typically hosted in norite, and consist of 90-95% pyrrhotite, with

minor chalcopyrite and pentlandite. They also contain maucherite and niccolite (Figs. 4E, F), and this is reflected in the elevated As content of sample DC-75 (Table 1). The massive sulfide pods and their noritic host are likely derived from *in situ* partial melting within the adjacent, sulfide-bearing country-rock xenoliths.

Several narrow lenses of massive sulfide reaching up to 5 cm in width occur in the basal mineralized rocks. They are usually at a sharp angle to the base of the intrusion, and are thus interpreted to originate as injections of sulfide liquid through a filter-pressing mechanism. The lenses contain 85-90% pyrrhotite, 5-10% pentlandite, and lesser chalcopyrite, cubanite and mackinawite. They are typically zoned, from a central core of massive pyrrhotite with minor flame-like pentlandite, to a narrow rim (1-2 mm) of subhedral pentlandite and marginal intergrowths of chalcopyrite, cubanite and minor mackinawite (Fig. 4G).

Chalcopyrite-rich disseminated sulfides

Chalcopyrite-rich disseminated sulfides are typically found in association with the pyrrhotite-rich lenses of massive sulfide. The disseminated sulfides occur as small interstitial grains to the silicate minerals or locally as very thin veinlets, and consist of 50-75% chalcopyrite, 15-30% pyrrhotite, 5-10% cubanite and 1-3% mackinawite, with minor sphalerite and bornite. Small subhedral grains of froodite surround pentlandite within a coarse-grained lamellar intergrowth of chalcopyrite and cubanite (Fig. 4H). The froodite appears to have nucleated on the pentlandite prior to the formation of the Cu-rich sulfide

phases, which favors a magmatic origin for the PGM, as opposed to its crystallization from a late hydrothermal fluid.

Sulfur isotopes

Sulfur isotope studies carried out on several Cu-Ni sulfide deposits of the Duluth Complex indicate that most of the sulfur has been derived from argillaceous rocks of the underlying Virginia Formation (Mainwaring & Naldrett 1977, Ripley 1981, 1986, Ripley & Al-Jassar 1987). Ripley (1981) obtained $\delta^{34}S$ values ranging from 0.2 to 15.3‰ from mineralized intrusive rocks of the Dunka Road deposit, values that cover a similar range to those he measured in the Virginia Formation.

Virginia Formation

Sulfur isotope measurements were obtained from six core samples of unmetamorphosed pyritiferous argillite taken approximately 20 km from the intrusive contact (drill hole #B2, Fig. 1). The samples are considered representative of the unit, having been collected between 3 and 345 m above the basal contact with the Biwabik Formation. Values of $\delta^{34}S$ range from 4.5 to 8.6‰ (Table 1, Fig. 5), and are similar to the value of 7.4‰ determined by Ripley (1981) on material from the same drill hole, and to the range of results of six analyses reported by Ripley & Al-Jassar (1987) (5.6 to 8.8‰) from core samples located 10 km from the margin of the Complex.

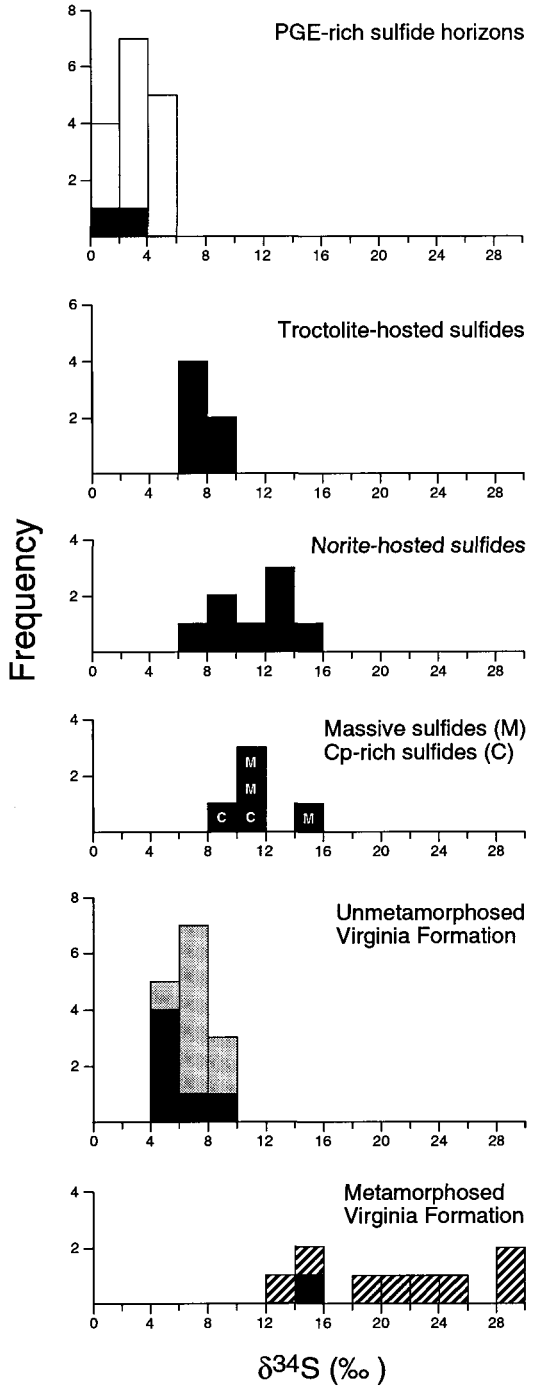

FIG. 5. Histogram showing the distribution of sulfur isotopic values for the five types of sulfide mineralization forming the Dunka Road deposit, as well as the bedded pyrrhotite unit and unmetamorphosed argillite of the Virginia Formation. Black boxes: this study; white boxes: Geerts (1994); grey boxes: Ripley (1981), Ripley & Al-Jassar (1987), Zanko *et al.* (1994); striped boxes: Severson (1994), Zanko *et al.* (1994).

One sample of metamorphosed argillite from the bedded pyrrhotite unit (DC-70; Table 1, Fig. 5) yielded a much higher value, 15.8‰, and falls within the range of $\delta^{34}S$ values determined by Severson (1994) (14.0 to 21.1‰). Sulfur isotope measurements of the same unit were also obtained by Zanko *et al.* (1994) from a 17-m-thick xenolith occurring along the base of the Serpentine deposit. The $\delta^{34}S$ values show a systematic increase from 6.3 to 29.1‰ (mean of 19.4‰) toward the top of the xenolith (their Fig. 10). This increase is associated with an upward increase in the grade of metamorphism; reported mineral assemblages and textures are indicative of complete dehydration and localized partial melting near the top, whereas relict chlorite and muscovite found at the base indicate that dehydration reactions did not go to completion. Similar variations in $\delta^{34}S$ values with proximity to the intrusive contact have also been reported from the Muskox Intrusion (Sasaki 1969) and the Pechenga ore field in Russia (Melezhik *et al.* 1994). Hence the strong positive correlation observed between $\delta^{34}S$ values of the argillaceous rocks and grade of metamorphism makes it improbable that the isotopic variability in the Virginia Formation is related to a primary process of bacterial fractionation, as was suggested by Zanko *et al.* (1994).

As proposed by Zheng (1990) for an open system, we argue that the significantly higher $\delta^{34}S$ values observed in metamorphosed argillaceous rocks near the contact originate from the breakdown of pyrite into pyrrhotite under hydrous conditions, with release of a light-sulfur-enriched vapor into the magma prior to the onset of crystallization. Such a process has previously been demonstrated experimentally by Kajiwara *et al.* (1981) through the thermal decomposition of pyrite into pyrrhotite at 600°C. They observed a significant depletion in

$\delta^{34}S$, by up to 12‰, in the early fraction of sulfur released, with the pyrrhotite residue having a $\delta^{34}S$ value about 4.5‰ higher than the starting material. Hence the early release of a light-sulfur-enriched vapor phase into the magma most likely led to a significant increase in the $\delta^{34}S$ of the residual pyrrhotite-bearing metasedimentary rocks, the later subsequently discharging important quantities of isotopically heavier sulfur near the base of the intrusion during their partial assimilation.

Norite-hosted, troctolite-hosted and PGE-rich disseminated sulfides

Sulfur isotope measurements obtained from these three types of disseminated sulfide mineralization show a general increase in $\delta^{34}S$ toward the base of the intrusion and in proximity to country-rock xenoliths (*i.e.*, where magma contamination is likely to be most important). Hence the average $\delta^{34}S$ value of the norite-hosted sulfides reaches 11.2‰, whereas that of the troctolite-hosted and PGE-rich sulfides is 7.8 and 2.1‰, respectively, with only a slight overlap between the groups of values (Table 1, Fig. 5). A similar variation with respect to distance from the basal contact was noted by Ripley (1981) based on 128 sulfur isotope analyses from the mineralized intrusive rocks. Of these, 14 samples from the uppermost PGE-rich horizon (the "Red Horizon" of Geerts 1994) yielded an average $\delta^{34}S$ value of 3.6‰ (Fig. 5), which is comparable to that of the present study.

Pyrrhotite-rich massive and chalcopyrite-rich disseminated sulfides

Sulfur isotope measurements obtained from the pyrrhotite-rich and chalcopyrite-rich sulfides yielded relatively high $\delta^{34}S$ values, ranging from 8.4 to 16.0‰ (Table 1), which suggest that a large proportion of the sulfur is sedimentary in origin. The very high value obtained for the massive sulfide pod (sample DC-75, 16.0‰) is almost identical to that measured for the bedded pyrrhotite unit. This is not surprising, as DC-75 was sampled directly adjacent to a country-rock xenolith. As for the pyrrhotite-rich lenses and associated chalcopyrite-rich disseminated sulfides, the very similar values obtained within each pair of samples imply that little to no isotopic fractionation occurred during their formation. A similar conclusion was reached by Ripley & Al-Jassar (1987) on the basis of $\delta^{34}S$ values of mineral separates from adjacent pyrrhotite and cubanite within the Babbitt deposit.

S/Se values

The ratio Se/S has been used effectively to determine the source of sulfur in magmatic Ni-Cu sulfide deposits (*e.g.*, Paktunc 1989, Eckstrand *et al.* 1989, Ripley 1990a, Thériault *et al.* 1997). Its usefulness is particularly significant where country-rock assimilation seems to have played a role in the genesis of mineralization, as sedimentary rocks are generally depleted in selenium relative to mantle-derived rocks (Eckstrand & Hulbert 1987).

Norite-hosted, troctolite-hosted and PGE-rich disseminated sulfides

Our data show that whole-rock S/Se values decrease systematically from the norite-hosted sulfides (mean of 9,700) to the troctolite-hosted sulfides (mean of 4,600), and reach a minimum in the PGE-rich sulfide horizons (mean of 2,600) (Table 1). In light of the elevated S/Se values of the argillite samples from the Virginia Formation, which range from 15,500 to 54,000, we attribute this regular decrease in S/Se to varying degrees of its assimilation by the mafic magma. Similar S/Se values (mean of 23,300) were also obtained in the district by Eckstrand & Cogulu (1986) from argillaceous rocks of the equivalent Rove Formation in proximity to the Ni-Cu sulfide deposit in the Crystal Lake Gabbro.

Pyrrhotite-rich massive and chalcopyrite-rich disseminated sulfides

The pyrrhotite-rich massive sulfides have significantly higher S/Se values than the chalcopyrite-rich disseminated sulfides (Table 1). The high value obtained for the massive sulfide pod (sample DC-75: 23,800) falls within the range for the argillaceous rocks; this is in agreement with its very high $\delta^{34}S$ value and points to a significant input of metasediment-derived sulfur.

Discussion

Country-rock assimilation

A number of lines of evidence presented above strongly support the assumption that country-rock assimilation was a key process in the genesis of the Dunka Road Cu-Ni-PGE

deposit. With respect to field observations, the abundance of hornfels xenoliths typically rimmed by granitic material, along with the common presence of norite near the base of the mineralized intrusion, are indicative of significant contamination of the parental magma through partial melting of the underlying Virginia Formation. There is also an apparent relationship between the relative abundances of pyrrhotite and arsenide minerals and the extent of contamination, owing to the Cu-Ni-poor and As-rich composition of the argillaceous country-rocks relative to the parental mafic magma.

Furthermore, sulfur isotope measurements and S/Se values of the mineralized rocks clearly demonstrate that a significant proportion of the sulfur is sedimentary in origin, being most likely derived in large part from the bedded pyrrhotite unit of the Virginia Formation. The wide range in $\delta^{34}S$ values of the mineralized intrusive rocks is consistent with a simple mixing model between "igneous" sulfur contained in the magma ($\delta^{34}S \sim 0.0‰$) and externally derived sedimentary sulfur represented by the bedded pyrrhotite unit ($\delta^{34}S \sim 15.8‰$). The assumed $\delta^{34}S$ value for magmatic sulfur is supported by recent isotopic measurements obtained by Lee & Ripley (1995) for 12 unmineralized samples of troctolite from the South Kawishiwi intrusion, which yielded values ranging from -3.4 to +1.2‰ (mean of +0.1‰). Assuming the two end members to be valid, an average of 71% of the sulfur within the norite-hosted sulfides seems to have been derived from the footwall rocks, as opposed to 49% for the troctolite-hosted sulfides and only 13% for the PGE-rich sulfides.

The observed increase in $\delta^{34}S$ values with degree of country-rock assimilation is associated with a concomitant increase in S/Se values (Fig. 6), as well as a decrease in the Pd

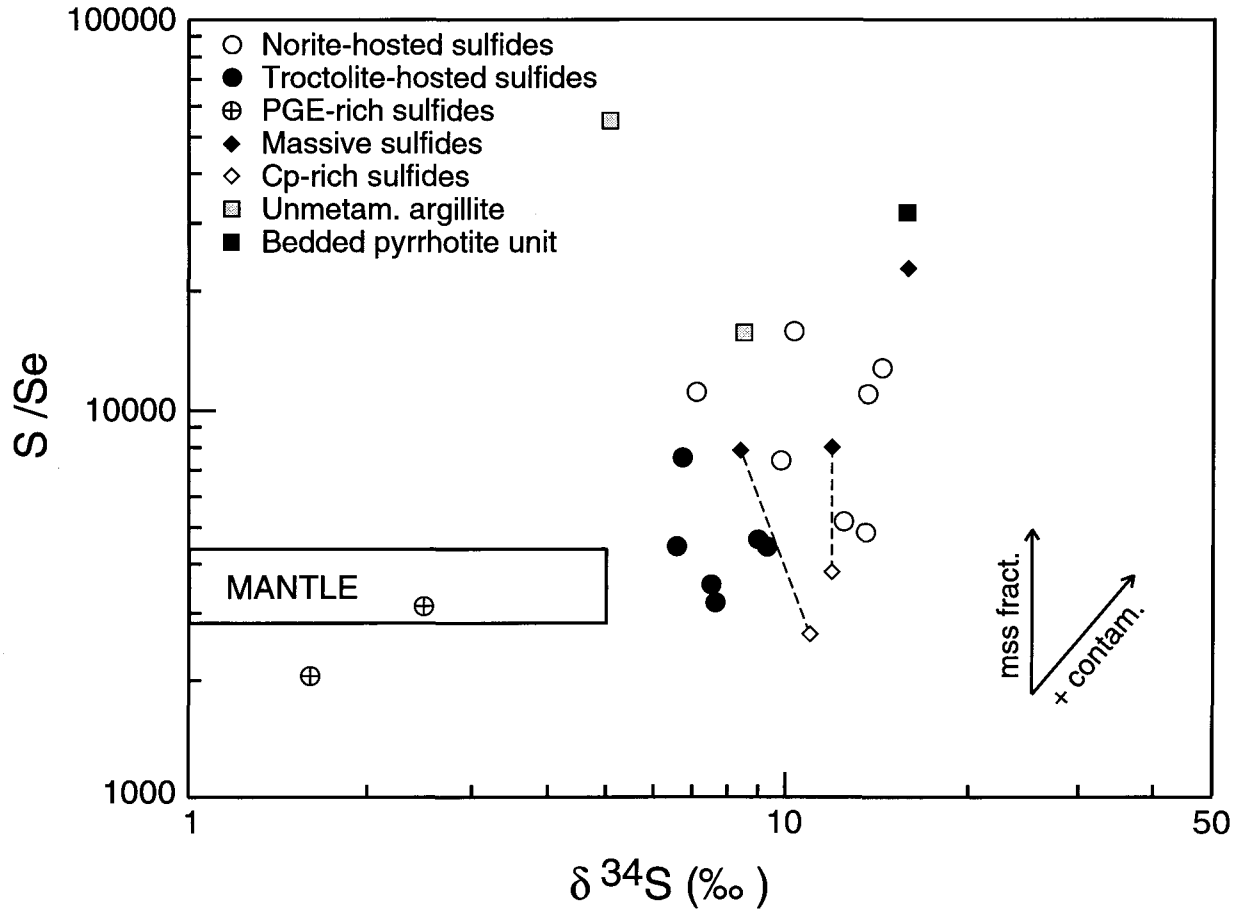

FIG. 6. Whole-rock S/Se ratio *versus* $\delta^{34}S$ value for the five types of sulfide mineralization, bedded pyrrhotite unit and unmetamorphosed argillite of the Virginia Formation. Range in S/Se ratio and $\delta^{34}S$ value of the mantle taken from Eckstrand & Hulbert (1987) and Hulbert *et al.* (1988), respectively.

+ Pt content of the sulfide fraction (Fig. 7). The latter is also suggestive of a mixing process between PGE-poor partial melts of the Virginia Formation and metal-bearing mafic magmas. Lower *R* factors (*i.e.* weight ratio of silicate magma to sulfide melt) attained in the more contaminated rocks also contribute to this gradual decrease in PGE (Thériault *et al.* 1997). Moreover, a plot of S/Se values *versus* Pd + Pt content of the sulfide fraction (Fig. 8) clearly illustrates the contaminated nature of the norite-hosted sulfides, which have S/Se values above those estimated for mantle-derived rocks (2850-4350: Eckstrand & Hulbert 1987). The low S/Se value and high Pd + Pt content of the PGE-rich sulfide horizons have been ascribed in part to elevated *R* factors achieved at the time of separation of the sulfide liquid (Thériault *et al.* 1997). These values are not unlike those of major PGE-rich deposits (Fig. 8), whose origin also has been linked to very large *R* factors (Campbell *et al.* 1983). As for the spatially associated pyrrhotite-rich and chalcopyrite-rich sulfide samples, the difference in S/Se values and Pd + Pt content likely relates to a difference in the extent of sulfide liquid fractionation, considering that both samples within a pair seem to have undergone comparable degrees of assimilation based on their similar $\delta^{34}S$ values (Table 1).

Additional geochemical evidence (Thériault *et al.* 1997) further confirm the importance of the assimilation process. For example, electron-microprobe analyses of the sulfide phases suggest a higher proportion of monoclinic to hexagonal pyrrhotite in the norite-hosted sulfides, which was interpreted to be due to the greater availability of locally derived sulfur from the sedimentary country-rocks. Moreover, an increase in the incompatible elements such as Cs, Rb, Ba and Th was noted in the more contaminated samples, as one would expect these

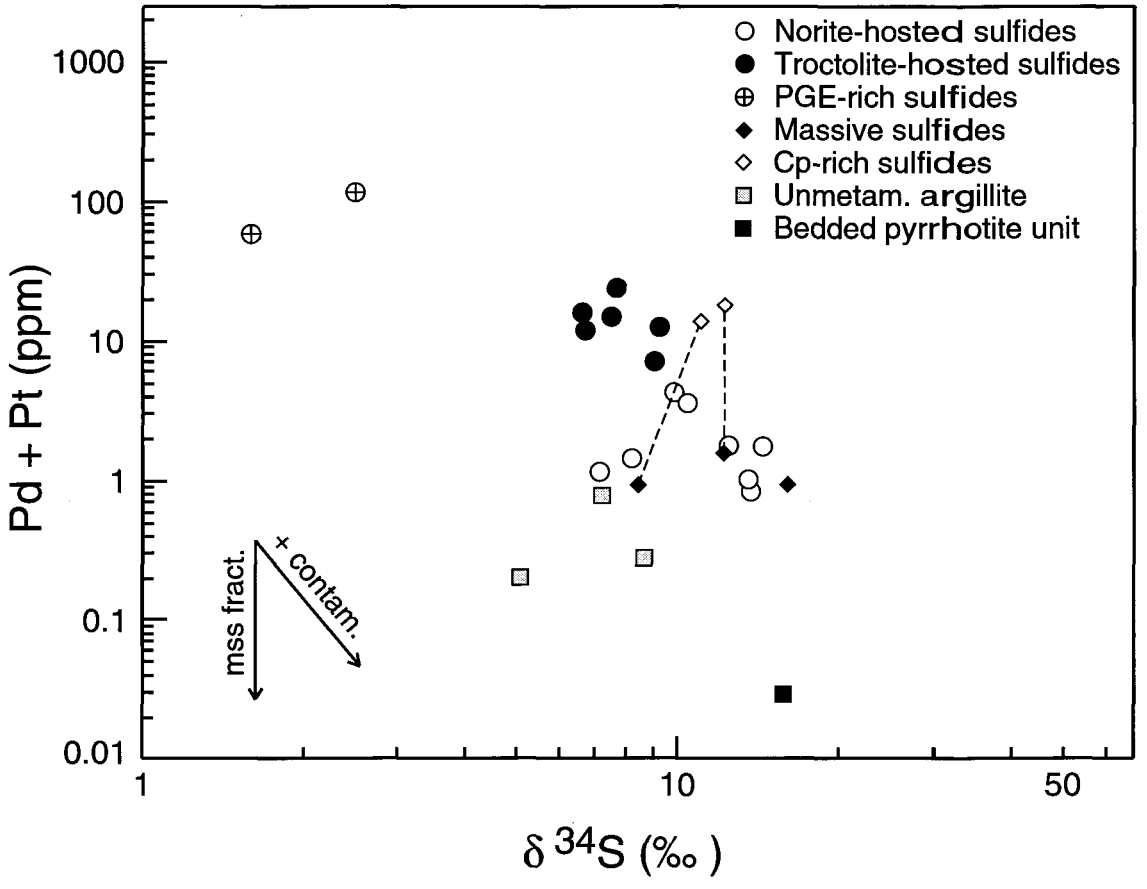

FIG. 7. Whole-rock $\delta^{34}S$ value *versus* Pd + Pt of sulfide fraction for the five types of sulfide mineralization, bedded pyrrhotite unit and unmetamorphosed argillite of the Virginia Formation. Broken lines join samples of pyrrhotite-rich massive sulfide lenses and associated chalcopyrite-rich disseminated sulfides. Arrows show compositional trend expected during *mss* fractionation and magma contamination. Symbols are the same as in Figure 6.

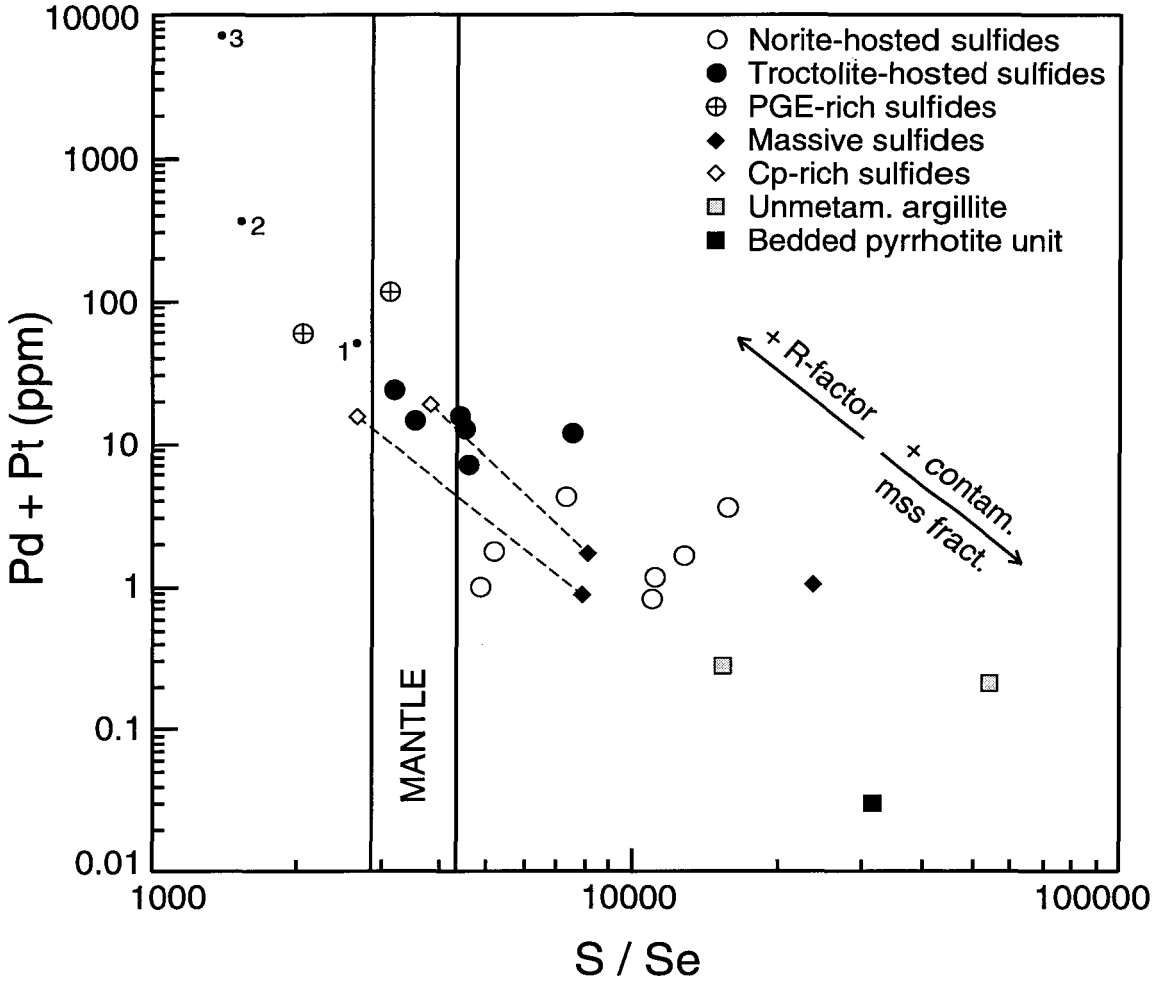

FIG. 8. Whole-rock S/Se ratio *versus* Pd + Pt of sulfide fraction for the five types of sulfide mineralization forming the Dunka Road deposit, bedded pyrrhotite unit and unmetamorphosed argillite of the Virginia Formation, and various PGE-dominant magmatic sulfide deposits (1: Crystal Lake gabbro, 2: Merensky Reef of the Bushveld Complex, 3: J-M Reef of the Stillwater intrusion). Data for other deposits taken from Naldrett (1981) and Eckstrand (unpubl. data, 1988). Symbols are the same as in Figure 6.

elements to be readily mobilized in a felsic partial melt.

Magmatic origin of the sulfides

A number of studies pertaining to the Babbitt deposit have emphasized the role of hydrothermal fluids in remobilizing the PGE (*e.g.*, Ripley 1990b, Mogessie *et al.* 1991, Mogessie & Stumpfl 1992, Ripley *et al.* 1993, Ripley & Chryssoulis 1994), on the basis of the common presence of platinum-group minerals (PGM) and secondary sulfides (bornite, vallerite and violarite) in strongly altered silicate rocks. However, studies carried out in the Dunka Road deposit report only minor evidence of hydrothermal alteration, and relate the origin of mineralization to primary magmatic processes (*e.g.* Ripley 1981, Rao & Ripley 1983, Severson & Hauck 1990, Geerts 1994, Thériault *et al.* 1997). In the present study, field and petrographic evidence suggest that the bulk of the mineralization (norite-hosted, troctolite-hosted, and PGE-rich sulfides) formed by the separation of sulfide liquid within a partially crystallized magma, which may explain the general lack of massive sulfides along the base of the intrusion. Where a relatively large volume of sulfide liquid did accumulate, it appears to have undergone fractional crystallization, producing an Fe-rich cumulate of monosulfide solid-solution (*mss*) and a Cu-rich fractionated sulfide liquid.

On a plot of Cu/Ir *versus* Ni/Pd (Fig. 9), two distinct features can be recognized: 1) a gradual decrease in Ni/Pd and Cu/Ir values from the norite-hosted to the troctolite-hosted sulfides, reaching a minimum in the PGE-rich sulfide horizons, and 2) a decrease in Ni/Pd ratio with concomitant increase in Cu/Ir ratio from the massive sulfide lenses to their associated

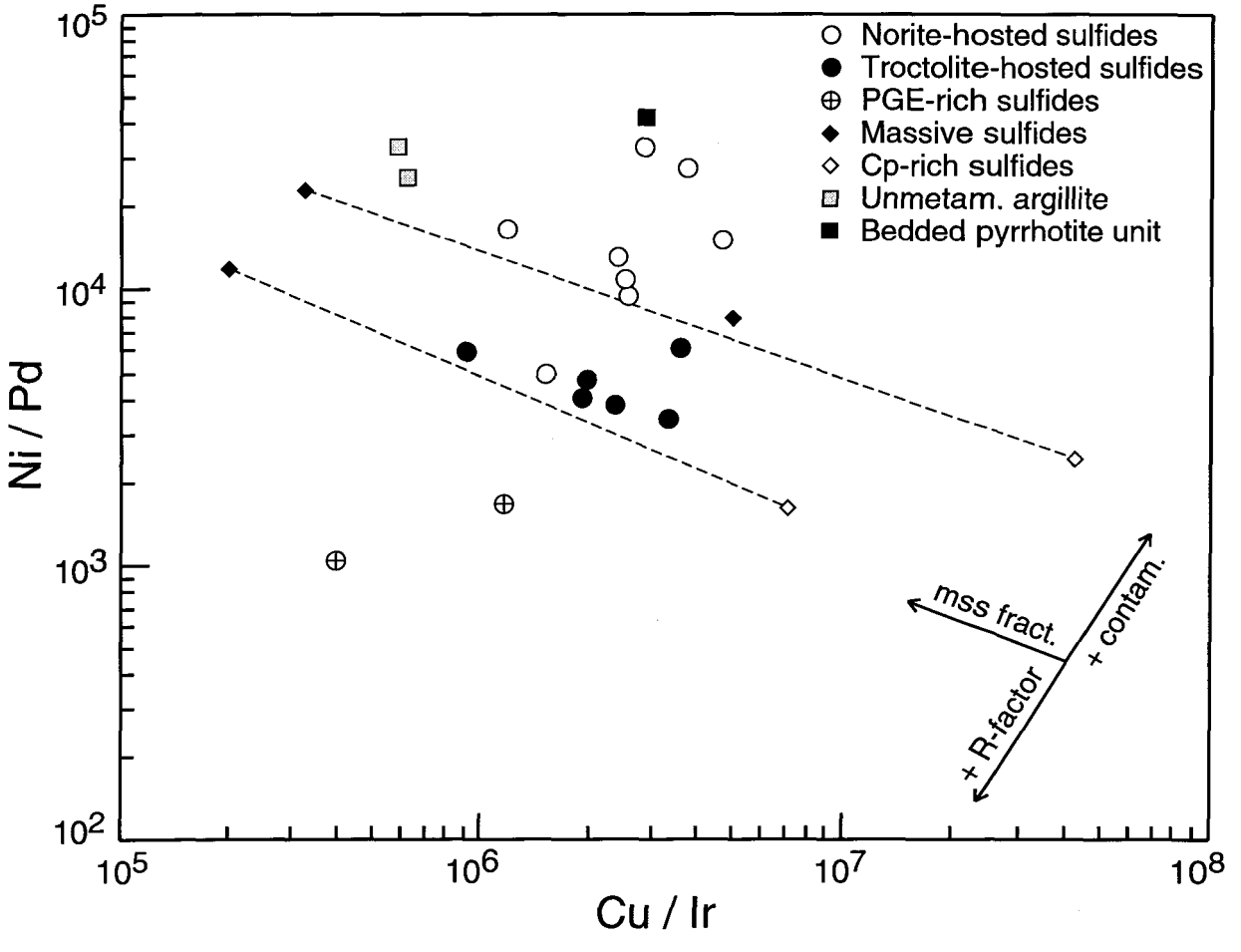

FIG. 9. Cu/Ir *versus Ni*/Pd diagram for the five types of sulfide mineralization, bedded pyrrhotite unit and unmetamorphosed argillite of the Virginia Formation. Symbols are the same as in Figure 6.

chalcopyrite-rich disseminated sulfides. In the first case, the systematic decrease in metal ratios is due to an increase in the PGE content of the sulfides, brought about by a rise in the *R* factor as the effect of country-rock assimilation diminishes away from the basal contact. This relationship was recently demonstrated by Thériault *et al.* (1997), who modeled the composition of the above three types of disseminated sulfide mineralization using the equation for equilibrium fractionation, obtaining average *R* factors of 175, 1300 and 8000 for the norite-hosted, troctolite-hosted and PGE-rich sulfides, respectively. A similar increase in PGE content (hence *R* factor) with distance away from the intrusive margins was also observed by Barnes & Francis (1995) in the Muskox intrusion, in the Northwest Territories. As for the associated massive sulfide lenses and chalcopyrite-rich sulfides, we explain the observed variation in metal ratios by the fractionation of Ir and, to a lesser extent, of Ni into *mss*, with Cu and Pd behaving as incompatible elements and being concentrated in the residual sulfide liquid. The metal ratio of the massive sulfide pod sample (DC-75) in proximity to the field of norite-hosted sulfides suggests that it has not undergone significant fractional crystallization, which is substantiated by the apparent lack of chalcopyrite-rich sulfides in the immediate area.

The whole-rock metal content of all mineralized samples was recalculated to 100% sulfides for the purpose of comparing the composition of the sulfide fraction of each type of mineralization (Table 2). The normative composition of the sulfide fraction was then calculated. Results clearly support the petrographic observations, and show that the proportion of base-metal sulfides (*i.e.*, chalcopyrite, cubanite, and pentlandite) increases relative to

TABLE 2. AVERAGE METAL CONCENTRATIONS AND NORMATIVE MINERALOGY OF THE SULFIDE FRACTION

Rock type	NOR	TROC	PGE	MS[1]	CP	ARG[2]
S (%)	36,1	35,7	35,2	36,3	35,5	36,4
Fe (%)	57,9	45,1	33,9	60,2	42,7	63,2
Cu (%)	4,45	15,3	22,5	1,39	19,9	0,08
Ni (%)	1,26	3,77	8,14	1,93	1,75	0,08
Os (ppb)	14	40	160	3	14	<55
Ir (ppb)	20	80	370	49	13	4
Ru (ppb)	170	260	1300	46	48	<370
Rh (ppb)	58	310	2100	140	50	11
Pt (ppb)	470	2900	15000	26	7400	190
Pd (ppb)	1500	11000	72000	1300	10000	180
Au (ppb)	330	1700	7000	47	3600	88
Re (ppb)	82	160	180	140	27	49
Co (ppm)	2300	1700	2000	1500	900	1200
As (ppm)	280	140	32	90	190	1100
Sb (ppm)	66	74	16	2	21	280
Se (ppm)	41	83	140	46	110	12
Cp+Cb (%)	13	44	64	4	57	0
Pn (%)	4	12	26	6	6	0
Po (%)	83	44	10	90	37	100

NOTES: Composition of the sulfide fraction calculated allowing 200 ppm Ni and 150 ppm Cu in the silicate component of the intrusive rocks. Details of the calculations in Barnes & Francis (1995). [1] : includes only massive sulfide lenses (i.e. DC-73 and DC-76); [2] : includes both argillite and bedded pyrrhotite unit.

pyrrhotite as the effect of country-rock assimilation wanes away from the basal contact. Furthermore, a striking increase in the normative proportion of Cu-rich sulfides is observed within the disseminated mineralization surrounding massive pyrrhotite-rich lenses, as predicted by the fractional crystallization model.

The recalculated composition of the sulfide fraction of each type of mineralization was plotted on mantle-normalized variation diagrams to better compare their level of metal enrichment. As shown in Figure 10A, the PGE-rich sulfides are strongly enriched in metals relative to the troctolite-hosted and norite-hosted sulfides, particularly in PGE and Au. In contrast, the sample from the bedded pyrrhotite unit shows a strong depletion in all metals, and plots closest to the field of norite-hosted sulfides. The following enrichment-factors were calculated between the average PGE-rich and norite-hosted sulfides: Cu(5), Ni(6), Os(11), Ru(16), Ir(18), Au(21), Pt(31), Rh(36), and Pd(49). The higher enrichment-factors of the Pd-group of PGE (Rh, Pt, and Pd: Barnes *et al.* 1985) possibly relates to their higher partition-coefficient into the sulfide liquid. The gradual increase in metal content observed from the norite-hosted to the PGE-rich sulfides probably reflects a number of factors, including the degree of country-rock assimilation, the ratio of silicate melt to sulfide liquid, and the partition-coefficient of metals into the sulfide liquid.

The mantle-normalized patterns of the massive sulfide lenses and associated chalcopyrite-rich disseminated sulfides show a clear antithetic relationship (Fig. 10B), with the former having higher contents in Ir, Ru and Rh, whereas the chalcopyrite-rich sulfides are strongly enriched in the more incompatible metals (*i.e.* Pt, Pd, Au and Cu). A striking

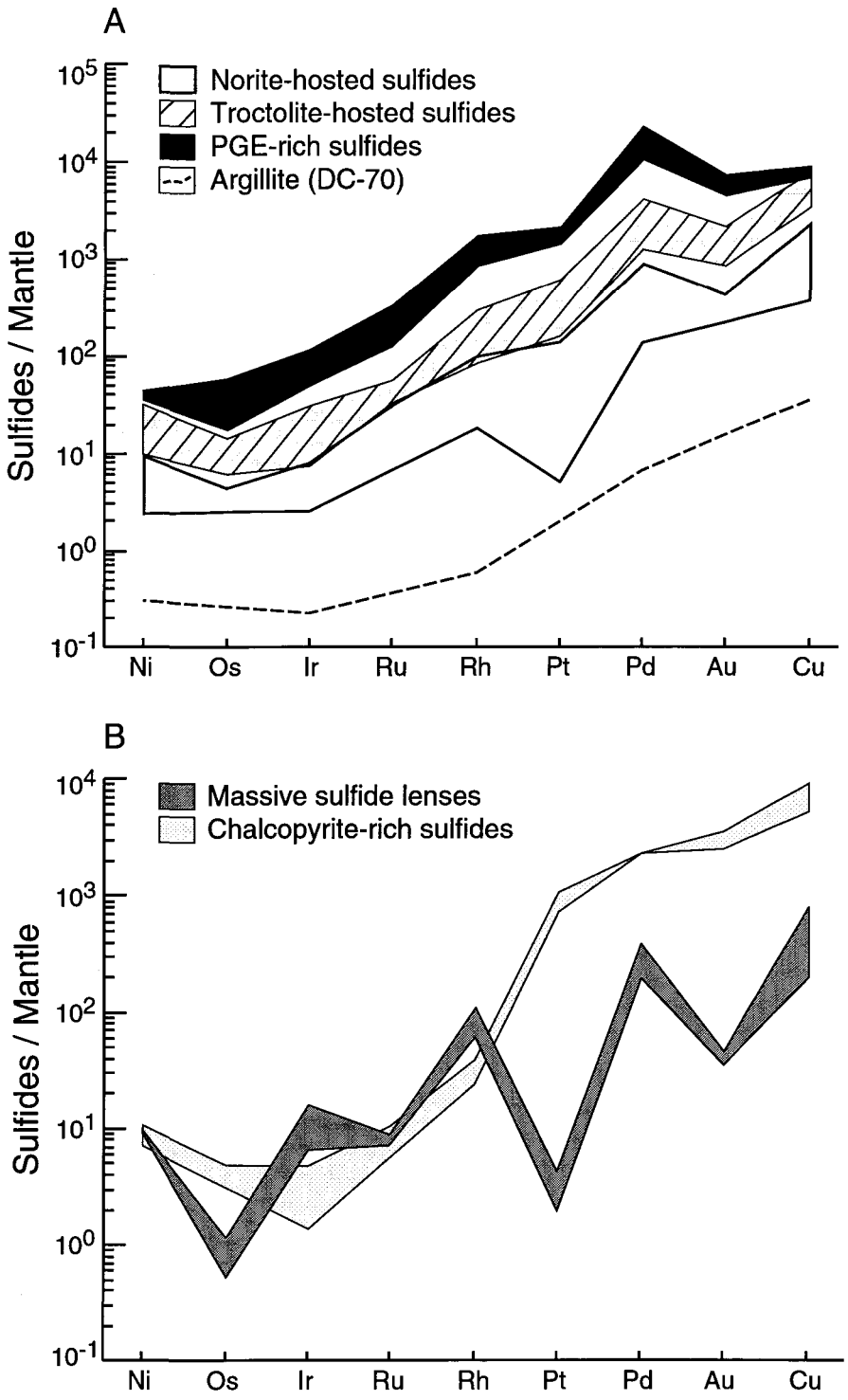

FIG. 10. Mantle-normalized metal patterns showing the range in composition of the sulfide fraction. A. Norite-hosted, troctolite-hosted and PGE-rich disseminated sulfides, and the bedded pyrrhotite unit of the Virginia Formation. B. Lenses of pyrrhotite-rich massive sulfide and associated chalcopyrite-rich disseminated sulfides. Normalization factors are from Barnes *et al.* (1988).

characteristic of the massive sulfides is their strong negative anomalies in Pt and Au relative to the smoother pattern of the chalcopyrite-rich assemblages. Similar patterns have also been described from sulfides of the Noril'sk-Talnakh District (Zientek *et al.* 1994, Barnes *et al.* 1997a), the Cape Smith Fold Belt (Barnes *et al.* 1997a) and the Stillwater Complex (Zientek *et al.* 1994), and illustrate the highly variable partitioning of metals between *mss* and the sulfide liquid.

To assess the degree of compatibility of metals in *mss*, the recalculated composition of each lens of pyrrhotite-rich massive sulfide was divided by that of its associated chalcopyrite-rich zone of disseminated sulfide mineralization (Fig. 11). Results show that Re, Ir and Rh appear to partition strongly into *mss*, whereas Pd, Sb, Cu, Au and Pt are highly incompatible and show an increasing affinity for the sulfide liquid. The average ratio of concentration in pyrrhotite-rich assemblage to that in chalcopyrite-rich assemblage was calculated for each metal, and yielded: Re(5.3), Ir(3.8), Rh(2.8), Co(1.6), Ni(1.1), Ru(0.96), As(0.47), Se(0.40), Pd(0.13), Sb(0.10), Cu(0.07), Au(0.01) and Pt (0.004). These values are quite similar to those obtained for other deposits (*e.g.,* Zientek *et al.* 1994, Li & Barnes 1996), and compare favorably with experimentally determined partition-coefficients (*e.g.* Fleet *et al.* 1993, Li *et al.* 1996, Barnes *et al.* 1997b), considering that the lenses of massive sulfide are not perfect *mss* adcumulates (*i.e.,* they contain some fractionated liquid component, manifested as a narrow Cu-rich rim). The apparently incompatible nature of Se with respect to *mss* could explain the lower S/Se of the chalcopyrite-rich sulfides relative to the lenses of massive sulfide (Table 1, Figs. 6, 8).

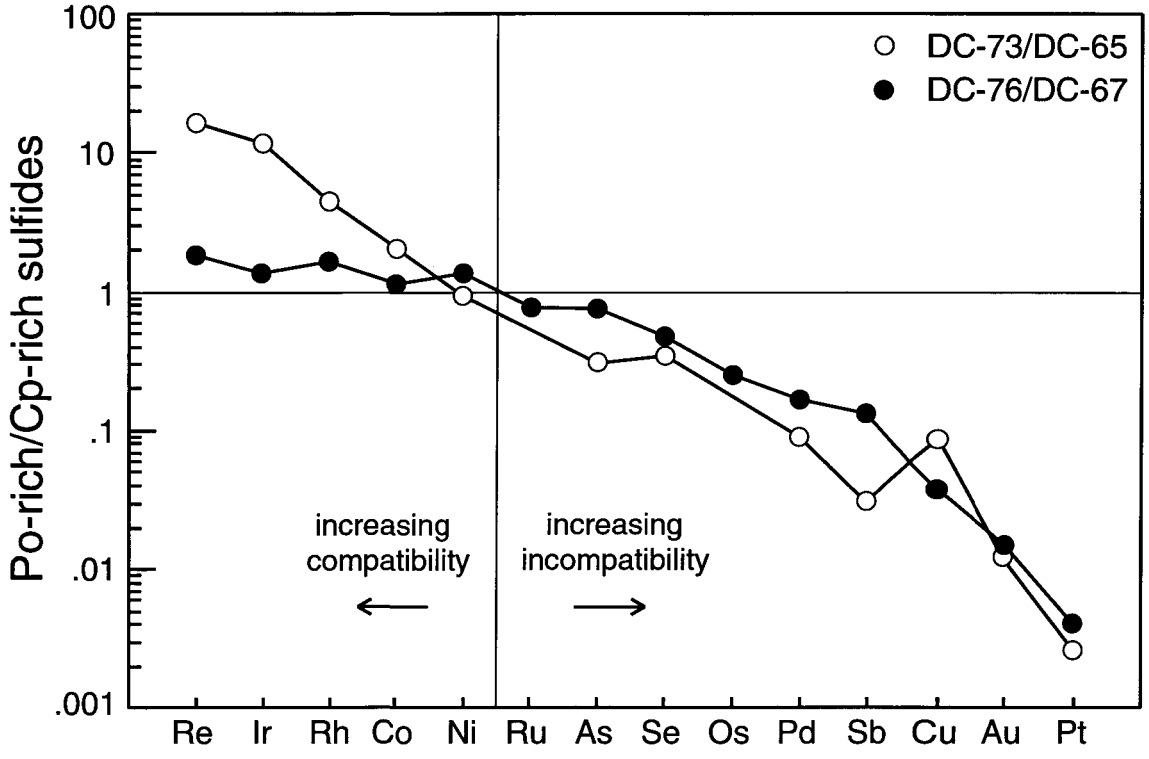

FIG. 11. Variation diagram showing the degree of compatibility of metals in the pyrrhotite-rich massive sulfide lenses relative to their associated chalcopyrite-rich disseminated sulfide mineralization.

Genesis of the Dunka Road deposit

The origin of the Dunka Road Cu-Ni-PGE deposit has been interpreted in terms of three main processes, which operated in sequence. Each of the five types of sulfide mineralization may be explained by the combined action of an externally derived process, country-rock assimilation, and two internal magmatic processes, namely the interaction between the sulfide liquid and the silicate melt, and fractional crystallization of the sulfide liquid. In light of the above, we interpret the sequence of events as follows (Fig. 12):

1) Early during emplacement of the Partridge River intrusion, the surrounding sedimentary rocks were contact-metamorphosed, leading to their partial dehydration and devolatilization. A light- sulfur-enriched H_2S vapor phase was released into the magma through the breakdown of pyrite into pyrrhotite, and either homogenized with the resident juvenile sulfur or escaped to surface *via* overlying flows of flood basalt (Fig. 12A).

2) The restitic, light-sulfur-depleted pyrrhotite-bearing metasedimentary rocks were subsequently assimilated by the magma, releasing a granitic partial melt and important quantities of ^{34}S- enriched sulfur near the base of the intrusion and in proximity to country-rock xenoliths. Owing to intense contamination by the granitic melt, the hybridized noritic magma was cooler than the surrounding troctolitic magma, which led to its early crystallization and formation of the norite-hosted disseminated sulfide mineralization (Fig. 12B). The sulfide liquid crystallized near its source and had less time to interact with the 4magma, resulting in low *R* factors. This hypothesis explains the metal-poor and pyrrhotite-rich nature of the norite-hosted sulfides. Furthermore, the sulfide liquid was As-rich and

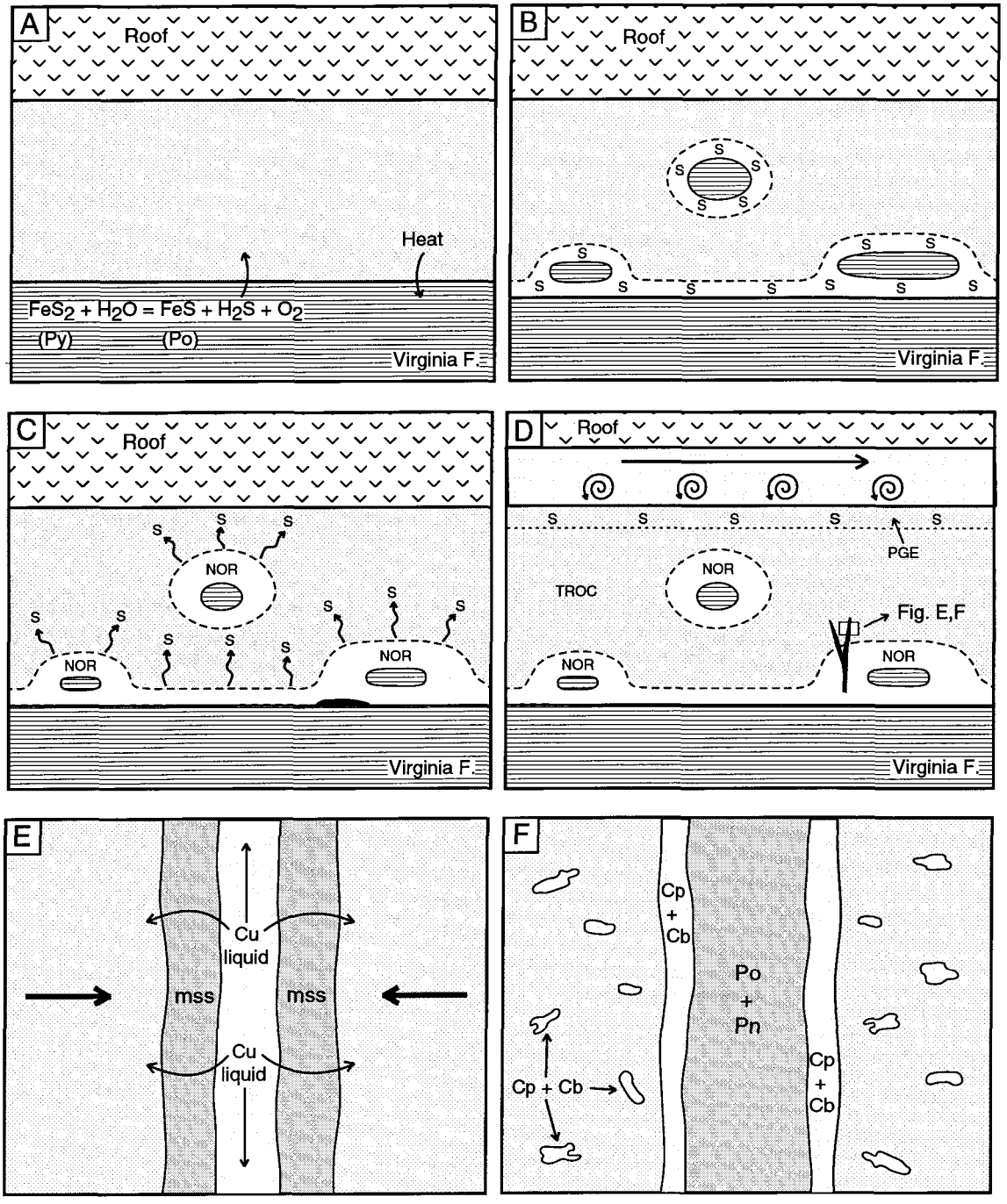
A
Roof
Heat
FeS2 + H2O = FeS + H2S + O2
(Py)
(Po)
Virginia F.
B
Roof
S
Virginia F.
C
Roof
NOR
S
Virginia F.
D
Roof
S
PGE
TROC
NOR
Fig. E,F
Virginia F.
E
Cu
liquid
mss
mss
Cu
liquid
F
Cp
+
Cb
Po
+
Pn
Cp + Cb
Cp
+
Cb

FIG. 12.

Fig. 12. Schematic diagram illustrating the processes involved in the formation of the five types of sulfide mineralization from the Dunka Road deposit. Figure not meant to be to scale. A. Early during contact metamorphism, a light sulfur enriched H_2S vapor phase is released into the troctolitic magma through the breakdown of pyrite into pyrrhotite. B. The restitic, light sulfur depleted metasedimentary rocks are later assimilated by the magma, releasing a granitic partial melt and important quantities of ^{34}S enriched sulfur near the base of the intrusion and in proximity to country-rock xenoliths. The hybridized magma and metal-poor sulfide liquid eventually crystallize, forming the norite-hosted disseminated sulfide mineralization. C. A significant proportion of ^{34}S enriched sulfur also diffuses into the surrounding troctolitic magma, mixing with juvenile igneous sulfur. The immiscible sulfide liquid interacts with a larger volume of silicate magma, and crystallizes to form troctolite-hosted disseminated sulfides having moderate PGE contents. D. A fresh input of uncontaminated troctolitic magma is injected above the basal mineralized unit. Sulfide liquid from this new injection is free to swirl within the turbulent magma, and eventually percolates downward into the partly consolidated rocks to form a PGE-rich disseminated sulfide horizon. Meanwhile, small pools of sulfide liquid near the base of the intrusion are filter pressed upwards to form subvertical injections. E. The sulfide liquid undergoes fractional crystallization, forming a cumulate of *mss* that crystallizes along the lens margins. Residual Cu-rich sulfide liquid accumulates in the central part of the lens, and is eventually expelled along the outer margins as well as into the surrounding crystal mush. F. With further cooling, the fractionated sulfide liquid crystallizes into chalcopyrite and cubanite while the *mss* exsolves into pyrrhotite and pentlandite, forming the observed pyrrhotite-rich massive sulfide lenses and associated chalcopyrite-rich disseminated sulfide mineralization.

Se-poor owing to the large contribution of sedimentary material to the magma, which is shown by the relative abundance of arsenide minerals and elevated S/Se values.

3) A significant proportion of ^{34}S-enriched sulfur also diffused into the surrounding troctolitic magma, mixing with juvenile igneous sulfur (Fig. 12C). The less contaminated and thus hotter troctolitic magma had longer to cool than the noritic magma. Therefore, the sulfide liquid had longer to interact with the silicate melt, which led to higher *R* factors. This finding explains the significant increase in the PGE content of the troctolite-hosted disseminated sulfides.

4) A fresh input of relatively uncontaminated troctolitic magma was later injected above the basal mineralized sequence. The low volume of sulfide liquid present near the base of this new injection was free to swirl within the turbulent magma, achieving very elevated *R* factors. Eventually, this ^{34}S-depleted sulfide liquid percolated downward into the partly consolidated troctolitic rocks, and crystallized to form a PGE-rich disseminated sulfide horizon (Fig. 12D). As these sulfides were largely derived from a mafic magma, they have low As concentrations and S/Se values close to those typical of the mantle.

5) In areas where significant amounts of sulfide liquid collected (*e.g.*, likely along the base, in proximity to the bedded pyrrhotite unit), it was filter-pressed upward to accumulate as subvertical injections (Fig. 12D). The sulfide liquid subsequently underwent fractional crystallization, forming an Fe-rich cumulate of *mss* that crystallized along the cooler margin of the lenses. The residual Cu-rich sulfide liquid, which would have accumulated within the central part of the lenses, was eventually expelled along the outer margin of the lenses as well as into the surrounding mush of crystals (Fig. 12E). This fractionated sulfide liquid ultimately

crystallized as chalcopyrite and cubanite along the outer margin of the lenses, as well as within the adjacent intrusive rocks, to form the chalcopyrite-rich disseminated sulfide mineralization. With further cooling, the *mss* exsolved into pyrrhotite and pentlandite, forming the inner part of the observed lenses of massive sulfide (Fig. 12F).

Post-crystallization hydrothermal remobilization of the metals appears to have been minimal, on the basis of the lack of significant alteration throughout the deposit.

Conclusions

Compositional variations in magmatic sulfides of the Dunka Road Cu-Ni-PGE deposit are best explained by varying degrees of country-rock assimilation, which in turn affected the amount of interaction between the sulfide liquid and the silicate melt (*R* factor). Fractional crystallization of sulfide liquid subsequently occurred within localized lenses of massive sulfide.

In this study, we have confirmed the significant role of country-rock assimilation in localizing the mineralization; this aspect had been emphasized in previous studies (*e.g.* Ripley 1981, Rao & Ripley 1983, Geerts 1991). In addition, however, we have been able to monitor systematic variations in the intensity of the process through detailed field, petrographic, geochemical and isotopic studies of the mineralization.

Acknowledgements

We gratefully acknowledge the significant collaboration throughout this study of Steven Hauck and Mark Severson of the Minnesota Natural Resources Research Institute. Special thanks are extended to John McGoran of Fleck Resources for his permission to publish the results, Penny Morton for her logistic support, Roger Eckstrand for allowing use of unpublished data, and Richard Lechasseur for his assistance with the analytical work. Ed Ripley (Indiana University) and Gilles St-Jean (Ottawa-Carleton Geoscience Centre) are also thanked for their $\delta^{34}S$ analyses and for informal discussion of results. Funding for this work was provided by a Fonds pour la Formation de Chercheurs et l'Aide à la Recherche research grant to R.D. Thériault and by a Natural Sciences and Engineering Research Council of Canada operating grant to S.-J. Barnes.

Références

Barnes, S.-J., Boyd, R., Korneliussen, A., Nilsson, L.P., Often, M., Pedersen, R.B. & Robins, B. (1988): The use of mantle normalization and metal ratios in discriminating between the effects of partial melting, crystal fractionation and sulphide segregation on platinum-group elements, gold, nickel and copper: examples from Norway. *In* Geo-platinum 87 (H.M. Prichard, P.J. Potts, J.F.W. Bowles & S. Cribb, eds.). Elsevier, Amsterdam, pp. 113-143.

Barnes, S.-J. & Francis, D. (1995): The distribution of platinum-group elements, nickel, copper, and gold in the Muskox layered intrusion, Northwest Territories, Canada. *Econ. Geol.* **90**, 135-154.

Barnes, S.-J., Makovicky, E., Makovicky, M., Rose-Hansen, J. & Karup-Moller, S. (1997b): Partition coefficients for Ni, Cu, Pd, Pt, Rh and Ir between monosulfide solid solution and sulfide liquid and the formation of compositionally zoned Ni-Cu sulfide bodies by fractional crystallization of sulfide liquid. *Can. J. Earth Sci.* **34**, 366-374.

Barnes, S.-J., Naldrett, A.J. & Gorton, M.P. (1985): The origin of the fractionation of platinum-group elements in terrestrial magmas. *Chem. Geol.* **53**, 303-323.

Barnes, S.-J., Zientek, M.L. & Severson, M.J. (1997a): Ni, Cu, Au and platinum-group element contents of sulphides associated with intraplate magmatism: a synthesis. *Can. J. Earth Sci.* **34**, 337-351.

Bédard, L.P. & Barnes, S.-J. (1990): Instrumental neutron activation analysis by collecting only one spectrum: Results for international geochemical reference samples. *Geostandards Newsletters* **14**, 479-484.

Campbell, I.H., Naldrett, A.J. & Barnes, S.J. (1983): A model for the origin of the platinum-rich sulfide horizons in the Bushveld and Stillwater Complexes. *J. Petrol.* **24**, 133-165.

Eckstrand, O.R. & Cogulu, E. (1986): Se/S evidence relating to genesis of sulphides in the Crystal Lake Gabbro, Thunder Bay, Ontario. Program with Abstracts, *Geol. Assoc. Can. - Mineral. Assoc. Can. Annual Meeting*, p. 66.

Eckstrand, O.R. & Hulbert, L.J. (1987): Selenium and the source of sulphur in magmatic nickel and platinum deposits. Program with Abstracts, *Geol. Assoc. Can. - Mineral. Assoc. Can. Annual Meeting*, p. 40.

Eckstrand, O.R., Grinenko, L.N., Krouse, H.R., Paktunc, A.D., Schwann, P.L. & Scoates, R.F.J. (1989): Preliminary data on sulphur isotopes and Se/S ratios, and the source of sulphur in magmatic sulphides from the Fox River Sill, Molson Dykes and Thompson nickel deposits, northern Manitoba. *In* Current research, part C, *Geol. Surv. Can., Pap.* **89-1C**, 235-242.

Fleet, M.E., Chryssoulis, S.L., Stone, W.E. & Weisener, C.G. (1993): Partitioning of platinum- group elements and Au in the Fe-Ni-Cu-S system: Experiments on the fractional crystallization of sulfide melt. *Contrib. Mineral. Petrol.* **115**, 36-44.

Foose, M. & Weiblen, P. (1986): The physical and petrologic setting and textural and compositional characteristics of sulfides from the South Kawishiwi Intrusion, Duluth Complex, Minnesota, U.S.A. *In* Geology and metallogeny of copper deposits (G.H. Friedrich, A.D. Genkin, A.J. Naldrett, J.D. Ridge, R.H. Sillitoe & F.M. Vokes, eds.). Springer-Verlag, Heidelberg, Germany, pp. 8-24.

Geerts, S.D. (1991): Geology, stratigraphy, and mineralization of the Dunka Road Cu-Ni prospect, northeastern Minnesota. Natural Resources Research Institute, Duluth, Minnesota, Technical Report 91-14, 63 p.

Geerts, S.D. (1994): Petrography and geochemistry of a platinum group element-bearing mineralized horizon in the Dunka Road prospect (Keweenawan), Duluth Complex, northeastern Minnesota. M.Sc. thesis, University of Minnesota, Duluth, Minn.

Hemming, S.R., McLennan, S.M. & Hanson, G.N. (1995): Geochemical and Nd/Pb isotopic evidence for the provenance of the Early Proterozoic Virginia Formation, Minnesota: Implications for the tectonic setting of the Animikie Basin. *J. Geol.* **103**, 147-168.

Hulbert, L.J., Duke, J.M., Eckstrand, O.R., Lydon, J.W., Scoates, R.F.J. & Cabri, L.J. (1988): Geological environments of the platinum group elements. *Geol. Surv. Can.*, Open File 1440, 148 p.

Kajiwara, Y., Sasaki, A. & Matsubaya, O. (1981): Kinetic sulfur isotope effects in the thermal decomposition of pyrite. *Geochem. J.* **15**, 193-197.

Lee, I. & Ripley, E.M. (1995): Genesis of Cu-Ni sulfide mineralization in the South Kawishiwi intrusion, Spruce Road area, Duluth Complex, Minnesota. *Can. Mineral.* **33**, 723-743.

Li, C. & Barnes, S.-J. (1996): Partitioning of platinum-group elements and Au in the Fe-Ni-Cu-S system: Experiments on the fractional crystallization of sulfide melt - A discussion. *Contrib. Mineral. Petrol.* **123**, 435-437.

Li, C., Barnes, S.-J., Makovicky, E., Rose-Hansen, J. & Makovicky, M. (1996): Partitioning of nickel, copper, iridium, rhenium, platinum, and palladium between monosulfide solid solution and sulfide liquid: Effects of composition and temperature. *Geochim. Cosmochim. Acta* **60**, 1231-1238.

Listerud, W.H. & Meineke, D.G. (1977): Mineral resources of a portion of the Duluth Complex and adjacent rocks in St. Louis and Lake Counties, northeastern Minnesota. Minnesota Department of Natural Resources, Division of Minerals, Report 93, 74 p.

Lucente, M.E. & Morey, G.B. (1983): Stratigraphy and sedimentology of the Lower Proterozoic Virginia Formation, Northern Minnesota. Minnesota Geological Survey, Report of Investigation **28**.

Mainwaring, P.R. & Naldrett, A.J. (1977): Country-rock assimilation and the genesis of Cu-Ni sulfides in the Water Hen Intrusion, Duluth Complex, Minnesota. *Econ. Geol.* **72**, 1269-1284.

Martineau, M.P. (1989): Empirically derived controls on Cu-Ni mineralization: a comparison between fertile and barren gabbros in the Duluth Complex, Minnesota, U.S.A. *In* Magmatic sulphides: the Zimbabwe volume (M.D. Prendergast & M.J. Jones, eds.). *Inst. Min. Metal.* pp. 117-137.

Melezhik, V.A., Hudson-Edwards, K.A., Green, A.H. & Grinenko, L.N. (1994): Pechenga area, Russia - Part 2: Nickel-copper deposits and related rocks. *Trans. Inst. Min. Metall. (Sect. B: Appl. Earth Sci.)* **103**, 146-152.

Mogessie, A. & Stumpfl, E.F. (1992): Platinum-group element and stable isotope geochemistry of PGM-bearing troctolitic rocks of the Duluth Complex, Minnesota. *Austr. J. Earth Sci.* **39**, 315-325.

Mogessie, A., Stumpfl, E.F. & Weiblen, P.W. (1991): The role of fluids in the formation of platinum-group minerals, Duluth Complex, Minnesota: mineralogic, textural, and chemical evidence. *Econ. Geol.* **86**, 1506-1518.

Morey, G.B. (1992): Chemical composition of the Eastern Biwabik Iron-Formation (Early Proterozoic), Mesabi Range, Minnesota. *Econ. Geol.* **87**, 1649-1658.

Naldrett, A.J. (1981): Platinum-group element deposits. *In* Platinum-group elements: mineralogy, geology, recovery (L.J. Cabri, ed.). *CIM Spec. Vol.* **23**, 197-231.

Naldrett, A.J. (1989): Ores associated with flood basalts. *In* Ore deposition associated with magmas. (J.A. Whitney & A.J. Naldrett, eds.). Society of Economic Geologists, *Rev. Econ. Geol.* **4**, 103-118.

Paces, J.B. & Miller, J.D., Jr. (1993): Precise U-Pb ages of Duluth Complex and related mafic intrusions, northeastern Minnesota: New insights for physical, petrogenetic, paleomagnetic and tectono-magmatic processes associated with 1.1 Ga Midcontinent rifting. *J. Geophys. Res.* **98B**, 13997-14013.

Paktunc, A.D. (1989): Petrology of the St. Stephen intrusion and the genesis of related nickel-copper sulfide deposits. *Econ. Geol.* **84**, 817-840.

Rao, B.V. & Ripley, E.M. (1983): Petrochemical studies of the Dunka Road Cu-Ni deposit, Duluth Complex, Minnesota. *Econ. Geol.* **78,** 1222-1238.

Ripley, E.M. (1981): Sulfur isotopic studies of the Dunka Road Cu-Ni deposit, Duluth Complex, Minnesota. *Econ. Geol.* **76**, 610-620.

Ripley, E.M. (1986): Application of stable isotopic studies to problems of magmatic sulfide ore genesis with special reference to the Duluth Complex, Minnesota. *In* Geology and metallogeny of copper deposits (G.H. Friedrich, A.D. Genkin, A.J. Naldrett, J.D. Ridge, R.H. Sillitoe & F.M. Vokes, eds.). Springer-Verlag, Heidelberg, Germany, pp. 8-24.

Ripley, E.M. (1990a): Se/S ratios of the Virginia Formation and Cu-Ni sulfide mineralization in the Babbitt area, Duluth Complex, Minnesota. *Econ. Geol.* **85**, 1935-1940.

Ripley, E.M. (1990b): Platinum-group element geochemistry of Cu-Ni mineralization in the basal zone of the Babbitt deposit, Duluth Complex, Minnesota. *Econ. Geol.* **85,** 830-841.

Ripley, E.M. & Alawi, J.A. (1988): Petrogenesis of pelitic xenoliths at the Babbitt Cu-Ni deposit, Duluth Complex, Minnesota, U.S.A. *Lithos* **21**, 143-159.

Ripley, E.M. & Al-Jassar, T.J. (1987): Sulfur and oxygen isotope studies of melt-country rock interaction, Babbitt Cu-Ni deposit, Duluth Complex, Minnesota. *Econ. Geol.* **82**, 87-107.

Ripley, E.M., Butler, B.K., Taib, N.I. & Lee, I. (1993): Hydrothermal alteration in the Babbitt Cu-Ni deposit, Duluth Complex: mineralogy and hydrogen isotope systematics. *Econ. Geol.* **88**, 679-696.

Ripley, E.M. & Chryssoulis, S.L. (1994): Ion microprobe analyses of platinum group elements in sulfide and arsenide minerals from the Babbitt Cu-Ni deposit, Duluth Complex, Minnesota. *Econ. Geol.* **80,** 201-210.

Robert, R.V.B., Van Wyk, E. & Palemer, R. (1971): Concentration of the noble metals by fire assay technique using nickel sulphide as the collector. *National Inst. Metall. Report* **1371**, pp. 1-14.

Sasaki, A. (1969): Sulphur isotope study of the Muskox Intrusion, District of Mackenzie. *Geol. Surv. Can., Pap.* **68-46**, 68 p.

Severson, M.J. (1994): Igneous stratigraphy of the South Kawishiwi intrusion, Duluth Complex, Minnesota. Natural Resources Research Institute, Duluth, Minnesota, Technical Report 93-34, 210 p.

Severson, M.J. & Hauck, S.A. (1990): Geology, geochemistry, and stratigraphy of a portion of the Partridge River intrusion. Natural Resources Research Institute, Duluth, Minnesota, Technical Report 89-11, 236 p.

Taylor, R.B. (1964): Geology of the Duluth Complex near Duluth, Minnesota. Minnesota *Geol. Surv. Bull.* **44**.

Thériault, R.D., Barnes, S.-J. & Severson, M.J. (1997): The influence of country rock assimilation and silicate to sulfide ratios (*R* factor) on the genesis of the Dunka Road Cu-Ni- PGE deposit, Duluth Complex, Minnesota. *Can. J. Earth Sci.* **34**, 373-389.

Tyson, R.M. & Chang, L.L.Y. (1984): The petrology and sulfide mineralization of the Partridge River Troctolite, Duluth Complex, Minnesota. *Can. Mineral.* **22**, 23-38.

Van Schmus, W.R. & Hinze, W.J. (1985): The Midcontinent Rift. *Annu. Rev. Earth Planet. Sci.* **13**, 345-383.

Weiblen, P.W. & Morey, G.B. (1980): A summary of the stratigraphy, petrology, and structure of the Duluth Complex. *Amer. J. Sci.* **280A**, 88-133.

Wright Engineers Limited (1991): Dunka Road Project: Preliminary Project Review for NERCO Minerals Co., Project 2046.

Zanko, L.M., Severson, M.J. & Ripley, E.M. (1994): Geology and mineralization of the Serpentine copper-nickel deposit. Natural Resources Research Institute, Duluth, Minnesota, Technical Report 93-52, 90 p.

Zheng, Y.F. (1990): Sulfur isotopes in metamorphic rocks. *Neues Jahrbuch Mineral. Abh.* **161**, 303-325.

Zientek, M.L., Likhachev, A.P., Kunilov, V.E., Barnes, S.-J., Meier, A.L., Carlson, R.R., Briggs, P.H., Fries, T.L. & Adrian, B.M. (1994): Cumulus processes and the composition of magmatic ore deposits: Examples from the Talnakh District, Russia. *In* The Sudbury-Noril'sk Symposium (P.C. Lightfoot & A.J. Naldrett, eds.). *Ont. Geol. Surv. Spec. Pub.* **5**, 373-392.

Economic Geology
Article accepté le 99-12-21

Origin of Cu-Ni-PGE sulfide mineralization in the Partridge River Intrusion, Duluth Complex, Minnesota.

Robert D. Thériault, Sarah-Jane Barnes

Département des Sciences Appliquées, Université du Québec à Chicoutimi,

Chicoutimi, Québec, G7H 2B1, Canada

and Mark J. Severson

Natural Resources Research Institute, Duluth, MN 55811, U.S.A.

Abstract

A total of four subeconomic Cu-Ni-PGE sulfide deposits occur near the base of the Partridge River Intrusion, a lopolith-shaped mafic layered intrusion emplaced along the northwestern margin of the Duluth Complex. The host troctolitic rocks are in contact with sulfide-bearing metasedimentary rocks of the Virginia Formation. The origin of the sulfide mineralization has generally been linked to contamination of the mafic magma through partial assimilation of the argillaceous country rocks. Three main types of sulfide mineralization have been recognized within the four deposits. These are: 1) PGE-poor disseminated sulfides; 2) PGE-rich disseminated sulfides; and 3) semi-massive to massive sulfides. The PGE-poor disseminated sulfides typically occur within the lower 250 m of the intrusion, and are hosted mainly by

heterogeneous norite and olivine gabbro that contain abundant country rock xenoliths. This type of mineralization shows a number of features suggesting that the magma had undergone substantial contamination, such as high proportions of pyrrhotite and arsenide minerals, and high Cu/Pd, Ni/Pd and Cu/Pt ratios. These sulfides appear to have formed at low to moderate ratios of silicate magma to sulfide melt (mean *R* factor= 600-2,400), as deduced from their metal-poor nature. The PGE-rich disseminated sulfides occur well within the intrusion directly beneath ultramafic layers, and show little signs of contamination. They are composed mainly of chalcopyrite and pentlandite, with lesser amounts of pyrrhotite and cubanite. They appear to have formed at high *R* factors (mean= 6,000-7,700), which explains their relatively high PGE and base metal contents. The semi-massive to massive sulfides occur mainly as veins and lenses both along the basal contact and within the underlying sedimentary country rocks. They are typically zoned, being composed of both pyrrhotite-rich (Fe-rich) and chalcopyrite/cubanite-rich (Cu-rich) portions, the latter often forming along the base or top of massive sulfide bodies. The zonation in the massive sulfides is interpreted to be the product of fractional crystallization of a sulfide liquid, the pyrrhotite-rich sulfides representing the cumulate of this crystallization and the Cu-rich sulfides the fractionated liquid. Based on the above evidence, we interpret the compositional variations observed between the different types of sulfide mineralization to originate from the combined action of three different processes, which operated in sequence from magma emplacement until complete crystallization of the sulfides. These are: 1) country rock assimilation; 2) interaction between the sulfide liquid and the silicate melt (*R* factor); and 3) fractional crystallization of the sulfide liquid.

Introduction

Numerous studies carried out in the Duluth Complex have focused on the subeconomic Cu-Ni-PGE sulfide occurrences of the Partridge River Intrusion, namely the Babbitt (e.g., Tyson and Chang, 1984; Ripley, 1990; Severson and Barnes, 1991; Severson et al., 1996), Dunka Road (e.g., Ripley, 1981; Rao and Ripley, 1983; Geerts, 1991; Thériault et al., 1997; Thériault and Barnes, 1998), Wetlegs (Severson and Hauck, 1990, 1997) and Wyman Creek (Severson and Hauck, 1990, 1997) deposits. Among these, a thorough investigation of a high grade massive sulfide occurrence from the Babbitt deposit (i.e. Local Boy ore zone) was completed in order to assess its economic potential (Severson, 1991; Severson and Barnes, 1991).

Recent work on the Dunka Road deposit (Thériault and Barnes, 1998) has shown that it consists of five different types of sulfide mineralization, referred to as: 1) norite-hosted disseminated sulfides; 2) troctolite-hosted disseminated sulfides; 3) PGE-rich disseminated sulfide horizons; 4) chalcopyrite-rich disseminated sulfides; and 5) pyrrhotite-rich massive sulfides. These have been explained by systematic variations in the degree of country rock assimilation and amount of interaction between the sulfide liquid and the silicate melt (*R* factor), with localized fractional crystallization of the sulfide liquid. Of particular economic interest is the presence of a number of laterally persistent PGE-rich sulfide horizons which contain up to 2.8 ppm Pd + Pt.

Although each of the deposits from the Partridge River Intrusion have been well documented, a comparative study of their mineralization for the purpose of elaborating an overall genetic model has yet to be accomplished. Hence, the main objectives of this paper are:

1) to determine if the various types of sulfide mineralization observed in the Dunka Road deposit also exist within the Babbitt, Wetlegs and Wyman Creek deposits, especially the PGE-rich horizons, which have been overlooked in the past and could potentially host a reef-type deposit; and 2) to propose a general model explaining the origin of the mineralization for the entire Partridge River Intrusion, with the use of field relationships, sulfide mineralogy and geochemistry, and quantitative modelling.

Regional Geology

The Duluth Complex consists of an arcuate mass of troctolitic and anorthositic intrusions of Middle Proterozoic age (1100 Ma) occurring within the Keweenawan flood basalt province of the Midcontinent Rift of North America (Van Schmus and Hinze, 1985). The complex extends for more than 220 km along the northwestern margin of Lake Superior, and was emplaced between comagmatic volcanic rocks of the North Shore Volcanic Group and older Proterozoic (1800-2300 Ma; Hemming et al., 1995) basement rocks of the Animikie Group (Fig. 1). On the basis of geophysical (Hutchinson et al., 1990) and isotopic evidence (Nicholson and Shirey, 1990), the voluminous mafic volcanic and intrusive rocks of the Keweenawan province have been explained by the ascent of a mantle plume (i.e. Keweenaw hot spot) in the Lake Superior area.

A total of 9 different Cu-Ni-PGE sulfide occurrences spread over a distance of 55 km occur along the basal contact of two adjacent troctolitic intrusions, namely the Partridge River and South Kawishiwi intrusions (Severson and Hauck 1990; Severson, 1994). These are the host to 4.4 billion tons of mineralization grading 0.66 percent Cu and 0.20 percent Ni

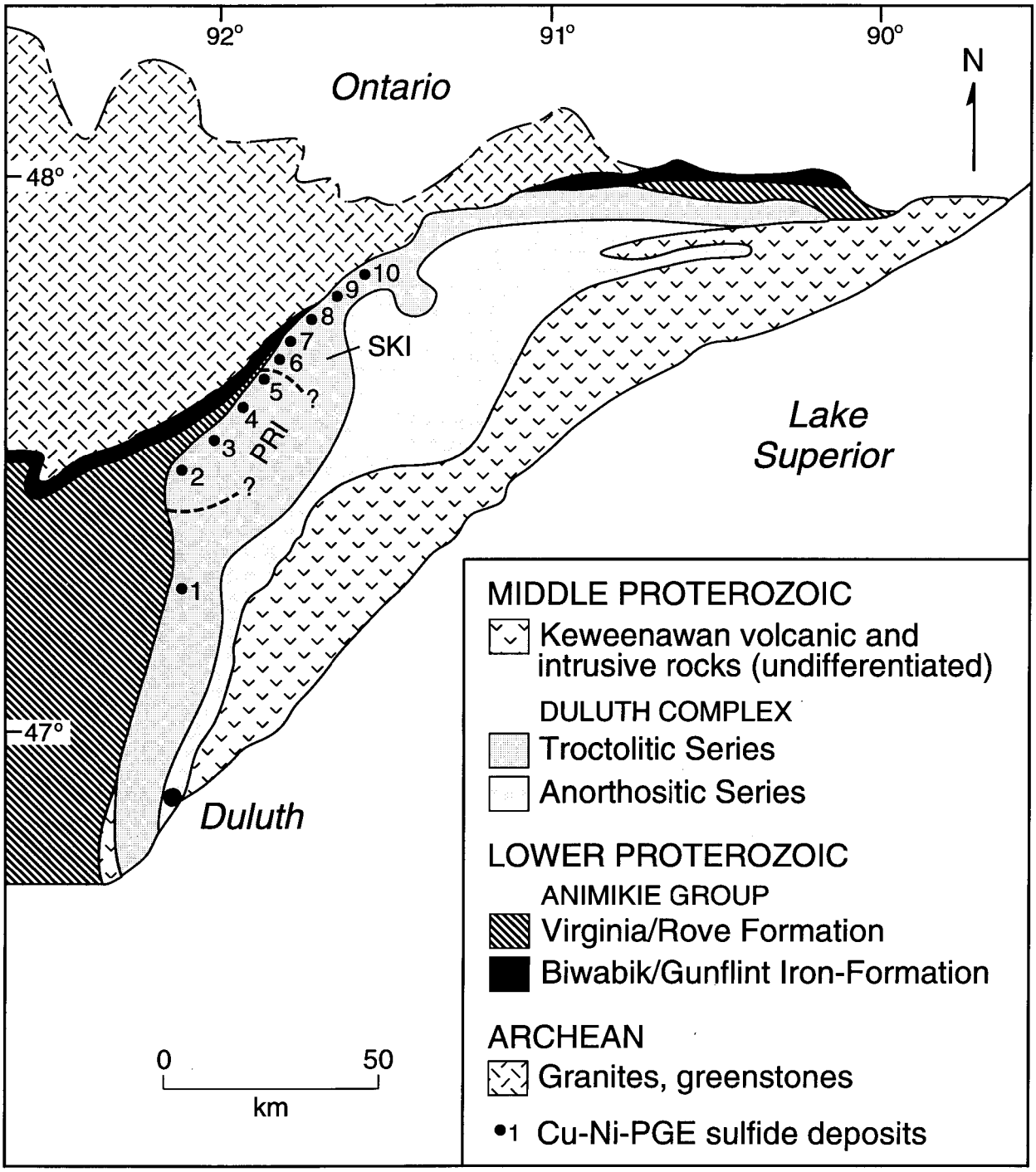

FIG. 1. Geological map showing the emplacement of the Duluth Complex and associated sulfide deposits within the Keweenawan flood basalt province of Central North America (modified after Naldrett 1989). PRI: Partridge River Intrusion, SKI: South Kawishiwi intrusion. Black circles represent Cu-Ni-PGE sulfide deposits (1: Water Hen; 2: Wyman Creek; 3: Wetlegs; 4: Dunka Road; 5: Babbitt; 6: Serpentine; 7: Dunka Pit; 8: Birch Lake; 9: Maturi; 10: Spruce Road).

(Listerud and Meineke, 1977). The sulfide-bearing intrusions occur along the northwestern margin of the complex, where they intrude Proterozoic metasedimentary rocks of the Virginia Formation and Biwabik Iron-formation (Fig. 1). The latter is composed of cherty and slaty banded-iron formation (Morey, 1992), whereas the overlying Virginia Formation consists mainly of argillite, siltstone, and greywacke. The argillaceous horizons are commonly graphitic and sulfide-bearing near the base of the Virginia Formation, and locally contain up to 15 percent thinly laminated pyrrhotite (i.e. bedded pyrrhotite unit; Severson et al., 1996). Magma contamination through assimilation of the sulfide-rich argillaceous rocks has generally been invoked to explain the origin of the Cu-Ni-PGE mineralization (Mainwaring and Naldrett, 1977; Ripley, 1981, 1986a; Rao and Ripley, 1983; Tyson and Chang, 1984; Foose and Weiblen, 1986; Severson and Hauck, 1990; Severson, 1994; Thériault et al., 1997; Thériault and Barnes, 1998).

Geology of the Partridge River Intrusion

The Partridge River Intrusion is a troctolitic lopolith emplaced within shallow dipping, sulfide-bearing argillaceous rocks of the Virginia Formation. Four large but low grade Cu-Ni-PGE sulfide deposits have been outlined along the base of the intrusion through extensive exploration drilling, and these are referred to from west to east as the Wyman Creek, Wetlegs, Dunka Road and Babbitt deposits. The Local Boy and Tiger Boy ore zones, which contain significant amounts of semi-massive to massive sulfide mineralization, comprise the eastern portion of the Babbitt deposit (Fig. 2; inset). Although the southern limit of the four deposits remains unknown, geophysical evidence (Chandler and Ferderer, 1989) suggest that they

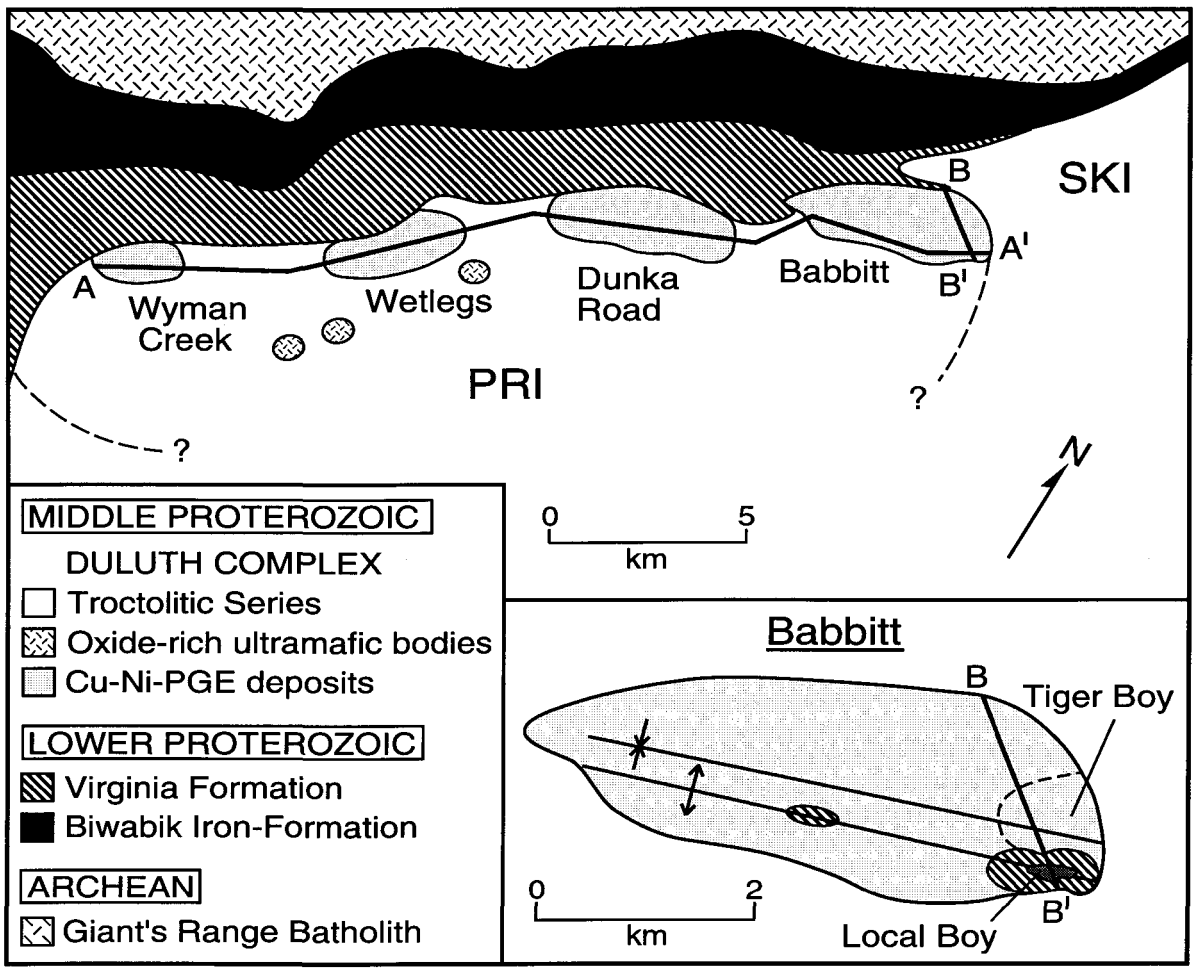

FIG. 2. Geological map showing the emplacement of the four Cu-Ni-PGE sulfide deposits of the Partridge River Intrusion (PRI). The inset shows the location of the Local Boy (dark grey) and Tiger Boy ore zones within the Babbitt deposit. Longitudinal cross sections A-A^1 and B-B^1 shown in figures 3 and 4 respectively.

could extend for some distance downdip due to the nearly coplanar nature of the basal contact with the Virginia Formation strata. Sulfide mineralization within each deposit appears to be largely concentrated along pre- and syn-Complex structural features present within the footwall Virginia Formation, namely northeast-trending normal faults and northwest-trending strike-slip faults at the Wyman Creek, Wetlegs, and Dunka Road deposits (Severson, 1988; Geerts, 1991; Severson and Hauck, 1997), and two parallel east-trending folds (i.e. Bathtub syncline and Local Boy anticline) at the Babbitt deposit (Severson and Barnes, 1991; Severson et al., 1994). Localized faulting and folding of the footwall rocks created important topographic irregularities along the basal contact, and thus greatly enhanced the potential for subsequent assimilation of the sulfide-bearing argillaceous rocks by the intruding mafic magma. This could have also changed the magma flow regime and possibly lead to massive sulfide formation.

Small discordant bodies of oxide-rich pyroxenite, peridotite and dunite occur predominantly in the vicinity of the Wetlegs and Wyman Creek deposits (Fig. 2). These ultramafic bodies represent potential Fe-Ti ore deposits (Severson, 1995), and possibly originate from partial melting of the Biwabik Iron-formation along the basal contact (Severson and Hauck, 1990).

As shown from a drill-hole-interpreted cross-section at the northern margin of the Partridge River Intrusion (Fig. 3), the igneous stratigraphy consists of a number of correlatable cyclic units, which for the most part, can be followed from Wyman Creek to the eastern portion of the Babbitt deposit (i.e. Local Boy and Tiger Boy ore zones) (Severson, 1994). Each cyclic unit generally consists of a thin ultramafic layer of melatroctolite to dunite (locally

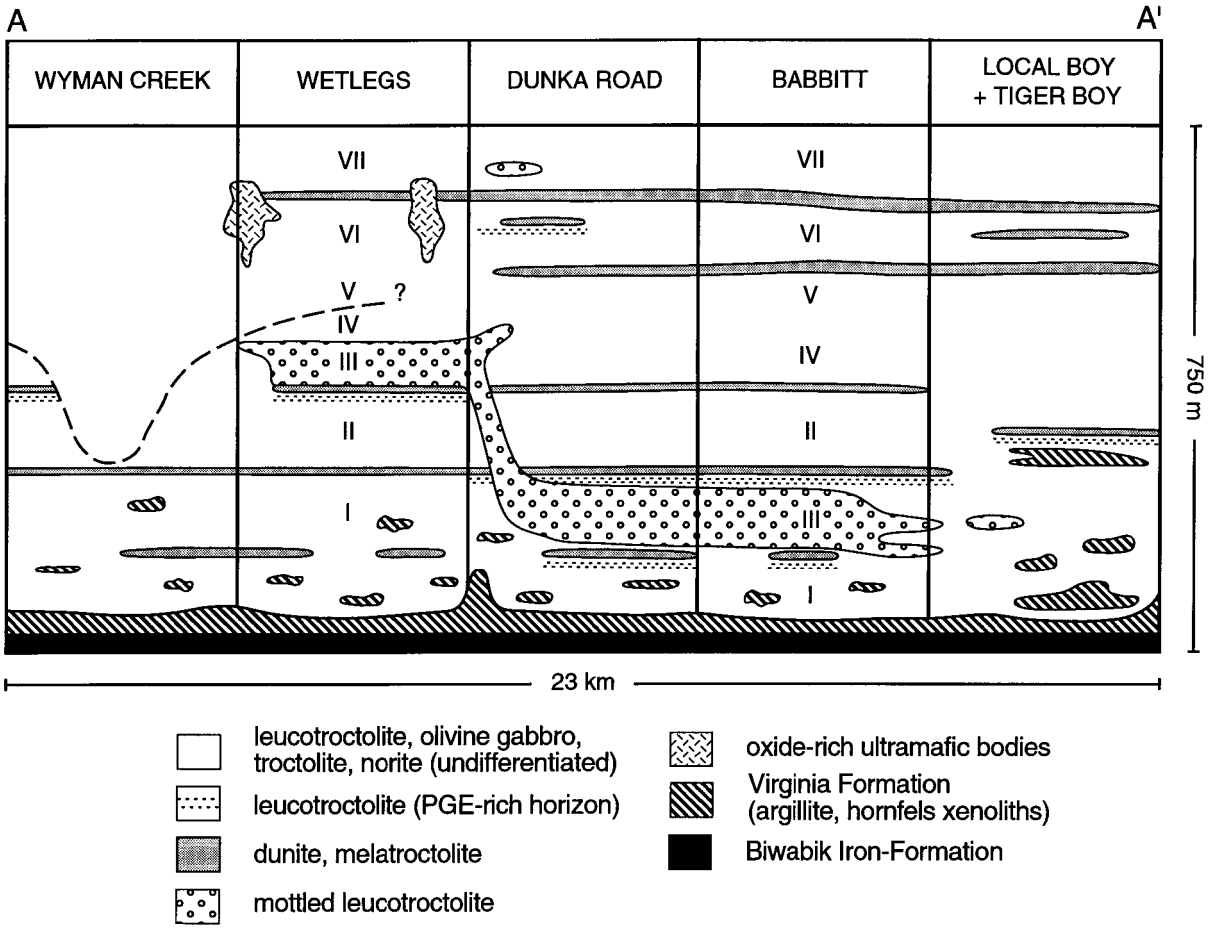

FIG. 3. SW-NE oriented longitudinal section across the four deposits of the Partridge River Intrusion, based on drill hole interpretation (modified after Severson and Hauck, 1997). Shallow drill holes in the Wyman Creek area prevented the extrapolation of the layering in the upper half of the section. Note that the uppermost mapped unit appears to have a downcutting relationship into older underlying layers.

discontinuous) overlain by a much thicker sequence of dominantly leucotroctolite and olivine gabbro, with minor troctolite and norite. The cyclic repetition of layers has been explained by periodic replenishment of new magma into the chamber (Severson and Hauck, 1990; Thériault et al., 1997). A unit of mottled leucotroctolite (Unit III of Severson, 1988) occurs along a 13 km strike length between the Wetlegs and Babbitt deposits. Although no definite intrusive relationships have been observed in drill core, the unit is here interpreted to be locally discordant to the igneous layering, based on its highly variable thickness and irregular distance away from the basal contact. Moreover, the presence of tongues and apophyses along its periphery also suggest that it was possibly intruded at a late stage in the crystallization history of the Partridge River Intrusion. The third author disagrees with the above interpretation, and believes that Unit III was emplaced at a much earlier stage, perhaps synchronous with the lowermost intrusive cycle, and that it is relatively flat lying (Hauck et al., 1997; their Fig. 6), whereas the basal contact is locally quite irregular as a result of the reactivation of pre- to syn-complex faults (Severson and Hauck, 1997).

While the upper cyclic units are generally well layered and contain very little sulfides, rocks forming the lower 200-300 m of the intrusion (i.e. Unit I of Severson and Hauck, 1990) are in contrast substantially mineralized and highly heterogeneous in terms of texture and composition. The proportion of olivine generally decreases at the expense of orthopyroxene towards the basal contact, such that olivine gabbro and norite become the most common rock types. Hornfels xenoliths derived from the underlying Virginia Formation comprise up to 25 percent of the lower sequence, and show a clear spatial relationship with a large part of the mineralization. Norite typically occurs in the vicinity of hornfels xenoliths, as well as directly

along the base of the intrusion. The norite has been interpreted to originate from mixing between the parental mafic magma and a granitic partial melt derived from the sulfide-bearing argillaceous country rocks (Thériault et al., 1997). Hence based on the above evidence, the highly heterogeneous and mineralized character of the basal part of the intrusion seemingly results from contamination of the parental troctolitic magma through mixing with derivatives from the underlying Virginia Formation.

A NW-SE trending cross-section of the Babbitt deposit in the Tiger Boy/Local Boy area (Fig. 4) clearly illustrates that the bulk of the sulfide mineralization occurs within the xenolith-bearing, lower portion of the intrusion. Semi-massive to massive sulfide lenses, which make up the Local Boy ore zone, are found along the axis and flanks of the Local Boy anticline, in the vicinity of two large xenoliths that reach up to 65 m in thickness and 600x1200 m in lateral extent (Figs. 2, 3, and 4) (Severson et al., 1996). The sulfide lenses occur both within and around xenoliths, as well as within the footwall rocks. A large xenolith measuring approximately 50x250x650 m in size also occurs above the anticlinal structure in the central part of the Babbitt deposit (see inset of Fig. 2). Although much less abundant than at Local Boy, semi-massive to massive sulfide lenses are also closely associated with this xenolith. The presence of such large raft-like xenoliths directly along the crest of the anticline strongly suggests that the magma was intruded within structurally-prepared footwall rocks. These likely consisted of sulfide-rich graphitic argillite (i.e. bedded pyrrhotite unit), on the basis of: 1) the relatively large amount of sulfides associated with the xenoliths and occurring within the footwall rocks; 2) the elevated and similar range of $\delta^{34}S$ and $\delta^{18}O$ values for both the basal

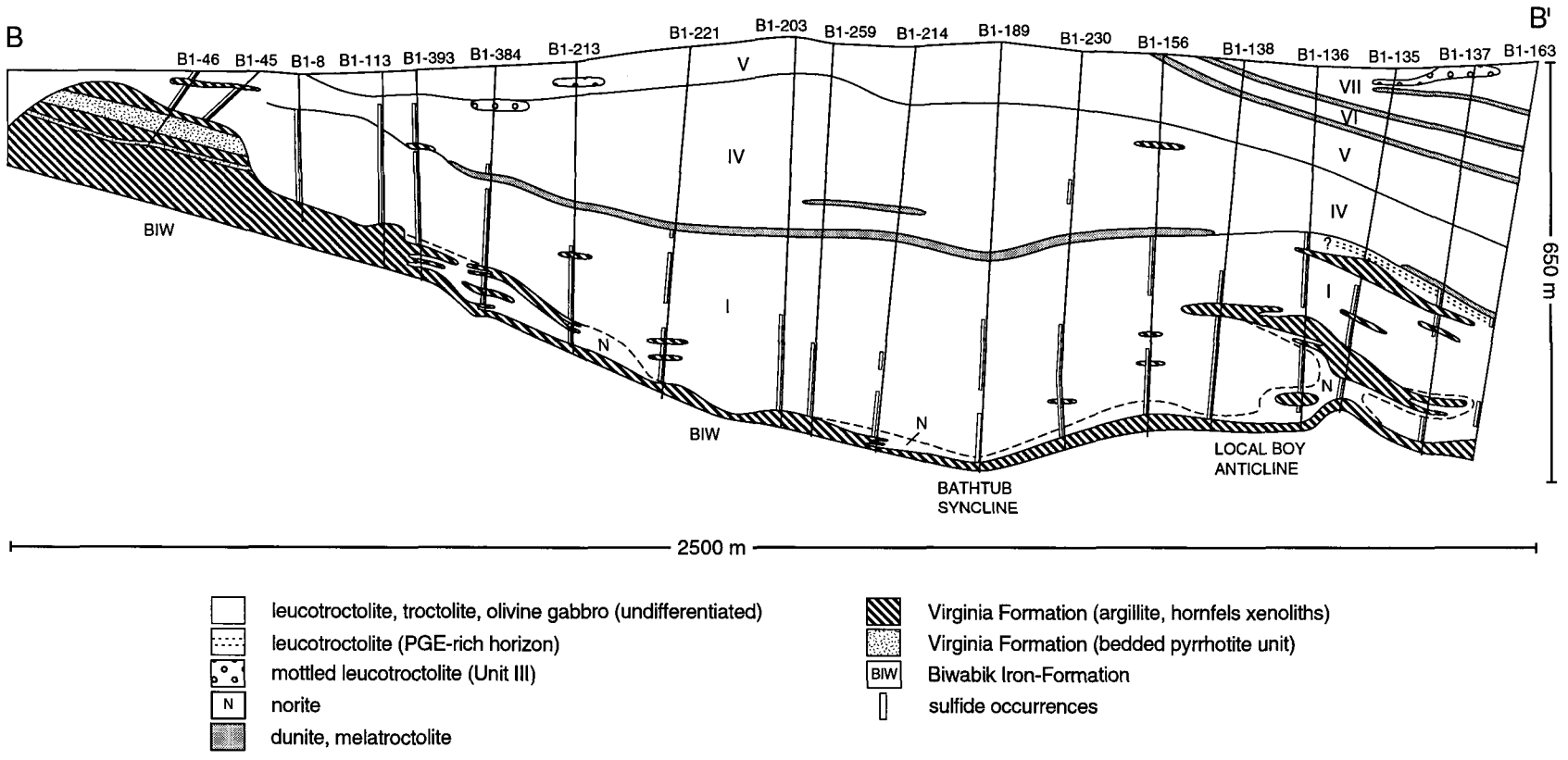

FIG. 4. NW-SE oriented longitudinal cross section of the eastern edge of the Babbitt deposit, based on drill hole interpretation (modified after Severson et al., 1996). Note that the Tiger Boy and Local Boy massive sulfide ore zones are spatially associated with the Bathtub syncline and Local Boy anticline, respectively.

mineralized rocks and adjacent metasedimentary rocks (Ripley and Al-Jassar, 1987); and 3) the abundance of preserved bedded pyrrhotite unit along the northern rim of the Partridge River Intrusion in the Babbitt area (see Fig. 4) (Severson et al., 1994). Geochemical modelling presented below also support such an origin for the sulfides. In contrast, Ripley (1986b) and Ripley and Al-Jassar (1987) suggest that the sulfides were transported from an underlying magma chamber.

A PGE-rich disseminated sulfide horizon was also found in the southern part of the Local Boy deposit (Fig. 4). Unfortunately, no samples were analyzed further to the north under the laterally persistent ultramafic layer present at the top of Unit I. It is however believed that the PGE-rich horizon likely extends in that direction based on the common presence of disseminated sulfides along this particular stratigraphic level.

Sulfide Mineralization in the Partridge River Intrusion

The four Cu-Ni-PGE sulfide deposits of the Partridge River Intrusion contain resources in excess of 2 billion tons. The bulk of the mineralization (>90 vol.%) consists of disseminated sulfides that typically occur within the lower 200-300 m of the intrusion. The disseminated sulfides generally comprise less than 5 vol. percent of the rock, and are dominantly interstitial to the silicate minerals. Significant amounts of semi-massive to massive sulfide mineralization, in the form of stringers, veins and lenses, occur near and within the basal contact in the Local Boy and Tiger Boy ore zones of the Babbitt deposit (Severson et al., 1994). Minor occurrences are also present in the western part of the Babbitt deposit (i.e. Bathtub area; Severson et al., 1994) as well as in the Dunka Road deposit (Thériault and

Barnes, 1998).

Sulfide mineralogy

The sulfide minerals generally consist of pyrrhotite, chalcopyrite, cubanite and pentlandite, with minor amounts of mackinawite, talnakhite, bornite, digenite, chalcocite, covellite, parkerite, sphalerite, and galena (Hauck et al., 1997, and references therein). The arsenide minerals maucherite, niccolite, and cobaltite-gersdorffite are also commonly found within sulfides near footwall rocks or country rock xenoliths (Severson and Barnes, 1991; Ripley and Chryssoulis, 1994; Thériault et al., 1997). Significant amounts of maucherite reaching up to 5 vol. percent was observed in footwall-hosted massive sulfides from the Local Boy ore zone (Severson and Barnes, 1991), occurring within Cu-rich sulfides (i.e. cubanite, chalcopyrite and talnakhite) in close association with sphalerite, native silver, and the bismuthian sulfide parkerite. Although uncommon, a number of occurrences of platinum-group minerals (PGM) were observed in association with the sulfide minerals (e.g., Ryan and Weiblen, 1984; Holst et al., 1986; Morton and Hauck, 1987; Kuhns et al., 1990; Mogessie et al., 1991; Thériault et al., 1997).

In this study, both PGE-poor (i.e. norite-hosted and troctolite-hosted sulfides of Thériault et al., 1997) and PGE-rich disseminated sulfides were observed in all four Cu-Ni-PGE deposits of the Partridge River Intrusion. This division in sulfide mineralization is clearly demonstrated at Dunka Road (Thériault et al., 1997; Thériault and Barnes, 1998), where disseminated sulfides found within heterogeneous and variably contaminated rocks of the lower part of the intrusion are generally PGE-poor, whereas disseminated sulfides occurring

within essentially uncontaminated leucotroctolitic rocks located directly beneath ultramafic layers are typically PGE-rich (see figs. 3 and 4). Although both types of disseminated sulfides are difficult to distinguish based on their sulfide mineralogy, the PGE-rich sulfides generally contain greater proportions of chalcopyrite, cubanite, and pentlandite, and are thus more enriched in Cu and Ni relative to the more pyrrhotite enriched, PGE-poor disseminated sulfides. Where present, massive sulfides generally have a higher pyrrhotite content than the PGE-poor disseminated sulfides.

Sulfide geochemistry

Table 1 shows the average metal concentrations of PGE-rich, PGE-poor, and semi-massive to massive sulfide mineralization for each Cu-Ni-PGE deposit of the Partridge River Intrusion, along with results of the modelling (i.e. degree of contamination and *R* factor). Both whole rock and recalculated values to 100 percent sulfides are given. The latter set of data was calculated for the purpose of comparing the different deposits in terms of the sulfide fraction composition for each type of mineralization.

Mantle normalized metal patterns of the sulfide fraction for each type of mineralization clearly illustrate differences in average composition for the different deposits (Figs. 5a-c). As shown in Figure 5a, patterns of the PGE-rich disseminated sulfides show a steady enrichment from Ni (25-35 x mantle) through to Pd (2,000-16,000 x mantle), with generally a slightly decreasing to flat pattern observed from Pd to Cu (8,000-10,000 x mantle). The Dunka Road and Wetlegs deposits are most strongly enriched in the noble metals Pd, Pt, and Au, with a moderate enrichment being observed at Babbitt and Local Boy. These all have a characteristic

Table 1. Average metal composition and results of the modelling of the different types of sulfide mineralization from the Cu-Ni-PGE deposits of the Partridge River Intrusion.

		n	S	Cu	Ni	Pd	Pt	Au	Cu/Pd	Cu/Ni	% cont.	*R* factor
BABBITT *(refs.: 1,2)*												
PGE-rich	(whole rock)	17	0,84	0,62	0,16	761	194	70	8200	3,89		
PGE-poor	(" ")	47	0,96	0,70	0,13	256	357	44	27500	5,29		
MS	(" ")	1	17,24	2,41	1,46	309	34	171	78200	1,65		
PGE-rich	(100%S)	17	36,00	26,85	7,24	36234	9556	2860	7400	3,71	10	7700
PGE-poor	(")	47	36,00	27,29	6,47	11067	5838	1151	24700	4,22	25	2400
MS	(")	1	36,00	5,04	3,05	644	72	358	78200	1,65	------	------
LOCAL BOY *(refs.: 1,2,3)*												
PGE-rich	(whole rock)	7	1,11	0,66	0,15	804	260	114	8200	4,50		
PGE-poor	(" ")	113	3,17	1,22	0,22	185	61	73	66100	5,63		
MS	(" ")	48	19,82	6,27	1,31	484	107	118	129600	4,78		
PGE-rich	(100%S)	7	36,00	21,75	4,78	28135	9214	4184	7700	4,55	5	6000
PGE-poor	(")	112	36,00	16,18	2,83	2683	905	923	60300	5,72	43	600
MS	(")	48	36,00	11,53	2,42	890	209	215	129500	4,76	~100	220
TIGER BOY *(refs.: 1,3)*												
PGE-poor	(whole rock)	44	2,07	1,12	0,22	211	133	49	53000	5,13		
MS	(" ")	8	19,20	5,36	1,30	262	15	19	204600	4,13		
PGE-poor	(100%S)	44	36,00	20,84	4,21	4624	1733	847	45100	4,95	35	1000
MS	(")	8	36,00	12,50	2,90	698	44	36	178400	4,31	~100	170
DUNKA ROAD *(refs.: 4,5,6,7,8)*												
PGE-rich	(whole rock)	69	------	0,57	0,13	1045	269	124	5400	4,50		
PGE-poor	(" ")	77	------	0,42	0,09	263	93	53	15900	4,43		
MS	(" ")	2	27,25	0,88	1,47	1035	22	35	8500	0,60		
PGE-rich	(100%S)	36	36,00	26,81	6,34	63831	15667	6706	4200	4,23	9	7100
PGE-poor	(")	23	36,00	15,09	4,25	9227	4275	2042	16400	3,55	18	1100
MS	(")	2	36,00	1,40	1,95	1257	26	47	11100	0,72	------	------
WETLEGS *(refs.: 2,4,8,9)*												
PGE-rich	(whole rock)	21	------	0,38	0,09	658	191	84	5700	4,21		
PGE-poor	(" ")	30	------	0,40	0,11	172	72	80	23200	3,92		
PGE-rich	(100%S)	10	36,00	29,35	7,11	58487	16197	7209	5000	4,13	13	6700
PGE-poor	(")	20	36,00	21,59	5,72	9685	4283	1452	22300	3,78	30	1200
WYMAN CREEK *(refs.: 2,4,7)*												
PGE-rich	(whole rock)	27	------	0,41	0,11	126	61	47	32100	3,66		
PGE-poor	(" ")	250	------	0,29	0,07	30	19	19	95300	4,20		
PGE-rich	(100%S)	22	36,00	23,35	6,32	8005	3829	2804	29200	3,69	9	7000
PGE-poor	(")	2	36,00	16,94	5,39	953	1725	960	177700	3,15	30	500
Parental magma *(ref: 10)*			<0,01	122	220	9,5	8,5	<1,5	12800	0,55		
Contaminant *(ref: 10)*			1,15	646	123	4,0	2,6	6,5	161500	5,25		

Notes: MS: includes semi-massive and massive sulfides; composition of the sulfide fraction (100% S) calculated assuming 36% S; % cont. (proportion of contaminant in hybrid magma) and *R* factor calculated using Cu and Pd values; references: 1: Patelke, 1994; 2: Severson and Hauck, 1997; 3: Ripley, 1990; 4: Severson and Hauck, 1990; 5: Geerts, 1991; 6: Thériault and Barnes, 1998; 7: Fleck Resources Ltd.; 8: International Platinum Company; 9: Department of Natural Resources, Minnesota; 10: Thériault et al., 1997

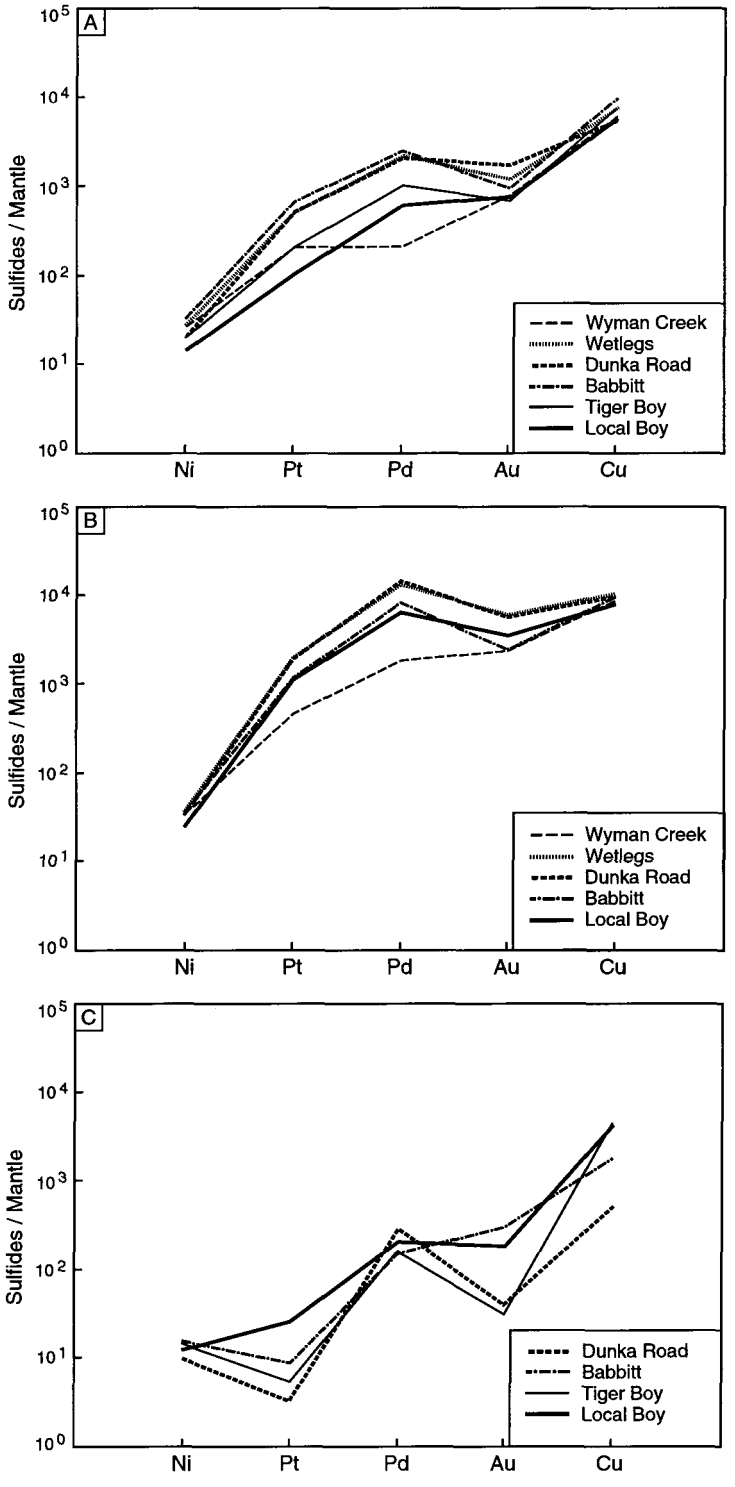

FIG. 5. Mantle-normalized metal patterns showing the range in composition of the three different types of sulfide mineralization; A) PGE-poor sulfides; B) PGE-rich sulfides; C) semi-massive to massive sulfides. Normalization factors are from Barnes et al. (1988).

arch-shaped pattern, which is typical of PGE-reefs throughout the world (Barnes et al., 1988). The PGE-rich sulfides of the Wyman Creek deposit contain, on the other hand, much lower noble metal concentrations that are in fact comparable to the PGE-poor disseminated sulfides of the Dunka Road and Wetlegs deposits (see Table 1). As for the base metals Ni and Cu, they have similar concentrations in the PGE-rich sulfides of the Dunka Road, Wetlegs, Wyman Creek and Babbitt deposits, while somewhat lower values are observed at the Local Boy ore zone. The higher PGE and Au content observed at Dunka Road and Wetlegs likely reflects the proximity of these deposits to the source of magma which fed the Partridge River Intrusion, as will be discussed later.

The mantle normalized metal patterns of the PGE-poor disseminated sulfides (Fig. 5b) show a steady enrichment from Ni (15-30 x mantle) to Cu (5,000-10,000 x mantle), with a slight negative Au anomaly. The Dunka Road, Wetlegs and Babbitt deposits generally have higher noble metal concentrations relative to the more depleted Tiger Boy and Local Boy ore zones and Wyman Creek deposit. This suggests that sulfides from the latter mineralized areas separated from a magma which had already segregated some sulfide liquid.

The mantle normalized metal patterns of the semi-massive to massive sulfides (Fig. 5c) have a different shape than that of the two types of disseminated sulfide mineralization, possessing negative anomalies for Pt and Au and generally much lower metal contents, especially at Dunka Road and Tiger Boy. The strong negative anomalies for Pt and Au of the massive sulfides from the Dunka Road deposit have been interpreted by Thériault and Barnes (1998) to represent a cumulate of monosulfide solid solution (*mss*), with Pt and Au being strongly incompatible and concentrating in the residual sulfide liquid. The same interpretation

is here given for the origin of the Tiger Boy massive sulfides. Similar shaped patterns have also been described from massive sulfides of the Noril'sk-Talnakh District (Zientek et al., 1994; Barnes et al., 1997), the Cape Smith Fold Belt (Barnes et al., 1997) and the Stillwater Complex (Zientek et al., 1994). The much less developed negative Pt and Au anomalies observed at Babbitt and Local Boy suggest that these massive sulfides are not *mss* cumulates, and like the two types of disseminated sulfides, likely represent near sulfide liquid compositions.

Modelling the Composition of the Sulfides

The composition of over 760 sulfide-bearing samples from the Partridge River Intrusion was modelled using the following equilibrium fractionation equation developed by Campbell and Naldrett (1979):

$$[1]\ C_C = C_L D(R+1)/(R + D)$$

where C_C= the concentration of the metal in the sulfide; C_L= the concentration of the metal in the silicate melt; D= the partition coefficient of the metal between the sulfide liquid and the silicate melt; and *R*= the ratio of silicate melt to sulfide liquid (*R* factor).

For each deposit, results of the modelling are plotted on the Cu/Pd versus Pd diagram of Barnes et al. (1993) (Figs. 6a-f). The diagram is subdivided into 3 separate fields: 1) "depleted", for rocks that have Cu/Pd ratios greater than mantle and are thus depleted in Pd relative to Cu; 2) "undepleted", which represents the range of mantle-derived rocks; and 3) "enriched", for PGE-rich rocks having a low Cu/Pd ratio indicative of Pd enrichment relative

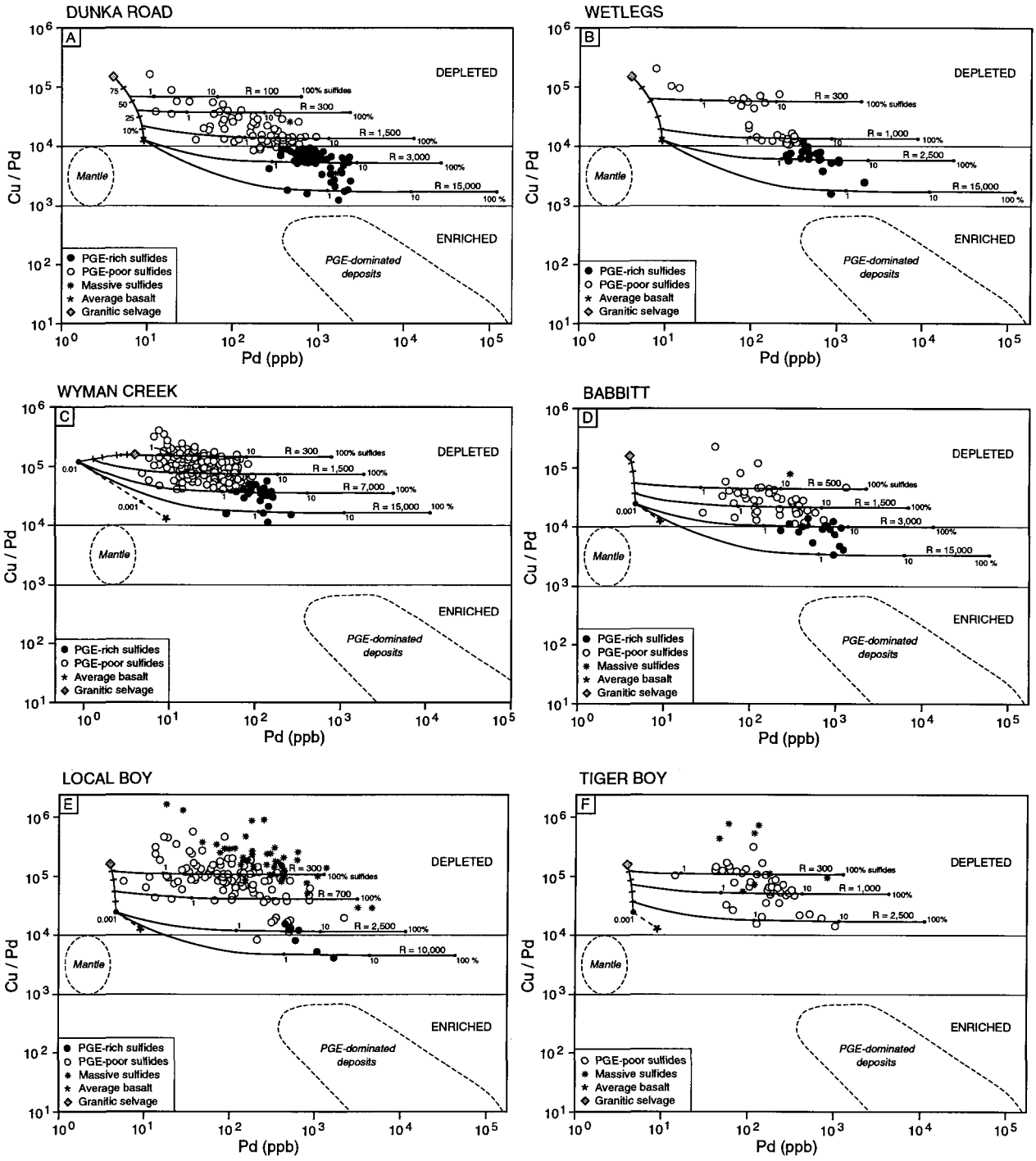

FIG. 6. Plot of Cu/Pd vs. Pd showing the composition of the three types of sulfide mineralization and the results of modelling for the six mineralized areas. Fields of mantle rocks and PGE-dominated deposits (e.g., PGE reefs from the Bushveld, Stillwater and Penikat intrusions) taken from Barnes et al. (1993).

to Cu.

As shown in Figures 6a and 6b, the proposed parental magma (i.e. average Keweenawan flood basalt composition; Table 1) from which the sulfides segregated to form the Dunka Road and Wetlegs deposits has a high Cu/Pd ratio (i.e., 12,800) which plots outside the expected range for mantle-derived rocks. This suggests that the basaltic magma segregated sulfides at depth, becoming depleted in Pd relative to Cu due to the much higher partition coefficient of the former into the sulfide melt (i.e. 100,000 and 2,000, respectively; Peach et al., 1994; Barnes and Francis, 1995). The metal content of the hypothetical initial magma prior to sulfide segregation may be estimated from the following equilibrium fractionation equation:

[2] $C_F/C_L = 1/[1 + X(D-1)/100]$

where C_F/C_L (depletion factor) = the concentration of the metal in the fractionated magma (i.e., parental basalt) divided by the concentration of the metal in the initial magma; D = the partition coefficient of the metal between the sulfide melt and the silicate magma; and X = the amount of segregated sulfides in weight percent. Assuming that the initial magma had a Cu/Pd value within the range of mantle-derived rocks, calculations show that 0.0005 to 0.01 wt. percent sulfide may have been removed from the magma at depth prior to emplacement of the Partridge River Intrusion at the actual site of the Dunka Road and Wetlegs deposits (Thériault et al., 1997, their Fig. 8). A similar interpretation was given by Saini-Eidukat (1991), who calculated that up to 0.1 wt. percent sulfide appears to have segregated at depth within a possible auxiliary magma chamber. Results of the modelling further suggest that an additional 0.001 wt. percent sulfide may have been removed from the magma prior to the segregation of

the sulfides in the Babbitt, Local Boy and Tiger Boy areas (see dashed curve in Figs. 6d, e and f, respectively). An even greater amount of sulfide (i.e., 0.01 wt.%) is interpreted to have segregated from the parental magma which gave rise to the Wyman Creek deposit (Fig. 6c). This additional event of sulfide extraction is clearly reflected in the metal depleted nature and low Cu/Pd values of the latter mineralized areas relative to the Dunka Road and Wetlegs deposits (see Table 1). The reason for this apparent decrease in noble metal content towards the southwestern and northeastern margins of the Partridge River Intrusion will be further discussed later.

The composition of the contaminant used in the modelling is represented by a granitic selvage sampled along the margin of a partially melted argillaceous xenolith, near the base of the Dunka Road deposit (Thériault et al., 1997; sample DC-80, their Table 1). The granitic partial melt has a very high Cu/Pd ratio (i.e., 159,900) which reflects the very low Pd content of the source argillite. For each of the deposits, the sulfides are interpreted to have interacted with a hybrid or daughter magma formed through the mixing of variable proportions of parental mafic magma and granitic partial melt. Hence in the modelling, magma compositions from which the sulfides segregated lie along a mixing line between the contaminant and the composition of the parental magma (Fig. 6). Each selected daughter magma represents the outset of a tie line linking its composition to that of sulfides in equilibrium with this magma. An infinite number of tie lines may be generated from the same daughter magma composition by simply changing the *R* factor. As shown on the diagram, increases in *R* factor yield compositions having lower Cu/Pd ratio and higher Pd contents due to the higher partition coefficient of Pd into sulfides relative to Cu. Hence the grade of the mineralization is

influenced by both the metal content of the daughter magma and the volume of silicate melt with which the sulfide liquid interacted (respectively C_L and R in equation 1). Finally, the black dots along each tie line indicate the Cu/Pd ratio and Pd content of rocks that would contain 1, 10, and 100 percent sulfides. An important constraint on the modelling is that the sulfide content of the analyzed samples must match the computed amount of sulfide, the latter being given by the location of the black dots along a particular tie line. Furthermore, the computed R factor and degree of contamination must be in accordance with the geochemical and mineralogical attributes characterizing each type of mineralization.

PGE-rich disseminated sulfides

Moderate to high R factors varying between approximately 2,500 and 17,000 were used to model the composition of the samples of PGE-rich disseminated sulfides from the various deposits, assuming a daughter magma that had undergone little to no contamination (i.e. 0-15%). The relatively uncontaminated nature of the magma is clearly supported by the mantle-like sulfur isotopic values and S/Se ratios measured from this type of mineralization at the Dunka Road deposit (Ripley, 1981; Thériault and Barnes, 1998). The average modelled R factor and degree of contamination for each mineralized area is given in Table 1. Although the composition of the daughter magma with which the PGE-rich disseminated sulfides interacted varies significantly between the deposits, their average R factor (i.e. 6,000 to 7,700) and degree of contamination (i.e. 5 to 13%) shows very little variation. Each area also shows a similar range in R factor for this type of mineralization (see Figs. 6a to 6f).

The similar results obtained for the different deposits, in modelling of the PGE-rich

disseminated sulfides, suggests that this type of mineralization formed by a similar process throughout the Partridge River Intrusion. As was previously suggested by Thériault et al. (1997), the origin of all PGE-rich sulfide horizons sampled within the intrusion are interpreted to have formed from mixing between evolved and primitive magmas following a magma replenishment event. A similar model was proposed to explain the origin of thin but highly enriched PGE horizons (i.e. reefs) within the Bushveld and Stillwater intrusions (e.g., Campbell et al., 1983; Irvine et al., 1983).

PGE-poor disseminated sulfides

Most samples of PGE-poor disseminated sulfides from the various deposits of the Partridge River Intrusion were successfully modelled using low to moderate *R* factors ranging between 100 and 3,000, at generally moderate to high degrees of contamination varying from 10 to 75 percent. The average modelled *R* factor and degree of contamination for each mineralized area is given in Table 1.

The composition of the PGE-poor disseminated sulfide samples from the Dunka Road (Fig. 6a) and Wetlegs (Fig. 6b) deposits were modelled using *R* factors between 100 and 2,000 (mean of 1,100 and 1,200, respectively), and a daughter magma which had undergone 10 to 60 percent contamination (mean of 18% and 30%, respectively). The PGE-poor sulfides from the Babbitt deposit (Fig. 6d) were modelled using *R* factors generally ranging from 500 to 3,000 (mean of 2,400), and low degrees of contamination between 10 and 35 percent (mean of 25%). As for the Local Boy (Fig. 6e) and Tiger Boy (Fig. 6f) ore zones, their PGE-poor disseminated sulfides were modelled using *R* factors between 300 and 2,500 (mean of 600 and 1,000,

respectively), at highly variable degrees of contamination ranging from 10 to 75 percent (mean of 43% and 35%, respectively). Finally, low to moderate *R* factors between 300 and 2,500 (mean of 500) at degrees of contamination ranging from 10 to 60 percent (mean of 30%) were used to model the composition of the PGE-poor disseminated sulfides from the Wyman Creek deposit (Fig. 6c).

Of significant importance is the fact that we failed to model several samples from the Local Boy ore zone. These have Cu/Pd ratios considerably higher than the composition of the assumed contaminant. Possible reasons for this discrepancy include: 1) locally more Cu and/or less Pd in the contaminant; 2) bulk assimilation of Cu-rich country rocks (i.e. bedded pyrrhotite unit); or, 3) extreme Pd depletion and/or Cu enrichment of the daughter magma. It appears most likely that the higher Cu/Pd ratios are related to a significant addition of externally derived Cu in the magma, either through very high degrees of partial melting (bulk assimilation) of the sedimentary country rocks, or more simply due to the greater availability of Cu within the latter.

Note that although no distinction could be made in this study between PGE-poor norite-hosted and PGE-poor troctolite-hosted disseminated sulfides, as had been the case in previous studies on the Dunka Road deposit (Thériault et al., 1997; Thériault and Barnes, 1998), we interpret that the samples with the highest Cu/Pd ratios were more intensely contaminated and thus, for the most part, represent PGE-poor norite-hosted sulfides.

Semi-massive to massive sulfides

Semi-massive to massive sulfide mineralization was mainly encountered along the base

of the Local Boy and Tiger Boy ore zones, with few minor occurrences present also within the Dunka Road and Babbitt deposits. Due to the scattered nature of the latter, modelling was attempted only for the Local Boy (Fig. 6e) and Tiger Boy (Fig. 6f) semi-massive to massive sulfides. Results show that very low *R* factors are needed to model their composition (i.e. mean *R* factor of 220 and 170, respectively), from a highly contaminated daughter magma which appears to more or less correspond to the composition of the partial melt derived from the underlying sedimentary country rocks. Many samples from both ore zones could not be modelled due to their very elevated Cu/Pd ratio, which exceeds that of the granitic partial melt. As was the case for the PGE-poor disseminated sulfides from the Local Boy area, the Cu-rich composition of these samples could well be related to bulk assimilation of Cu-bearing sedimentary rocks, more specifically the bedded pyrrhotite unit, which is a dominant footwall rock along the northeastern margin of the Partridge River Intrusion (Severson et al., 1996). The high variability in Cu/Pd ratio of the semi-massive to massive sulfides is also likely due to the fact that they are probably, for the most part, not representative of true sulfide liquid compositions, having apparently fractionated early into Fe-rich cumulates of monosulfide solid solution (*mss*), with subsequent formation of evolved Cu-rich sulfides. Localized remobilization of this Cu-rich liquid could also explain some of the samples with extremely elevated Cu/Pd ratios.

Ni/Pd vs. Cu/Pt diagram

Mineralized samples from the various deposits are also presented on a metal ratio plot of Ni/Pd vs. Cu/Pt (Fig. 7), which was first introduced by Barnes et al. (1988) in order to evaluate

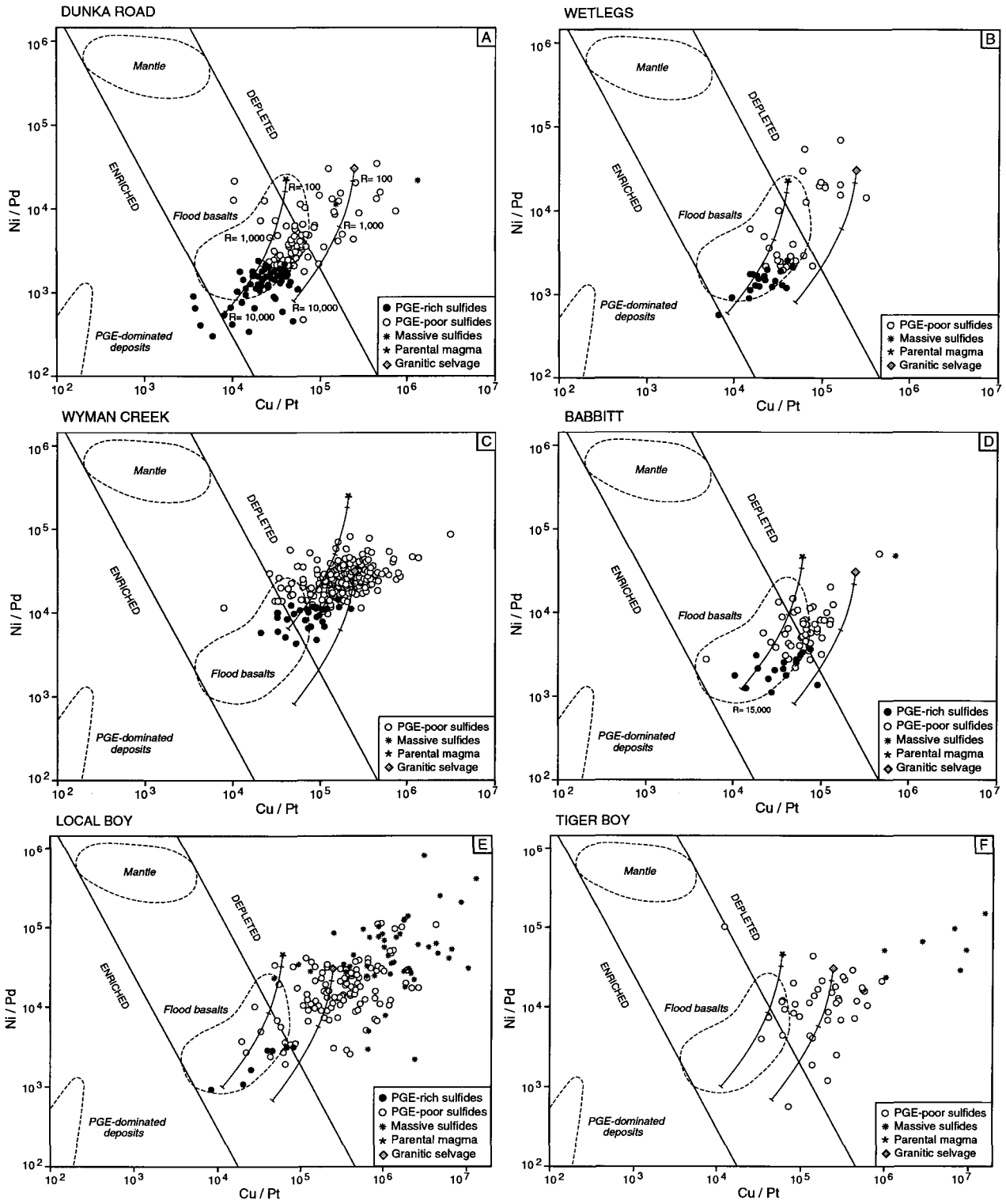

FIG. 7. Plot of Ni/Pd vs. Cu/Pt showing the composition of the three types of sulfide mineralization and the results of modelling for the six mineralized areas. Fields of mantle rocks, flood basalts and PGE-dominated deposits (e.g., PGE reefs from the Bushveld, Stillwater and Penikat intrusions) taken from Barnes et al. (1993).

the effects of partial melting, crystal fractionation and sulfide segregation on the composition of sulfides. As the Cu/Pd vs. Pd diagram, this plot is very useful in prospecting for PGE-rich, reef-type deposits (Barnes, 1990). Furthermore, the fact that it is a metal ratio plot enables one to compare the composition of different types of mineralization regardless of their sulfide content. As in the Cu/Pd vs. Pd diagram, the plot has been subdivided into three main fields (i.e. enriched; depleted; mantle), which allows comparison of the composition of each sample relative to that of the mantle in terms of the level of PGE enrichment. Also illustrated on the diagram are fields showing the range in composition of flood basalts, as well as reef-type PGE-dominated deposits. Note that the composition of the Keweenawan flood basalts plots slightly in the depleted field (Figs. 7a, b), further supporting the assumption that the magma became depleted in PGE en route to the surface through early precipitation of sulfides.

Samples from all types of sulfide mineralization are plotted on the diagram for the various deposits of the Partridge River Intrusion (Figs. 7a to 7f). Modelled curves at increasing *R* factor are also shown for both the parental magma and the granitic partial melt (i.e. end member compositions). Samples from PGE-rich disseminated sulfide horizons have typically lower Ni/Pd and Cu/Pt ratios than samples from PGE-poor disseminated sulfides, with very little overlap between the two types of mineralization. The PGE-rich samples from the Dunka Road (Fig. 7a), Wetlegs (Fig. 7b), Babbitt (Fig. 7d) and Local Boy (Fig. 7e) areas plot in the mantle field, with a few samples from the Dunka Road and Wetlegs deposits falling in the enriched field, whereas PGE-rich samples from the Wyman Creek deposit (Fig. 7c), although occurring along similar «reef-type» horizons, are characteristically depleted in PGE relative to the mantle. This feature further demonstrates the significant depletion in PGE of the parental

magma from which sulfides segregated to form the Wyman Creek deposit. Hence, the variation in composition of the PGE-rich disseminated sulfides observed across the Partridge River Intrusion is seemingly related to the variable metal content of the magma at the time of sulfide segregation. However, the similarity in the computed *R* factor and degree of contamination clearly point to a common mode of origin for this type of mineralization throughout the Partridge River Intrusion.

As was the case with the Cu/Pd vs. Pd diagram, most samples of semi-massive to massive sulfides from the Tiger Boy and Local Boy ore zone (as well as PGE-poor disseminated sulfides from the latter) show a very strong depletion in PGE, as illustrated by their very elevated Cu/Pt and Ni/Pd ratios (Figs. 7e, f). The positive correlation observed between the two ratios suggest that significant amounts of both Cu and Ni were likely added from the sedimentary rocks through partial melting, with external addition of PGE being minimal. Furthermore, samples having Cu/Pt and Ni/Pd ratios above 10^5 and 10^4, respectively, appear to become gradually more enriched in Cu relative to Ni with increasing degree of PGE depletion, as is suggested by the general decrease in slope observed when all samples are compared together. This also characterizes PGE-poor disseminated sulfide samples from the Dunka Road and Wyman Creek deposits, and further supports an external source for a large part of the Cu.

Discussion

Origin of sulfide mineralization

As pointed out by Thériault and Barnes (1998) for the Dunka Road deposit, compositional variations observed in the Cu-Ni-PGE magmatic sulfides for the various deposits of the Partridge River Intrusion may best be explained by varying degrees of country rock assimilation, which in turn had a strong control on the amount of interaction between the sulfide liquid and the silicate melt (*R* factor). Although irregular on a small scale of observation (i.e. <10 m), variations in sulfide composition (manifested ultimately by changes in the type of mineralization) are somewhat systematic when the Dunka Road deposit is interpreted as a whole. This relationship is expressed by the general decrease in the metal concentration of the sulfides towards the base of the intrusion. Such changes in composition are clearly associated with an increase in the degree of contamination, with a concomitant decrease in the *R* factor. This likely results from the introduction of partial melt from the underlying metasedimentary country rocks during emplacement of the mafic magma, the partial melt being cooler than the latter, leading to early crystallization of the magma at low *R* factors in areas where the effects of contamination were more important. We would apply the same interpretation to the PGE-poor and PGE-rich disseminated sulfides found within the Wyman Creek, Wetlegs and Babbitt deposits, as well as the Local Boy and Tiger Boy ore zones.

The systematic relationship between the degree of contamination and the *R* factor for the different types of sulfide mineralization is illustrated in Figure 8 for the six mineralized areas. A sharp increase in the mean *R* factor is observed from the massive sulfides (150-220) to the PGE-rich sulfides (6,000-7,700), with the PGE-poor sulfides having intermediate values (500-

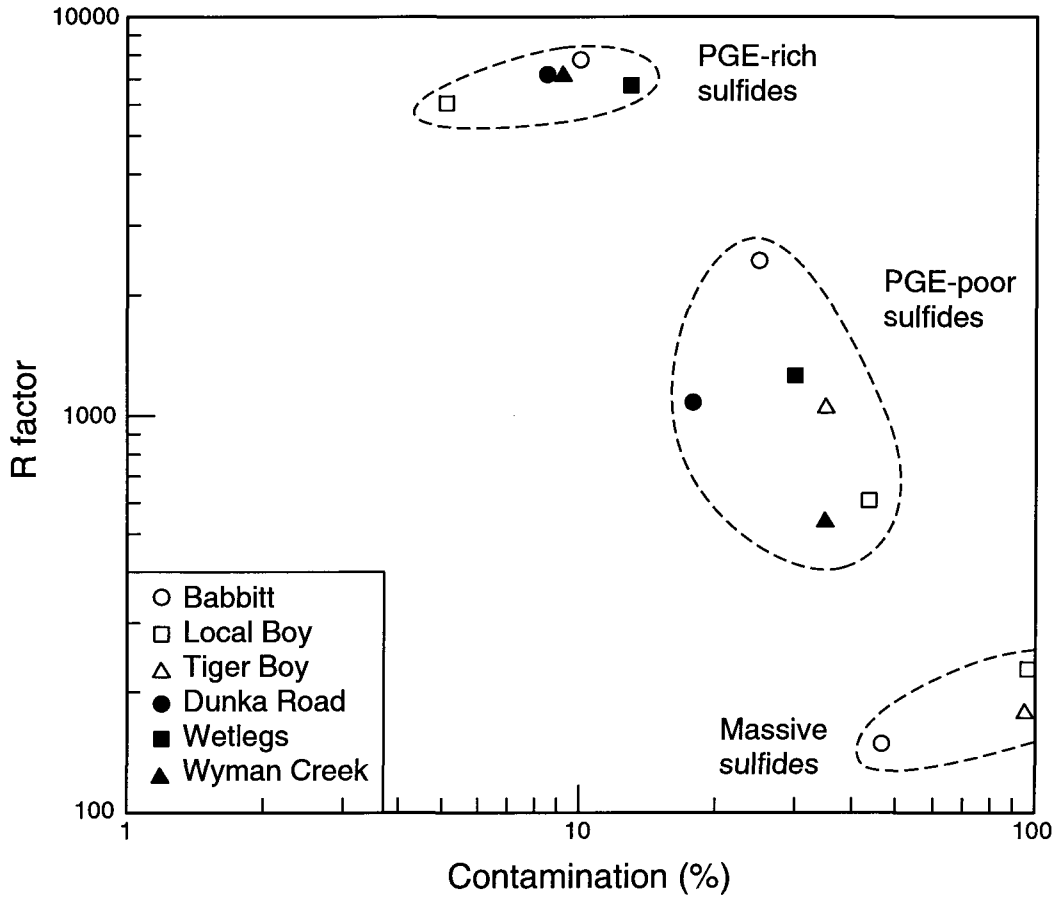

FIG. 8. Plot of *R* factor vs. degree of contamination (%) comparing the three types of sulfide mineralization from the different deposits and ore zones of the Partridge River Intrusion. Values refer to those of Table 1.

2,400). This is associated with a concomitant decrease in the degree of contamination from near 100 percent contamination for the massive sulfides down to approximately 10 percent contamination in the case of the PGE-rich sulfides, while the PGE-poor sulfides have intermediate values averaging about 30 percent contamination.

In all the deposits, the PGE-poor sulfides occur largely within the lower 250 m of the intrusion. The more contaminated and metal-depleted samples from this type of mineralization typically formed along the basal contact or surrounding country rock xenoliths, that is where the effects of country rock assimilation were most significant. Mixing between a silica-rich, sulfide-bearing partial melt and the intruding tholeiitic mafic magma led to the early crystallization of metal-depleted, sulfide-bearing norite (referred as norite-hosted sulfide mineralization at Dunka Road; Thériault et al., 1997). The remaining PGE-poor disseminated sulfides likely formed at a slightly later stage, thus having the opportunity to interact with a greater volume of mafic magma and attain larger *R* factors, which explains their higher metal content. Hence, magma contamination by the silica-rich partial melt was less important, such that the mineralization is hosted mostly in leucotroctolite or olivine gabbro (referred as troctolite-hosted sulfide mineralization at Dunka Road; Thériault et al., 1997). Apart from host rock composition, further evidence of country rock assimilation noted towards the base of the intrusion in the Dunka Road area include: 1) increase in sulfur isotopic values and S/Se ratios; 2) increase in pyrrhotite and arsenide minerals at the expense of base metal sulfides; 3) increase in the proportion of hexagonal pyrrhotite relative to the monoclinic variety; 4) increase in the content of orthopyroxene and ilmenite at the expense of olivine and magnetite, respectively; 5) increase in the content of biotite and sulfide; and 6) increase in incompatible

trace elements such as Ta, Cs, Rb, Ba, Th, U and K, as well as the metals As and Sb (Thériault et al., 1997; Thériault and Barnes, 1998).

The PGE-rich sulfide mineralization occurs anywhere between 100 and 600 meters above the basal contact, forming thin (<25 m) but laterally persistent horizons of disseminated sulfides located directly underneath ultramafic layers. While the PGE-poor sulfides are more or less confined to the mineralized areas, the PGE-rich sulfide horizons probably extend laterally for considerable distances between the deposits (see Fig. 3). The metal enriched sulfides are interpreted to have separated from relatively uncontaminated batches of tholeiitic magma following their injection above the partly solidified, mineralized units of the lower part of the intrusion. The intruding primitive magma mixed with the resident fractionated magma present above the cumulate pile, leading to sulfide saturation and formation of a sulfide liquid. It is interpreted that a relatively low volume of sulfide liquid swirled within the turbulently flowing mafic magma, hence achieving very elevated *R* factors in the order of 5,000 to 15,000. As the flow rate of the magma decreased, the metal enriched sulfide liquid percolated downward into the partly consolidated troctolitic crystal mush, and eventually crystallized to form a PGE-rich disseminated sulfide horizon. It appears that the sulfur was largely derived from the mafic magma (i.e. little to no contamination), since the PGE-rich mineralized rocks exhibit low sulfur isotopic values ($\delta^{34}S$= +1.6 to +2.5‰) and S/Se ratios (2100-3100) close to those typical of the mantle (Thériault and Barnes, 1998).

Significant quantities of semi-massive to massive sulfides in the form of stringers, veins and lenses occur along the basal contact at the Local Boy and Tiger Boy ore zones. Minor

occurrences are also present within the Dunka Road deposit and the western part of the Babbitt deposit. When all types of disseminated and massive sulfide mineralization are compared at 100 percent sulfides, it becomes clear that the massive sulfides found throughout the Partridge River Intrusion are significantly depleted in metals relative to the disseminated sulfides (see Table 1). Modelling, with use of the Cu/Pd vs. Pd diagram, demonstrates that the lower metal content of the massive sulfides relates to an increase in the degree of contamination observed toward the base of the intrusion. This effect, in turn, reduced the amount of interaction between the silicate magma and the sulfide melt (i.e. the *R* factor). In other words, mixing of a silica-rich partial melt with the mafic magma lowered the temperature of the hybrid noritic magma, and thus, the sulfide melt had less time to interact with the magma as its liquidus temperature was attained at a relatively early stage. Furthermore, it is well known that felsification of a mafic magma through assimilation of a silica-rich partial melt is one of the key factors that can lead to sulfide immiscibility, and ultimately to the formation of a Ni-Cu magmatic sulfide deposit (MacLean, 1969; Naldrett, 1997). The lower metal content of the massive sulfides may also be explained partly by the dilution of metals in the mafic magma as a result of its mixing with a metal depleted granitic melt.

The Local Boy ore zone of the Babbitt Cu-Ni deposit represents by far the largest accumulation of semi-massive to massive sulfides known in the Duluth Complex. The mineralization typically occurs both along and below the base of the intrusion in an area measuring approximately 250 by 700 meters. Reserves in the order of 5.3 million tons of ore grading 2.71 percent Cu and 0.55 percent Ni, at a cut-off grade of 1.0 percent Cu, have been

calculated by Severson and Barnes (1991). A large proportion of the massive sulfide mineralization occurs as veins and lenses within the fractured footwall rocks, which suggests that the sulfides could be derived from partial melting of sulfide-rich sedimentary units within the Virginia Formation (i.e. bedded pyrrhotite unit), as was originally proposed by Hauck et al. (1995). Of particular interest is the fact that these sulfides are mainly found along the crest and flanks of the Local Boy anticline (see Figs. 2 and 4), which is counter-intuitive considering the higher density of the sulfide melt. The accumulation of large amounts of massive sulfides within the anticlinal fold strongly suggests that structural preparation of the footwall rocks (i.e. buckling) exerted a strong control on the emplacement of the mineralization by providing dilatant zones (Severson and Barnes, 1991). The absence of the uppermost two submembers (termed A and B) of the Biwabik Formation along the north flank of the Bathtub syncline led Severson et al. (1994) to suggest that folding of the underlying sedimentary strata was initiated at the end of the depositional period of the Biwabik Formation, that is well before the emplacement of the Partridge River Intrusion. The fact that there is no systematic downward increase in sulfide content within the basal troctolitic rocks (Severson, 1998), as would be expected if the sulfides had accumulated via a gravitational settling mechanism, also points to an origin whereby the sulfides originate from the partial melting of the underlying, S-rich sedimentary rocks of the Virginia Formation. It is however uncertain weather the massive sulfides formed in situ or were injected into the anticlinal structure, although the later interpretation is here favored in light of the apparent increase in the thickness of the massive sulfides towards a possible feeder vent to the east (i.e. Grano fault) (Severson, 1998). Important quantities of maucherite ($Ni_{11}As_8$) are identified within the massive sulfides, in

close association with sphalerite, zincian hercynite, parkerite ($Ni_3Bi_2S_2$) and native silver (Severson and Barnes, 1991). The common presence and intimate association of these phases in the massive sulfides suggest a sedimentary derivation of As, Zn, Bi and Ag owing to their typically elevated concentrations in the bedded pyrrhotite unit (from Patelke, 1994), which further supports the contention that wholesale assimilation was a key process in the genesis of the Local Boy ore zone. It is noteworthy mentioning that massive sulfides from the Serpentine deposit, which occurs 4 km to the north within the adjacent South Kawishiwi troctolitic intrusion, also accumulated along and within the basal contact in close association with sulfide-rich footwall units of the Virginia Formation. An origin by partial to complete melting of the sulfide-bearing sedimentary rocks was also proposed for the formation of these massive sulfides (Hauck et al., 1997).

Although the average composition of massive sulfides from a particular deposit shows a significant depletion in all metals relative to PGE-poor and PGE-rich disseminated sulfides (when recalculated at 100% sulfides), a number of massive sulfide samples are nonetheless significantly enriched in Cu, especially from the Local Boy and Tiger Boy ore zones. These Cu-rich samples usually contain 20-30 percent Cu when recalculated to 100 percent sulfides, which implies that they consist of 60-90 percent chalcopyrite and cubanite, with lower amounts of pyrrhotite and pentlandite. They also have very elevated Cu/Ni ratios that range between 7 and 32. Contrastingly, a second group of massive sulfide samples are Fe-rich, and contain low levels of Cu (1-5%) and Ni (1-3%) associated with relatively low Cu/Ni ratios that vary between 1 and 2. As was demonstrated at Dunka Road (Thériault and Barnes, 1998), this association of Cu-rich and Fe-rich massive sulfides strongly suggests that the sulfide liquid

underwent fractional crystallization, forming an Fe-rich cumulate of monosulfide solid solution (*mss*), with concentration of Cu in the residual sulfide liquid. This Cu-rich liquid accumulated along the margins of the massive sulfide veins and lenses, and eventually crystallized into mainly chalcopyrite and cubanite. Meanwhile, the *mss* exsolved into pyrrhotite and pentlandite, forming the metal-poor and Fe-rich portions of the massive sulfide bodies. Such an interpretation was also recently proposed by Severson (1998) and Peterson (1998) for the Local Boy ore zone, and is in accordance with the observation that the Cu-rich sulfides often occur well into the footwall rocks or along the top and/or basal part of massive sulfide lenses (Severson and Barnes, 1991). Injection of Cu-rich ore into underlying footwall rocks is characteristic of the vein-like massive sulfide mineralization described from the Sudbury Igneous Complex (e.g. Naldrett et al., 1982; Li et al., 1992; Naldrett et al., 1994).

Feeder zone of the Partridge River Intrusion

Several lines of evidence suggest that the feeder zone for the Partridge River Intrusion may be situated somewhere between the Wetlegs and Dunka Road deposits. These include: 1) lateral variations in the Cu/Pd ratio of the assumed parental magma; 2) presence of a mottled leucotroctolite unit (i.e. Unit III of Severson, 1988) of limited lateral extent that shows important thickness variations; and 3) presence of a ramp of Virginia Formation strata along the basal contact.

As was demonstrated by modelling, sulfides forming the different deposits of the Partridge River Intrusion are interpreted to have separated from a magma that was sulfide saturated prior to emplacement. Of significant importance is the sharp increase noted in the

Cu/Pd ratio of the "residual" magma, from which sulfides segregated to form the "more distal" Wyman Creek and Babbitt deposits (including the Local Boy and Tiger Boy ore zones). These deposits are situated respectively along the southwestern and northeastern margins of the Partridge River Intrusion, which strongly suggests that the parental magma was emplaced originally along the central part of the intrusion, that is, in the vicinity of the Dunka Road and Wetlegs deposits (see Fig. 2). Results of the modelling show that sulfides from these two deposits formed from a magma that had a much lower Cu/Pd ratio than the other deposits (see Fig. 6), implying that it contained a greater amount of metals, particularly in the highly chalcophile platinum-group elements. Segregation of sulfides at the site of the Dunka Road and Wetlegs deposits could have caused the resultant magma to become depleted in metals prior to its arrival in the Wyman Creek and Babbitt area, as suggested by its apparent increase in Cu/Pd ratio. Hence, sulfides that ultimately separated from this metal-depleted magma during formation of the latter deposits have very elevated Cu/Pd ratios (see Table 1). The application of Cu/Pd ratios as a geochemical tool in the exploration for PGE-rich horizons in layered mafic intrusions has been demonstrated very efficiently in the case of the Bushveld Complex (Maier et al., 1996, 1998) and the Munni Munni Complex (Barnes et al., 1993). Interestingly, a similar lateral increase in Cu/Pd ratio with distance away from an apparent feeder zone has been interpreted by Maier et al. (1998) for the western Bushveld Complex.

As described earlier, a unit of mottled leucotroctolite averaging 80 m in thickness occurs anywhere between 100 and 400 meters from the base of the intrusion in the Wetlegs, Dunka Road and southwestern part of the Babbitt deposits (Fig. 3). The unit varies from less than 10 m to as much as 150 m in thickness, and was first recognized by Severson (1988) during

detailed relogging of over 30 000 m of drill core throughout the Partridge River Intrusion. A number of key characteristics of the mottled leucotroctolite unit suggest that it was emplaced as a separate injection of magma, and that the feeder to this magma was located approximately between the Wetlegs and Dunka Road deposit. Several of these salient features were originally described by Severson (1988) and Severson and Hauck (1990, 1997), and include: 1) the usually sharp upper (+/- lower) contact of the mottled leucotroctolite unit with the overlying units, especially near the assumed location of the feeder zone (see Fig. 3); 2) the apparent presence of tongues and apophyses along its periphery and the fact it pinches out laterally; 3) the typically finer grained (1-2 mm) texture of plagioclase laths relative to other units; 4) the presence of large (1-3 cm) poikilitic crystals of olivine, which is a texture unique to this unit and is suggestive of different cooling conditions and/or magma composition; 5) the presence of a thin oxide-rich zone at the top of the unit in the Wetlegs area, consisting of Cr-bearing titanomagnetite poikilitically enclosed in both plagioclase and olivine; and 6) the presence of partly resorbed plagioclase xenocrysts within a very fine grained mafic rock of unknown origin found only in 3-4 drill holes underneath the mottled leucotroctolite unit in the area of the Wetlegs and Dunka Road deposits.

Another striking feature which supports the assumption that a feeder zone to the Partridge River Intrusion is located in between the Wetlegs and the Dunka Road deposits is the presence of a thick promontory of Virginia Formation strata which rises 130 meters above both the level of the basal contact and the top of the Biwabik Formation (see Fig. 3). This ramp has a very limited extent, and occurs along the southwestern limit of the Dunka Road deposit (hole 26143; see Plate II of Severson and Hauck, 1990). The sudden increase in the thickness of the

Virginia Formation in this area is quite peculiar, considering that it generally ranges between 0 and 50 m in thickness throughout the Partridge River Intrusion. The reason why the Virginia Formation was locally preserved from erosion and assimilation in this area may be related to the presence of an important pre-Complex fault, which may have acted as an eventual conduit for the injection of magma.

The presence of a possible feeder zone in the vicinity of the Wetlegs and Dunka Road deposits may have some important economic implications. One question that must be addressed is the possibility of finding higher grade sulfides (i.e. PGE-rich) at depth towards the central and deeper portion of the Partridge River Intrusion, that is in a downdip direction.

Summary

The four different Cu-Ni-PGE sulfide deposits that occur along the northern margin of the Partridge River Intrusion are interpreted to result from the interplay of three main processes that operated in sequence from the time of magma emplacement until complete solidification of a sulfide liquid. More specifically, the mineralization is explained by the combined action of an externally derived process, country-rock assimilation, and two internal magmatic processes, namely the interaction between the sulfide liquid and the silicate melt (*R* factor), and fractional crystallization of the sulfide liquid. Based on the results of modelling, and on key evidence given by field relationships and sulfide mineralogy and geochemistry, the following sequence of events are favored to explain the origin of the different types of sulfide mineralization comprising the Cu-Ni-PGE deposits of the Partridge River Intrusion:

1) During emplacement of the Partridge River Intrusion, the footwall sulfide-bearing sedimentary rocks of the Virginia Formation were partly assimilated by the intruding magma, releasing a sulfide-bearing granitic partial melt near the base of the intrusion. Owing to contamination by the granitic melt, the resulting hybrid magma was cooler than the original troctolitic magma and crystallized more rapidly, such that the sulfide liquid had little time to interact with the magma. This resulted in low to moderate *R* factors, and explains the relatively low metal content of the PGE-poor disseminated sulfide mineralization.

2) A fresh input of relatively uncontaminated troctolitic magma was later injected above the basal mineralized sequence. The low volume of sulfide liquid present near the base of this new injection was free to swirl within the turbulent magma, achieving elevated *R* factors. The sulfide liquid eventually percolated downward into the partly consolidated troctolitic rocks, and crystallized to form laterally persistent horizons of PGE-rich disseminated sulfides.

3) In areas where significant amounts of sulfide liquid was collected, such as in the Local Boy and Tiger Boy area, it underwent fractional crystallization, forming an Fe-rich cumulate of *mss* and a residual Cu-rich sulfide liquid that accumulated along the edges of the massive sulfide veins and lenses. Upon cooling, the *mss* crystallized into pyrrhotite±pentlandite, and the fractionated sulfide liquid into mainly chalcopyrite and cubanite.

Acknowledgements

The authors would like to thank Steven Hauck of the Minnesota Natural Resources Research Institute for his collaboration throughout this study. Appreciation is also expressed to

the Minnesota Department of Natural Resources for providing drill core samples, and to Richard Lechasseur for his assistance with the analytical work. Thoughtful reviews by xx and xx improved the quality of the manuscript. Funding for this work was provided by a Natural Sciences and Engineering Research Council of Canada operating grant to S.-J. Barnes.

References

Barnes, S.-J., 1990, The use of metal ratios in prospecting for platinum-group element deposits in mafic and ultramafic intrusions: Journal of Geochemical Exploration, v. 37, p. 91-99.

Barnes, S.-J., and Francis, D., 1995, The distribution of platinum-group elements, nickel, copper, and gold in the Muskox layered intrusion, Northwest Territories, Canada: ECONOMIC GEOLOGY, v. 90, p. 135-154.

Barnes, S.-J., Boyd, R., Korneliussen, A., Nilsson, L.P., Often, M., Pedersen, R.B., and Robins, B., 1988, The use of mantle normalization and metal ratios in discriminating between the effects of partial melting, crystal fractionation and sulphide segregation on platinum-group elements, gold, nickel and copper: examples from Norway, *In* Prichard, H.M., Potts, P.J., Bowles, J.F.W., and Cribb, S., eds., Geo-platinum 87:Elsevier, Barking, p. 113-143.

Barnes, S.-J., Couture, J.-F., Sawyer, E.W., and Bouchaib, C., 1993, Nickel-copper occurrences in the Belleterre-Angliers Belt of the Pontiac Subprovince and the use of Cu-Pd ratios in interpreting platinum-group element distributions: ECONOMIC GEOLOGY, v. 88., p. 1402-1418.

Barnes, S.-J., Zientek, M.L., and Severson, M.J., 1997, Ni, Cu, Au and platinum-group element contents of sulphides associated with intraplate magmatism: a synthesis: Canadian Journal of Earth Sciences, v. 34, p. 337-351.

Campbell, I.H., and Naldrett, A.J., 1979, The influence of silicate:sulfide ratios on the geochemistry of magmatic sulfides : ECONOMIC GEOLOGY, v. 74, p. 1503-1505.

Campbell, I.H., Naldrett, A.J., and Barnes, S.J., 1983, A model for the origin of the platinum-rich sulfide horizons in the Bushveld and Stillwater Complexes: Journal of Petrology, v. 24, p. 133-165.

Chandler, V.W., and Ferderer, R.J., 1989, Copper-Nickel mineralization of the Duluth Complex, Minnesota: A gravity and magnetic perspective: ECONOMIC GEOLOGY, v. 84, p. 1690-1696.

Foose, M., and Weiblen, P., 1986, The physical and petrologic setting and textural and compositional characteristics of sulfides from the South Kawishiwi Intrusion, Duluth Complex, Minnesota, U.S.A., *In* Friedrich, G.H., Genkin, A.D., Naldrett, A.J., Ridge, J.D., Sillitoe, R.H., and Vokes, F.M., eds., Geology and metallogeny of copper deposits: Springer-Verlag, Berlin, Germany, p. 8-24.

Geerts, S.D., 1991, Geology, stratigraphy, and mineralization of the Dunka Road Cu-Ni prospect, northeastern Minnesota: Natural Resources Research Institute, Duluth, Minnesota, Technical Report 91-14, 63 p.

—— 1994, Petrography and geochemistry of a platinum group element-bearing mineralized horizon in the Dunka Road prospect (Keweenawan), Duluth Complex, northeastern Minnesota: Unpublished M.Sc. thesis, Duluth, University of Minnesota, 155 p.

Hauck, S., Severson, M., Zanko, L., Barnes, S.-J., Morton, P., Aiminas, H., Foord, E.E., and Dahlberg, E.H. 1995. A review of sulfide, platinum group element and oxide mineralization along the western contact of the Duluth Complex: as related to structural development, *In* Ojakangas, R.W., Dickas, A.B., and Green, J.C., eds., Basement Tectonics 10, Kluwer Academic Publishers, p. 47-54.

—— 1997, An overview of the geology and oxide, sulfide, and platinum-group element mineralization along the western and northern contacts of the Duluth Complex, *In* Ojakangas, R.W., Dickas, A.B., and Green, J.C., eds., Middle Proterozoic to Cambrian rifting, Central North America: Geological Society of America Special Paper 312, p. 137-186.

Hemming, S.R., McLennan, S.M., and Hanson, G.N., 1995, Geochemical and Nd/Pb isotopic evidence for the provenance of the Early Proterozoic Virginia Formation, Minnesota: Implications for the tectonic setting of the Animikie Basin: Journal of Geology, v. 103, p. 147-168.

Holst, T.B., Mullenmeister, E.E., Chandler, V.W., Green, J.C., and Weiblen, P.W., 1986, Relationship of structural geology of the Duluth Complex to economic mineralization: Minnesota Department of Natural Resources, Division of Minerals, Report 241-2, 165 p.

Hutchinson, D.R., White, R.S., Cannon, W.F., and Schulz, K.J., 1990, Keweenaw hot spot: Geophysical evidence for a 1.1 Ga mantle plume beneath the midcontinent rift system: Journal of Geophysical Research, v. 95, p. 10,869-10,884.

Irvine, T.N., Keith, D.W., and Todd, S.G., 1983, The J-M platinum palladium reef: II. Origin by double diffusive convective magma mixing and implications for the Bushveld Complex: ECONOMIC GEOLOGY, v. 78, p. 1287-1334.

Kuhns, M.J.P., Hauck, S.A., and Barnes, R.J., 1990, Origin and occurrence of platinum group elements, gold and silver in the South Filson Creek copper-nickel mineral deposit, Lake County, Minnesota: Natural Resources Research Institute, Duluth, Minnesota, Technical Report 89-15, 67 p.

Li, C., Naldrett, A.J., Coats, C.J.A., and Johannessen, P., 1992, Platinum, palladium, gold, and copper-rich stringers at the Strathcona mine, Sudbury: Their enrichment by fractionation of a sulfide liquid: ECONOMIC GEOLOGY, v. 87, p. 1584-1598.

Listerud, W.H., and Meineke, D.G., 1977, Mineral resources of a portion of the Duluth Complex and adjacent rocks in St. Louis and Lake Counties, northeastern Minnesota: Minnesota Department of Natural Resources, Division of Minerals, Report 93, 74 p.

MacLean, W.H., 1969, Liquidus phase relations in the FeS-FeO-Fe_3O_4-SiO_2 system, and their application in geology: ECONOMIC GEOLOGY, v. 64, p. 865-884.

Maier, W.D., Barnes, S.-J., Teigler, B., De Klerk, W.J., and Mitchell, A.A., 1996, Cu/Pd and Cu/Pt of silicate rocks in the Bushveld Complex: Implications for platinum-group element exploration: ECONOMIC GEOLOGY, v. 91, p. 1151-1158.

Maier, W.D., Barnes, S.-J., and de Waal, S.A., 1998, Exploration for magmatic Ni-Cu-PGE sulphide deposits: A review of recent advances in the use of geochemical tools, and their application to some South African ores: South African Journal of Geology, v. 101(3), p. 237-253.

Mainwaring, P.R., and Naldrett, A.J., 1977, Country-rock assimilation and the genesis of Cu-Ni sulfides in the Water Hen Intrusion, Duluth Complex, Minnesota: ECONOMIC GEOLOGY, v. 72, p. 1269-1284.

Mogessie, A., Stumpfl, E.F., and Weiblen, P.W., 1991, The role of fluids in the formation of platinum-group minerals, Duluth Complex, Minnesota: Mineralogic, textural, and chemical evidence: ECONOMIC GEOLOGY, v. 86, p. 1506-1518.

Morey, G.B., 1992, Chemical composition of the Eastern Biwabik Iron-Formation (Early Proterozoic), Mesabi Range, Minnesota: ECONOMIC GEOLOGY, v. 87, p. 1649-1658.

Morton, P., and Hauck, S.A., 1987, PGE, Au and Ag contents of Cu-Ni sulfides found at the base of the Duluth Complex, northeastern Minnesota: Natural Resources Research Institute, Duluth, Minnesota, Technical Report 87-04, 85 p.

Naldrett, A.J. 1989. Ores associated with flood basalts, *In* Whitney, J.A., and Naldrett, A.J., eds., Ore deposition associated with magmas: Society of Economic Geologists, Reviews in Economic Geology, v. 4, p. 103-118.

Naldrett, A.J. 1997. Ni-Cu-PGE deposits of the Noril'sk region and other world-class nickel sulfide deposits: Australian Journal of Earth Sciences, v. 44, p. 283-315.

Naldrett, A.J., Innes, D.G., Sowa, J., and Gorton, M., 1982, Compositional variation within and between five Sudbury ore deposits: ECONOMIC GEOLOGY, v. 77, p. 1519-1534.

Naldrett, A.J., Pessaran, R., Asif, M., and Li, C., 1994, Compositional variation in the Sudbury ores and prediction of the proximity of footwall copper-PGE ore bodies; , *In* Proceedings of the Sudbury-Noril'sk Symposium: Ontario Geological Survey Special Paper 5, p. 133-143.

Nicholson, S.W., and Shirey, S.B., 1990, Midcontinent rift volcanism in the Lake Superior region: Sr, Nd, and Pb isotopic evidence for a mantle plume origin: Journal of Geophysical Research, v. 95, p. 10,851-10,868.

Patelke, R.L., 1994, The Babbitt copper-nickel deposit. Part A: Digital drill hole data files for the Babbitt and Serpentine copper-nickel deposits: Natural Resources Research Institute, Duluth, Minnesota, Technical Report 94-21a, 48 p.

Peach, C.L., Mathez, E.A., Keays, R.R., and Reeves, S.J., 1994, Experimentally determined sulfide melt-silicate melt partition coefficients for iridium and palladium: Chemical Geology, v. 117, p. 361-377.

Peterson, D.M., 1998, Ore deposit modeling and exploration criteria for footwall Cu-PGE mineralization, Duluth Complex: The Minnesota Prospector, Minnesota Exploration Association, December 1998, p. 22-23.

Rao, B.V., and Ripley, E.M., 1983, Petrochemical studies of the Dunka Road Cu-Ni deposit, Duluth Complex, Minnesota: ECONOMIC GEOLOGY, v. 78, p. 1222-1238.

Ripley, E.M., 1981, Sulfur isotopic studies of the Dunka Road Cu-Ni deposit, Duluth Complex, Minnesota: ECONOMIC GEOLOGY, v. 76, p. 610-620.

—— 1986a, Application of stable isotopic studies to problems of magmatic sulfide ore genesis with special reference to the Duluth Complex, Minnesota, *In* Friedrich, G.H., Genkin, A.D., Naldrett, A.J., Ridge, J.D., Sillitoe, R.H., and Vokes, F.M., eds., Geology and metallogeny of copper deposits: Springer-Verlag, Berlin, Germany, p. 8-24.

—— 1986b, Origin and concentration mechanisms of copper and nickel in Duluth Complex sulfide zones: A dilemma: ECONOMIC GEOLOGY, v. 81, p. 974-978.

—— 1990, Platinum-group element geochemistry of Cu-Ni mineralization in the basal zone of the Babbitt deposit, Duluth Complex, Minnesota: ECONOMIC GEOLOGY, v. 85, p. 830-841.

Ripley, E.M., and Al-Jassar, T.J., 1987, Sulfur and oxygen isotope studies of melt-country rock interaction, Babbitt Cu-Ni deposit, Duluth Complex, Minnesota: ECONOMIC GEOLOGY, v. 82, p. 87-107.

Ripley, E.M., and Chryssoulis, S.L., 1994, Ion microprobe analysis of platinum-group elements in sulfide and arsenide minerals from the Babbitt Cu-Ni deposit, Duluth Complex, Minnesota. ECONOMIC GEOLOGY, v. 89, p. 201-210.

Ryan, R.J., and Weiblen, P.W., 1984, Pt and Ni arsenide minerals in the Duluth Complex. *In* 20th annual Institute on Lake Superior geology: Wausau, Wisconsin, v. 20, p. 58-60.

Saini-Eidukat, B., 1991, Platinum group elements in anorthositic rocks of the Duluth Complex, Minnesota: petrogenetic and economic implications. Unpublished Ph.D. thesis, Minneapolis, University of Minnesota.

Severson, M.J., 1988, Geology and structure of a portion of the Partridge River Intrusion: A progress report: Natural Resources Research Institute, Duluth, Minnesota, Technical Report 88-08, 78 p.

—— 1991, Geology, mineralization, and geostatistics of the Minnamax/Babbitt Cu-Ni deposit (Local Boy area), Minnesota. Part I: Geology: Natural Resources Research Institute, Duluth, Minnesota, Technical Report 91-13, 96 p.

—— 1994, Igneous stratigraphy of the South Kawishiwi intrusion, Duluth Complex, Minnesota: Natural Resources Research Institute, Duluth, Minnesota, Technical Report 93-34, 210 p.

—— 1995, Geology of the southern portion of the Duluth Complex: Natural Resources Research Institute, Duluth, Minnesota, Technical Report 95-26, 185 p.

—— 1998, Geology and mineralogy of the Local Boy high grade Cu-Ni-PGE body, Babbitt Cu-Ni deposit: The Minnesota Prospector, Minnesota Exploration Association, December 1998, p. 20-21.

Severson, M.J., and Barnes, R.J., 1991, Geology, mineralization, and geostatistics of the Minnamax/Babbitt Cu-Ni deposit (Local Boy area), Minnesota. Part II: Mineralization and geostatistics: Natural Resources Research Institute, Duluth, Minnesota, Technical Report 91-13b, 216 p.

Severson, M.J., and Hauck, S.A., 1990, Geology, geochemistry, and stratigraphy of a portion of the Partridge River intrusion: Natural Resources Research Institute, Duluth, Minnesota, Technical Report 89-11, 236 p.

—— 1997, Igneous stratigraphy and mineralization in the basal portion of the Partridge River Intrusion, Duluth Complex, Allen Quadrangle, Minnesota: Natural Resources Research Institute, Duluth, Minnesota, Technical Report 97-19, 102 p.

Severson, M.J., Patelke, R.L., Hauck, S.A, and Zanko, L.M., 1994, The Babbitt copper-nickel deposit. Part B: Structural datums: Natural Resources Research Institute, Duluth, Minnesota, Technical Report 94-21b, 48 p.

—— 1996, The Babbitt copper-nickel deposit. Part C: Igneous geology, footwall lithologies, and cross-sections: Natural Resources Research Institute, Duluth, Minnesota, Technical Report 94-21c, 79 p.

Thériault, R.D., and Barnes, S.-J., 1998, Compositional variations in Cu-Ni-PGE sulfides of the Dunka Road deposit, Duluth Complex, Minnesota: The importance of combined assimilation and magmatic processes: The Canadian Mineralogist, v. 36, p. 869-886.

Thériault, R.D., Barnes, S.-J., and Severson, M.J., 1997, The influence of country rock assimilation and silicate to sulfide ratios (*R* factor) on the genesis of the Dunka Road Cu-Ni-PGE deposit, Duluth Complex, Minnesota: Canadian Journal of Earth Sciences, v. 34, p. 373-389.

Tyson, R.M., and Chang, L.L.Y., 1984, The petrology and sulfide mineralization of the Partridge River Troctolite, Duluth Complex, Minnesota: Canadian Mineralogist, v. 22, p. 23-38.

Van Schmus, W.R., and Hinze, W.J., 1985, The Midcontinent Rift: Annual Review of Earth Planetary Sciences, v. 13, p. 345-383.

Zientek, M.L., Likhachev, A.P., Kunilov, V.E., Barnes, S.-J., Meier, A.L., Carlson, R.R., Briggs, P.H., Fries, T.L., and Adrian, B.M., 1994, Cumulus processes and the composition of magmatic ore deposits: Examples from the Talnakh District, Russia, *In* Lightfoot, P.C., and Naldrett, A.J., eds., The Sudbury-Noril'sk Symposium: Ontario Geological Survey Special Publication 5, p. 373-392.

CONCLUSIONS

L'intrusion de Partridge River est située le long de la marge nord-ouest du complexe de Duluth, et repose sur des roches sédimentaires sulfurés de la Formation de Virginia. Un total de quatre gisements non exploités de Cu-Ni-ÉGP se retrouvent près de la base de l'intrusion, soit ceux de Dunka Road, Babbitt, Wetlegs et Wyman Creek. Dans la première phase du projet (premier et deuxième article), une étude détaillée du gisement de Dunka Road a mené à l'identification et la caractérisation de cinq différents types de minéralisation en sulfures, soit: 1) sulfures disséminés dans la norite hôte; 2) sulfures disséminés dans la troctolite hôte; 3) horizons de sulfures disséminés enrichis en ÉGP; 4) sulfures massifs à pyrrhotite; et 5) sulfures disséminés enrichis en cuivre. Cette étude détaillée a permis de circonscrire les principaux facteurs ayant influé sur la genèse du gisement, et ultimement, de démontrer que les cinq types de minéralisation se sont formés suite à l'action progressive de trois principaux processsus, qui sont: 1) l'assimilation de roches sédimentaires encaissantes; 2) l'interaction entre le liquide sulfuré et le magma silicaté (facteur *R*); et 3) la cristallisation fractionnée du liquide sulfuré. Dans la deuxième partie de la thèse (troisième article), une étude géochimique des autres gisements de l'intrusion de Partridge River a permis de reconnaître les mêmes types de minéralisation en sulfures que ceux retrouvés dans le gisement de Dunka Road, et d'expliquer leur origine par l'action des mêmes processus.

Ainsi, en tenant compte des observations de terrain, de la composition minéralogique et géochimique des sulfures et des silicates, et des résultats de la modélisation, les

interprétations suivantes ont été retenues pour expliquer l'origine des différents types de mineralisation en sulfures formant les gisements de Cu-Ni-ÉGP de l'intrusion de Partridge River:

1) Durant la mise en place de l'intrusion de Partridge River, les roches sédimentaires encaissantes de la Formation de Virginia ont été partiellement assimilées par le magma mafique, libérant un produit de fusion partielle granitique et une grande quantité de sulfures enrichis en ^{34}S près de la base de l'intrusion et des enclaves. Dû à son importante contamination par le produit de fusion granitique, le magma hybride de composition noritique était plus froid que le magma troctolitique environnant, ce qui mena à sa cristallisation hâtive et à la formation de la minéralisation en sulfures disséminés dans la norite. Le liquide sulfuré cristallisa près de sa source (*i.e.* roches encaissantes et enclaves) de telle sorte qu'il eut moins de temps pour interagir avec le magma, expliquant les faibles valeurs du facteur *R* associées à ce type de minéralisation. Les autres évidences suggérant que les sulfures disséminés dans la norite se sont formés à partir d'un magma fortement contaminé sont nombreuses, et incluent : 1) les valeurs élevées de $\delta^{34}S$ et de S/Se; 2) les teneurs élevées en As et Sb; 3) les faibles teneurs en ÉGP et métaux de base; et 4) la proportion élevée de pyrrhotite par rapport à la chalcopyrite, cubanite et pentlandite.

2) Une certaine quantité de produit de fusion granitique et de liquide sulfuré enrichie en ^{34}S se sont aussi dispersés dans le magma troctolitique environnant. Ce magma était moins contaminé et donc plus chaud que le magma noritique, de telle sorte que le liquide sulfuré a pu interagir plus longuement avec le magma mafique avant sa cristallisation. Cela explique

les plus grandes valeurs du facteur *R* obtenues pour la minéralisation en sulfures disséminés dans la troctolite par rapport au type de minéralisation précédent. De plus, les sulfures disséminés dans la troctolite sont plus riches en ÉGP et métaux de base et montrent des valeurs plus faible de $\delta^{34}S$ et de S/Se, ce qui témoigne d'un plus faible taux de contamination du magma.

3) Une nouvelle injection de magma troctolitique non contaminé s'est par la suite mise en place au-dessus de la séquence de roches basales minéralisées. Le liquide sulfuré présent dans ce magma a atteint des valeurs du facteur *R* très élevées dû à son interaction prolongée avec le magma en convection, s'enrichissant par le fait même en éléments chalcophiles tels les ÉGP. Le liquide sulfuré a éventuellement percolé à l'intérieur des roches sous-jacentes partiellement consolidées, cristallisant pour former les horizons de sulfures disséminés enrichis en ÉGP.

4) Finalement, aux endroits où une importante quantité de liquide sulfuré s'est accumulé (*i.e.* zones minéralisées de Local Boy et de Tiger Boy), sa cristallisation fractionnée a mené à la formation d'une solution solide de monosulfure enrichie en fer et d'un liquide sulfuré résiduel enrichi en cuivre. Avec une baisse de température, le liquide sulfuré fractionné a migré vers la bordure du sulfure massif pour ultimement cristalliser en chalcopyrite et en cubanite, alors que la solution solide de monosulfure s'est exsolvée en pyrrhotite et en pentlandite.

5) Certaines évidences d'altération hydrothermale post-magmatique ont été observées, en particulier le long de la bordure est du gisement de Babbitt à proximité d'une faille tardive.

Cependant, il s'agit d'un phénomène local qui ne semble pas avoir affecté la distribution et la composition des sulfures, tel que le laisse suggérer les résultats de la modélisation, qui s'appuie sur un modèle magmatique.

Cette étude a permis de confirmer l'hypothèse que l'assimilation de roches sédimentaires encaissantes a eu une influence marquée sur la formation des volumineux gisements de sulfures de Cu-Ni-ÉGP de l'intrusion de Partridge River, considérant l'importante quantité de soufre d'origine sédimentaire introduit dans le magma mafique. De plus, une contribution importante de ce travail est d'avoir été en mesure de reconnaître à l'intérieur de chacun des gisements des variations systématiques au niveau de la composition minéralogique et géochimique des minéralisations en sulfures, et d'avoir identifié ces variations comme étant le résultat de l'action progressive et variable de trois principaux processus. Ainsi, une augmentation systématique des effets de contamination associée à une diminution graduelle du degré d'interaction entre le liquide sulfuré et le magma silicaté (facteur *R*) ont été observées en s'approchant des zones à enclaves et du contact avec les roches encaissantes.

Cette étude a également permis de démontrer que les horizons enrichis en ÉGP découvert précédemment à l'intérieur du gisement de Dunka Road se retrouvent également dans les autres gisements de l'intrusion de Partridge River, se prolongeant ainsi latéralement sur plusieurs dizaines de km. Ces horizons représentent une très bonne cible pour l'exploration des gîtes d'ÉGP, considérant entre autre la hausse importante du prix du platine et du palladium au cours des dernières années. D'ailleurs, un projet pilote de grande

envergure est actuellement en cours par la compagnie PolyMet Mining afin d'évaluer la rentabilité du gisement de Dunka Road (renommé NorthMet). Une récente étude métallurgique effectuée sur le gisement en utilisant une nouvelle technique d'extraction par bio-oxidation a grandement augmenté sa valeur, en faisant l'un des plus importants gisements non exploités de ce type au monde. Les ressources du gisement sont évaluées à 1,45 milliards de tonnes de minerais à des teneurs de 0,40% Cu, 0,10% Ni, 0,01% Co, 447 ppb Pd, 119 ppb Pt, 61 ppb Au et 1,5 ppm Ag, ce qui représente une valeur de plus de 30 milliards de dollars U.S. (PolyMet Mining Corporation, communiqué de presse, janvier 1999). L'exploitation de ce gisement en ferait le seul producteur de nickel et de cobalt aux États-Unis, et le deuxième producteur de palladium et de platine au pays après la mine Stillwater.

Dans l'optique d'une exploitation prochaine du gisement de Dunka Road, des recherches futures sont recommandées sur les autres gisements de l'intrusion de Partridge River, plus particulièrement en ce qui a trait à l'origine et au potentiel économique des horizons de sulfures disséminés enrichis en ÉGP. Il est à souligner qu'une étude doctorale est présentement en cours par Jean Lafrance (Université du Québec à Chicoutimi) sous la supervision de Dr. Sarah-Jane Barnes, et qui a pour but de circonscrire les principaux mécanismes impliqués lors du transfert du soufre des roches sédimentaires encaissantes vers les roches mafiques de l'intrusion de Partridge River. Un aspect intéressant de ce projet est de déterminer l'origine d'un niveau particulièrement enrichi en sulfures de la Formation de Virginia (désigné le «bedded pyrrhotite unit»), et qui semble être le contaminant

principal pour les gisements de Cu-Ni-ÉGP de l'intrusion de Partridge River. Ce niveau est caractérisé par des valeurs isotopiques du soufre extrêmement élevées ($\delta^{34}S$= +12‰ à +29‰) qui suggère une perte hâtive de ^{32}S par dévolatilisation tôt lors de la mise en place de l'intrusion.

ANNEXE 1

RÉSULTATS D'ANALYSES GÉOCHIMIQUES (ROCHE TOTALE)

PAR

FLUORESCENCE-X ET ACTIVATION NEUTRONIQUE

Abréviations

VIRG : Formation de Virginia (argillite; grauwacke)
BIW : Formation de Biwabik (formation de fer; marbre)
POK : Formation de Pokegama (quartzite)
NOP : Formation de Nopeming (grès quartzitique)
GIANT : Batholite de Giant's Range (granite)
DYKE : Dyke de diabase (essaim de Carlton County (DC-34) et de Duluth (DC-35))
ELYS : Formation de Ely`s Peak (basalte)
KEW : Formation de Keweenawan (basalte de plateau)
LOGAN : Filon-couche de Logan (gabbro)
CBB : Complexe de Beaver Bay (troctolite)
BASE : Contact basal du Complexe de Duluth (troctolite)
CORN : Cornéenne de la Formation de Virginia
VIRG-Po : Formation de Virginia (argillite à pyrrhotite)
GRAN : Produit de fusion partielle de composition granitique
IUO : Intrusions ultramafiques à oxydes (pyroxénite; péridotite)
PD : Péridotite
TROC : Troctolite, gabbro à olivine ou leucotroctolite
NOR : Norite
S-TROC : Troctolite, gabbro à olivine ou leucotroctolite à sulfures
S-NOR : Norite à sulfures
S-ÉGP : Leucotroctolite à sulfures enrichis en ÉGP
CU : Troctolite, gabbro à olivine ou leucotroctolite à sulfures enrichis en cuivre
SM : Veines de sulfures massifs à semi-massifs
DUP38; DUP67 : Duplicata des échantillons DC-38 et DC-67

ST-ARG : Standard SH-19 (argillite)
ST-BAS : Standard EV-55 (basalte)
ST-KOM : Standard AX-90 (komatiite)
P.A.F. : Perte au feu

Notes

- FeO (silicates) : quantité de FeO dans les phases silicatées

- Fe (sulfures) : quantité de Fe dans les phases sulfurées

- les éléments majeurs (sauf Fe_2O_3T et Na_2O), S, Cu et Ni analysés par fluorescence X à Analabs-Caleb Brett en Angleterre

- les éléments du groupe du platine, les éléments en traces, Fe_2O_3T et Na_2O analysés par INAA à l'Université du Québec à Chicoutimi

- Se analysé par absorption atomique à Laboratoires Chemex Ltée. de Vancouver pour les échantillons suivants : DC-1; DC-3; DC-5; DC-7; DC-8; DC-9; DC-27; DC-49; DC-52; DC-53; DC-54; DC-60; DC-63; DC-70

No. Échantillon	DC-1	DC-2	DC-3	DC-4	DC-5	DC-6	DC-7	DC-8	DC-9	DC-10
Type de roche	VIRG	VIRG	VIRG	VIRG	VIRG	VIRG	VIRG	VIRG	VIRG	BIW
No. Forage	B2	B2	B2	B2	B2	B2	B2	B2	B2	B2
Profondeur (m)	135,9	432,0	390,3	482,1	464,8	314,6	479,7	443,2	245,3	654,5
SiO_2 (%)	63,58	28,98	62,04	15,18	61,85	69,66	66,73	60,08	59,92	54,62
TiO_2	0,71	0,36	0,63	0,24	0,76	0,55	0,69	0,80	0,79	0,01
Al_2O_3	15,44	6,32	13,38	3,74	15,51	12,81	12,62	17,00	17,17	0,19
FeO (silicates)	7,57	2,61	5,17	0,59	5,35	6,14	5,86	5,03	8,11	37,52
MnO	0,06	0,35	0,08	0,15	0,05	0,05	0,06	0,05	0,06	0,11
MgO	3,34	1,62	2,66	1,02	3,19	2,53	2,52	3,20	3,71	4,47
CaO	0,75	29,50	3,37	42,20	0,66	0,99	2,09	0,55	0,54	0,43
Na_2O	3,16	0,87	2,83	0,16	1,98	4,13	2,23	2,04	2,67	0,02
K_2O	2,36	1,31	2,01	1,38	3,18	1,17	2,27	3,62	3,08	0,01
P_2O_5	0,18	0,12	0,16	0,08	0,17	0,12	0,17	0,19	0,15	0,03
S	0,02	0,97	0,31	0,08	0,53	<0,01	0,09	1,08	0,03	0,07
Fe (sulfures)	0,03	1,70	0,54	0,15	0,92	0,00	0,16	1,88	0,05	0,12
P.A.F.	1,97	23,27	5,40	34,46	5,64	2,49	3,68	4,49	4,37	3,90
TOTAL	99,18	97,98	98,59	99,43	99,81	100,65	99,18	100,01	100,66	101,50
Fe_2O_3T	8,46	5,33	6,52	0,87	7,26	6,83	6,74	8,27	9,08	41,87
Os (ppb)	<0,6	0,7	0,9	<0,5	<1,2	<0,6	<0,6	<0,7	<0,5	<0,7
Ir	0,14	0,03	0,07	<0,02	<0,07	0,02	0,04	0,10	0,09	0,02
Ru	<3,3	<3,8	<5,0	<4,1	<9,8	<5,4	<3,4	<5,3	<3,5	<2,0
Rh	0,17	0,23	0,23	0,11	<0,37	0,26	<0,31	<0,20	0,13	0,08
Pt	3,1	<3,8	<3,2	<3,5	6,5	8,2	<4,2	3,5	3,9	3,8
Pd	1,8	<2,1	2,4	<2,5	4,9	2,7	3,3	2,6	<3,2	<3,1
Au	5,4	4,4	<5,9	<1,2	2,8	2,4	<1,6	<3,5	<1,6	<2,0
Re	0,07	<0,11	0,67	<0,08	0,68	<0,09	0,34	2,1	0,20	<0,09
Cu (ppm)	39	19	43	5	73	30	46	58	59	<2
Ni	67	19	61	9	89	41	48	85	78	<2
Ag	2,0	26	2,7	0,98	5,0	0,53	1,5	4,2	0,46	2,6
As	7,2	110	13	3,7	26	4,5	9,0	27	3,8	20
Co	39	14	34	7	26	43	32	28	35	56
Sb	1,83	3,67	4,56	1,05	5,09	1,33	2,47	5,98	1,83	0,55
Se	<0,2	1,1	0,2	<0,47	<0,2	<2,3	<0,2	0,2	<0,2	<1,4
Ba (ppm)	600	197	351	148	479	228	471	598	546	48
Ce	91	34	58	15	53	48	50	52	56	0,86
Cr	176	73	146	68	175	120	156	181	197	6
Cs	7,2	2,2	5,6	4,3	9,7	2,4	6,0	10	8,4	1,6
Eu	1,9	1,5	2,0	0,44	1,6	0,69	1,1	1,4	1,4	0,07
Hf	3,4	1,6	2,5	0,39	4,2	2,3	5,0	4,4	4,6	0,37
La	44	16	26	7,0	25	23	24	25	25	1,4
Lu	0,46	0,24	0,46	0,11	0,47	0,29	0,43	0,46	0,48	0,01
Nd	33	16	31	5,7	14	20	19	15	20	2,4
Rb	89	37	51	44	131	38	77	136	125	5,7
Sc	21	8,5	17	5,3	22	13	17	25	26	0,38
Sm	7,8	4,8	7,0	1,5	6,0	4,1	4,6	5,2	5,6	0,25
Ta	1,3	0,25	0,96	0,13	1,0	1,1	1,0	0,92	0,74	0,84
Tb	0,99	1,0	1,3	0,22	0,97	0,79	0,60	0,86	0,76	<0,15
Th	11	3,5	6,8	1,8	9,7	6,1	7,8	11	10	0,11
U	4,1	1,4	3,9	1,5	9,4	2,0	3,9	8,1	3,9	<0,15
Yb	2,4	1,4	2,6	0,58	2,7	1,5	2,3	2,5	2,6	0,13

No. Échantillon	DC-11	DC-12	DC-13	DC-14	DC-15	DC-16	DC-17	DC-18	DC-19	DC-20
Type de roche	BIW	BIW	BIW	BIW	BIW	BIW	BIW	POK	NOP	GIANT
No. Forage	B2	B2	B2	B2	B2	B2	-----	B2	-----	KA-2
Profondeur (m)	598,3	535,6	499,8	495,5	491,0	487,0	-----	688,6	-----	340,5
SiO_2 (%)	54,72	33,06	39,90	36,90	24,21	14,71	41,79	75,48	91,49	64,01
TiO_2	0,09	0,03	0,07	0,07	0,36	0,18	0,02	0,04	0,22	0,40
Al_2O_3	1,16	0,36	0,61	0,94	6,17	3,92	0,28	5,88	3,60	16,75
FeO (silicates)	23,01	49,72	8,35	6,79	6,84	1,04	53,99	11,42	0,29	3,46
MnO	0,49	0,53	0,52	0,56	1,58	0,25	0,17	0,08	<0,01	0,06
MgO	2,80	1,63	7,06	7,91	8,83	0,94	1,12	2,99	0,10	2,17
CaO	2,46	5,32	17,01	19,20	20,20	42,20	0,65	0,11	0,16	2,65
Na_2O	0,08	0,02	0,02	0,02	0,04	0,03	0,01	0,01	0,04	6,47
K_2O	0,20	0,11	0,19	0,20	1,92	1,45	0,02	0,22	2,16	3,41
P_2O_5	0,02	0,15	0,04	0,67	0,43	0,03	<0,01	0,02	0,05	0,23
S	0,17	0,09	0,23	0,22	0,19	0,02	0,09	<0,01	<0,01	<0,01
Fe (sulfures)	0,30	0,16	0,40	0,38	0,33	0,03	0,16	0,00	0,00	0,00
P.A.F.	13,70	10,09	24,33	24,87	27,71	33,72	3,44	2,11	0,00	0,79
TOTAL	99,19	101,27	98,73	98,73	98,81	98,52	101,74	98,36	98,11	100,40
Fe_2O_3T	25,99	55,48	9,85	8,09	8,07	1,20	60,23	12,69	0,32	3,84
Os (ppb)	0,6	<0,5	<0,6	<0,6	<1,0	<0,7	<0,7	<0,6	<0,6	<0,9
Ir	0,15	<0,03	<0,03	0,11	0,05	0,05	<0,02	0,05	0,04	<0,03
Ru	<1,9	<3,6	<3,3	<4,6	<3,8	<2,2	<2,9	<4,1	<2,2	<5,0
Rh	0,19	<0,09	<0,12	0,33	<0,22	0,13	<0,09	<0,17	<0,15	<0,15
Pt	7,2	<3,1	2,4	5,1	2,6	<4,0	<3,0	2,8	<3,5	4,4
Pd	5,6	<4,6	<2,8	4,3	<2,4	<2,6	1,4	<2,7	<1,7	2,4
Au	1,3	<,9	<1,0	<2,4	<2,1	<2,1	<1,9	<1,3	<1,6	<2,3
Re	0,19	<0,11	0,14	<0,35	0,35	<0,18	<0,07	<0,08	0,10	<0,12
Cu (ppm)	4	<2	2	8	15	5	<2	3	4	9
Ni	<2	<2	<2	3	15	4	<2	38	9	6
Ag	1,4	0,35	1,5	9,0	4,0	0,30	0,32	<0,13	0,77	<0,36
As	30	13	13	37	16	1,3	0,86	0,62	5,9	<1,0
Co	38	35	38	31	20	8	68	36	93	50
Sb	0,46	0,47	0,96	1,3	2,2	3,1	0,94	0,64	1,7	0,55
Se	0,94	1,4	1,4	<1,9	<1,0	1,0	1,9	<1,7	2,9	2,8
Ba (ppm)	<15	15	21	<20	128	62	<53	48	552	2222
Ce	6,0	8,5	6,2	35	86	47	<1,1	2,9	27	107
Cr	9	7	6	9	56	7	9	9	15	22
Cs	6,8	0,92	<0,14	0,18	5,4	6,1	0,47	0,55	0,56	2,3
Eu	0,34	0,19	0,16	1,6	1,6	0,87	0,05	0,18	0,23	2,0
Hf	0,22	<0,07	0,31	0,41	4,0	3,5	<0,23	0,27	2,7	3,5
La	3,4	4,4	2,9	26	37	20	0,80	1,5	8,2	50
Lu	0,06	0,04	0,06	0,36	0,51	0,86	0,01	0,01	0,20	0,10
Nd	3,4	3,0	4,5	25	37	18	1,8	4,8	13	53
Rb	14	<3,4	2,3	2,0	83	57	<3,4	<3,1	36	60
Sc	2,1	0,45	0,46	1,0	7,8	2,3	0,62	1,2	2,1	5,2
Sm	0,76	0,71	0,50	5,7	8,0	5,7	0,18	0,27	1,5	6,8
Ta	0,93	1,1	0,95	0,73	0,66	0,56	2,1	0,97	3,1	1,3
Tb	0,15	0,12	<0,05	0,98	0,99	1,2	<0,10	<0,05	<0,08	<0,08
Th	0,76	0,04	0,48	0,40	6,1	2,7	0,11	0,61	4,3	5,3
U	0,41	<0,09	0,33	6,4	4,4	4,3	<0,10	0,10	0,62	0,96
Yb	0,33	0,26	0,34	2,1	2,9	4,9	0,19	0,11	1,2	0,45

No. Échantillon	DC-34	DC-35	DC-36	DC-37	DC-38	DC-39	DC-40	DC-41	DC-42	DC-51
Type de roche	DYKE	DYKE	ELYS	KEW	KEW	DUP38	LOGAN	CBB	BASE	BASE
No. Forage	-----	-----	-----	-----	-----	-----	-----	-----	-----	-----
Profondeur (m)	-----	-----	-----	-----	-----	-----	-----	-----	-----	-----
SiO_2 (%)	49,04	47,01	50,48	49,10	48,87	49,46	51,39	48,74	49,33	48,07
TiO_2	1,39	0,96	2,38	0,82	0,95	0,94	3,63	1,38	1,78	2,69
Al_2O_3	16,26	16,98	11,20	17,16	16,90	16,89	13,20	16,24	16,56	15,76
FeO (silicates)	12,17	9,29	13,35	8,37	8,96	9,24	14,48	10,83	11,35	13,62
MnO	0,18	0,29	0,21	0,14	0,15	0,15	0,18	0,25	0,16	0,18
MgO	8,20	8,36	7,05	8,28	8,55	8,52	3,39	7,94	6,92	6,48
CaO	10,50	9,88	10,60	10,60	10,80	10,70	6,68	10,10	10,60	7,91
Na_2O	2,89	2,45	2,47	2,37	2,51	2,57	3,13	2,46	2,96	3,31
K_2O	0,44	0,23	0,37	0,36	0,36	0,36	1,48	0,41	0,61	1,08
P_2O_5	0,13	0,09	0,29	0,07	0,10	0,10	0,51	0,14	0,14	0,39
S	<0,01	<0,01	<0,01	<0,01	<0,01	<0,01	0,11	<0,01	<0,01	0,10
Fe (sulfures)	0,00	0,00	0,00	0,00	0,00	0,00	0,18	0,00	0,00	0,16
P.A.F.	0,87	6,00	1,44	2,68	1,57	0,95	1,50	1,81	0,85	0,81
TOTAL	102,10	101,57	99,87	99,98	99,75	99,91	99,90	100,33	101,28	100,60
Fe_2O_3T	13,52	10,32	14,84	9,30	9,96	10,27	16,34	12,04	12,61	15,37
Os (ppb)	<0,4	<0,5	0,4	<0,5	<1,1	<0,7	<0,4	<0,5	<0,8	0,8
Ir	0,05	0,03	0,87	0,19	0,21	0,16	0,05	0,07	0,13	0,10
Ru	<2,8	<3,4	<2,1	<1,4	<5,0	<2,3	<2,3	<1,9	<1,4	<2,7
Rh	0,25	<0,13	0,69	0,35	0,35	0,31	0,34	0,09	0,22	0,39
Pt	<3,1	<3,4	21	10	7,0	4,7	7,2	<6,4	11	3,5
Pd	2,3	3,3	12	9,2	11	8,3	8,2	1,7	8,6	4,1
Au	<3,6	<1,7	<5,1	<1,7	<1,2	<1,2	<4,2	<2,6	<1,5	<2,0
Re	0,21	0,15	1,7	0,09	0,41	0,25	0,36	2,8	0,28	0,27
Cu (ppm)	102	74	190	97	117	117	371	130	151	244
Ni	181	181	91	221	218	217	109	170	98	180
Ag	<0,36	<0,24	6,0	<0,48	<0,48	<0,42	<0,45	<0,38	<0,50	<0,30
As	0,46	0,57	110	<0,20	0,21	0,24	2,5	0,19	0,52	2,2
Co	85	57	83	59	62	61	55	66	70	60
Sb	0,50	0,51	21	0,65	1,4	0,79	0,61	1,6	5,0	2,9
Se	<1,5	<1,0	4,1	<0,80	<0,80	<1,4	2,2	<1,1	<1,8	<1,1
Ba (ppm)	123	65	258	79	84	91	422	171	124	336
Ce	29	16	104	13	15	15	87	30	26	59
Cr	196	177	453	332	337	345	23	186	224	159
Cs	<0,31	1,8	0,26	<0,56	0,44	<0,64	3,5	<0,51	0,54	1,6
Eu	1,6	1,3	3,0	0,61	0,94	1,1	3,0	1,6	1,6	2,4
Hf	3,0	1,4	6,5	0,81	0,95	1,0	7,5	2,2	1,1	5,4
La	12	7,5	47	4,6	5,4	5,6	37	12	11	25
Lu	0,38	0,23	0,34	0,22	0,29	0,31	0,61	0,36	0,34	0,56
Nd	12	8,3	56	5,9	5,8	8,5	46	14	10	31
Rb	<4,3	2,9	4,3	<11	<6,2	<9,4	47	<7,7	5,9	29
Sc	31	29	34	28	29	30	26	29	35	21
Sm	4,1	2,3	9,9	1,9	2,5	2,5	9,9	4,0	3,2	7,0
Ta	1,5	0,21	3,1	0,23	0,39	0,44	2,0	0,92	0,95	1,2
Tb	0,81	0,47	1,0	0,30	0,44	0,52	1,6	0,62	0,69	1,3
Th	1,2	0,54	4,6	0,22	0,38	0,47	5,8	1,2	1,5	3,8
U	0,23	<0,24	2,7	<0,16	<0,16	<0,10	1,6	0,16	0,29	1,1
Yb	2,3	1,4	1,8	1,3	1,7	1,8	3,5	2,1	2,0	3,2

No. Échantillon	DC-26	DC-69	DC-71	DC-77	DC-78	DC-81	DC-70	DC-80	DC-47	DC-48
Type de roche	CORN	CORN	CORN	CORN	CORN	CORN	VIRG-Po	GRAN	IUO	IUO
No. Forage	26117	26117	26117	26117	26117	26107	-----	26107	-----	26117
Profondeur (m)	708,3	706,8	731,7	722,6	715,9	719,6	-----	718,4	-----	163,6
SiO_2 (%)	46,94	38,05	37,11	65,72	44,11	46,74	56,17	60,61	39,97	48,90
TiO_2	0,10	0,58	0,58	0,40	1,70	1,62	0,72	0,75	5,62	2,13
Al_2O_3	29,04	25,61	15,76	11,74	26,63	22,06	15,82	17,24	2,33	2,63
FeO (silicates)	8,20	9,48	3,25	6,50	12,42	14,49	0,56	6,15	24,34	19,15
MnO	0,06	0,05	0,05	0,17	0,07	0,11	0,03	0,05	0,35	0,32
MgO	10,94	8,94	4,18	1,49	9,12	10,13	2,56	3,41	14,85	16,85
CaO	0,45	0,20	1,21	11,92	0,07	0,42	1,11	0,87	10,15	8,85
Na_2O	0,23	0,18	1,99	0,74	0,18	0,97	1,75	4,73	0,32	0,24
K_2O	0,58	0,61	2,44	0,10	0,64	0,65	3,24	4,29	0,15	0,17
P_2O_5	<0,01	<0,01	0,04	0,08	0,02	0,02	0,13	0,11	0,01	0,41
S	0,70	5,90	10,20	0,01	1,56	0,40	4,45	0,15	0,37	0,15
Fe (sulfures)	1,20	10,09	17,12	0,00	2,65	0,66	7,75	0,22	0,46	0,24
P.A.F.	1,29	1,80	7,67	0,95	1,83	2,86	5,86	1,22	1,21	1,91
TOTAL	99,78	101,73	102,35	99,93	101,11	101,20	100,18	99,88	100,37	102,01
Fe_2O_3T	10,82	24,96	28,09	7,22	17,59	17,05	11,70	7,15	27,71	21,62
Os (ppb)	0,7	1,2	-----	<0,5	0,7	0,6	<1,5	<0,6	0,9	0,8
Ir	0,33	0,82	-----	0,04	0,22	0,26	0,06	0,08	0,40	0,46
Ru	<2,9	7,5	-----	<2,2	1,7	<2,6	<5,0	<2,5	<5,0	<4,4
Rh	0,57	1,2	-----	<0,17	0,43	0,31	0,12	0,07	1,4	0,90
Pt	6,0	13	-----	2,0	9,0	7,4	<4,7	2,6	26	12
Pd	2,9	36	-----	<1,1	5,3	8,3	3,5	4,0	46	25
Au	3,1	28	23	<1,0	12	7,2	<2,8	6,5	15	2,5
Re	1,4	5,8	-----	<0,05	1,5	0,80	0,10	0,34	0,77	0,61
Cu (ppm)	422	1335	5823	825	732	420	170	646	1936	207
Ni	150	1035	1706	235	355	291	144	123	432	343
Ag	2,3	5,2	1,9	<0,15	<0,41	1,4	1,2	<0,33	<0,40	<0,29
As	14	96	62	3,1	6,0	38	9,4	6,0	<0,42	0,27
Co	166	227	124	21	69	83	33	25	124	103
Sb	1,1	0,35	1,5	0,93	0,20	1,1	5,4	1,9	0,95	1,4
Se	6,3	2,4	3,7	<0,65	1,0	2,0	1,4	0,77	2,3	<1,5
Ba (ppm)	24	23	548	39	18	102	477	539	<25	<32
Ce	<0,83	<1,7	50	35	3,6	13	73	72	5,9	20
Cr	608	2730	238	123	768	609	179	177	511	359
Cs	5,6	3,7	6,2	0,71	3,2	6,2	11	5,1	<0,37	<0,25
Eu	<0,13	<0,07	2,2	1,2	0,03	0,45	1,7	1,2	0,72	0,72
Hf	<0,38	0,28	1,9	2,4	0,81	1,3	3,9	3,5	1,6	1,2
La	0,43	0,62	26	16	1,8	6,4	43	34	1,4	6,7
Lu	0,05	0,05	0,35	0,27	0,13	0,37	0,78	0,40	0,31	0,36
Nd	3,3	1,9	21	14	1,1	3,2	36	32	4,3	12
Rb	53	39	76	2,4	43	40	142	133	<4,8	<2,6
Sc	18	15	21	13	42	62	27	24	73	55
Sm	0,09	0,14	4,4	3,4	0,37	1,0	9,1	6,4	2,6	3,7
Ta	5,0	0,11	0,55	0,41	0,64	0,90	0,55	0,62	1,2	0,60
Tb	<0,13	<0,05	0,63	0,51	<0,04	0,08	1,3	0,77	0,67	0,75
Th	<0,15	0,21	4,4	3,0	0,49	1,1	10	15	<0,09	0,39
U	<0,19	0,12	7,6	1,2	0,14	0,25	23	5,3	<0,08	<0,11
Yb	0,19	0,23	1,8	1,6	0,57	1,9	4,0	1,7	1,7	2,1

No. Échantillon	DC-43	DC-44	DC-45	DC-46	DC-21	DC-22	DC-23	DC-24	DC-25	DC-28
Type de roche	PD	PD	PD	PD	TROC	TROC	TROC	TROC	TROC	TROC
No. Forage	26117	26117	26117	26117	26107	26117	26117	26107	26117	26107
Profondeur (m)	151,1	492,5	327,7	603,4	249,6	505,6	134,7	400,7	485,2	185,7
SiO_2 (%)	38,06	36,58	39,13	39,50	49,37	47,51	46,78	47,85	49,16	47,55
TiO_2	0,14	1,17	0,21	0,53	0,55	0,41	0,55	1,41	0,79	0,32
Al_2O_3	8,59	6,16	8,62	8,98	17,53	21,94	20,42	20,21	21,70	21,30
FeO (silicates)	19,64	21,94	18,74	20,14	9,44	9,18	10,94	11,37	7,07	8,48
MnO	0,23	0,27	0,23	0,24	0,14	0,11	0,13	0,15	0,09	0,11
MgO	18,41	21,76	20,01	19,38	8,97	7,75	8,02	6,68	5,50	8,36
CaO	2,72	3,74	3,70	4,20	11,40	10,00	9,49	9,56	11,20	9,36
Na_2O	0,63	0,64	0,92	1,06	2,73	2,89	2,36	3,13	3,18	3,04
K_2O	0,11	0,15	0,16	0,22	0,36	0,35	0,29	0,51	0,46	0,41
P_2O_5	<0,01	0,02	0,01	0,02	0,02	0,06	0,04	0,16	0,07	0,02
S	0,07	0,08	0,05	0,03	0,25	0,01	0,01	0,06	<0,01	0,01
Fe (sulfures)	0,06	0,05	0,04	0,00	0,43	0,00	0,00	0,10	0,00	0,01
P.A.F.	12,65	8,60	9,52	7,04	0,84	0,72	0,89	0,67	0,02	2,05
TOTAL	101,41	101,29	101,42	101,44	102,06	100,98	99,97	101,90	99,27	101,05
Fe_2O_3T	21,91	24,45	20,89	22,39	11,11	10,20	12,16	12,78	7,86	9,44
Os (ppb)	0,8	4,3	<0,9	2,4	<1,0	<0,5	<1,3	1,1	0,4	<1,3
Ir	0,49	1,9	0,24	1,4	0,18	0,03	0,33	0,12	0,32	0,41
Ru	<3,1	7,3	<5,0	6,9	<8,2	<5,4	4,9	<2,7	<2,0	<3,1
Rh	0,44	0,14	0,19	0,43	0,18	<0,18	0,65	0,20	0,39	0,12
Pt	5,3	9,3	5,4	9,0	4,5	<2,4	6,7	3,1	<5,3	<5,1
Pd	13	5,7	13	3,5	4,5	<2,8	11	3,7	6,1	<2,8
Au	<1,5	2,1	<2,4	2,7	<2,7	<1,5	<2,1	<3,0	<1,5	<1,1
Re	0,16	0,11	0,15	<0,17	0,11	0,15	0,10	0,26	0,13	0,14
Cu (ppm)	66	327	74	221	112	169	189	164	129	62
Ni	892	946	693	658	228	295	273	189	198	266
Ag	<0,19	<0,26	<0,20	<0,21	<0,39	0,17	<0,17	<0,18	<0,20	<0,18
As	<0,13	<0,23	<0,20	<0,18	<0,33	<0,33	<0,28	0,86	0,34	<0,39
Co	130	147	137	134	76	85	85	74	62	74
Sb	0,66	1,3	0,69	2,2	0,34	0,47	0,85	1,6	0,31	0,45
Se	<0,70	<0,90	0,62	<0,50	<1,9	1,4	1,9	0,90	<0,70	<0,8
Ba (ppm)	33	<23	21	28	117	136	68	176	115	99
Ce	1,7	4,0	1,4	2,1	4,8	8,0	5,1	22	13	3,8
Cr	94	4705	174	221	666	72	238	238	699	326
Cs	0,95	<0,46	0,42	<0,36	<0,57	<0,23	0,72	0,48	0,65	1,2
Eu	0,31	0,38	0,36	0,44	0,92	0,96	0,96	1,5	1,2	0,66
Hf	<0,14	<0,18	<0,24	0,14	0,32	0,22	<0,23	2,2	0,38	0,32
La	1,1	1,1	1,0	1,4	2,3	4,1	2,8	10	5,3	2,0
Lu	0,03	0,07	0,04	0,06	0,11	0,06	0,06	0,21	0,11	0,02
Nd	<1,1	<1,5	<1,7	0,8	5,1	5,9	4,9	11	6,1	4,2
Rb	<5,4	4,4	<3,6	<3,3	<5,2	9,5	5,5	8,3	7,2	4,0
Sc	7,0	17	9,9	11	34	4,3	7,8	13	16	4,2
Sm	0,14	0,47	0,28	0,35	1,2	0,87	0,56	2,8	1,6	0,35
Ta	<0,14	<0,19	<0,17	<0,13	0,55	1,0	0,81	1,0	1,3	0,52
Tb	<0,09	<0,10	<0,10	<0,08	0,18	0,11	0,08	0,38	0,19	<0,05
Th	<0,11	<0,09	<0,07	<0,12	<0,15	0,27	<0,15	1,3	0,68	0,12
U	<0,05	<0,07	<0,06	<0,08	<0,14	0,08	<0,07	0,28	0,24	<0,16
Yb	0,14	0,32	0,29	0,31	0,61	0,33	0,27	1,3	0,71	0,18

No. Échantillon	DC-29	DC-30	DC-32	DC-33	DC-59	DC-31	DC-50	DC-53	DC-49	DC-54
Type de roche	TROC	TROC	TROC	TROC	TROC	NOR	NOR	S-TROC	S-NOR	S-NOR
No. Forage	26143	26117	26107	26117	-----	26117	26117	26117	26117	-----
Profondeur (m)	391,6	529,0	311,0	656,9	-----	580,6	471,5	741,2	727,5	-----
SiO_2 (%)	48,38	48,73	46,49	47,82	46,93	50,34	45,56	48,24	49,27	46,03
TiO_2	1,00	0,44	0,33	0,63	0,77	0,78	5,05	2,29	2,87	1,39
Al_2O_3	23,58	23,19	20,81	19,32	18,11	16,03	13,81	16,46	15,53	20,17
FeO (silicates)	4,77	7,23	8,20	11,86	10,51	7,99	14,44	12,55	14,91	13,83
MnO	0,05	0,09	0,11	0,14	0,15	0,14	0,20	0,18	0,18	0,12
MgO	2,80	6,19	7,40	8,98	9,06	7,72	7,37	6,42	5,35	8,63
CaO	10,20	10,80	10,10	8,48	8,20	12,70	10,50	8,58	7,03	2,01
Na_2O	4,15	3,15	2,84	2,86	3,18	2,76	2,48	3,19	2,84	1,55
K_2O	0,49	0,38	0,51	0,39	0,69	0,37	0,39	1,05	0,48	0,75
P_2O_5	0,04	0,05	0,03	0,04	0,15	0,02	0,05	0,31	0,54	0,02
S	0,03	<0,01	0,03	0,06	0,12	<0,01	0,09	0,15	0,20	0,31
Fe (sulfures)	0,05	0,00	0,05	0,10	0,09	0,00	0,12	0,22	0,32	0,48
P.A.F.	2,60	0,50	2,24	0,34	0,25	0,71	0,53	0,78	1,13	5,86
TOTAL	98,18	100,77	99,18	101,06	98,37	99,58	100,65	100,49	100,70	101,23
Fe_2O_3T	5,38	8,04	9,18	13,32	11,81	8,88	16,21	14,26	17,03	16,05
Os (ppb)	<0,6	<0,7	<1,0	<0,8	<1,4	0,5	<1,2	<0,8	<0,5	0,7
Ir	0,39	0,30	0,13	0,10	0,13	0,10	0,31	0,57	0,10	0,22
Ru	<2,5	<3,3	<1,7	<4,1	<3,1	<5,0	<2,2	<5,0	<5,0	<5,0
Rh	0,36	1,2	0,33	0,27	0,21	0,73	0,40	1,2	<0,21	0,46
Pt	8,5	<6,0	5,5	<4,7	<5,4	9,6	7,4	10	2,5	6,9
Pd	6,9	17	3,3	3,1	5,1	2,0	14	39	5,4	8,1
Au	<1,8	<1,4	118	<1,3	<1,5	<1,7	<1,1	<2,1	<3,2	2,3
Re	0,07	0,22	<0,14	0,17	0,42	0,57	0,49	0,46	0,22	1,2
Cu (ppm)	155	38	132	173	1014	87	501	514	373	622
Ni	123	188	244	190	567	97	155	230	151	265
Ag	<0,31	<0,27	0,15	0,26	0,19	<0,28	<0,31	<0,27	<0,23	<0,57
As	0,82	<0,46	<0,50	<0,43	0,34	<0,44	<0,19	2,2	2,0	2,8
Co	44	70	69	97	68	62	63	55	52	62
Sb	4,4	0,62	1,1	0,50	1,1	0,64	0,96	1,0	1,6	0,80
Se	<1,6	0,89	0,85	1,1	0,71	1,0	<1,6	0,2	<0,2	0,6
Ba (ppm)	165	113	133	118	150	88	116	276	199	198
Ce	10	9,5	5,7	9,3	22	7,4	13	48	45	23
Cr	124	283	281	354	32	339	310	143	170	526
Cs	<0,36	0,33	1,1	0,19	0,55	<0,34	<0,50	1,7	0,64	2,8
Eu	1,6	0,98	0,75	1,2	1,6	1,3	1,4	2,4	2,8	2,0
Hf	0,64	0,79	0,24	0,33	1,8	0,40	2,0	4,3	2,3	0,96
La	4,7	4,4	2,5	4,4	9,6	2,4	5,2	21	19	14
Lu	0,06	0,09	0,06	0,07	0,18	0,18	0,30	0,47	0,50	0,34
Nd	4,5	5,0	2,3	2,8	11	4,0	7,7	25	24	7,5
Rb	3,8	3,4	4,4	6,9	11	4,9	<7,3	34	7,3	31
Sc	4,4	5,3	8,6	8,2	8,5	43	47	20	29	55
Sm	0,85	1,0	0,62	0,66	2,5	1,4	2,6	5,9	6,0	1,2
Ta	0,58	0,94	0,61	0,54	0,27	0,90	0,77	0,88	1,2	0,71
Tb	<0,11	0,16	0,06	<0,10	0,36	0,39	0,55	1,1	0,92	<0,17
Th	0,46	0,53	0,09	0,28	1,3	<0,18	<0,11	3,8	0,84	0,48
U	<0,11	0,10	<0,08	<0,22	0,36	<0,13	<0,13	1,0	1,3	0,26
Yb	0,29	0,50	0,31	0,34	1,0	0,88	1,6	2,7	2,8	1,7

No. Échantillon	DC-64	DC-52	DC-27	DC-79	DC-55	DC-56	DC-57	DC-61	DC-60	DC-62
Type de roche	S-ÉGP	S-NOR	S-NOR	S-TROC	S-TROC	S-TROC	CU	S-TROC	S-NOR	S-ÉGP
No. Forage	26117	-----	26117	26107	26117	26107	26117	26117	26117	26107
Profondeur (m)	609,2	-----	708,3	718,0	753,9	702,8	727,5	627,8	683,4	627,5
SiO_2 (%)	45,02	54,38	42,89	45,31	46,06	45,08	52,01	44,37	38,99	43,65
TiO_2	0,59	1,02	6,81	0,65	1,71	1,26	2,13	0,25	7,13	1,46
Al_2O_3	19,43	18,14	6,51	19,73	16,23	16,89	18,72	19,45	13,81	14,19
FeO (silicates)	9,95	8,51	23,29	10,11	12,84	13,28	7,22	9,12	18,89	14,56
MnO	0,13	0,08	0,25	0,10	0,17	0,15	0,09	0,10	0,22	0,18
MgO	8,59	5,44	11,88	9,02	7,32	8,23	2,54	8,50	7,16	11,41
CaO	9,35	2,12	4,10	8,02	8,09	8,25	8,25	8,75	6,66	7,41
Na_2O	2,41	2,85	0,79	2,16	2,82	2,71	3,67	2,57	2,15	2,20
K_2O	0,43	3,98	0,17	0,49	0,82	0,55	1,24	0,35	0,48	0,59
P_2O_5	0,10	0,07	0,51	0,08	0,23	0,12	0,99	0,04	0,13	0,19
S	0,59	0,66	0,77	1,12	1,11	1,44	1,49	1,50	1,57	1,69
Fe (sulfures)	0,60	1,12	1,22	1,14	1,54	1,87	1,73	1,82	2,38	1,54
P.A.F.	0,56	2,19	1,29	1,32	0,47	0,78	1,13	0,86	0,94	0,36
TOTAL	98,26	100,62	100,64	100,19	99,88	101,36	102,21	98,60	100,92	101,03
Fe_2O_3T	11,91	11,07	27,63	12,86	16,47	17,43	10,50	12,74	24,40	18,38
Os (ppb)	4,1	<0,9	<0,6	1,3	0,9	1,6	2,5	2,5	<1,3	3,2
Ir	8,6	0,25	0,28	3,0	1,0	2,8	7,6	3,8	1,2	11
Ru	31	4,9	<2,6	10	6,9	13	7,7	16	<5,0	34
Rh	48	0,53	0,74	15	4,2	12	14	15	4,0	66
Pt	299	3,7	13	164	42	112	554	124	50	560
Pd	1630	11	23	583	174	402	423	501	105	2251
Au	89	<3,2	11	67	32	48	31	59	19	421
Re	4,1	0,93	0,86	8,8	3,6	6,1	1,3	6,0	2,7	5,1
Cu (ppm)	3382	293	1296	7120	3652	5550	8140	7129	3000	12249
Ni	1684	186	348	2246	1073	1909	1885	2051	1140	3742
Ag	0,29	<0,82	0,98	1,0	0,28	1,4	3,9	1,2	0,75	1,6
As	0,56	6,3	13	4,7	1,6	3,5	29	<0,38	3,4	1,5
Co	83	40	114	120	89	170	96	113	127	150
Sb	0,39	1,4	0,89	0,60	1,5	2,9	2,5	0,56	0,57	0,44
Se	1,8	0,6	0,6	3,5	2,4	3,2	6,4	4,2	1,0	8,2
Ba (ppm)	76	673	30	117	204	162	434	81	164	152
Ce	13	60	25	17	36	22	79	6,5	21	27
Cr	112	318	859	101	161	143	83	193	360	258
Cs	0,32	2,6	<0,40	2,1	1,5	0,43	4,2	<0,27	0,49	0,74
Eu	0,93	2,7	1,4	1,3	1,9	1,3	3,5	0,87	1,6	1,4
Hf	1,3	2,5	1,8	1,4	3,3	2,2	1,2	0,27	2,5	2,7
La	6,0	32	11	7,4	16	9,4	31	2,9	8,7	11
Lu	0,16	0,60	0,42	0,15	0,37	0,25	0,37	0,04	0,27	0,29
Nd	6,7	21	12	8,4	19	8,3	51	1,1	11	14
Rb	3,0	86	<6,2	19	21	9,4	39	<6,3	12	13
Sc	12	38	88	10	18	14	13	4,7	32	18
Sm	1,8	3,9	3,9	1,8	4,4	2,5	11	0,59	3,1	3,6
Ta	0,28	<0,29	2,5	0,22	0,72	0,25	0,62	<0,11	1,3	0,40
Tb	0,19	0,62	0,87	0,26	0,82	0,38	1,7	<0,09	0,56	0,57
Th	0,66	4,7	0,44	1,1	2,2	1,3	3,9	0,18	1,4	1,5
U	0,19	2,1	0,16	0,26	0,63	0,33	4,6	<0,21	0,44	0,39
Yb	0,82	3,2	2,3	0,86	2,1	1,4	2,3	0,18	1,5	1,7

No. Échantillon	DC-58	DC-65	DC-63	DC-67	DUP67	DC-66	DC-72	DC-73	DC-74	DC-75
Type de roche	S-TROC	CU	S-NOR	CU	CU	S-NOR	S-NOR	SM	SM	SM
No. Forage	26107	26143	26143	26143	26143	26107	26117	26143	-----	26117
Profondeur (m)	682,5	288,5	252,3	329,2	329,2	721,7	703,5	283,9	-----	716,5
SiO_2 (%)	44,83	44,22	40,21	51,70	52,20	43,05	31,93	19,98	21,12	8,37
TiO_2	1,28	4,19	2,85	2,51	2,48	2,04	7,75	2,55	0,44	0,36
Al_2O_3	18,42	13,10	11,82	12,95	13,04	13,98	6,37	3,99	6,55	3,06
FeO (silicates)	10,03	14,37	16,78	8,18	8,33	16,51	27,40	12,30	7,40	1,47
MnO	0,13	0,18	0,22	0,09	0,09	0,17	0,29	0,15	0,10	0,03
MgO	7,22	5,24	9,03	3,18	3,17	5,85	10,62	5,19	2,32	1,69
CaO	8,92	9,26	6,67	4,82	4,78	7,21	3,33	3,61	0,47	1,02
Na_2O	2,86	2,21	1,93	3,44	3,47	1,96	0,91	0,54	0,82	0,24
K_2O	0,58	0,59	0,55	2,14	2,15	0,66	0,30	0,18	1,27	0,11
P_2O_5	0,07	0,31	0,07	0,65	0,64	0,26	0,11	0,02	0,02	<0,01
S	2,00	2,17	2,45	3,42	3,39	4,32	4,65	19,64	22,20	31,20
Fe (sulfures)	2,38	2,29	4,02	4,61	4,55	6,76	7,69	32,15	35,71	52,72
P.A.F.	0,14	0,91	1,06	0,69	0,47	1,15	1,06	1,52	3,47	2,45
TOTAL	100,13	100,75	97,96	99,93	100,32	104,79	102,89	104,10	105,16	104,54
Fe_2O_3T	14,55	19,25	24,40	15,67	15,76	28,02	41,45	59,64	59,28	77,01
Os (ppb)	1,9	2,3	1,2	4,1	2,9	2,2	1,3	1,2	3,5	3,8
Ir	3,1	0,37	0,92	2,0	1,7	4,3	1,5	38	9,3	2,3
Ru	10	<5,0	<5,0	5,3	<5,3	20	<5,0	27	19	<9,3
Rh	16	2,4	2,7	5,8	5,9	19	4,7	96	26	9,7
Pt	161	371	16	835	642	35	5,4	89	32	23
Pd	712	601	63	974	932	464	120	470	627	877
Au	144	265	18	276	213	45	45	29	347	131
Re	8,8	0,79	4,9	4,0	4,6	27	2,8	115	74	8,0
Cu (ppm)	10228	15662	2210	13996	14052	6395	3699	12154	18206	11369
Ni	2439	1465	824	1570	1553	2283	1138	10691	14518	6840
Ag	0,79	3,9	0,48	2,0	2,5	1,0	2,4	1,1	2,0	12
As	0,71	15	6,8	14	12	15	38	41	50	387
Co	113	109	180	138	137	310	290	1097	1586	1245
Sb	2,7	1,4	0,57	1,9	1,3	0,71	0,58	0,37	0,94	0,84
Se	4,6	8,2	2,2	9,0	8,0	5,9	9,6	25	22	13
Ba (ppm)	143	116	146	300	258	276	83	56	99	<59
Ce	14	27	18	61	62	44	19	3,7	11	<0,88
Cr	113	322	186	160	163	242	569	198	180	431
Cs	<0,33	1,1	1,2	9,2	9,2	1,5	0,82	<0,43	0,87	<0,48
Eu	1,4	2,0	1,5	1,4	1,4	1,8	1,1	0,58	0,37	0,23
Hf	1,1	3,7	1,3	2,5	2,7	6,0	2,6	0,91	0,59	<0,19
La	5,6	11	8,5	27	27	19	8,5	2,4	6,6	1,5
Lu	0,17	0,46	0,22	0,42	0,41	0,51	0,27	0,11	0,11	<0,02
Nd	7,0	17	11	35	36	26	7,8	5,0	3,7	<2,8
Rb	7,5	<7,9	16	124	122	21	16	12	28	<7,8
Sc	13	54	27	17	17	28	32	23	11	5,8
Sm	1,8	4,9	2,4	7,6	7,7	6,2	2,3	1,2	0,97	0,15
Ta	0,17	1,4	0,66	0,97	1,1	0,89	1,6	0,48	0,19	<0,14
Tb	0,33	0,90	0,43	1,2	1,0	1,1	0,32	0,28	<0,09	<0,08
Th	0,69	1,4	0,89	7,2	7,2	2,6	1,3	0,66	3,1	1,3
U	0,22	0,44	0,12	4,6	5,0	0,75	0,30	<0,31	0,29	1,1
Yb	0,80	2,6	1,3	2,1	2,2	2,8	1,5	0,89	0,36	<0,12

No. Échantillon	DC-76	SH-19(1)	SH-19(2)	EV-55	AX-90(1)	AX-90(2)	AX-90(3)	AX-90(4)	AX-90(5)
Type de roche	SM	ST-ARG	ST-ARG	ST-BAS	ST-KOM	ST-KOM	ST-KOM	ST-KOM	ST-KOM
No. Forage	26143	-----	-----	-----	-----	-----	-----	-----	-----
Profondeur (m)	328,9	-----	-----	-----	-----	-----	-----	-----	-----
SiO_2 (%)	3,38	58,28	-----	50,27	-----	-----	-----	36,81	-----
TiO_2	0,46	0,90	-----	1,31	-----	-----	-----	0,23	-----
Al_2O_3	0,55	12,88	-----	13,47	-----	-----	-----	4,52	-----
FeO (silicates)	1,47	0,71	-----	15,35	-----	-----	-----	8,23	-----
MnO	0,03	0,04	-----	0,22	-----	-----	-----	0,17	-----
MgO	0,66	2,72	-----	5,45	-----	-----	-----	27,16	-----
CaO	1,44	1,77	-----	9,05	-----	-----	-----	4,97	-----
Na_2O	0,11	1,03	0,99	2,90	0,05	0,05	0,05	0,05	-----
K_2O	0,15	6,28	-----	0,18	-----	-----	-----	0,15	-----
P_2O_5	0,19	0,08	-----	0,11	-----	-----	-----	0,02	-----
S	34,90	1,25	-----	0,07	-----	-----	-----	3,26	-----
Fe (sulfures)	58,56	2,20	-----	0,13	-----	-----	-----	4,98	-----
P.A.F.	0,28	12,20	-----	3,75	-----	-----	-----	8,86	-----
TOTAL	104,59	100,35	-----	102,28	-----	-----	-----	100,18	-----
Fe_2O_3T	85,35	3,93	3,84	17,25	15,96	16,26	16,26	16,26	-----
Os (ppb)	4,6	-----	-----	-----	2,6	2,8	2,7	3,5	2,5
Ir	27	-----	-----	-----	3,6	3,2	3,2	2,9	3,1
Ru	40	-----	-----	-----	25	20	23	20	18
Rh	96	-----	-----	-----	13	12	13	12	12
Pt	35	-----	-----	-----	146	143	126	119	161
Pd	1590	-----	-----	-----	365	343	363	331	343
Au	40	-----	-----	-----	3,3	4,9	4,0	4,0	-----
Re	73	-----	-----	-----	1,7	1,7	1,6	1,5	1,6
Cu (ppm)	5423	19	-----	138	-----	-----	-----	846	-----
Ni	18731	58	-----	37	-----	-----	-----	6888	-----
Ag	0,7	3,9	1,4	0,51	<0,29	<0,24	<0,27	-----	-----
As	102	25	24	5,5	0,37	<0,33	0,43	-----	-----
Co	1051	32	31	54	236	233	241	-----	-----
Sb	2,6	1,6	1,8	0,06	0,52	1,3	0,65	-----	-----
Se	43	1,5	1,5	<0,8	1,9	1,7	1,3	-----	-----
Ba (ppm)	<19	750	711	<33	<40	<28	<26	-----	-----
Ce	12	67	69	19	<1,9	<1,9	<2,0	-----	-----
Cr	83	131	129	90	4257	4202	4278	-----	-----
Cs	0,36	3,4	3,4	0,68	<0,76	<0,56	<0,32	-----	-----
Eu	0,05	1,3	1,3	1,4	0,17	0,20	0,09	-----	-----
Hf	<0,12	5,1	4,1	2,9	0,53	0,19	0,35	-----	-----
La	7,6	35	34	6,6	0,42	0,43	0,47	-----	-----
Lu	0,05	0,60	0,53	0,45	0,08	0,09	0,09	-----	-----
Nd	8,2	30	29	10	1,2	<1,4	1,4	-----	-----
Rb	8,7	131	132	<3,5	3,6	<5,0	<4,4	-----	-----
Sc	3,9	22	21	38	18	17	18	-----	-----
Sm	2,8	5,7	5,9	3,8	0,43	0,39	0,46	-----	-----
Ta	0,23	1,2	1,2	0,13	<0,13	<0,07	0,15	-----	-----
Tb	0,24	0,78	0,77	0,93	0,14	0,09	0,11	-----	-----
Th	1,3	10	10	0,60	<0,13	<0,09	0,2	-----	-----
U	<0,52	4,8	4,8	0,11	<0,13	<0,10	<0,11	-----	-----
Yb	0,34	3,2	3,1	2,7	0,50	0,51	0,43	-----	-----

ANNEXE 2

RÉSULTATS D'ANALYSES GÉOCHIMIQUES (MINÉRAUX)

PAR

MICROSONDE ÉLECTRONIQUE

Abréviations

HEX : Pyrrhotite du type hexagonal (FeS)
MON : Pyrrhotite du type monoclinique ($Fe_{1-X}S$)

Notes

- limites de détection en % poids, à 3σ (50% d'erreur) : S= 0,10%; Fe= 0,14%; Ni= 0,03%; Cu= 0,03%; Co= 0,03%; As= 0,17%; Sb= 0,08%; Pd= 0,12%; Pt= 0,05%; Rh= 0,16%; Ag= 1,13%; Bi= 0,26%
- analyses effectuées par dispersion de longueur d'onde (WDS) à 20 kV et 7 ηA; diamètre du faisceau= 5 μm; intervalle de comptage= 100 secondes; S, Fe et As analysé par dispersion d'énergie (EDS); intervalle de comptage= 50 secondes

Pyrrhotite - $Fe_{1-X}S$

% poids

No. lame mince	DC-20A	DC-20A	DC-20A	DC-20A	DC-20A	DC-43	DC-43	DC-44	DC-44	DC-62	DC-62	DC-21	DC-21	DC-21
No. échantillon	DC-76	DC-76	DC-76	DC-76	DC-76	DC-64	DC-64	DC-61	DC-61	DC-55	DC-55	DC-67	DC-67	DC-67
S	36,73	36,80	36,29	36,73	36,34	37,03	36,79	36,79	36,43	38,72	38,78	36,17	36,18	36,65
Fe	62,23	63,06	63,05	63,13	62,38	63,00	63,33	62,87	63,03	60,70	61,15	62,01	62,37	62,90
Ni	0,00	0,00	0,00	0,04	0,00	0,00	0,00	0,04	0,00	0,12	0,00	0,00	0,00	0,00
Co	0,00	0,00	0,00	0,00	0,00	0,00	0,00	0,00	0,00	0,00	0,00	0,00	0,00	0,00
Cu	0,00	0,00	0,04	0,00	0,04	0,08	0,00	0,00	0,04	0,00	0,00	0,00	0,00	0,00
Total	98,96	99,85	99,38	99,90	98,76	100,11	100,12	99,70	99,50	99,54	99,92	98,18	98,55	99,55
% atomique														
S	50,69	50,41	50,05	50,31	50,35	50,56	50,29	50,46	50,16	52,58	52,48	50,40	50,26	50,37
Fe	49,31	49,59	49,92	49,66	49,62	49,38	49,71	49,51	49,82	47,33	47,52	49,60	49,74	49,63
Ni	0,00	0,00	0,00	0,03	0,00	0,00	0,00	0,03	0,00	0,09	0,00	0,00	0,00	0,00
Co	0,00	0,00	0,00	0,00	0,00	0,00	0,00	0,00	0,00	0,00	0,00	0,00	0,00	0,00
Cu	0,00	0,00	0,03	0,00	0,03	0,06	0,00	0,00	0,03	0,00	0,00	0,00	0,00	0,00
Total	100,00	100,00	100,00	100,00	100,00	100,00	100,00	100,00	100,00	100,00	100,00	100,00	100,00	100,00
Formule chimique														
S	1,01	1,01	1,00	1,01	1,01	1,01	1,01	1,01	1,00	1,05	1,05	1,01	1,01	1,01
Fe	0,99	0,99	1,00	0,99	0,99	0,99	0,99	0,99	1,00	0,95	0,95	0,99	0,99	0,99
Ni	0,00	0,00	0,00	0,00	0,00	0,00	0,00	0,00	0,00	0,00	0,00	0,00	0,00	0,00
Co	0,00	0,00	0,00	0,00	0,00	0,00	0,00	0,00	0,00	0,00	0,00	0,00	0,00	0,00
Cu	0,00	0,00	0,00	0,00	0,00	0,00	0,00	0,00	0,00	0,00	0,00	0,00	0,00	0,00
Total	2,00	2,00	2,00	2,00	2,00	2,00	2,00	2,00	2,00	2,00	2,00	2,00	2,00	2,00
Type	HEX	HEX	HEX	HEX	HEX	HEX	HEX	HEX	HEX	MON	MON	HEX	HEX	HEX

Pyrrhotite - $Fe_{1-X}S$

% poids

No. lame mince	DC-69	DC-69	DC-18	DC-18	DC-18	DC-19B	DC-55	DC-55	DC-20B	DC-20B
No. échantillon	DC-66	DC-66	DC-73	DC-73	DC-73	DC-65	DC-26	DC-26	DC-76	DC-76
S	38,59	38,72	38,28	37,84	38,33	38,16	38,07	38,56	35,98	36,02
Fe	59,25	59,05	58,65	59,30	59,48	59,85	61,02	60,85	63,45	62,60
Ni	0,57	0,55	0,21	0,20	0,18	0,12	0,22	0,18	0,00	0,05
Co	0,00	0,00	0,00	0,00	0,00	0,00	0,00	0,00	0,00	0,00
Cu	0,00	0,00	0,00	0,00	0,42	0,05	0,00	0,00	0,10	0,00
Total	98,41	98,32	97,14	97,34	98,42	98,18	99,31	99,59	99,53	98,67
% atomique										
S	52,93	53,10	53,12	52,56	52,66	52,56	51,99	52,39	49,65	50,04
Fe	46,65	46,49	46,72	47,29	46,91	47,32	47,84	47,47	50,28	49,93
Ni	0,42	0,41	0,16	0,15	0,14	0,09	0,17	0,14	0,00	0,04
Co	0,00	0,00	0,00	0,00	0,00	0,00	0,00	0,00	0,00	0,00
Cu	0,00	0,00	0,00	0,00	0,29	0,03	0,00	0,00	0,07	0,00
Total	100,00	100,00	100,00	100,00	100,00	100,00	100,00	100,00	100,00	100,00
Formule chimique										
S	1,06	1,06	1,06	1,05	1,05	1,05	1,04	1,05	0,99	1,00
Fe	0,93	0,93	0,93	0,95	0,94	0,95	0,96	0,95	1,01	1,00
Ni	0,01	0,01	0,00	0,00	0,00	0,00	0,00	0,00	0,00	0,00
Co	0,00	0,00	0,00	0,00	0,00	0,00	0,00	0,00	0,00	0,00
Cu	0,00	0,00	0,00	0,00	0,01	0,00	0,00	0,00	0,00	0,00
Total	2,00	2,00	2,00	2,00	2,00	2,00	2,00	2,00	2,00	2,00
Type	MON	MON	MON	MON	MON	MON	MON	MON	HEX	HEX

Pentlandite - $(Fe,Ni,Co)_9S_8$

% poids

No. lame mince	DC-20A	DC-20A	DC-20A	DC-20A	DC-43	DC-43	DC-43	DC-43	DC-44	DC-44	DC-44	DC-62	DC-62	DC-21
No. échantillon	DC-76	DC-76	DC-76	DC-76	DC-64	DC-64	DC-64	DC-64	DC-61	DC-61	DC-61	DC-55	DC-55	DC-67
S	33,14	33,38	33,26	33,25	33,61	33,19	33,61	33,60	33,45	33,33	33,01	33,48	33,53	33,41
Fe	33,89	33,29	34,37	34,01	38,08	37,31	36,22	37,72	37,93	34,99	34,95	33,34	32,32	33,53
Ni	31,03	30,95	29,83	29,95	27,70	28,91	29,77	28,66	27,91	29,83	29,80	31,44	32,22	31,00
Co	1,17	1,04	0,95	0,82	0,00	0,00	0,00	0,07	0,20	0,68	0,50	1,33	1,66	2,05
Total	99,23	98,66	98,41	98,03	99,39	99,41	99,60	100,05	99,50	98,84	98,26	99,60	99,72	99,99
% atomique														
S	47,22	47,71	47,65	47,79	47,60	47,14	47,56	47,35	47,39	47,56	47,41	47,48	47,50	47,25
Fe	27,72	27,32	28,27	28,06	30,97	30,42	29,43	30,52	30,85	28,66	28,82	27,14	26,29	27,22
Ni	24,15	24,16	23,34	23,51	21,43	22,43	23,01	22,07	21,60	23,25	23,38	24,36	24,94	23,95
Co	0,91	0,81	0,74	0,64	0,00	0,00	0,00	0,05	0,15	0,53	0,39	1,03	1,28	1,58
Total	100,00	100,00	100,00	100,00	100,00	100,00	100,00	100,00	100,00	100,00	100,00	100,00	100,00	100,00
Formule chimique														
S	8,03	8,11	8,10	8,12	8,09	8,01	8,08	8,05	8,06	8,08	8,06	8,07	8,07	8,03
Fe	4,71	4,64	4,81	4,77	5,26	5,17	5,00	5,19	5,24	4,87	4,90	4,61	4,47	4,63
Ni	4,11	4,11	3,97	4,00	3,64	3,81	3,91	3,75	3,67	3,95	3,97	4,14	4,24	4,07
Co	0,15	0,14	0,13	0,11	0,00	0,00	0,00	0,01	0,03	0,09	0,07	0,17	0,22	0,27
Total	17,00	17,00	17,00	17,00	17,00	17,00	17,00	17,00	17,00	17,00	17,00	17,00	17,00	17,00

Pentlandite - $(Fe,Ni,Co)_9 S_8$

% poids

No. lame mince	DC-21	DC-21	DC-69	DC-69	DC-69	DC-18	DC-18	DC-19B	DC-55	DC-20B	DC-20B
No. échantillon	DC-67	DC-67	DC-66	DC-66	DC-66	DC-73	DC-73	DC-65	DC-26	DC-76	DC-76
S	32,98	32,93	32,96	33,03	32,56	32,34	32,80	33,03	33,18	33,22	32,96
Fe	33,77	34,62	29,90	30,07	29,61	31,55	31,75	33,70	32,11	34,03	33,52
Ni	31,24	30,71	33,62	33,06	32,77	31,95	32,08	32,43	32,23	29,60	29,25
Co	1,96	1,75	3,28	3,28	3,56	2,40	2,59	1,07	2,94	1,34	1,67
Total	99,95	100,01	99,76	99,43	98,50	98,24	99,23	100,24	100,46	98,19	97,40

% atomique

S	46,78	46,68	46,90	47,09	46,92	46,73	46,88	46,73	46,85	47,69	47,70
Fe	27,50	28,18	24,42	24,61	24,49	26,17	26,06	27,38	26,03	28,05	27,86
Ni	24,21	23,79	26,14	25,75	25,80	25,22	25,05	25,07	24,86	23,21	23,13
Co	1,52	1,35	2,54	2,55	2,79	1,88	2,01	0,82	2,26	1,05	1,31
Total	100,00	100,00	100,00	100,00	100,00	100,00	100,00	100,00	100,00	100,00	100,00

Formule chimique

S	7,95	7,94	7,97	8,01	7,98	7,94	7,97	7,94	7,96	8,11	8,11
Fe	4,68	4,79	4,15	4,18	4,16	4,45	4,43	4,65	4,43	4,77	4,74
Ni	4,12	4,04	4,44	4,38	4,39	4,29	4,26	4,26	4,23	3,95	3,93
Co	0,26	0,23	0,43	0,43	0,47	0,32	0,34	0,14	0,38	0,18	0,22
Total	17,00	17,00	17,00	17,00	17,00	17,00	17,00	17,00	17,00	17,00	17,00

Chalcopyrite - $CuFeS_2$

% poids

No. lame mince	DC-20A	DC-20A	DC-20A	DC-20A	DC-43	DC-43	DC-44	DC-44	DC-62	DC-62	DC-21	DC-21	DC-21	DC-21
No. échantillon	DC-76	DC-76	DC-76	DC-76	DC-64	DC-64	DC-61	DC-61	DC-55	DC-55	DC-67	DC-67	DC-67	DC-67
S	34,89	35,05	34,62	34,76	35,05	35,10	34,91	34,82	35,02	35,39	34,10	33,43	34,52	34,69
Fe	30,54	30,38	30,37	29,97	30,13	29,81	30,49	29,61	30,35	30,89	30,00	28,07	29,51	29,84
Ni	0,00	0,00	0,00	0,04	0,00	0,00	0,00	0,00	0,00	0,00	0,13	0,00	0,16	0,00
Cu	34,51	34,51	33,65	33,84	34,76	34,68	34,52	33,70	36,35	34,60	33,82	35,43	35,31	34,37
Total	99,94	99,94	98,63	98,61	99,94	99,59	99,92	98,13	101,72	100,88	98,04	96,93	99,50	98,90

% atomique

S	49,96	50,14	50,15	50,33	50,15	50,35	49,99	50,59	49,47	50,14	49,81	49,58	49,76	50,16
Fe	25,11	24,95	25,26	24,92	24,75	24,55	25,07	24,70	24,61	25,12	25,16	23,90	24,43	24,77
Ni	0,00	0,00	0,00	0,03	0,00	0,00	0,00	0,00	0,00	0,00	0,10	0,00	0,13	0,00
Cu	24,93	24,91	24,60	24,72	25,10	25,10	24,94	24,71	25,91	24,73	24,93	26,51	25,68	25,07
Total	100,00	100,00	100,00	100,00	100,00	100,00	100,00	100,00	100,00	100,00	100,00	100,00	100,00	100,00

Formule chimique

S	2,00	2,01	2,01	2,01	2,01	2,01	2,00	2,02	1,98	2,01	1,99	1,98	1,99	2,01
Fe	1,00	1,00	1,01	1,00	0,99	0,98	1,00	0,99	0,98	1,00	1,01	0,96	0,98	0,99
Ni	0,00	0,00	0,00	0,00	0,00	0,00	0,00	0,00	0,00	0,00	0,00	0,00	0,01	0,00
Cu	1,00	1,00	0,98	0,99	1,00	1,00	1,00	0,99	1,04	0,99	1,00	1,06	1,03	1,00
Total	4,00	4,00	4,00	4,00	4,00	4,00	4,00	4,00	4,00	4,00	4,00	4,00	4,00	4,00

Chalcopyrite - $CuFeS_2$

% poids

No. lame mince	DC-69	DC-18	DC-19B	DC-55	DC-20B
No. échantillon	DC-66	DC-73	DC-65	DC-26	DC-76
S	34,69	34,07	34,51	34,17	34,86
Fe	29,89	29,54	29,94	30,53	30,43
Ni	0,00	0,00	0,00	0,00	0,00
Cu	35,95	37,51	36,28	37,70	35,75
Total	100,53	101,12	100,72	102,40	101,04

% atomique

S	49,56	48,70	49,30	48,32	49,54
Fe	24,52	24,24	24,55	24,78	24,83
Ni	0,00	0,00	0,00	0,00	0,00
Cu	25,92	27,05	26,15	26,90	25,64
Total	100,00	100,00	100,00	100,00	100,00

Formule chimique

S	1,98	1,95	1,97	1,93	1,98
Fe	0,98	0,97	0,98	0,99	0,99
Ni	0,00	0,00	0,00	0,00	0,00
Cu	1,04	1,08	1,05	1,08	1,03
Total	4,00	4,00	4,00	4,00	4,00

Cubanite - $CuFe_2S_3$

% poids

No. lame mince	DC-20A	DC-20A	DC-20A	DC-43	DC-43	DC-43	DC-44	DC-44	DC-62	DC-62	DC-62	DC-21
No. échantillon	DC-76	DC-76	DC-76	DC-64	DC-64	DC-64	DC-61	DC-61	DC-55	DC-55	DC-55	DC-67
S	35,65	35,58	35,51	35,55	35,51	35,66	35,63	36,14	35,69	35,31	35,83	35,82
Fe	40,55	41,02	40,58	40,67	41,04	41,74	41,26	41,40	41,34	40,97	41,40	40,80
Ni	0,04	0,00	0,00	0,00	0,04	0,00	0,00	0,00	0,00	0,00	0,04	0,00
Cu	23,17	23,25	23,01	22,96	23,06	23,99	23,05	23,36	23,99	23,45	23,61	24,53
Total	99,41	99,84	99,10	99,18	99,64	101,38	99,94	100,90	101,02	99,73	100,88	101,15
% atomique												
S	50,46	50,21	50,42	50,43	50,20	49,71	50,21	50,41	49,89	49,97	50,09	50,01
Fe	32,96	33,24	33,09	33,13	33,31	33,41	33,39	33,15	33,18	33,28	33,23	32,71
Ni	0,03	0,00	0,00	0,00	0,03	0,00	0,00	0,00	0,00	0,00	0,03	0,00
Cu	16,55	16,56	16,49	16,44	16,45	16,88	16,39	16,44	16,92	16,74	16,65	17,28
Total	100,00	100,00	100,00	100,00	100,00	100,00	100,00	100,00	100,00	100,00	100,00	100,00
Formule chimique												
S	3,03	3,01	3,03	3,03	3,01	2,98	3,01	3,02	2,99	3,00	3,01	3,00
Fe	1,98	1,99	1,99	1,99	2,00	2,00	2,00	1,99	1,99	2,00	1,99	1,96
Ni	0,00	0,00	0,00	0,00	0,00	0,00	0,00	0,00	0,00	0,00	0,00	0,00
Cu	0,99	0,99	0,99	0,99	0,99	1,01	0,98	0,99	1,02	1,00	1,00	1,04
Total	6,00	6,00	6,00	6,00	6,00	6,00	6,00	6,00	6,00	6,00	6,00	6,00

Mackinawite - (Fe,Ni) S

% poids

No. lame mince	DC-20A	DC-20A	DC-20A	DC-62	DC-21	DC-21	DC-18
No. échantillon	DC-76	DC-76	DC-76	DC-55	DC-67	DC-67	DC-73
S	36,22	36,52	36,05	36,63	36,22	36,46	35,59
Fe	56,95	57,43	56,80	56,28	57,32	56,66	54,31
Ni	5,84	5,68	5,66	6,40	5,86	5,97	6,37
Co	0,00	0,00	0,00	0,00	0,00	0,00	0,00
Cu	0,00	0,00	0,00	0,06	0,00	0,00	0,34
Total	99,02	99,62	98,51	99,37	99,39	99,09	96,61

% atomique

S	50,23	50,30	50,24	50,54	50,07	50,46	50,53
Fe	45,34	45,42	45,45	44,59	45,50	45,03	44,28
Ni	4,43	4,28	4,31	4,83	4,43	4,51	4,94
Co	0,00	0,00	0,00	0,00	0,00	0,00	0,00
Cu	0,00	0,00	0,00	0,04	0,00	0,00	0,24
Total	100,00	100,00	100,00	100,00	100,00	100,00	100,00

Formule chimique

S	1,00	1,01	1,00	1,01	1,00	1,01	1,01
Fe	0,91	0,91	0,91	0,89	0,91	0,90	0,89
Ni	0,09	0,09	0,09	0,10	0,09	0,09	0,10
Co	0,00	0,00	0,00	0,00	0,00	0,00	0,00
Cu	0,00	0,00	0,00	0,00	0,00	0,00	0,00
Total	2,00	2,00	2,00	2,00	2,00	2,00	2,00

Maucherite - $(Ni,Fe,Co,Pd,Pt,Ag,Cu)_{11}$ $(As,Sb,S)_8$

% poids

No. lame mince	DC-21	DC-21	DC-69	DC-69	DC-69	DC-69	DC-69	DC-69	DC-69	DC-69
No échantillon	DC-67	DC-67	DC-66	DC-66	DC-66	DC-66	DC-66	DC-66	DC-66	DC-66
S	0,00	0,12	0,00	0,12	0,13	0,19	0,15	0,17	0,89	3,69
Fe	0,45	0,24	0,78	0,28	1,57	3,30	6,29	2,53	3,27	2,97
Ni	46,23	47,03	50,69	50,81	50,07	42,32	23,70	48,12	32,23	29,84
Cu	0,00	0,00	0,00	0,00	0,00	0,00	0,00	0,00	0,00	0,00
As	46,31	46,00	48,31	47,40	48,15	41,85	24,50	47,36	33,84	36,03
Sb	1,12	0,94	0,00	0,00	0,00	4,76	8,66	0,25	13,82	12,08
Pd	0,00	0,33	0,00	0,42	0,52	2,33	6,26	0,35	10,27	7,71
Rh	0,00	0,00	0,00	0,00	0,00	0,00	0,00	0,00	0,00	0,00
Pt	0,36	0,08	0,06	0,00	0,00	0,00	0,07	0,09	0,17	0,07
Ag	0,00	0,00	0,00	0,00	0,00	2,26	2,98	0,00	5,66	5,25
Co	0,29	0,32	0,94	0,99	0,97	0,80	0,40	0,94	1,65	4,59
Total	94,76	95,06	100,79	100,03	101,42	97,80	73,01	99,80	101,79	102,23

% atomique

S	0,00	0,27	0,00	0,25	0,27	0,40	0,48	0,34	2,01	7,90
Fe	0,56	0,30	0,91	0,32	1,81	4,11	11,11	2,98	4,25	3,66
Ni	55,09	55,64	56,13	56,65	55,06	50,07	39,86	53,79	39,84	34,91
Cu	0,00	0,00	0,00	0,00	0,00	0,00	0,00	0,00	0,00	0,00
As	43,23	42,63	41,90	41,41	41,47	38,79	32,29	41,47	32,77	33,03
Sb	0,64	0,54	0,00	0,00	0,00	2,72	7,02	0,13	8,24	6,82
Pd	0,00	0,21	0,00	0,26	0,32	1,52	5,80	0,21	7,00	4,98
Rh	0,00	0,00	0,00	0,00	0,00	0,00	0,00	0,00	0,00	0,00
Pt	0,13	0,03	0,02	0,00	0,00	0,00	0,03	0,03	0,06	0,02
Ag	0,00	0,00	0,00	0,00	0,00	1,45	2,73	0,00	3,80	3,34
Co	0,35	0,38	1,04	1,10	1,07	0,94	0,67	1,05	2,03	5,35
Total	100,00	100,00	100,00	100,00	100,00	100,00	100,00	100,00	100,00	100,00

Formule chimique

S	0,00	0,01	0,00	0,01	0,01	0,01	0,01	0,01	0,04	0,16
Fe	0,01	0,01	0,02	0,01	0,04	0,08	0,22	0,06	0,09	0,07
Ni	1,10	1,11	1,12	1,13	1,10	1,00	0,80	1,08	0,80	0,70
Cu	0,00	0,00	0,00	0,00	0,00	0,00	0,00	0,00	0,00	0,00
As	0,86	0,85	0,84	0,83	0,83	0,78	0,65	0,83	0,66	0,66
Sb	0,01	0,01	0,00	0,00	0,00	0,05	0,14	0,00	0,16	0,14
Pd	0,00	0,00	0,00	0,01	0,01	0,03	0,12	0,00	0,14	0,10
Rh	0,00	0,00	0,00	0,00	0,00	0,00	0,00	0,00	0,00	0,00
Pt	0,00	0,00	0,00	0,00	0,00	0,00	0,00	0,00	0,00	0,00
Ag	0,00	0,00	0,00	0,00	0,00	0,03	0,05	0,00	0,08	0,07
Co	0,01	0,01	0,02	0,02	0,02	0,02	0,01	0,02	0,04	0,11
Total	2,00	2,00	2,00	2,00	2,00	2,00	2,00	2,00	2,00	2,00
As+Sb+S	8,00	8,00	8,00	8,00	8,00	8,00	8,00	8,00	8,00	8,00
Ni+Fe+Co+Pd +Pt+Ag+Cu	10,24	10,37	11,08	11,20	11,10	11,09	12,10	11,07	10,59	8,75

Maucherite - $(Ni,Fe,Co,Pd,Pt,Ag,Cu)_{11}$ $(As,Sb,S)_8$

% poids

No. lame mince	DC-69	DC-69	DC-69	DC-69	DC-69	DC-69	DC-69	DC-18	DC-18	DC-18
No échantillon	DC-66	DC-66	DC-66	DC-66	DC-66	DC-66	DC-66	DC-73	DC-73	DC-73
S	0,16	0,14	0,16	0,00	1,42	0,00	0,25	0,13	0,00	0,11
Fe	0,38	0,85	1,93	1,89	3,18	2,24	2,52	1,06	0,82	0,82
Ni	50,74	49,36	49,36	49,78	46,32	48,65	48,94	51,24	51,21	51,33
Cu	0,00	0,00	0,00	0,00	1,15	0,00	0,00	0,00	0,00	0,00
As	48,36	48,44	48,32	49,59	47,72	49,70	49,46	49,69	49,26	50,03
Sb	0,00	0,00	0,00	0,00	0,00	0,00	0,00	0,00	0,00	0,00
Pd	0,50	0,43	0,43	0,50	0,39	0,70	0,70	0,00	0,83	0,00
Rh	0,00	0,00	0,00	0,00	0,00	0,00	0,00	0,00	0,00	0,00
Pt	0,00	0,08	0,07	0,10	0,07	0,00	0,00	0,07	0,17	0,10
Ag	0,00	0,00	0,00	0,00	0,00	0,00	0,00	0,00	0,00	0,00
Co	1,54	1,68	1,64	1,67	1,57	1,43	1,68	0,77	0,63	1,04
Total	101,68	100,98	101,91	103,52	101,79	102,72	103,55	102,96	102,92	103,44

% atomique

S	0,33	0,29	0,33	0,00	2,80	0,00	0,49	0,26	0,00	0,22
Fe	0,44	0,99	2,22	2,14	3,61	2,56	2,86	1,21	0,94	0,94
Ni	55,68	54,60	53,99	53,78	50,08	53,03	52,71	55,50	55,79	55,39
Cu	0,00	0,00	0,00	0,00	1,14	0,00	0,00	0,00	0,00	0,00
As	41,57	41,98	41,40	41,96	40,42	42,43	41,73	42,17	42,03	42,30
Sb	0,00	0,00	0,00	0,00	0,00	0,00	0,00	0,00	0,00	0,00
Pd	0,30	0,26	0,26	0,30	0,23	0,42	0,42	0,00	0,50	0,00
Rh	0,00	0,00	0,00	0,00	0,00	0,00	0,00	0,00	0,00	0,00
Pt	0,00	0,03	0,02	0,03	0,02	0,00	0,00	0,02	0,05	0,03
Ag	0,00	0,00	0,00	0,00	0,00	0,00	0,00	0,00	0,00	0,00
Co	1,68	1,85	1,79	1,79	1,69	1,55	1,80	0,83	0,68	1,12
Total	100,00	100,00	100,00	100,00	100,00	100,00	100,00	100,00	100,00	100,00

Formule chimique

S	0,01	0,01	0,01	0,00	0,06	0,00	0,01	0,01	0,00	0,00
Fe	0,01	0,02	0,04	0,04	0,07	0,05	0,06	0,02	0,02	0,02
Ni	1,11	1,09	1,08	1,08	1,00	1,06	1,05	1,11	1,12	1,11
Cu	0,00	0,00	0,00	0,00	0,02	0,00	0,00	0,00	0,00	0,00
As	0,83	0,84	0,83	0,84	0,81	0,85	0,83	0,84	0,84	0,85
Sb	0,00	0,00	0,00	0,00	0,00	0,00	0,00	0,00	0,00	0,00
Pd	0,01	0,01	0,01	0,01	0,00	0,01	0,01	0,00	0,01	0,00
Rh	0,00	0,00	0,00	0,00	0,00	0,00	0,00	0,00	0,00	0,00
Pt	0,00	0,00	0,00	0,00	0,00	0,00	0,00	0,00	0,00	0,00
Ag	0,00	0,00	0,00	0,00	0,00	0,00	0,00	0,00	0,00	0,00
Co	0,03	0,04	0,04	0,04	0,03	0,03	0,04	0,02	0,01	0,02
Total	2,00	2,00	2,00	2,00	2,00	2,00	2,00	2,00	2,00	2,00
As+Sb+S	8,00	8,00	8,00	8,00	8,00	8,00	8,00	8,00	8,00	8,00
Ni+Fe+Co+Pd +Pt+Ag+Cu	11,04	10,92	11,17	11,00	10,46	10,77	10,87	10,85	10,93	10,81

Niccolite - (Ni,Fe,Co,Pd,Pt) (As,Sb,S)

% poids

No. lame mince	DC-21	DC-21	DC-21	DC-69	DC-69
No. échantillon	DC-67	DC-67	DC-66	DC-66	DC-66
S	0,10	0,12	0,18	0,11	0,26
Fe	0,23	0,00	0,00	2,20	2,19
Ni	38,13	39,50	36,27	43,61	43,69
Cu	0,00	0,00	0,00	0,00	0,00
As	53,38	53,14	52,37	58,33	57,89
Sb	1,40	1,31	1,31	0,19	0,15
Pd	0,00	0,00	0,30	0,00	0,00
Rh	0,00	0,00	0,00	0,00	0,00
Pt	0,26	0,00	0,00	0,12	0,00
Ag	0,00	0,00	0,00	0,00	0,00
Co	0,30	0,40	0,26	0,94	0,87
Total	93,81	94,47	90,69	105,51	105,04

% atomique

S	0,23	0,27	0,43	0,22	0,51
Fe	0,30	0,00	0,00	2,49	2,48
Ni	46,82	47,95	46,10	46,95	47,10
Cu	0,00	0,00	0,00	0,00	0,00
As	51,35	50,52	52,13	49,20	48,89
Sb	0,83	0,76	0,80	0,10	0,08
Pd	0,00	0,00	0,21	0,00	0,00
Rh	0,00	0,00	0,00	0,00	0,00
Pt	0,10	0,00	0,00	0,04	0,00
Ag	0,00	0,00	0,00	0,00	0,00
Co	0,37	0,49	0,32	1,01	0,94
Total	100,00	100,00	100,00	100,00	100,00

Formule chimique

S	0,00	0,01	0,01	0,00	0,01
Fe	0,01	0,00	0,00	0,05	0,05
Ni	0,94	0,96	0,92	0,94	0,94
Cu	0,00	0,00	0,00	0,00	0,00
As	1,03	1,01	1,04	0,98	0,98
Sb	0,02	0,02	0,02	0,00	0,00
Pd	0,00	0,00	0,00	0,00	0,00
Rh	0,00	0,00	0,00	0,00	0,00
Pt	0,00	0,00	0,00	0,00	0,00
Ag	0,00	0,00	0,00	0,00	0,00
Co	0,01	0,01	0,01	0,02	0,02
Total	2,00	2,00	2,00	2,00	2,00
As+Sb+S	1,05	1,03	1,07	0,99	0,99
Ni+Fe+Co+Pd+Pt	0,95	0,97	0,93	1,01	1,01

Cobaltite-Gersdorffite - (Co,Fe,Ni,Cu,Pd,Rh,Pt) (As,Sb) S

% poids

No. lame mince	DC-69	DC-69	DC-69	DC-69	DC-18	DC-18	DC-18
No échantillon	DC-66	DC-66	DC-66	DC-66	DC-73	DC-73	DC-73
S	18,66	17,84	17,64	21,16	21,26	24,28	27,37
Fe	4,85	4,70	5,77	12,89	6,67	12,28	17,35
Ni	6,47	6,44	7,99	5,99	3,07	2,94	1,83
Cu	0,00	0,00	0,00	0,00	4,24	10,40	16,46
As	42,83	42,14	38,97	35,79	41,98	35,93	28,82
Sb	0,13	2,03	3,21	2,77	0,00	0,00	0,00
Pd	0,22	0,89	1,55	1,71	0,51	0,98	0,96
Rh	0,00	0,00	0,00	0,00	0,33	1,97	2,08
Pt	0,16	0,00	0,11	0,00	0,00	0,07	0,09
Ag	0,00	0,00	0,00	0,00	0,00	0,00	0,00
Co	22,37	22,64	18,64	17,29	24,24	16,08	12,47
Total	95,69	96,69	93,88	97,60	102,31	104,92	107,44

% atomique

S	33,56	32,30	33,00	36,61	35,24	38,40	41,03
Fe	5,01	4,89	6,20	12,80	6,35	11,15	14,93
Ni	6,36	6,37	8,16	5,66	2,78	2,54	1,50
Cu	0,00	0,00	0,00	0,00	3,55	8,30	12,45
As	32,97	32,67	31,19	26,50	29,79	24,32	18,49
Sb	0,06	0,97	1,58	1,26	0,00	0,00	0,00
Pd	0,12	0,49	0,87	0,89	0,25	0,47	0,43
Rh	0,00	0,00	0,00	0,00	0,17	0,97	0,97
Pt	0,05	0,00	0,03	0,00	0,00	0,02	0,02
Ag	0,00	0,00	0,00	0,00	0,00	0,00	0,00
Co	21,89	22,31	18,97	16,27	21,87	13,83	10,17
Total	100,00	100,00	100,00	100,00	100,00	100,00	100,00

Formule chimique

S	1,01	0,97	0,99	1,10	1,06	1,15	1,23
Fe	0,15	0,15	0,19	0,38	0,19	0,33	0,45
Ni	0,19	0,19	0,24	0,17	0,08	0,08	0,05
Cu	0,00	0,00	0,00	0,00	0,11	0,25	0,37
As	0,99	0,98	0,94	0,79	0,89	0,73	0,55
Sb	0,00	0,03	0,05	0,04	0,00	0,00	0,00
Pd	0,00	0,01	0,03	0,03	0,01	0,01	0,01
Rh	0,00	0,00	0,00	0,00	0,01	0,03	0,03
Pt	0,00	0,00	0,00	0,00	0,00	0,00	0,00
Ag	0,00	0,00	0,00	0,00	0,00	0,00	0,00
Co	0,66	0,67	0,57	0,49	0,66	0,42	0,31
Total	3,00	3,00	3,00	3,00	3,00	3,00	3,00
S	1,01	0,97	0,99	1,10	1,06	1,15	1,23
As+Sb	0,99	1,01	0,98	0,83	0,89	0,73	0,55
Co+Fe+Ni+Cu+ Pd+Rh+Pt	1,00	1,02	1,03	1,07	1,05	1,12	1,21

Gersdorffite - (Ni,Co,Fe,Cu) (As,Sb) S

% poids

No. lame mince	DC-21	DC-69
No. échantillon	DC-67	DC-66
S	17,79	13,45
Fe	3,03	2,92
Ni	18,62	14,81
Cu	0,62	1,53
As	44,29	36,96
Sb	0,69	0,00
Pd	0,00	0,00
Rh	0,00	0,00
Pt	0,00	0,00
Ag	0,00	0,00
Co	9,86	17,41
Total	94,91	87,07

% atomique

S	32,63	27,30
Fe	3,19	3,40
Ni	18,66	16,42
Cu	0,57	1,56
As	34,77	32,09
Sb	0,34	0,00
Pd	0,00	0,00
Rh	0,00	0,00
Pt	0,00	0,00
Ag	0,00	0,00
Co	9,84	19,22
Total	100,00	100,00

Formule chimique

S	0,98	0,82
Fe	0,10	0,10
Ni	0,56	0,49
Cu	0,02	0,05
As	1,04	0,96
Sb	0,01	0,00
Pd	0,00	0,00
Rh	0,00	0,00
Pt	0,00	0,00
Ag	0,00	0,00
Co	0,30	0,58
Total	3,00	3,00
S	0,98	0,82
As+Sb	1,05	0,96
Ni+Co+Fe+Cu	0,97	1,22

Froodite - (Pd,Fe,Cu,Ni,Pt,Rh) $(Bi,Ag,Sb,Te)_2$

% poids

No. lame mince	DC-21	DC-21	DC-21	DC-21	DC-21	DC-21	DC-21
No échantillon	DC-67	DC-67	DC-67	DC-67	DC-67	DC-67	DC-67
Fe	1,47	0,32	0,31	0,60	1,23	0,53	0,51
Ni	0,40	0,00	0,00	0,37	0,32	0,00	0,35
Cu	0,61	0,39	0,38	0,56	0,50	0,60	0,97
Sb	0,00	0,09	0,09	0,13	0,20	0,00	0,00
Pd	19,13	19,53	19,66	18,91	19,51	19,26	19,78
Rh	0,00	0,00	0,00	0,16	0,00	0,00	0,16
Pt	1,74	1,92	1,90	1,74	1,84	1,71	1,76
Te	0,00	0,00	0,00	0,00	0,00	0,32	0,00
Bi	79,94	78,57	78,45	77,08	78,30	78,17	81,04
Ag	2,85	2,74	-----	-----	-----	-----	-----
Total	106,14	103,57	100,80	99,55	101,90	100,60	104,57

% atomique

Fe	4,11	0,96	0,97	1,83	3,63	1,61	1,48
Ni	1,06	0,00	0,00	1,08	0,90	0,00	0,97
Cu	1,51	1,02	1,03	1,52	1,31	1,63	2,48
Sb	0,00	0,12	0,13	0,18	0,27	0,00	0,00
Pd	28,07	30,22	31,73	30,43	30,34	30,93	30,25
Rh	0,00	0,00	0,00	0,27	0,00	0,00	0,26
Pt	1,39	1,62	1,67	1,53	1,56	1,50	1,47
Te	0,00	0,00	0,00	0,00	0,00	0,43	0,00
Bi	59,73	61,89	64,47	63,16	61,99	63,90	63,10
Ag	4,12	4,18	-----	-----	-----	-----	-----
Total	100,00	100,00	100,00	100,00	100,00	100,00	100,00

Formule chimique

Fe	0,12	0,03	0,03	0,06	0,11	0,05	0,04
Ni	0,03	0,00	0,00	0,03	0,03	0,00	0,03
Cu	0,05	0,03	0,03	0,05	0,04	0,05	0,07
Sb	0,00	0,00	0,00	0,01	0,01	0,00	0,00
Pd	0,84	0,91	0,95	0,91	0,91	0,93	0,91
Rh	0,00	0,00	0,00	0,01	0,00	0,00	0,01
Pt	0,04	0,05	0,05	0,05	0,05	0,04	0,04
Te	0,00	0,00	0,00	0,00	0,00	0,01	0,00
Bi	1,79	1,86	1,93	1,89	1,86	1,92	1,89
Ag	0,12	0,13	-----	-----	-----	-----	-----
Total	3,00	3,00	3,00	3,00	3,00	3,00	3,00
Bi+Ag+Sb+Te	1,92	1,99	1,94	1,90	1,87	1,93	1,89
Pd+Fe+Cu+ Ni+Pt+Rh	1,08	1,01	1,06	1,10	1,13	1,07	1,11

Arséniure de Pd-Sb - (Pd,Co,Ag,Ni,Fe,Pt) (As,Sb,S)

% poids

No. lame mince No échantillon	DC-69 DC-66	DC-69 DC-66	DC-69 DC-66
S	8,41	7,99	10,93
Fe	4,04	4,09	3,89
Ni	5,01	4,87	5,92
Cu	0,00	0,00	0,00
As	26,77	25,27	31,68
Sb	22,82	25,04	17,52
Pd	19,42	17,85	14,42
Rh	0,00	0,00	0,00
Pt	0,25	0,12	0,00
Ag	12,06	11,81	7,98
Co	10,71	11,02	13,37
Total	109,49	108,06	105,71

% atomique

S	18,19	17,63	22,50
Fe	5,01	5,18	4,60
Ni	5,92	5,87	6,66
Cu	0,00	0,00	0,00
As	24,78	23,87	27,92
Sb	13,00	14,55	9,50
Pd	12,66	11,87	8,95
Rh	0,00	0,00	0,00
Pt	0,09	0,04	0,00
Ag	7,75	7,75	4,88
Co	12,60	13,23	14,98
Total	100,00	100,00	100,00

Formule chimique

S	0,36	0,35	0,45
Fe	0,10	0,10	0,09
Ni	0,12	0,12	0,13
Cu	0,00	0,00	0,00
As	0,50	0,48	0,56
Sb	0,26	0,29	0,19
Pd	0,25	0,24	0,18
Rh	0,00	0,00	0,00
Pt	0,00	0,00	0,00
Ag	0,16	0,16	0,10
Co	0,25	0,26	0,30
Total	2,00	2,00	2,00
As+S+Sb	1,12	1,12	1,20
Pd+Co+Ag+ Ni+Fe+Pt	0,88	0,88	0,80

ANNEXE 3

RÉSULTATS DES ISOTOPES DU SOUFRE (ROCHE TOTALE)

PAR

TECHNIQUE KIBA

Abréviations

VIRG : Formation de Virginia (argillite)
VIRG-Po : Formation de Virginia (argillite à pyrrhotite)
S-NOR : Norite à sulfures
S-TROC : Troctolite, gabbro à olivine ou leucotroctolite à sulfures
S-ÉGP : Leucotroctolite à sulfures enrichis en ÉGP
SM : Veines de sulfures massifs à semi-massifs
CU : Troctolite, gabbro à olivine ou leucotroctolite à sulfures enrichis en cuivre

Notes

- précision à 2σ d'erreur= 0,3‰ (standards internationaux IAEA-S1 et IAEA-S2)

No. Échantillon	Type de roche	No. Forage	Profondeur (m)	$\delta^{34}S$ (‰)
DC-27	S-NOR	26117	708,3	14,5
DC-49	S-NOR	26117	727,5	8,2
DC-52	S-NOR	-----	-----	13,7
DC-54	S-NOR	-----	-----	12,5
DC-60	S-NOR	26117	683,4	10,4
DC-63	S-NOR	26143	252,3	7,1
DC-66	S-NOR	26107	721,7	9,8
DC-72	S-NOR	26117	703,5	13,6
DC-53	S-TROC	26117	741,2	6,7
DC-55	S-TROC	26117	753,9	9,0
DC-56	S-TROC	26107	702,8	9,2
DC-58	S-TROC	26107	682,5	6,6
DC-61	S-TROC	26117	627,8	7,5
DC-79	S-TROC	26107	718,0	7,6
DC-62	S-ÉGP	26107	627,5	1,6
DC-64	S-ÉGP	26117	609,2	2,5
DC-73	SM	26143	284,0	8,4
DC-75	SM	26117	716,5	16,0
DC-76	SM	26143	328,9	12,0
DC-65	CU	26143	288,2	11,0
DC-67	CU	26143	329,0	11,9
DC-1	VIRG	B2	135,9	5,3
DC-3	VIRG	B2	390,3	8,6
DC-5	VIRG	B2	464,8	7,2
DC-7	VIRG	B2	479,7	4,5
DC-8	VIRG	B2	443,2	5,1
DC-9	VIRG	B2	245,3	4,7
DC-70	VIRG-Po	-----	-----	15,8

ANNEXE 4

RÉSULTATS D'ANALYSES GÉOCHIMIQUES

TIRÉES DE LA LITTÉRATURE (ARTICLE #3)

Abréviations

S-ÉGP : Leucotroctolite, gabbro à olivine ou troctolite à sulfures enrichis en ÉGP
S-TROC : Troctolite, gabbro à olivine, norite ou leucotroctolite à sulfures
SM : Veines de sulfures massifs à semi-massifs
IPCO : International Platinum Company
DNR : Department of Natural Resources, Minnesota
UQAC : Université du Québec à Chicoutimi
n : nombre d'échantillons

Notes

la composition des sulfures a été recalculée à 100% sulfures en assumant 36% S

DUNKA ROAD - ROCHE TOTALE

No. forage	Profondeur (pieds)	Type de roche	Références	S(%)	Cu(ppm)	Ni(ppm)	Au(ppb)	Pt(ppb)	Pd(ppb)
A4-11	240-251	S-ÉGP	IPCO	-----	1200	500	192	317	759
A4-11	251-258	S-ÉGP	IPCO	0,38	4100	900	317	950	2200
A4-11	285	S-TROC	IPCO	0,42	4500	700	54	80	190
A4-11	295-305	S-TROC	IPCO	0,47	4300	700	85	175	400
A4-11	305	S-TROC	IPCO	0,89	4500	900	47	60	180
A4-11	434-444	S-ÉGP	IPCO	-----	800	400	51	221	444
A4-11	1335-1345	S-ÉGP	IPCO	0,52	3900	1100	50	100	620
A4-11	1345-1355	S-ÉGP	IPCO	0,49	4100	800	68	230	490
A4-11	1355-1365	S-ÉGP	IPCO	0,75	5600	1300	68	200	870
A4-11	1365-1375	S-ÉGP	IPCO	0,61	4700	1400	82	190	700
A4-11	1375-1385	S-ÉGP	IPCO	0,56	3800	1700	69	190	710
A4-11	1385-1395	S-ÉGP	IPCO	0,17	1200	600	24	50	285
A4-11	1395-1405	S-ÉGP	IPCO	0,52	4200	900	69	120	460
A4-11	1405	S-TROC	IPCO	-----	2400	600	19	45	227
A4-11	1425	S-TROC	IPCO	-----	1300	500	18	48	108
013	101-111	S-ÉGP	Geerts, 1991	0,47	3582	871	164	361	2081
013	111-119	S-ÉGP	Geerts, 1991	0,31	2180	538	170	367	1759
015	286-296	S-ÉGP	Geerts, 1991	-----	3536	1104	74	276	1432
017	585-593	S-ÉGP	Geerts, 1991	1,16	6300	1100	113	141	889
027	506	S-TROC	Fleck Resources	-----	932	287	17	11	47
027	516	S-TROC	Fleck Resources	-----	1794	385	13	4	11
027	526	S-TROC	Fleck Resources	-----	1775	414	11	7	20
027	556	S-TROC	Fleck Resources	-----	1769	424	13	4	32
027	566	S-TROC	Fleck Resources	-----	2341	732	33	16	83
031	719-729	S-ÉGP	Geerts, 1991	1,34	9577	2275	218	512	1999
033	535-540	S-ÉGP	Geerts, 1991	0,84	5680	1520	120	290	950
034	1058-1068	S-ÉGP	Geerts, 1991	1,17	7400	1800	78	341	1010
042	973	S-TROC	Severson et Hauck, 1990	0,42	3226	869	71	100	330
045	369-375	S-ÉGP	Geerts, 1991	0,56	3100	1140	81	90	540
046	465-470	S-ÉGP	Geerts, 1991	0,78	4790	1590	160	340	1400
058	8	S-TROC	Fleck Resources	-----	8815	1394	175	246	633
060	109-119	S-ÉGP	Geerts, 1991	1,42	9715	1801	442	329	2026
064	765	S-TROC	Geerts, 1991	1,40	4440	1360	42	100	370
065	2235	S-TROC	Severson et Hauck, 1990	0,17	237	254	3	20	8
073	1697-1707	S-ÉGP	Geerts, 1991	1,02	6700	1600	62	161	963
073	1717-1727	S-ÉGP	Geerts, 1991	0,82	4900	1000	75	239	937
075	2240-2250	S-ÉGP	Geerts, 1991	1,58	12276	2133	121	219	1928
080	315-325	S-ÉGP	Fleck Resources	0,48	3802	761	171	405	1132
080	325-339	S-ÉGP	Fleck Resources	0,51	4221	857	175	525	1568
086	463-473	S-ÉGP	Geerts, 1991	1,38	7900	2500	67	339	1286
098	428-438	S-ÉGP	Geerts, 1991	0,64	5100	1100	38	124	599
098	438-448	S-ÉGP	Geerts, 1991	0,89	6717	1257	95	384	1903
107	2005	S-TROC	Severson et Hauck, 1990	0,09	212	176	2	20	8
107	2064	S-ÉGP	Thériault et Barnes, 1998	1,69	12200	3740	420	560	2300
107	2245	S-TROC	Thériault et Barnes, 1998	2,00	10200	2440	140	160	710
107	2312	S-TROC	Thériault et Barnes, 1998	1,44	5550	1910	48	110	400
107	2362	S-TROC	Thériault et Barnes, 1998	1,12	7120	2250	67	160	580
107	2374	S-TROC	Thériault et Barnes, 1998	4,32	6400	2280	45	35	460
109	187	S-TROC	Fleck Resources	-----	4288	1052	49	69	285
109	198	S-TROC	Fleck Resources	-----	3494	807	55	51	225
115	1532	S-TROC	Fleck Resources	-----	2793	808	36	45	166
115	1542-1552	S-ÉGP	Fleck Resources	-----	6951	1643	69	410	900
115	1552-1562	S-ÉGP	Fleck Resources	-----	5407	1327	69	164	744
115	1572	S-TROC	Fleck Resources	-----	6048	1344	58	119	503
115	1579	S-TROC	Fleck Resources	-----	5780	1289	35	177	260

DUNKA ROAD - ROCHE TOTALE

No. forage	Profondeur (pieds)	Type de roche	Références	S(%)	Cu(ppm)	Ni(ppm)	Au(ppb)	Pt(ppb)	Pd(ppb)
115	1589	S-TROC	Fleck Resources	-----	5837	1364	42	95	390
115	1600-1610	S-ÉGP	Fleck Resources	-----	6543	1403	97	545	738
115	1610	S-TROC	Fleck Resources	-----	4266	947	36	111	391
115	2037	S-TROC	Fleck Resources	-----	5262	1217	25	36	129
115	2047	S-TROC	Fleck Resources	-----	4127	1051	23	394	81
115	2057	S-TROC	Fleck Resources	-----	3466	988	19	7	62
116	1701-1711	S-ÉGP	Geerts, 1991	0,84	6372	850	267	410	2454
117		S-TROC	Severson et Hauck, 1990	0,14	1043	411	27	50	55
117	2004	S-ÉGP	Thériault et Barnes, 1998	0,59	3380	1680	89	300	1600
117	2043-2048	S-ÉGP	Geerts, 1991	0,78	7419	863	64	150	1886
117	2065	S-TROC	Thériault et Barnes, 1998	1,50	7130	2050	59	120	500
117	2248	S-TROC	Thériault et Barnes, 1998	1,57	3000	1140	19	50	100
117	2314	S-TROC	Thériault et Barnes, 1998	4,65	3700	1140	45	5	120
117	2330	S-TROC	Thériault et Barnes, 1998	0,77	1300	348	11	13	23
117	2393	S-TROC	Thériault et Barnes, 1998	0,20	373	151	0	3	5
117	2438	S-TROC	Thériault et Barnes, 1998	0,15	514	230	0	10	39
117	2480	S-TROC	Thériault et Barnes, 1998	1,11	3650	1070	32	42	170
121	313	S-ÉGP	Geerts, 1991	1,38	9600	1800	48	382	1435
122	205-215	S-ÉGP	Geerts, 1991	1,22	15217	1420	368	410	2347
122	215-227	S-ÉGP	Geerts, 1991	1,06	11513	1777	254	376	2064
125	2102-2109	S-ÉGP	Fleck Resources	-----	3027	912	82	80	584
125	2141-2151	S-ÉGP	Geerts, 1991	0,90	5937	1321	48	257	862
125	2151-2161	S-ÉGP	Geerts, 1991	1,09	7481	1595	41	360	988
125	2161-2174	S-ÉGP	Fleck Resources	-----	5439	1153	179	118	851
125	2201	S-TROC	Fleck Resources	-----	3137	698	62	61	261
125	2211	S-TROC	Fleck Resources	-----	1603	494	24	34	123
125	2217	S-TROC	Fleck Resources	-----	1230	418	20	40	57
127	491	S-TROC	Fleck Resources	-----	1673	552	52	26	84
127	501	S-TROC	Fleck Resources	-----	1524	481	34	21	178
127	538	S-TROC	Fleck Resources	-----	1116	297	38	10	84
127	555	S-TROC	Fleck Resources	-----	4813	1035	70	111	482
127	565	S-TROC	Fleck Resources	-----	4486	1056	65	95	351
127	575	S-TROC	Fleck Resources	-----	3176	905	57	61	293
127	585	S-TROC	Fleck Resources	-----	4265	1118	65	75	371
127	595	S-TROC	Fleck Resources	-----	3586	824	45	76	329
141	153-163	S-ÉGP	Fleck Resources	-----	4493	956	91	176	827
141	163-168	S-ÉGP	Fleck Resources	-----	4081	945	80	192	767
141	168-179	S-ÉGP	Fleck Resources	-----	2629	674	47	110	374
141	179-189	S-ÉGP	Fleck Resources	-----	4100	880	93	240	543
141	189-199	S-ÉGP	Fleck Resources	-----	6661	1393	153	414	1104
141	199-209	S-ÉGP	Fleck Resources	-----	4268	1037	115	217	819
141	209-219	S-ÉGP	Fleck Resources	-----	4363	1013	68	198	714
141	219-228	S-ÉGP	Fleck Resources	-----	5191	1049	115	211	666
141	228-238	S-ÉGP	Fleck Resources	-----	2779	648	62	101	374
141	238-248	S-ÉGP	Fleck Resources	-----	7396	1335	109	320	816
141	248-258	S-ÉGP	Fleck Resources	-----	4028	884	111	180	481
141	258-269	S-ÉGP	Fleck Resources	-----	4628	1001	141	212	600
141	425	S-TROC	Fleck Resources	-----	2921	676	57	99	271
141	435	S-TROC	Fleck Resources	-----	6143	950	124	120	451
141	447	S-TROC	Fleck Resources	-----	2022	432	72	83	216
141	457	S-TROC	Fleck Resources	-----	1881	468	52	63	214
141	650-655	S-ÉGP	Fleck Resources	-----	6177	1366	243	441	1410
141	655-665	S-ÉGP	Fleck Resources	-----	3887	836	76	108	481
141	665-675	S-ÉGP	Fleck Resources	-----	5027	1178	93	298	677
141	675-685	S-ÉGP	Fleck Resources	-----	5458	1216	102	152	878

DUNKA ROAD - ROCHE TOTALE

No. forage	Profondeur (pieds)	Type de roche	Références	S(%)	Cu(ppm)	Ni(ppm)	Au(ppb)	Pt(ppb)	Pd(ppb)
141	685-695	S-ÉGP	Fleck Resources	-----	7791	2069	194	242	1284
141	695-705	S-ÉGP	Fleck Resources	-----	6560	1544	91	168	806
141	705-715	S-ÉGP	Fleck Resources	-----	6056	1475	182	158	666
141	715	S-TROC	Fleck Resources	-----	5787	1306	72	152	576
141	725	S-TROC	Fleck Resources	-----	4730	1447	90	134	512
141	731	S-TROC	Fleck Resources	-----	3793	972	61	146	413
141	738-748	S-ÉGP	Fleck Resources	-----	6382	1547	153	266	764
141	748	S-TROC	Fleck Resources	-----	5429	1219	84	171	556
142	252-262	S-ÉGP	Geerts, 1991	1,10	7500	1700	222	183	1055
142	262-271	S-ÉGP	Fleck Resources	-----	7846	1373	103	356	917
142	306-316	S-ÉGP	Fleck Resources	-----	7627	1051	106	222	798
142	316-324	S-ÉGP	Fleck Resources	-----	9435	1684	89	314	1158
142	324-334	S-ÉGP	Fleck Resources	-----	3420	775	43	132	379
142	334-345	S-ÉGP	Fleck Resources	-----	3896	805	69	133	443
143	320	S-ÉGP	Severson et Hauck, 1990	0,50	3560	920	88	270	640
143	830	S-TROC	Thériault et Barnes, 1998	2,45	2210	824	18	16	63
143	852	S-TROC	Fleck Resources	-----	1914	507	24	46	79
143	865	S-TROC	Fleck Resources	-----	509	203	7	3	13
143	876	S-TROC	Fleck Resources	-----	3637	799	17	13	91
143	886	S-TROC	Fleck Resources	-----	2672	778	24	57	177
143	927	S-TROC	Fleck Resources	-----	5595	2487	27	34	199
143	934	SM	Thériault et Barnes, 1998	19,60	12200	10700	29	9	470
143	937	S-TROC	Fleck Resources	-----	2728	756	17	40	72
143	946	S-TROC	Fleck Resources	-----	11206	1963	119	161	390
143	949	S-TROC	Thériault et Barnes, 1998	2,17	15700	1470	270	370	600
143	956	S-TROC	Fleck Resources	-----	13017	1452	123	80	346
143	961	S-TROC	Fleck Resources	-----	2692	466	32	11	104
143	970	S-TROC	Fleck Resources	-----	5904	1144	46	115	181
143	1082	SM	Thériault et Barnes, 1998	34,90	5420	18700	40	35	1600
143	1083	S-TROC	Thériault et Barnes, 1998	3,42	14000	1570	280	840	970
143	1121	S-TROC	Fleck Resources	-----	5650	708	94	86	393
143	1134	S-TROC	Fleck Resources	-----	2943	529	53	75	224
143	1143	S-TROC	Fleck Resources	-----	6313	1088	46	210	346
143	1153	S-TROC	Fleck Resources	-----	5781	1007	72	136	525
143	1163	S-TROC	Fleck Resources	-----	6199	711	45	63	319
143	1173	S-TROC	Fleck Resources	-----	5041	1314	91	82	399
143	2021	S-TROC	Severson et Hauck, 1990	0,26	702	252	5	30	20
Moyenne	S-ÉGP	n=69		-----	5693	1266	124	269	1045
Moyenne	S-TROC	n=77		-----	4183	945	53	93	263
Moyenne	SM	n=2		27,25	8810	14700	35	22	1035
Moyenne	TOTAL	n=148		-----	4950	1281	86	174	638

DUNKA ROAD - 100% SULFURES

No. forage	Profondeur (pieds)	Type de roche	Références	S(%)	Cu(%)	Ni(%)	Au(ppb)	Pt(ppb)	Pd(ppb)
A4-11	251-258	S-ÉGP	IPCO	36,0	38,8	8,53	30032	90000	208421
A4-11	285	S-TROC	IPCO	36,0	38,6	6,00	4629	6857	16286
A4-11	295-305	S-TROC	IPCO	36,0	32,9	5,36	6511	13404	30638
A4-11	305	S-TROC	IPCO	36,0	18,2	3,64	1901	2427	7281
A4-11	1335-1345	S-ÉGP	IPCO	36,0	27,0	7,62	3462	6923	42923
A4-11	1345-1355	S-ÉGP	IPCO	36,0	30,1	5,88	4996	16898	36000
A4-11	1355-1365	S-ÉGP	IPCO	36,0	26,9	6,24	3264	9600	41760
A4-11	1365-1375	S-ÉGP	IPCO	36,0	27,7	8,26	4839	11213	41311
A4-11	1375-1385	S-ÉGP	IPCO	36,0	24,4	10,9	4436	12214	45643
A4-11	1385-1395	S-ÉGP	IPCO	36,0	25,4	12,7	5082	10588	60353
A4-11	1395-1405	S-ÉGP	IPCO	36,0	29,1	6,23	4777	8308	31846
013	101-111	S-ÉGP	Geerts, 1991	36,0	27,4	6,67	12562	27651	159396
013	111-119	S-ÉGP	Geerts, 1991	36,0	25,3	6,25	19742	42619	204271
017	585-593	S-ÉGP	Geerts, 1991	36,0	19,6	3,41	3507	4376	27590
031	719-729	S-ÉGP	Geerts, 1991	36,0	25,7	6,11	5857	13755	53704
033	535-540	S-ÉGP	Geerts, 1991	36,0	24,3	6,51	5143	12429	40714
034	1058-1068	S-ÉGP	Geerts, 1991	36,0	22,8	5,54	2400	10492	31077
042	973	S-TROC	Severson et Hauck, 1990	36,0	27,7	7,45	6086	8571	28286
045	369-375	S-ÉGP	Geerts, 1991	36,0	19,9	7,33	5207	5786	34714
046	465-470	S-ÉGP	Geerts, 1991	36,0	22,1	7,34	7385	15692	64615
060	109-119	S-ÉGP	Geerts, 1991	36,0	24,6	4,57	11206	8341	51363
064	765	S-TROC	Geerts, 1991	36,0	11,4	3,50	1080	2571	9514
065	2235	S-TROC	Severson et Hauck, 1990	36,0	5,02	5,38	635	4235	1694
073	1697-1707	S-ÉGP	Geerts, 1991	36,0	23,6	5,65	2188	5682	33988
073	1717-1727	S-ÉGP	Geerts, 1991	36,0	21,5	4,39	3293	10493	41137
075	2240-2250	S-ÉGP	Geerts, 1991	36,0	28,0	4,86	2757	4990	43929
080	315-325	S-ÉGP	Fleck Resources	36,0	28,5	5,71	12825	30375	84900
080	325-339	S-ÉGP	Fleck Resources	36,0	29,8	6,05	12353	37059	110682
086	463-473	S-ÉGP	Geerts, 1991	36,0	20,6	6,52	1748	8843	33548
098	428-438	S-ÉGP	Geerts, 1991	36,0	28,7	6,19	2138	6975	33694
098	438-448	S-ÉGP	Geerts, 1991	36,0	27,2	5,08	3843	15533	76975
107	2005	S-TROC	Severson et Hauck, 1990	36,0	8,48	7,04	800	8000	3200
107	2064	S-ÉGP	Thériault et Barnes, 1998	36,0	26,0	7,97	8947	11929	48994
107	2245	S-TROC	Thériault et Barnes, 1998	36,0	18,4	4,39	2520	2880	12780
107	2312	S-TROC	Thériault et Barnes, 1998	36,0	13,9	4,78	1200	2750	10000
107	2362	S-TROC	Thériault et Barnes, 1998	36,0	22,9	7,23	2154	5143	18643
107	2374	S-TROC	Thériault et Barnes, 1998	36,0	5,33	1,90	375	292	3833
116	1701-1711	S-ÉGP	Geerts, 1991	36,0	27,3	3,64	11443	17571	105171
117	1925	S-TROC	Severson et Hauck, 1990	36,0	26,8	10,6	6943	12857	14143
117	2004	S-ÉGP	Thériault et Barnes, 1998	36,0	20,6	10,3	5431	18305	97627
117	2043-2048	S-ÉGP	Geerts, 1991	36,0	34,2	3,98	2954	6923	87046
117	2065	S-TROC	Thériault et Barnes, 1998	36,0	17,1	4,92	1416	2880	12000
117	2248	S-TROC	Thériault et Barnes, 1998	36,0	6,88	2,61	436	1146	2293
117	2314	S-TROC	Thériault et Barnes, 1998	36,0	2,86	0,88	348	39	929
117	2330	S-TROC	Thériault et Barnes, 1998	36,0	6,08	1,63	514	608	1075
117	2393	S-TROC	Thériault et Barnes, 1998	36,0	6,71	2,72	0	540	900
117	2438	S-TROC	Thériault et Barnes, 1998	36,0	12,3	5,52	0	2400	9360
117	2480	S-TROC	Thériault et Barnes, 1998	36,0	11,8	3,47	1038	1362	5514
121	313	S-ÉGP	Geerts, 1991	36,0	25,0	4,70	1252	9965	37435
122	205-215	S-ÉGP	Geerts, 1991	36,0	44,9	4,19	10859	12098	69256
122	215-227	S-ÉGP	Geerts, 1991	36,0	39,1	6,04	8626	12770	70098
125	2141-2151	S-ÉGP	Geerts, 1991	36,0	23,7	5,28	1920	10280	34480
125	2151-2161	S-ÉGP	Geerts, 1991	36,0	24,7	5,27	1354	11890	32631
143	320	S-ÉGP	Severson et Hauck, 1990	36,0	25,6	6,62	6336	19440	46080
143	830	S-TROC	Thériault et Barnes, 1998	36,0	3,25	1,21	264	235	926

DUNKA ROAD - 100% SULFURES

No. forage	Profondeur (pieds)	Type de roche	Références	S(%)	Cu(%)	Ni(%)	Au(ppb)	Pt(ppb)	Pd(ppb)
143	934	SM	Thériault et Barnes, 1998	36,0	2,24	1,97	53	17	863
143	949	S-TROC	Thériault et Barnes, 1998	36,0	26,0	2,44	4479	6138	9954
143	1082	SM	Thériault et Barnes, 1998	36,0	0,56	1,93	41	36	1650
143	1083	S-TROC	Thériault et Barnes, 1998	36,0	14,7	1,65	2947	8842	10211
143	2021	S-TROC	Severson et Hauck, 1990	36,0	9,72	3,49	692	4154	2769
Moyenne	S-ÉGP	n=36		36,0	26,8	6,34	6706	15667	63831
Moyenne		n=23		36,0	15,1	4,25	2042	4275	9227
Moyenne	SM	n=2		36,0	1,40	1,95	47	26	1257
Moyenne	TOTAL	n=61		36,0	21,6	5,41	4729	10859	41191

WETLEGS - ROCHE TOTALE

No. forage	Profondeur (pieds)	Type de roche	Références	S(%)	Cu(ppm)	Ni(ppm)	Au(ppb)	Pt(ppb)	Pd(ppb)
A4-12	1029	S-TROC	UQAC	1,02	3711	1278	11	23	62
A4-13	1240-1244	S-ÉGP	UQAC	0,60	6289	1829	166	282	1090
A4-14	1487	S-TROC	IPCO	-----	1900	600	28	125	98
A4-14	1634-1644	S-ÉGP	IPCO	-----	4000	1300	81	169	650
A4-14	1644-1654	S-ÉGP	IPCO	-----	1900	700	23	47	277
W-1	566-571	S-ÉGP	UQAC	1,03	5210	2005	325	552	2167
W-1	757	S-TROC	Severson et Hauck, 1990	0,26	1206	362	8	20	12
W-2	124	S-TROC	IPCO	-----	3500	600	1562	46	270
W-2	867-877	S-ÉGP	IPCO	0,32	1600	500	33	97	284
W-2	877-887	S-ÉGP	IPCO	0,36	4500	800	95	126	602
W-2	887-897	S-ÉGP	IPCO	0,36	3700	800	77	193	636
W-2	897-907	S-ÉGP	IPCO	0,34	2900	600	50	105	480
W-2	907-917	S-ÉGP	IPCO	0,29	2200	500	44	101	297
W-2	917	S-TROC	IPCO	0,40	3000	700	37	95	277
W-2	926	S-TROC	IPCO	0,63	4200	700	83	108	330
W-2	936-946	S-ÉGP	IPCO	0,60	4900	900	60	105	419
W-2	946	S-TROC	IPCO	0,54	4300	800	16	90	355
W-2	956	S-TROC	IPCO	0,73	4900	900	13	80	307
W-2	966	S-TROC	IPCO	0,37	3300	700	17	107	235
W-2	976-986	S-ÉGP	IPCO	0,54	4100	800	14	272	450
W-2	986	S-TROC	IPCO	0,25	4700	800	15	141	328
W-3	926	S-TROC	UQAC	0,17	724	485	7	22	48
W-3	1460	S-TROC	UQAC	1,43	5865	2456	42	36	35
W-8	429	S-TROC	UQAC	1,69	3678	1404	20	38	63
W-9	359	S-TROC	DNR	1,87	16100	4400	49	150	220
W-9	925	S-TROC	DNR	1,00	5200	1800	52	<15	95
W-9	935	S-TROC	DNR	1,65	9000	3000	58	<15	130
W-10	630	S-TROC	UQAC	1,63	5252	1295	16	33	84
W-11	433	S-TROC	Severson et Hauck, 1990	0,26	1386	298	12	15	15
W-11	653	S-TROC	UQAC	1,09	3566	1481	25	33	78
W-12	340-350	S-ÉGP	DNR	0,22	1400	500	89	213	887
W-12	682	S-TROC	UQAC	1,22	4667	1367	46	71	110
W-13	209-219	S-ÉGP	IPCO	-----	2500	600	51	110	399
W-13	229	S-TROC	IPCO	-----	2900	600	33	86	270
W-13	239	S-TROC	IPCO	-----	3200	600	30	73	211
W-13	248	S-TROC	IPCO	-----	4000	700	66	110	352
W-13	258-268	S-ÉGP	IPCO	-----	4500	900	56	132	466
W-13	268	S-TROC	IPCO	-----	2900	700	40	67	279
W-13	278	S-TROC	IPCO	-----	3600	700	55	73	276
W-13	288	S-TROC	IPCO	-----	3500	600	41	98	275
W-13	298-308	S-ÉGP	IPCO	-----	4100	800	56	224	476
W-13	308-318	S-ÉGP	IPCO	-----	3300	600	41	112	412
W-13	318-328	S-ÉGP	IPCO	-----	3600	600	93	90	496
W-13	328	S-TROC	IPCO	-----	1700	500	17	67	138
W-13	347	S-TROC	IPCO	-----	2200	400	25	96	183
W-14	434	S-TROC	DNR	1,42	8000	2200	71	25	150
W-14	824-834	S-ÉGP	IPCO	-----	5000	1000	81	259	642
W-14	834-844	S-ÉGP	IPCO	-----	5800	1400	153	330	1091
W-14	844-854	S-ÉGP	IPCO	-----	2700	800	73	176	715
W-14	854-863	S-ÉGP	IPCO	-----	4600	800	94	309	879
W-14	863	S-TROC	IPCO	-----	1700	600	20	75	121
W-14	873	S-TROC	IPCO	-----	2200	400	28	46	99
W-14	1185	S-TROC	Severson et Hauck, 1990	0,40	1591	442	10	25	8

WETLEGS - ROCHE TOTALE

No. forage	Profondeur (pieds)	Type de roche	Références	S(%)	Cu(ppm)	Ni(ppm)	Au(ppb)	Pt(ppb)	Pd(ppb)
Moyenne	S-ÉGP	n=21		-----	3752	892	84	191	658
Moyenne	S-TROC	n=32		-----	3989	1058	80	72	172
Moyenne	TOTAL	n=53		-----	3895	992	81	119	365

WETLEGS - 100% SULFURES

No. forage	Profondeur (pieds)	Type de roche	Références	S(%)	Cu(%)	Ni(%)	Au(ppb)	Pt(ppb)	Pd(ppb)
A4-12	1029	S-TROC	UQAC	36,0	13,1	4,51	388	812	2188
A4-13	1240-1244	S-ÉGP	UQAC	36,0	37,7	11,0	9960	16920	65400
W-1	566-571	S-ÉGP	UQAC	36,0	18,2	7,01	11359	19293	75740
W-1	757	S-TROC	Severson et Hauck, 1990	36,0	16,7	5,01	1108	2769	1662
W-2	867-877	S-ÉGP	IPCO	36,0	18,0	5,63	3713	10913	31950
W-2	877-887	S-ÉGP	IPCO	36,0	45,0	8,00	9500	12600	60200
W-2	887-897	S-ÉGP	IPCO	36,0	37,0	8,00	7700	19300	63600
W-2	897-907	S-ÉGP	IPCO	36,0	30,7	6,35	5294	11118	50824
W-2	907-917	S-ÉGP	IPCO	36,0	27,3	6,21	5462	12538	36869
W-2	917	S-TROC	IPCO	36,0	27,0	6,30	3330	8550	24930
W-2	926	S-TROC	IPCO	36,0	24,0	4,00	4743	6171	18857
W-2	936-946	S-ÉGP	IPCO	36,0	29,4	5,40	3600	6300	25140
W-2	946	S-TROC	IPCO	36,0	28,7	5,33	1067	6000	23667
W-2	956	S-TROC	IPCO	36,0	24,2	4,44	641	3945	15140
W-2	966	S-TROC	IPCO	36,0	32,1	6,81	1654	10411	22865
W-2	976-986	S-ÉGP	IPCO	36,0	27,3	5,33	933	18133	30000
W-2	986	S-TROC	IPCO	36,0	67,7	11,5	2160	20304	47232
W-3	926	S-TROC	UQAC	36,0	15,3	10,3	1482	4659	10165
W-3	1460	S-TROC	UQAC	36,0	14,8	6,18	1057	906	881
W-8	429	S-TROC	UQAC	36,0	7,83	2,99	426	809	1342
W-9	359	S-TROC	DNR	36,0	31,0	8,47	943	2888	4235
W-9	925	S-TROC	DNR	36,0	18,7	6,48	1872	-----	3420
W-9	935	S-TROC	DNR	36,0	19,6	6,55	1265	-----	2836
W-10	630	S-TROC	UQAC	36,0	11,6	2,86	353	729	1855
W-11	433	S-TROC	Severson et Hauck, 1990	36,0	19,2	4,13	1662	2077	2077
W-11	653	S-TROC	UQAC	36,0	11,8	4,89	826	1090	2576
W-12	340-350	S-ÉGP	DNR	36,0	22,9	8,18	14564	34855	145145
W-12	682	S-TROC	UQAC	36,0	13,8	4,03	1357	2095	3246
W-14	434	S-TROC	DNR	36,0	20,3	5,58	1800	634	3803
W-14	1185	S-TROC	Severson et Hauck, 1990	36,0	14,3	3,98	900	2250	720
Moyenne	S-ÉGP	n=10		36,0	29,35	7,11	7209	16197	58487
Moyenne	S-TROC	n=20		36,0	21,59	5,72	1452	4283	9685
Moyenne	TOTAL	n=30		36,0	24,1747	6,18	3371	8538	25952

WYMAN CREEK - ROCHE TOTALE

No. forage	Profondeur (pieds)	Type de roche	Références	S(%)	Cu(ppm)	Ni(ppm)	Au(ppb)	Pt(ppb)	Pd(ppb)
126	361-368	S-ÉGP	Fleck Resources	0,32	2091	586	25	39	133
126	368-378	S-ÉGP	Fleck Resources	0,79	5204	1169	22	89	109
126	373	S-TROC	Fleck Resources	-----	2973	850	22	16	61
126	388	S-TROC	Fleck Resources	-----	3868	1023	24	31	72
126	398	S-TROC	Fleck Resources	-----	4556	1112	29	56	90
126	837	S-TROC	Fleck Resources	-----	1518	375	7	4	17
126	860	S-TROC	Fleck Resources	-----	3471	698	17	3	15
126	870	S-TROC	Fleck Resources	-----	3201	548	13	7	30
126	880	S-TROC	Fleck Resources	-----	3104	481	19	5	9
126	920	S-TROC	Fleck Resources	-----	5375	675	28	124	35
126	928	S-TROC	Fleck Resources	-----	3336	611	17	9	20
126	936	S-TROC	Fleck Resources	-----	4373	894	16	14	21
126	946	S-TROC	Fleck Resources	-----	2358	540	12	9	23
126	953	S-TROC	Fleck Resources	-----	2248	612	17	8	19
126	980	S-TROC	Fleck Resources	-----	2595	568	19	9	24
126	990	S-TROC	Fleck Resources	-----	3191	844	19	24	37
126	1030	S-TROC	Fleck Resources	-----	3163	782	26	<2	9
126	1040	S-TROC	Fleck Resources	-----	4447	871	30	14	34
126	1098	S-TROC	Fleck Resources	-----	2430	383	15	1	18
126	1109	S-TROC	Fleck Resources	-----	3794	598	24	29	21
126	1119	S-TROC	Fleck Resources	-----	2243	348	14	3	14
126	1127	S-TROC	Fleck Resources	-----	3091	524	18	12	23
126	1133	S-TROC	Fleck Resources	-----	1077	453	14	6	20
126	1143	S-TROC	Fleck Resources	-----	3012	631	15	8	25
126	1155	S-TROC	Fleck Resources	-----	2112	555	13	6	10
126	1166	S-TROC	Fleck Resources	-----	340	100	11	7	6
126	1174	S-TROC	Fleck Resources	-----	3182	462	21	21	8
126	1184	S-TROC	Fleck Resources	-----	1824	237	34	7	10
126	1194	S-TROC	Fleck Resources	-----	2242	315	48	6	4
126	1204-1214	S-ÉGP	Severson et Hauck, 1997	1,20	3900	900	44	40	96
132	27	S-TROC	Fleck Resources	-----	4843	1068	60	37	86
132	37	S-TROC	Fleck Resources	-----	4561	1082	48	31	71
132	47-57	S-ÉGP	Severson et Hauck, 1997	0,29	2300	900	20	10	80
132	57-67	S-ÉGP	Severson et Hauck, 1997	0,58	4000	1300	50	80	132
132	67	S-TROC	Fleck Resources	-----	3542	757	38	25	47
132	77	S-TROC	Fleck Resources	-----	5910	1292	41	34	97
132	87	S-TROC	Fleck Resources	-----	5193	1074	44	17	63
132	97	S-TROC	Fleck Resources	-----	4931	1090	43	16	49
132	107	S-TROC	Fleck Resources	-----	3540	795	32	14	39
132	132	S-TROC	Fleck Resources	-----	4224	940	65	21	45
132	142	S-TROC	Fleck Resources	-----	3243	791	31	19	40
132	152	S-TROC	Fleck Resources	-----	3432	793	35	19	40
132	162-172	S-ÉGP	Fleck Resources	0,89	4382	977	58	62	90
132	172-177	S-ÉGP	Fleck Resources	0,85	4806	1013	54	71	124
132	403	S-TROC	Fleck Resources	-----	2246	699	19	10	18
132	413	S-TROC	Fleck Resources	-----	3516	853	57	31	32
132	421	S-TROC	Fleck Resources	-----	1904	600	13	9	15
132	1040	S-TROC	Fleck Resources	-----	2693	549	31	25	53
132	1050	S-TROC	Fleck Resources	-----	3585	660	29	454	57
132	1061	S-TROC	Fleck Resources	-----	2013	567	23	12	24
132	1074	S-TROC	Fleck Resources	-----	2359	761	28	10	29
133	589	S-TROC	Fleck Resources	-----	902	488	11	4	14
133	595	S-TROC	Fleck Resources	-----	2783	816	43	12	43
133	610-620	S-ÉGP	Fleck Resources	0,48	3028	768	33	73	90
133	620-631	S-ÉGP	Fleck Resources	0,55	3169	804	54	44	122

WYMAN CREEK - ROCHE TOTALE

No. forage	Profondeur (pieds)	Type de roche	Références	S(%)	Cu(ppm)	Ni(ppm)	Au(ppb)	Pt(ppb)	Pd(ppb)
133	631-636	S-ÉGP	Fleck Resources	-----	2937	781	43	32	88
133	638-648	S-ÉGP	Fleck Resources	0,44	3632	763	42	34	97
133	1251	S-TROC	Fleck Resources	-----	4492	714	26	16	27
133	1261	S-TROC	Fleck Resources	-----	1689	318	10	8	12
133	1266	S-TROC	Fleck Resources	-----	2165	410	8	11	7
133	1457	S-TROC	Fleck Resources	-----	6314	1381	43	46	67
133	1483	S-TROC	Fleck Resources	-----	4311	703	20	24	41
134	127	S-TROC	Fleck Resources	-----	3061	756	22	19	37
134	137	S-TROC	Fleck Resources	-----	1158	550	8	8	17
134	148	S-TROC	Fleck Resources	-----	1790	482	21	13	24
134	155	S-TROC	Fleck Resources	-----	4926	892	31	20	52
134	166	S-TROC	Fleck Resources	-----	2823	746	20	26	28
134	176	S-TROC	Fleck Resources	-----	4671	1021	41	18	61
134	186	S-TROC	Fleck Resources	-----	2800	658	14	14	26
134	222	S-TROC	Fleck Resources	-----	2829	650	12	8	15
134	232	S-TROC	Fleck Resources	-----	2128	546	7	7	11
134	242	S-TROC	Fleck Resources	-----	1942	575	9	10	13
134	247	S-TROC	Fleck Resources	-----	1358	401	6	2	10
134	251	S-TROC	Fleck Resources	-----	1616	431	12	8	22
134	261	S-TROC	Fleck Resources	-----	2919	617	14	12	24
134	271	S-TROC	Fleck Resources	-----	1678	524	11	6	13
134	276	S-TROC	Fleck Resources	-----	520	299	5	8	13
134	283	S-TROC	Fleck Resources	-----	2097	526	14	9	12
134	293	S-TROC	Fleck Resources	-----	700	305	11	1	7
134	299	S-TROC	Fleck Resources	-----	3148	651	15	4	22
134	309	S-TROC	Fleck Resources	-----	2497	565	15	9	27
134	319	S-TROC	Fleck Resources	-----	2840	655	18	13	33
134	329	S-TROC	Fleck Resources	-----	2719	673	18	14	26
134	339	S-TROC	Fleck Resources	-----	1699	586	17	22	35
134	526	S-TROC	Fleck Resources	-----	1220	354	11	11	15
134	536	S-TROC	Fleck Resources	-----	1568	418	25	11	17
134	565	S-TROC	Fleck Resources	-----	1383	393	19	14	19
134	576	S-TROC	Fleck Resources	-----	3425	787	21	18	27
134	608	S-TROC	Fleck Resources	-----	2874	764	22	10	21
134	618	S-TROC	Fleck Resources	-----	2326	586	15	10	22
134	643	S-TROC	Fleck Resources	-----	2419	532	20	12	24
134	653	S-TROC	Fleck Resources	-----	4235	865	21	16	35
134	661	S-TROC	Fleck Resources	-----	2212	484	17	11	19
134	670	S-TROC	Fleck Resources	-----	3928	821	19	17	27
134	680	S-TROC	Fleck Resources	-----	3479	765	28	21	33
134	690	S-TROC	Fleck Resources	-----	5017	1069	42	35	54
134	701	S-TROC	Fleck Resources	-----	2190	500	15	10	11
134	713	S-TROC	Fleck Resources	-----	3294	682	18	11	25
134	718	S-TROC	Fleck Resources	-----	1402	357	6	4	13
134	969	S-TROC	Fleck Resources	-----	4401	1400	38	22	42
134	981	S-TROC	Fleck Resources	-----	2370	844	31	13	23
134	991	S-TROC	Fleck Resources	-----	3165	1241	22	20	31
134	1001	S-TROC	Fleck Resources	-----	1133	442	12	7	14
134	1010	S-TROC	Fleck Resources	-----	2842	954	23	25	33
134	1018	S-TROC	Fleck Resources	-----	1965	697	21	14	33
134	1027	S-TROC	Fleck Resources	-----	2922	1390	34	21	45
134	1037	S-TROC	Fleck Resources	-----	2671	999	23	16	38
134	1058	S-TROC	Fleck Resources	-----	2705	764	33	12	29
134	1068	S-TROC	Fleck Resources	-----	2362	712	26	9	23
135	287-297	S-ÉGP	Fleck Resources	0,53	4927	808	44	54	168

WYMAN CREEK - ROCHE TOTALE

No. forage	Profondeur (pieds)	Type de roche	Références	S(%)	Cu(ppm)	Ni(ppm)	Au(ppb)	Pt(ppb)	Pd(ppb)
135	297	S-TROC	Fleck Resources	-----	2611	662	22	25	46
135	307-317	S-ÉGP	Fleck Resources	-----	2369	640	34	32	64
135	317	S-TROC	Fleck Resources	-----	2137	642	15	16	35
135	327	S-TROC	Fleck Resources	-----	2737	670	27	23	57
135	337	S-ÉGP	Fleck Resources	-----	2259	690	29	27	58
135	494	S-TROC	Fleck Resources	-----	1609	388	8	5	9
135	504	S-TROC	Fleck Resources	-----	910	321	23	6	11
135	514	S-TROC	Fleck Resources	-----	1300	356	9	4	11
135	524	S-TROC	Fleck Resources	-----	2905	607	15	12	18
135	534	S-TROC	Fleck Resources	-----	2513	654	11	8	22
135	544	S-TROC	Fleck Resources	-----	1223	392	11	10	15
135	554	S-TROC	Fleck Resources	-----	1366	328	13	5	11
135	564	S-TROC	Fleck Resources	-----	1422	408	11	8	15
135	574	S-TROC	Fleck Resources	-----	1573	406	13	8	14
135	584	S-TROC	Fleck Resources	-----	794	215	4	2	6
135	594	S-TROC	Fleck Resources	-----	1368	408	9	7	15
136	52	S-TROC	Fleck Resources	-----	3845	937	31	81	41
136	62	S-TROC	Fleck Resources	-----	3391	792	22	24	31
136	72	S-TROC	Fleck Resources	-----	3935	850	27	29	33
136	82	S-TROC	Fleck Resources	-----	3402	881	12	6	28
136	92	S-TROC	Fleck Resources	-----	4617	894	7	9	31
136	102	S-TROC	Fleck Resources	-----	2655	628	2	12	24
136	112	S-TROC	Fleck Resources	-----	4930	1027	14	24	76
136	122	S-TROC	Fleck Resources	-----	3646	931	8	16	27
136	133	S-TROC	Fleck Resources	-----	2145	630	1	23	22
136	143	S-TROC	Fleck Resources	-----	2545	695	37	25	27
136	153	S-TROC	Fleck Resources	-----	3047	602	12	16	37
136	163	S-TROC	Fleck Resources	-----	1953	524	1	15	17
136	173	S-TROC	Fleck Resources	-----	1329	391	1	17	20
136	183	S-TROC	Fleck Resources	-----	3681	578	1	15	15
136	189	S-TROC	Fleck Resources	-----	4667	927	9	41	43
136	195	S-TROC	Fleck Resources	-----	9356	1554	31	66	67
136	205	S-TROC	Fleck Resources	-----	8458	1504	27	30	65
136	215	S-TROC	Fleck Resources	-----	9853	1699	19	54	65
136	225	S-TROC	Fleck Resources	-----	6164	1037	8	23	43
136	230	S-TROC	Fleck Resources	-----	5514	1034	15	65	65
136	240	S-TROC	Fleck Resources	-----	2350	479	6	20	33
136	245	S-TROC	Fleck Resources	-----	5576	867	3	24	49
136	255	S-TROC	Fleck Resources	-----	5147	1149	13	19	44
136	265	S-TROC	Fleck Resources	-----	5715	914	7	27	53
136	275	S-TROC	Fleck Resources	-----	5943	1117	5	44	63
136	281	S-TROC	Fleck Resources	-----	3159	740	5	16	36
136	291	S-TROC	Fleck Resources	-----	2107	581	1	9	25
136	302	S-TROC	Fleck Resources	-----	2398	583	6	21	53
136	305	S-TROC	Fleck Resources	-----	6363	1151	23	71	98
136	313	S-TROC	Fleck Resources	-----	3436	780	29	30	52
136	323	S-TROC	Fleck Resources	-----	2246	634	1	16	30
136	333	S-TROC	Fleck Resources	-----	2729	742	18	18	43
136	343	S-TROC	Fleck Resources	-----	1842	545	1	6	32
136	353	S-TROC	Fleck Resources	-----	2474	614	13	20	63
136	644	S-TROC	Fleck Resources	-----	4669	838	1	10	35
136	656	S-TROC	Fleck Resources	-----	1330	357	1	8	13
136	664	S-TROC	Fleck Resources	-----	2676	535	1	6	18
136	674	S-TROC	Fleck Resources	-----	3111	592	1	29	22
136	702	S-TROC	Fleck Resources	-----	1716	347	1	5	15

WYMAN CREEK - ROCHE TOTALE

No. forage	Profondeur (pieds)	Type de roche	Références	S(%)	Cu(ppm)	Ni(ppm)	Au(ppb)	Pt(ppb)	Pd(ppb)
136	712	S-TROC	Fleck Resources	-----	3442	656	17	12	29
136	719	S-TROC	Fleck Resources	-----	2415	469	10	6	13
136	725	S-TROC	Fleck Resources	-----	2547	607	13	7	20
137	867-877	S-ÉGP	Fleck Resources	0,46	4712	1019	55	42	149
137	877-887	S-ÉGP	Fleck Resources	0,69	5615	1206	52	177	135
137	887-899	S-ÉGP	Fleck Resources	0,79	5798	1913	139	36	165
137	899-906	S-ÉGP	Fleck Resources	-----	3191	872	21	31	79
137	1075	S-TROC	Fleck Resources	-----	671	269	6	3	12
137	1082	S-TROC	Fleck Resources	-----	3267	640	19	11	17
137	1089	S-TROC	Fleck Resources	-----	1867	457	24	13	27
137	1175	S-TROC	Fleck Resources	-----	2583	612	17	12	24
137	1188	S-TROC	Fleck Resources	-----	1383	409	9	20	29
137	1283	S-TROC	Fleck Resources	-----	1989	476	17	10	22
137	1293	S-TROC	Fleck Resources	-----	2615	577	24	9	25
137	1390	S-TROC	Fleck Resources	-----	2752	673	12	11	26
137	1398	S-TROC	Fleck Resources	-----	9384	2028	24	22	71
137	1409	S-TROC	Fleck Resources	-----	9460	1763	33	29	89
138	129-135	S-ÉGP	Fleck Resources	0,40	3195	807	61	79	154
138	135	S-TROC	Fleck Resources	-----	3331	910	38	20	55
138	232	S-TROC	Fleck Resources	-----	3947	835	29	37	67
138	240	S-TROC	Fleck Resources	-----	4217	950	32	32	82
138	280	S-TROC	Fleck Resources	-----	1913	523	26	31	36
138	290	S-TROC	Fleck Resources	-----	2875	703	46	26	43
138	300	S-TROC	Fleck Resources	-----	3162	780	27	17	39
138	711	S-TROC	Fleck Resources	-----	3840	1251	44	35	43
138	721	S-TROC	Fleck Resources	-----	4348	1367	52	34	47
138	731	S-TROC	Fleck Resources	-----	2433	705	16	38	20
138	742	S-TROC	Fleck Resources	-----	1199	475	13	13	11
138	752	S-TROC	Fleck Resources	-----	377	263	7	5	5
138	762	S-TROC	Fleck Resources	-----	1539	580	10	4	11
138	897	S-TROC	Fleck Resources	-----	3304	538	17	28	23
138	907	S-TROC	Fleck Resources	-----	2411	414	10	12	14
138	1009	S-TROC	Fleck Resources	-----	1227	275	9	7	11
138	1017	S-TROC	Fleck Resources	-----	1894	441	9	5	13
138	1080	S-TROC	Fleck Resources	-----	1215	382	13	11	23
138	1087-1097	S-ÉGP	Fleck Resources	0,67	4551	850	42	138	136
138	1097-1107	S-ÉGP	Fleck Resources	1,02	8037	1621	73	68	146
138	1107	S-TROC	Fleck Resources	-----	370	238	6	14	8
138	1118-1124	S-ÉGP	Fleck Resources	0,91	6107	1985	69	68	167
139	30	S-TROC	Fleck Resources	-----	1743	493	26	9	24
139	35	S-TROC	Fleck Resources	-----	3627	873	34	16	43
139	45	S-TROC	Fleck Resources	-----	3481	830	19	11	25
139	55	S-TROC	Fleck Resources	-----	951	416	11	6	10
139	62	S-TROC	Fleck Resources	-----	5112	1133	31	40	62
139	72	S-TROC	Fleck Resources	-----	4676	1060	33	34	64
139	78	S-TROC	Fleck Resources	-----	2546	676	17	18	31
139	119	S-TROC	Fleck Resources	-----	5578	1347	30	29	62
139	125	S-TROC	Fleck Resources	-----	6653	1539	34	34	56
139	131	S-TROC	Fleck Resources	-----	3436	779	21	21	30
139	138	S-TROC	Fleck Resources	-----	3360	846	23	20	38
139	147	S-TROC	Fleck Resources	-----	1312	414	19	8	17
139	154	S-TROC	Fleck Resources	-----	2513	692	26	12	30
140	53	S-TROC	Fleck Resources	-----	1548	415	9	7	16
140	63	S-TROC	Fleck Resources	-----	830	262	6	9	8
140	71	S-TROC	Fleck Resources	-----	3609	838	35	17	32
140	81	S-TROC	Fleck Resources	-----	3531	799	19	16	29

WYMAN CREEK - ROCHE TOTALE

No. forage	Profondeur (pieds)	Type de roche	Références	S(%)	Cu(ppm)	Ni(ppm)	Au(ppb)	Pt(ppb)	Pd(ppb)
140	91	S-TROC	Fleck Resources	-----	2046	550	20	11	16
140	101	S-TROC	Fleck Resources	-----	1915	772	20	20	41
140	111	S-TROC	Fleck Resources	-----	2939	735	37	10	64
140	122	S-TROC	Fleck Resources	-----	1654	489	9	2	18
140	129	S-TROC	Fleck Resources	-----	2713	757	15	6	25
140	139	S-TROC	Fleck Resources	-----	616	349	8	2	15
140	149	S-TROC	Fleck Resources	-----	1682	564	14	11	17
140	184	S-TROC	Fleck Resources	-----	2309	659	15	7	16
140	194	S-TROC	Fleck Resources	-----	2354	571	17	7	32
140	204	S-TROC	Fleck Resources	-----	1116	457	12	7	18
140	211	S-TROC	Fleck Resources	-----	2343	580	13	14	17
140	221	S-TROC	Fleck Resources	-----	2216	570	22	16	33
140	230	S-TROC	Fleck Resources	-----	1194	375	9	7	20
140	240	S-TROC	Fleck Resources	-----	712	259	9	4	13
140	246	S-TROC	Fleck Resources	-----	2452	573	15	4	20
140	255	S-TROC	Fleck Resources	-----	1450	426	10	9	14
140	260	S-TROC	Fleck Resources	-----	1268	406	16	20	16
140	265	S-TROC	Fleck Resources	-----	2048	500	15	21	22
140	275	S-TROC	Fleck Resources	-----	1088	312	6	6	11
140	285	S-TROC	Fleck Resources	-----	1047	279	5	3	9
140	295	S-TROC	Fleck Resources	-----	884	285	5	8	10
140	305	S-TROC	Fleck Resources	-----	320	173	2	7	3
140	313	S-TROC	Fleck Resources	-----	2499	766	15	7	18
140	318	S-TROC	Fleck Resources	-----	1037	364	8	9	15
140	328	S-TROC	Fleck Resources	-----	770	289	8	5	15
140	340	S-TROC	Fleck Resources	-----	5076	1159	65	27	50
140	350	S-TROC	Fleck Resources	-----	3287	674	29	16	27
140	355	S-TROC	Fleck Resources	-----	2585	536	11	7	25
140	364	S-TROC	Fleck Resources	-----	2582	624	17	12	21
140	374	S-TROC	Fleck Resources	-----	2273	571	13	4	18
140	384	S-TROC	Fleck Resources	-----	1543	410	18	5	15
140	395	S-TROC	Fleck Resources	-----	2590	865	21	20	22
140	401	S-TROC	Fleck Resources	-----	1737	625	22	18	33
140	408	S-TROC	Fleck Resources	-----	1956	637	23	55	32
140	417	S-TROC	Fleck Resources	-----	3729	961	35	49	50
140	427	S-TROC	Fleck Resources	-----	3830	923	32	22	40
140	435	S-TROC	Fleck Resources	-----	4222	1003	29	24	35
140	445	S-TROC	Fleck Resources	-----	4292	1230	26	19	35
140	453	S-TROC	Fleck Resources	-----	5167	917	28	21	41
140	463	S-TROC	Fleck Resources	-----	3566	842	24	11	26
140	470	S-TROC	Fleck Resources	-----	2740	731	15	17	21
140	480	S-TROC	Fleck Resources	-----	2135	491	9	9	13
140	490	S-TROC	Fleck Resources	-----	2680	450	9	2	10
140	500	S-TROC	Fleck Resources	-----	1363	293	7	4	12
140	510	S-TROC	Fleck Resources	-----	1665	364	9	4	13
149	303-307	S-ÉGP	UQAC	1,06	4087	1899	67	52	278
149	307-312	S-ÉGP	UQAC	0,94	4161	1554	24	89	125
151	306	S-TROC	UQAC	0,41	2245	805	16	10	10
151	905	S-TROC	Severson et Hauck, 1990	0,28	1102	288	4	20	8
152	880	S-TROC	Severson et Hauck, 1990	0,09	1825	730	17	40	45
153	506-508	S-ÉGP	Severson et Hauck, 1990	0,34	1702	870	35	80	150
153	519-521	S-ÉGP	UQAC	1,78	5173	2075	29	32	145
153	605	S-TROC	Severson et Hauck, 1990	0,07	1351	394	6	40	15
Moyenne	S-ÉGP	n=26		-----	4051	1107	47	61	126
Moyenne	S-TROC	n=249		-----	2858	680	19	19	30
Moyenne	TOTAL	n=275		-----	2971	720	22	23	39

WYMAN CREEK - 100% SULFURES

No. forage	Profondeur (pieds)	Type de roche	Références	S(%)	Cu(%)	Ni(%)	Au(ppb)	Pt(ppb)	Pd(ppb)
126	361-368	S-ÉGP	Fleck Resources	36,0	23,5	6,59	2813	4388	14963
126	368-378	S-ÉGP	Fleck Resources	36,0	23,7	5,33	1003	4056	4967
126	1204-1214	S-ÉGP	Severson et Hauck, 1997	36,0	11,7	2,70	1320	1200	2880
132	47-57	S-ÉGP	Severson et Hauck, 1997	36,0	28,6	11,2	2483	1241	9931
132	57-67	S-ÉGP	Severson et Hauck, 1997	36,0	24,8	8,07	3103	4966	8193
132	162-172	S-ÉGP	Fleck Resources	36,0	17,7	3,95	2346	2508	3640
132	172-177	S-ÉGP	Fleck Resources	36,0	20,4	4,29	2287	3007	5252
133	610-620	S-ÉGP	Fleck Resources	36,0	22,7	5,76	2475	5475	6750
133	620-631	S-ÉGP	Fleck Resources	36,0	20,7	5,26	3535	2880	7985
133	638-648	S-ÉGP	Fleck Resources	36,0	29,7	6,24	3436	2782	7936
135	287-297	S-ÉGP	Fleck Resources	36,0	33,5	5,49	2989	3668	11411
137	867-877	S-ÉGP	Fleck Resources	36,0	36,9	7,97	4304	3287	11661
137	877-887	S-ÉGP	Fleck Resources	36,0	29,3	6,29	2713	9235	7043
137	887-899	S-ÉGP	Fleck Resources	36,0	26,4	8,72	6334	1641	7519
138	129-135	S-ÉGP	Fleck Resources	36,0	28,8	7,26	5490	7110	13860
138	1087-1097	S-ÉGP	Fleck Resources	36,0	24,5	4,57	2257	7415	7307
138	1097-1107	S-ÉGP	Fleck Resources	36,0	28,4	5,72	2576	2400	5153
138	1118-1124	S-ÉGP	Fleck Resources	36,0	24,2	7,85	2730	2690	6607
149	303-307	S-ÉGP	UQAC	36,0	13,9	6,45	2275	1766	9442
149	307-312	S-ÉGP	UQAC	36,0	15,9	5,95	919	3409	4787
151	306	S-TROC	UQAC	36,0	19,7	7,07	1405	878	878
151	905	S-TROC	Severson et Hauck, 1990	36,0	14,2	3,70	514	2571	1029
153	506-508	S-ÉGP	Severson et Hauck, 1990	36,0	18,0	9,21	3706	8471	15882
153	519-521	S-ÉGP	UQAC	36,0	10,5	4,20	587	647	2933
Moyenne	S-ÉGP	n=22		36,0	23,3	6,32	2804	3829	8005
Moyenne	S-TROC	n=2		36,0	16,9	5,39	960	1725	953
Moyenne	TOTAL	n=24		36,0	22,8	6,24	2650	3654	7417

BABBITT - ROCHE TOTALE

No. forage	Profondeur (pieds)	Type de roche	Références	S(%)	Cu(ppm)	Ni(ppm)	Au(ppb)	Pt(ppb)	Pd(ppb)
B1-58	1433-1441	SM	Patelke, 1994	17,2	24120	14630	171	34	309
B1-60	1731-1735	S-TROC	Patelke, 1994	6,49	62740	3770	686	12684	1371
B1-66	2078-2083	S-ÉGP	Severson et Hauck, 1997	0,61	5200	2200	127	496	1267
B1-82	237-248	S-TROC	Patelke, 1994	0,31	3100	700	-----	50	90
B1-82	655-665	S-TROC	Patelke, 1994	0,29	2500	600	-----	25	120
B1-90	511-514	S-TROC	Patelke, 1994	1,13	9800	1700	-----	195	770
B1-90	514-518	S-TROC	Patelke, 1994	0,24	2400	700	-----	30	60
B1-90	535-541	S-TROC	Patelke, 1994	0,23	1600	1100	-----	45	125
B1-90	1330-1335	S-TROC	Patelke, 1994	1,18	8300	1500	46	126	332
B1-90	1425-1430	S-TROC	Patelke, 1994	1,75	12200	2600	140	136	450
B1-91	131-136	S-ÉGP	Patelke, 1994	0,77	6800	1200	-----	270	750
B1-91	136-149	S-TROC	Patelke, 1994	0,13	500	300	-----	10	30
B1-91	157-167	S-TROC	Patelke, 1994	0,11	1000	400	-----	45	70
B1-92	118-125	S-ÉGP	Patelke, 1994	0,23	2100	500	-----	70	245
B1-92	634-640	S-ÉGP	Patelke, 1994	0,43	3000	700	-----	230	570
B1-100	750-756	S-ÉGP	Severson et Hauck, 1997	1,20	8300	2300	26	216	910
B1-103	115-119	S-ÉGP	Patelke, 1994	0,39	3200	1200	-----	175	400
B1-103	119-128	S-TROC	Patelke, 1994	0,68	5300	1800	-----	175	465
B1-144	665-675	S-TROC	Patelke, 1994	0,47	4000	1100	67	100	360
B1-144	675-685	S-ÉGP	Patelke, 1994	1,11	8400	1700	180	440	800
B1-144	1412-1417	S-TROC	Patelke, 1994	0,74	15100	1300	64	130	130
B1-144	1435-1445	S-TROC	Patelke, 1994	0,89	6750	1400	51	100	220
B1-144	1462-1472	S-TROC	Patelke, 1994	0,82	6400	1400	62	50	180
B1-147	1485-1494	S-TROC	Patelke, 1994	0,94	6100	1200	94	60	380
B1-147	1556-1566	S-TROC	Patelke, 1994	0,96	6800	1400	120	100	220
B1-147	1566-1575	S-TROC	Patelke, 1994	1,02	7700	1450	68	80	180
B1-216	355-369	S-TROC	Patelke, 1994	0,36	3400	1100	-----	25	90
B1-263	55-65	S-TROC	Patelke, 1994	1,07	2800	1000	-----	85	75
B1-263	115-125	S-TROC	Patelke, 1994	0,29	2300	700	-----	35	130
B1-289	215-225	S-TROC	Patelke, 1994	0,23	2000	500	-----	35	125
B1-289	225-235	S-ÉGP	Patelke, 1994	0,65	4500	1200	-----	85	445
B1-289	745-755	S-TROC	Patelke, 1994	0,47	3300	1000	-----	50	120
B1-295	1375-1435	S-TROC	Patelke, 1994	1,08	10600	1700	100	140	620
B1-295	1385-1395	S-ÉGP	Severson et Hauck, 1997	1,53	12200	2600	70	237	1008
B1-295	2095-2235	S-TROC	Patelke, 1994	1,58	6600	1400	72	90	400
B1-296	1287-1387	S-TROC	Patelke, 1994	1,07	8900	2000	-----	145	395
B1-296	1387-1477	S-TROC	Patelke, 1994	1,00	7000	1500	-----	55	190
B1-296	1477-1567	S-TROC	Patelke, 1994	1,03	6000	1500	-----	80	135
B1-296	1567-1657	S-TROC	Patelke, 1994	1,13	6500	1500	-----	120	140
B1-296	1667-1697	S-TROC	Patelke, 1994	1,80	6300	1600	-----	50	80
B1-316	45-55	S-TROC	Patelke, 1994	0,22	1700	500	-----	20	70
B1-316	175-185	S-TROC	Patelke, 1994	0,37	2800	700	-----	45	95
B1-316	205-215	S-TROC	Patelke, 1994	0,19	1600	400	-----	15	50
B1-327	1473	S-ÉGP	Severson et Hauck, 1997	0,90	6900	1700	33	113	508
B1-327	1493	S-TROC	Severson et Hauck, 1997	1,50	9300	2000	48	202	495
B1-330	1587	S-TROC	Severson et Hauck, 1997	0,93	6800	1800	39	112	361
B1-330	1607	S-TROC	Severson et Hauck, 1997	0,42	3700	600	26	137	135
B1-356	1075	S-TROC	Severson et Hauck, 1997	1,24	8700	1800	45	202	423
B1-356	1225	S-TROC	Severson et Hauck, 1997	1,15	4600	1300	24	115	235
B1-356	1400-1545	S-ÉGP	Patelke, 1994	1,34	8400	2100	80	160	830
B1-359	1695	S-ÉGP	Severson et Hauck, 1997	0,85	5100	1500	53	87	486
B1-361	1504-1514	S-ÉGP	Severson et Hauck, 1997	0,42	3300	1100	126	119	988
B1-361	1624-1634	S-ÉGP	Severson et Hauck, 1997	1,29	7500	1800	169	189	1017
B1-363	298-310	S-TROC	Patelke, 1994	0,68	6300	1000	-----	50	140
B1-369	1305-1445	S-TROC	Patelke, 1994	1,53	9200	2040	11	20	41

BABBITT - ROCHE TOTALE

No. forage	Profondeur (pieds)	Type de roche	Références	S(%)	Cu(ppm)	Ni(ppm)	Au(ppb)	Pt(ppb)	Pd(ppb)
B1-371	1365	S-TROC	Severson et Hauck, 1997	1,57	3700	1000	32	50	238
B1-371	1594	S-ÉGP	Severson et Hauck, 1997	0,62	3400	1100	19	46	312
B1-371	1634-1644	S-ÉGP	Severson et Hauck, 1997	0,88	5400	1600	87	59	1161
B1-372	119-134	S-TROC	Patelke, 1994	1,15	6700	1400	-----	155	505
B1-372	651-662	S-TROC	Patelke, 1994	0,48	3100	800	-----	65	55
B1-380	365	S-TROC	Severson et Hauck, 1997	1,00	8900	2100	84	211	327
B1-386	185-195	S-ÉGP	Severson et Hauck, 1997	1,12	11800	2600	217	314	1234
B1-386		S-TROC	Severson et Hauck, 1997	0,90	7200	1800	109	106	250
B1-386	255	S-TROC	Severson et Hauck, 1997	1,27	10600	2100	77	139	361
Moyenne	S-ÉGP	n=17		0,84	6206	1594	70	194	761
Moyenne	S-TROC	n=47		0,96	7040	1331	44	357	256
Moyenne	SM	n=1		17,2	24120	14630	171	34	309
Moyenne	TOTAL	n=65		1,18	7085	1604	53	310	389

BABBITT - 100% SULFURES

No. forage	Profondeur (pieds)	Type de roche	Références	S(%)	Cu(%)	Ni(%)	Au(ppb)	Pt(ppb)	Pd(ppb)
B1-58	1433-1441	SM	Patelke, 1994	36,0	5,04	3,05	358	72	644
B1-60	1731-1735	S-TROC	Patelke, 1994	36,0	34,8	2,09	3803	70356	7606
B1-66	2078-2083	S-ÉGP	Severson et Hauck, 1997	36,0	30,7	13,0	7495	29272	74774
B1-82	237-248	S-TROC	Patelke, 1994	36,0	36,0	8,13	-----	5806	10452
B1-82	655-665	S-TROC	Patelke, 1994	36,0	31,0	7,45	-----	3103	14897
B1-90	511-514	S-TROC	Patelke, 1994	36,0	31,2	5,42	-----	6212	24531
B1-90	514-518	S-TROC	Patelke, 1994	36,0	36,0	10,5	-----	4500	9000
B1-90	535-541	S-TROC	Patelke, 1994	36,0	25,0	17,2	-----	7043	19565
B1-90	1330-1335	S-TROC	Patelke, 1994	36,0	25,3	4,58	1395	3844	10129
B1-90	1425-1430	S-TROC	Patelke, 1994	36,0	25,1	5,35	2870	2798	9257
B1-91	131-136	S-ÉGP	Patelke, 1994	36,0	31,8	5,61	-----	12623	35065
B1-91	136-149	S-TROC	Patelke, 1994	36,0	13,8	8,31	-----	2769	8308
B1-91	157-167	S-TROC	Patelke, 1994	36,0	32,7	13,1	-----	14727	22909
B1-92	118-125	S-ÉGP	Patelke, 1994	36,0	32,9	7,83	-----	10957	38348
B1-92	634-640	S-ÉGP	Patelke, 1994	36,0	25,1	5,86	-----	19256	47721
B1-100	750-756	S-ÉGP	Severson et Hauck, 1997	36,0	24,9	6,90	780	6480	27300
B1-103	115-119	S-ÉGP	Patelke, 1994	36,0	29,5	11,1	-----	16154	36923
B1-103	119-128	S-TROC	Patelke, 1994	36,0	28,1	9,53	-----	9265	24618
B1-144	665-675	S-TROC	Patelke, 1994	36,0	30,6	8,43	5132	7660	27574
B1-144	675-685	S-ÉGP	Patelke, 1994	36,0	27,2	5,51	5838	14270	25946
B1-144	1412-1417	S-TROC	Patelke, 1994	36,0	73,5	6,32	3114	6324	6324
B1-144	1435-1445	S-TROC	Patelke, 1994	36,0	27,3	5,66	2063	4045	8899
B1-144	1462-1472	S-TROC	Patelke, 1994	36,0	28,1	6,15	2722	2195	7902
B1-147	1485-1494	S-TROC	Patelke, 1994	36,0	23,4	4,60	3600	2298	14553
B1-147	1556-1566	S-TROC	Patelke, 1994	36,0	25,5	5,25	4500	3750	8250
B1-147	1566-1575	S-TROC	Patelke, 1994	36,0	27,2	5,12	2400	2824	6353
B1-216	355-369	S-TROC	Patelke, 1994	36,0	34,0	11,0	-----	2500	9000
B1-263	55-65	S-TROC	Patelke, 1994	36,0	9,42	3,36	-----	2860	2523
B1-263	115-125	S-TROC	Patelke, 1994	36,0	28,6	8,69	-----	4345	16138
B1-289	215-225	S-TROC	Patelke, 1994	36,0	31,3	7,83	-----	5478	19565
B1-289	225-235	S-ÉGP	Patelke, 1994	36,0	24,9	6,65	-----	4708	24646
B1-289	745-755	S-TROC	Patelke, 1994	36,0	25,3	7,66	-----	3830	9191
B1-295	1375-1435	S-TROC	Patelke, 1994	36,0	35,3	5,67	3333	4667	20667
B1-295	1385-1395	S-ÉGP	Severson et Hauck, 1997	36,0	28,7	6,12	1647	5576	23718
B1-295	2095-2235	S-TROC	Patelke, 1994	36,0	15,0	3,19	1641	2051	9114
B1-296	1287-1387	S-TROC	Patelke, 1994	36,0	29,9	6,73	-----	4879	13290
B1-296	1387-1477	S-TROC	Patelke, 1994	36,0	25,2	5,40	-----	1980	6840
B1-296	1477-1567	S-TROC	Patelke, 1994	36,0	21,0	5,24	-----	2796	4718
B1-296	1567-1657	S-TROC	Patelke, 1994	36,0	20,7	4,78	-----	3823	4460
B1-296	1667-1697	S-TROC	Patelke, 1994	36,0	12,6	3,20	-----	1000	1600
B1-316	45-55	S-TROC	Patelke, 1994	36,0	27,8	8,18	-----	3273	11455
B1-316	175-185	S-TROC	Patelke, 1994	36,0	27,2	6,81	-----	4378	9243
B1-316	205-215	S-TROC	Patelke, 1994	36,0	30,3	7,58	-----	2842	9474
B1-327	1473	S-ÉGP	Severson et Hauck, 1997	36,0	27,6	6,80	1320	4520	20320
B1-327	1493	S-TROC	Severson et Hauck, 1997	36,0	22,3	4,80	1152	4848	11880
B1-330	1587	S-TROC	Severson et Hauck, 1997	36,0	26,3	6,97	1510	4335	13974
B1-330	1607	S-TROC	Severson et Hauck, 1997	36,0	31,7	5,14	2229	11743	11571
B1-356	1075	S-TROC	Severson et Hauck, 1997	36,0	25,3	5,23	1306	5865	12281
B1-356	1225	S-TROC	Severson et Hauck, 1997	36,0	14,4	4,07	751	3600	7357
B1-356	1400-1545	S-ÉGP	Patelke, 1994	36,0	22,6	5,64	2149	4299	22299
B1-359	1695	S-ÉGP	Severson et Hauck, 1997	36,0	21,6	6,35	2245	3685	20584
B1-361	1504-1514	S-ÉGP	Severson et Hauck, 1997	36,0	28,3	9,43	10800	10200	84686
B1-361	1624-1634	S-ÉGP	Severson et Hauck, 1997	36,0	20,9	5,02	4716	5274	28381
B1-363	298-310	S-TROC	Patelke, 1994	36,0	33,4	5,29	-----	2647	7412
B1-369	1305-1445	S-TROC	Patelke, 1994	36,0	21,6	4,80	259	471	965

BABBITT - 100% SULFURES

No. forage	Profondeur (pieds)	Type de roche	Références	S(%)	Cu(%)	Ni(%)	Au(ppb)	Pt(ppb)	Pd(ppb)
B1-371	1365	S-TROC	Severson et Hauck, 1997	36,0	8,48	2,29	734	1146	5457
B1-371	1594	S-ÉGP	Severson et Hauck, 1997	36,0	19,7	6,39	1103	2671	18116
B1-371	1634-1644	S-ÉGP	Severson et Hauck, 1997	36,0	22,1	6,55	3559	2414	47495
B1-372	119-134	S-TROC	Patelke, 1994	36,0	21,0	4,38	-----	4852	15809
B1-372	651-662	S-TROC	Patelke, 1994	36,0	23,3	6,00	-----	4875	4125
B1-380	365	S-TROC	Severson et Hauck, 1997	36,0	32,0	7,56	3024	7596	11772
B1-386	185-195	S-ÉGP	Severson et Hauck, 1997	36,0	37,9	8,36	6975	10093	39664
B1-386		S-TROC	Severson et Hauck, 1997	36,0	28,8	7,20	4360	4240	10000
B1-386	255	S-TROC	Severson et Hauck, 1997	36,0	30,0	5,95	2183	3940	10233
Moyenne	S-ÉGP	n=17		36,0	26,9	7,24	2860	9556	36234
Moyenne	S-TROC	n=47		36,0	27,1	6,55	2563	6074	11429
Moyenne	SM	n=1		36,0	5,04	3,05	358	72	644
Moyenne	TOTAL	n=65		36,0	26,7	6,63	2945	6764	17623

TIGER BOY - ROCHE TOTALE

No. forage	Profondeur (pieds)	Type de roche	Références	S(%)	Cu(ppm)	Ni(ppm)	Au(ppb)	Pt(ppb)	Pd(ppb)
B1-189	1858	S-TROC	Ripley, 1990	0,78	6100	900	95	47	210
B1-189	1863	SM	Ripley, 1990	10,0	61000	20700	10	59	900
B1-189	1898	S-TROC	Ripley, 1990	1,83	10000	1500	19	120	180
B1-189	1953	SM	Ripley, 1990	20,7	20900	18300	83	3	192
B1-189	2004	S-TROC	Ripley, 1990	1,11	6400	600	13	51	54
B1-189	2037	S-TROC	Ripley, 1990	3,64	15000	1300	1100	71	1100
B1-189	2041	S-TROC	Ripley, 1990	0,35	1500	100	2	7	15
B1-189	2043	S-TROC	Ripley, 1990	2,31	8900	1400	0	26	64
B1-189	2046	SM	Ripley, 1990	29,5	9000	6600	19	9	130
B1-189	2050	SM	Ripley, 1990	27,3	47100	9500	4	3	64
B1-197	1360-1459	S-TROC	Patelke, 1994	0,99	5900	2150	64	95	175
B1-197	1530-1536	S-TROC	Patelke, 1994	0,28	1800	800	12	30	71
B1-197	1536-1540	S-TROC	Patelke, 1994	2,50	14300	3400	120	230	770
B1-197	1540-1550	S-TROC	Patelke, 1994	2,06	13400	2900	59	50	260
B1-197	1651-1661	S-TROC	Patelke, 1994	2,44	11500	2300	53	40	190
B1-197	1674-1679	S-TROC	Patelke, 1994	2,74	18900	7100	100	20	340
B1-197	1684-1690	S-TROC	Patelke, 1994	2,46	16000	800	86	60	320
B1-197	1756-1766	S-TROC	Patelke, 1994	3,11	9800	1800	45	120	90
B1-197	1781-1786	S-TROC	Patelke, 1994	2,30	5400	1300	27	10	74
B1-214	1695	S-TROC	Ripley, 1990	1,04	8900	800	79	64	430
B1-214	1761	SM	Ripley, 1990	18,2	107000	25000	0	11	491
B1-214	1769	S-TROC	Ripley, 1990	1,00	9000	3400	25	65	78
B1-214	1856	S-TROC	Ripley, 1990	3,44	17800	3700	19	98	174
B1-214	1885	S-TROC	Ripley, 1990	8,93	37100	12300	17	3000	122
B1-221	1434	S-TROC	Ripley, 1990	2,87	25200	4500	5	59	155
B1-221	1510	S-TROC	Ripley, 1990	2,82	12700	1500	28	54	100
B1-221	1564	SM	Ripley, 1990	15,9	98000	4000	12	12	142
B1-221	1579	S-TROC	Ripley, 1990	1,55	5500	800	13	21	45
B1-221	1583	SM	Ripley, 1990	12,0	65700	8500	16	23	129
B1-221	1603	SM	Ripley, 1990	20,0	20400	11200	4	0	49
B1-221	1614	S-TROC	Ripley, 1990	1,98	6300	300	17	21	45
B1-254	1753-1763	S-TROC	Patelke, 1994	0,40	2000	600	0	0	135
B1-254	1763-1773	S-TROC	Patelke, 1994	0,37	1900	700	0	0	60
B1-254	1773-1783	S-TROC	Patelke, 1994	0,99	8800	1800	0	135	195
B1-254	1783-1793	S-TROC	Patelke, 1994	2,09	18800	2400	0	90	275
B1-254	1793-1803	S-TROC	Patelke, 1994	1,50	12400	2300	0	90	570
B1-254	1803-1813	S-TROC	Patelke, 1994	2,16	18200	3000	0	125	220
B1-254	1813-1823	S-TROC	Patelke, 1994	2,19	16700	2800	0	170	370
B1-254	1823-1833	S-TROC	Patelke, 1994	1,59	13200	2100	0	30	295
B1-254	1833-1843	S-TROC	Patelke, 1994	2,17	14700	2600	0	170	240
B1-254	1843-1853	S-TROC	Patelke, 1994	1,96	12300	3300	0	75	200
B1-254	1863-1873	S-TROC	Patelke, 1994	1,81	10100	2300	0	35	195
B1-254	1873-1883	S-TROC	Patelke, 1994	1,54	8700	1800	0	15	115
B1-254	1883-1893	S-TROC	Patelke, 1994	2,22	11800	2200	0	25	190
B1-254	1893-1903	S-TROC	Patelke, 1994	2,79	15800	2100	0	25	205
B1-254	1903-1913	S-TROC	Patelke, 1994	3,05	13800	2200	0	25	135
B1-254	1913-1923	S-TROC	Patelke, 1994	4,06	9700	2600	0	0	60
B1-254	1923-1933	S-TROC	Patelke, 1994	1,06	3100	600	0	90	155
B1-333	545-615	S-TROC	Patelke, 1994	1,51	7100	1400	30	25	110
B1-381	325-375	S-TROC	Patelke, 1994	0,99	8400	1800	80	200	250
B1-390	1235-1335	S-TROC	Patelke, 1994	2,25	8100	1600	42	25	67
Moyenne	S-TROC	n=44		2,07	11193	2181	49	133	211
Moyenne	SM	n=8		19,2	53638	12975	19	15	262
Moyenne	TOTAL	n=52		4,70	17723	3841	44	115	219

TIGER BOY - 100% SULFURES

No. forage	Profondeur (pieds)	Type de roche	Références	S(%)	Cu(%)	Ni(%)	Au(ppb)	Pt(ppb)	Pd(ppb)
B1-189	1858	S-TROC	Ripley, 1990	36,0	28,2	4,15	4385	2169	9692
B1-189	1863	SM	Ripley, 1990	36,0	22,0	7,45	36	212	3240
B1-189	1898	S-TROC	Ripley, 1990	36,0	19,7	2,95	374	2361	3541
B1-189	1953	SM	Ripley, 1990	36,0	3,63	3,18	144	5	334
B1-189	2004	S-TROC	Ripley, 1990	36,0	20,8	1,95	422	1654	1751
B1-189	2037	S-TROC	Ripley, 1990	36,0	14,8	1,29	10879	702	10879
B1-189	2041	S-TROC	Ripley, 1990	36,0	15,4	1,03	206	720	1543
B1-189	2043	S-TROC	Ripley, 1990	36,0	13,9	2,18	0	405	997
B1-189	2046	SM	Ripley, 1990	36,0	1,10	0,81	23	11	159
B1-189	2050	SM	Ripley, 1990	36,0	6,21	1,25	5	4	84
B1-197	1360-1459	S-TROC	Patelke, 1994	36,0	21,5	7,82	2327	3455	6364
B1-197	1530-1536	S-TROC	Patelke, 1994	36,0	23,1	10,3	1543	3857	9129
B1-197	1536-1540	S-TROC	Patelke, 1994	36,0	20,6	4,90	1728	3312	11088
B1-197	1540-1550	S-TROC	Patelke, 1994	36,0	23,4	5,07	1031	874	4544
B1-197	1651-1661	S-TROC	Patelke, 1994	36,0	17,0	3,39	782	590	2803
B1-197	1674-1679	S-TROC	Patelke, 1994	36,0	24,8	9,33	1314	263	4467
B1-197	1684-1690	S-TROC	Patelke, 1994	36,0	23,4	1,17	1259	878	4683
B1-197	1756-1766	S-TROC	Patelke, 1994	36,0	11,3	2,08	521	1389	1042
B1-197	1781-1786	S-TROC	Patelke, 1994	36,0	8,45	2,03	423	157	1158
B1-214	1695	S-TROC	Ripley, 1990	36,0	30,8	2,77	2735	2215	14885
B1-214	1761	SM	Ripley, 1990	36,0	21,2	4,95	0	22	971
B1-214	1769	S-TROC	Ripley, 1990	36,0	32,4	12,2	900	2340	2808
B1-214	1856	S-TROC	Ripley, 1990	36,0	18,6	3,87	199	1026	1821
B1-214	1885	S-TROC	Ripley, 1990	36,0	15,0	4,96	69	12094	492
B1-221	1434	S-TROC	Ripley, 1990	36,0	31,6	5,64	63	740	1944
B1-221	1510	S-TROC	Ripley, 1990	36,0	16,2	1,91	357	689	1277
B1-221	1564	SM	Ripley, 1990	36,0	22,2	0,91	27	27	322
B1-221	1579	S-TROC	Ripley, 1990	36,0	12,8	1,86	302	488	1045
B1-221	1583	SM	Ripley, 1990	36,0	19,7	2,55	48	69	387
B1-221	1603	SM	Ripley, 1990	36,0	3,67	2,02	7	0	88
B1-221	1614	S-TROC	Ripley, 1990	36,0	11,5	0,55	309	382	818
B1-254	1753-1763	S-TROC	Patelke, 1994	36,0	18,0	5,40	0	0	12150
B1-254	1763-1773	S-TROC	Patelke, 1994	36,0	18,5	6,81	0	0	5838
B1-254	1773-1783	S-TROC	Patelke, 1994	36,0	32,0	6,55	0	4909	7091
B1-254	1783-1793	S-TROC	Patelke, 1994	36,0	32,4	4,13	0	1550	4737
B1-254	1793-1803	S-TROC	Patelke, 1994	36,0	29,8	5,52	0	2160	13680
B1-254	1803-1813	S-TROC	Patelke, 1994	36,0	30,3	5,00	0	2083	3667
B1-254	1813-1823	S-TROC	Patelke, 1994	36,0	27,5	4,60	0	2795	6082
B1-254	1823-1833	S-TROC	Patelke, 1994	36,0	29,9	4,75	0	679	6679
B1-254	1833-1843	S-TROC	Patelke, 1994	36,0	24,4	4,31	0	2820	3982
B1-254	1843-1853	S-TROC	Patelke, 1994	36,0	22,6	6,06	0	1378	3673
B1-254	1863-1873	S-TROC	Patelke, 1994	36,0	20,1	4,57	0	696	3878
B1-254	1873-1883	S-TROC	Patelke, 1994	36,0	20,3	4,21	0	351	2688
B1-254	1883-1893	S-TROC	Patelke, 1994	36,0	19,1	3,57	0	405	3081
B1-254	1893-1903	S-TROC	Patelke, 1994	36,0	20,4	2,71	0	323	2645
B1-254	1903-1913	S-TROC	Patelke, 1994	36,0	16,3	2,60	0	295	1593
B1-254	1913-1923	S-TROC	Patelke, 1994	36,0	8,60	2,31	0	0	532
B1-254	1923-1933	S-TROC	Patelke, 1994	36,0	10,5	2,04	0	3057	5264
B1-333	545-615	S-TROC	Patelke, 1994	36,0	16,9	3,34	715	596	2623
B1-381	325	S-TROC	Patelke, 1994	36,0	30,5	6,55	2909	7273	9091
B1-390	1235	S-TROC	Patelke, 1994	36,0	13,0	2,56	672	400	1072
Moyenne	TOTAL	n=52		36,0	19,5	4,00	720	1468	4008
Moyenne	S-TROC	n=44		36,0	20,8	4,21	847	1733	4624
Moyenne	SM	n=8		36,0	18,0	5,54	37	41	569

LOCAL BOY - ROCHE TOTALE

No. forage	Profondeur (pieds)	Type de roche	Références	S(%)	Cu(ppm)	Ni(ppm)	Au(ppb)	Pt(ppb)	Pd(ppb)
B1-105	1624-1667	S-TROC	Patelke, 1994	1,36	5800	1350	94	90	500
B1-105	1768-1778	S-TROC	Patelke, 1994	7,69	41750	4500	417	65	885
B1-105	1778-1783	SM	Patelke, 1994	14,4	77500	7400	39	120	310
B1-105	1783-1788	SM	Patelke, 1994	12,2	31300	10300	19	30	150
B1-105	1788-1793	S-TROC	Patelke, 1994	5,89	13800	4800	11	10	50
B1-105	1793-1798	S-TROC	Patelke, 1994	1,74	4300	1200	10	20	35
B1-105	1798-1803	S-TROC	Patelke, 1994	2,19	6500	1000	20	10	43
B1-105	1803-1808	S-TROC	Patelke, 1994	1,63	5000	900	11	10	46
B1-105	1808-1830	S-TROC	Patelke, 1994	2,33	8500	1200	46	35	125
B1-105	1830-1834	S-TROC	Patelke, 1994	0,53	3700	500	10	40	29
B1-105	1834-1842	S-TROC	Patelke, 1994	9,56	42100	8700	170	80	370
B1-105	1842-1849	SM	Patelke, 1994	17,8	58200	10800	51	1200	460
B1-105	1849-1855	SM	Patelke, 1994	12,7	31100	9600	14	30	170
B1-116	1650-1655	S-TROC	Patelke, 1994	1,87	13500	1300	65	60	190
B1-116	1655-1660	S-TROC	Patelke, 1994	0,49	8700	800	15	10	25
B1-116	1660-1665	S-TROC	Patelke, 1994	3,94	56000	2700	600	220	900
B1-116	1665-1670	SM	Patelke, 1994	18,4	164000	5000	494	151	640
B1-116	1670-1675	SM	Patelke, 1994	27,0	244000	8300	67	610	260
B1-116	1675-1680	S-TROC	Patelke, 1994	8,46	43000	13000	120	90	520
B1-116	1680-1685	SM	Patelke, 1994	22,7	196000	6800	420	290	1400
B1-116	1685-1690	SM	Patelke, 1994	22,5	112000	19700	320	60	1100
B1-116	1690-1695	SM	Patelke, 1994	16,0	94000	15400	17	280	450
B1-116	1695-1698	SM	Patelke, 1994	30,2	166000	24100	2	90	190
B1-116	1698-1705	S-TROC	Patelke, 1994	0,89	3900	800	3	10	32
B1-116	1705-1709	S-TROC	Patelke, 1994	0,38	1200	500	2	10	12
B1-116	1709-1712	SM	Patelke, 1994	19,8	67000	22700	30	190	840
B1-116	1712-1715	S-TROC	Patelke, 1994	0,44	1900	500	11	5	20
B1-120	1305-1315	S-ÉGP	Severson et Hauck, 1997	1,01	7200	1600	241	837	1728
B1-120	1325-1335	S-ÉGP	Severson et Hauck, 1997	0,79	5100	1000	52	197	618
B1-124	1754-1824	S-TROC	Patelke, 1994	2,06	10800	1700	85	55	235
B1-124	1824-1829	S-TROC	Patelke, 1994	3,29	16000	1800	66	20	140
B1-124	1829-1834	S-TROC	Patelke, 1994	2,99	16100	1900	51	20	150
B1-124	1834-1838	S-TROC	Patelke, 1994	5,45	31600	2600	140	200	220
B1-129	1751-1757	S-TROC	Patelke, 1994	1,65	900	200	7	5	22
B1-129	1757-1775	S-TROC	Patelke, 1994	0,70	3000	250	6	15	16
B1-130	1665-1668	S-TROC	Patelke, 1994	6,50	36500	4300	390	30	410
B1-130	1668-1686	S-TROC	Patelke, 1994	0,68	2700	400	26	45	70
B1-130	1686-1689	SM	Patelke, 1994	27,9	30000	7800	22	34	103
B1-130	1704-1710	SM	Patelke, 1994	16,1	55100	11200	120	69	446
B1-130	1710-1717	SM	Patelke, 1994	21,0	44200	15800	29	34	446
B1-133	985	S-ÉGP	Severson et Hauck, 1997	1,20	6300	1600	33	90	509
B1-134	1146	S-ÉGP	Severson et Hauck, 1997	1,21	7500	1500	34	89	471
B1-134	1156-1166	S-TROC	Patelke, 1994	1,14	6800	1300	53	100	360
B1-134	1216-1226	S-TROC	Patelke, 1994	1,44	7800	1600	110	100	480
B1-134	1256-1266	S-TROC	Patelke, 1994	0,85	5300	1100	49	60	320
B1-134	1696-1706	S-TROC	Patelke, 1994	0,20	1800	600	39	80	220
B1-134	1706-1716	S-TROC	Patelke, 1994	0,81	6300	1200	71	140	500
B1-135	1625-1655	S-TROC	Patelke, 1994	1,13	11100	540	285	165	280
B1-135	1657-1685	S-TROC	Patelke, 1994	7,74	36400	4600	73	40	420
B1-135	1685-1702	SM	Patelke, 1994	15,0	40800	11200	19	33	430
B1-135	1702-1708	S-TROC	Patelke, 1994	0,56	4300	370	3	10	14
B1-136	1034	S-TROC	Ripley, 1990	1,51	6600	3400	23	52	520
B1-136	1108	S-TROC	Ripley, 1990	1,58	13500	1400	12	47	191
B1-136	1433	S-TROC	Ripley, 1990	2,34	7700	3900	20	91	120
B1-136	1504	S-TROC	Ripley, 1990	7,11	22800	7700	34	17	152

LOCAL BOY - ROCHE TOTALE

No. forage	Profondeur (pieds)	Type de roche	Références	S(%)	Cu(ppm)	Ni(ppm)	Au(ppb)	Pt(ppb)	Pd(ppb)
B1-136	1568	SM	Ripley, 1990	30,0	26300	18500	3	3	90
B1-136	1635-1645	S-TROC	Patelke, 1994	1,86	6200	1800	31	20	59
B1-136	1645-1653	S-TROC	Patelke, 1994	3,42	8200	2200	24	20	83
B1-136	1653-1659	S-TROC	Patelke, 1994	8,55	18900	6200	47	10	320
B1-136	1725-1729	S-TROC	Patelke, 1994	0,67	1800	700	12	5	24
B1-136	1729-1735	SM	Patelke, 1994	19,4	99000	7300	960	40	3300
B1-136	1735-1741	SM	Patelke, 1994	25,4	65000	11800	120	30	420
B1-136		SM	Patelke, 1994	23,5	107200	10600	170	10	350
B1-136	1747-1755	S-TROC	Patelke, 1994	2,57	16800	1000	48	20	150
B1-136	1755-1758	S-TROC	Patelke, 1994	7,87	22000	4200	31	5	39
B1-136	1758-1765	S-TROC	Patelke, 1994	2,91	12500	1700	53	10	140
B1-136	1765-1770	S-TROC	Patelke, 1994	0,34	700	400	13	5	11
B1-136	1784-1793	S-TROC	Patelke, 1994	2,82	22500	1600	37	50	110
B1-137	1154-1164	S-ÉGP	Severson et Hauck, 1997	0,86	5800	1200	309	279	1115
B1-138	1645-1725	S-TROC	Patelke, 1994	2,27	11600	2050	44	85	190
B1-138	1725-1730	S-TROC	Patelke, 1994	0,96	8500	1800	3	5	18
B1-138	1730-1735	S-TROC	Patelke, 1994	4,38	6700	1600	13	10	40
B1-138	1735-1743	S-TROC	Patelke, 1994	7,47	9800	2600	15	5	91
B1-138	1761-1766	S-TROC	Patelke, 1994	0,23	600	200	5	5	14
B1-138	1766-1774	S-TROC	Patelke, 1994	7,23	34000	3300	2100	1700	880
B1-138	1774-1779	S-TROC	Patelke, 1994	0,28	1700	300	11	10	29
B1-139	1651-1655	S-TROC	Patelke, 1994	4,91	24500	2000	130	30	290
B1-139	1655-1665	S-TROC	Patelke, 1994	1,30	6100	1500	11	10	120
B1-139	1665-1669	S-TROC	Patelke, 1994	2,48	20200	1400	89	60	100
B1-139	1669-1676	S-TROC	Patelke, 1994	1,86	9400	1400	22	20	38
B1-139	1676-1685	S-TROC	Patelke, 1994	0,77	3700	800	17	10	41
B1-139	1685-1693	S-TROC	Patelke, 1994	5,00	42200	2000	31	230	90
B1-139	1693-1699	S-TROC	Patelke, 1994	0,36	1900	500	9	10	19
B1-139	1699-1705	S-TROC	Patelke, 1994	6,63	45200	5800	120	110	2300
B1-139	1705-1710	S-TROC	Patelke, 1994	1,98	14500	1800	25	40	80
B1-139	1710-1715	SM	Patelke, 1994	21,0	142500	14000	670	210	4800
B1-139	1715-1719	SM	Patelke, 1994	13,4	75200	15100	22	130	160
B1-139	1719-1721	S-TROC	Patelke, 1994	0,42	4600	700	16	30	33
B1-139	1721-1725	SM	Patelke, 1994	24,0	120000	29100	260	270	640
B1-139	1725-1730	SM	Patelke, 1994	24,3	48500	27500	19	30	340
B1-139	1730-1735	SM	Patelke, 1994	26,3	44500	28000	140	70	860
B1-139	1735-1740	SM	Patelke, 1994	14,0	50200	15900	97	50	190
B1-139	1740-1747	SM	Patelke, 1994	15,2	35800	18600	21	10	330
B1-140	1899-1914	S-TROC	Patelke, 1994	6,35	21500	5800	45	30	190
B1-140	1914-1917	SM	Patelke, 1994	14,9	65000	13100	46	670	380
B1-142	1665-1667	S-TROC	Patelke, 1994	6,39	5100	3500	9	10	89
B1-142	1667-1675	S-TROC	Patelke, 1994	0,34	500	200	12	10	6
B1-142	1675-1679	S-TROC	Patelke, 1994	3,82	8900	2200	6	10	20
B1-142	1679-1681	SM	Patelke, 1994	31,8	31500	15100	10	10	19
B1-142	1681-1690	S-TROC	Patelke, 1994	4,27	11800	2100	71	25	130
B1-142	1690-1695	S-TROC	Patelke, 1994	7,78	9400	4100	9	10	36
B1-146	1628	S-TROC	Ripley, 1990	1,29	8700	1300	25	28	122
B1-146	1658	SM	Ripley, 1990	19,9	39500	12400	3	3	30
B1-146	1751-1775	S-TROC	Patelke, 1994	2,76	10600	2000	84	35	155
B1-146	1782	SM	Ripley, 1990	19,1	20300	4300	3	3	81
B1-146	1775-1785	S-TROC	Patelke, 1994	3,17	9200	2300	92	30	110
B1-146	1785-1790	S-TROC	Patelke, 1994	1,13	4300	1000	52	20	110
B1-146	1790-1798	SM	Patelke, 1994	17,2	14000	12100	26	20	160
B1-146	1798-1799	S-TROC	Patelke, 1994	3,50	10600	2000	79	370	200
B1-146	1799-1809	S-TROC	Patelke, 1994	2,35	8600	2200	22	20	89

LOCAL BOY - ROCHE TOTALE

No. forage	Profondeur (pieds)	Type de roche	Références	S(%)	Cu(ppm)	Ni(ppm)	Au(ppb)	Pt(ppb)	Pd(ppb)
B1-146	1809-1819	S-TROC	Patelke, 1994	1,34	10400	1900	17	10	67
B1-146	1819-1829	S-TROC	Patelke, 1994	2,02	7800	1600	38	30	120
B1-146	1829-1839	S-TROC	Patelke, 1994	2,40	7300	1700	110	20	89
B1-146	1839-1849	S-TROC	Patelke, 1994	2,35	10000	1800	62	30	150
B1-146	1849-1855	S-TROC	Patelke, 1994	1,95	8300	1500	45	20	83
B1-146	1855-1860	SM	Patelke, 1994	13,6	22000	8900	35	5	140
B1-146	1860-1865	SM	Patelke, 1994	28,4	25000	18000	6	5	72
B1-146	1865-1880	SM	Patelke, 1994	23,7	44300	17600	40	10	280
B1-146	1880-1897	S-TROC	Patelke, 1994	9,79	34300	5600	131	35	185
B1-153	1135	S-TROC	Severson et Hauck, 1997	1,05	5900	1700	57	175	340
B1-154	1755-1757	SM	Patelke, 1994	17,7	13400	8400	12	5	140
B1-154	1765-1768	SM	Patelke, 1994	15,0	18100	6000	17	10	49
B1-154	1813-1815	S-TROC	Patelke, 1994	6,11	8400	2800	25	10	100
B1-154	1815-1825	S-TROC	Patelke, 1994	2,59	8100	1200	26	20	85
B1-154	1825-1831	S-TROC	Patelke, 1994	3,51	7000	1400	16	20	60
B1-154	1860-1862	S-TROC	Patelke, 1994	1,44	4900	1200	110	20	110
B1-154	1862-1866	SM	Patelke, 1994	15,2	35000	18600	170	30	420
B1-154	1866-1875	S-TROC	Patelke, 1994	1,20	4100	800	18	20	42
B1-154	1875-1879	S-TROC	Patelke, 1994	2,26	5000	1000	22	10	110
B1-154	1879-1883	SM	Patelke, 1994	25,6	29500	15100	27	20	200
B1-154	1883-1884	S-TROC	Patelke, 1994	4,62	13700	3100	71	30	360
B1-156	1739-1740	SM	Patelke, 1994	20,7	17800	6800	5	9	49
B1-159	1740-1807	S-TROC	Patelke, 1994	1,84	9500	1800	55	180	265
B1-159	1807-1815	S-TROC	Patelke, 1994	4,05	11300	2300	52	200	120
B1-159	1815-1820	S-TROC	Patelke, 1994	7,06	18100	3500	31	120	110
B1-159	1820-1825	SM	Patelke, 1994	13,3	25500	7800	13	100	90
B1-159	1825-1830	S-TROC	Patelke, 1994	3,28	8900	1400	13	40	87
B1-159	1830-1835	S-TROC	Patelke, 1994	0,77	3200	500	5	10	37
B1-159	1835-1839	S-TROC	Patelke, 1994	6,30	6200	2900	10	5	58
B1-159	1839-1843	S-TROC	Patelke, 1994	9,57	18000	4300	34	140	480
B1-159	1843-1850	S-TROC	Patelke, 1994	1,80	8200	1100	27	20	74
B1-159	1850-1855	S-TROC	Patelke, 1994	1,46	6400	1000	26	30	77
B1-159	1855-1870	S-TROC	Patelke, 1994	2,66	9200	1500	147	25	525
B1-159	1870-1903	S-TROC	Patelke, 1994	2,10	8500	1200	26	30	90
B1-159	1903-1904	SM	Patelke, 1994	12,2	36500	3300	12	20	120
B1-160	1745-1749	S-TROC	Patelke, 1994	3,70	6400	1500	6	30	48
B1-160	1749-1755	S-TROC	Patelke, 1994	6,51	19200	5300	44	40	180
B1-160	1755-1760	SM	Patelke, 1994	19,4	62500	12600	52	30	430
B1-160	1760-1765	SM	Patelke, 1994	16,5	46500	9000	150	10	190
B1-160	1765-1769	S-TROC	Patelke, 1994	1,02	7500	900	41	50	94
B1-160	1769-1775	SM	Patelke, 1994	14,0	71500	6400	34	30	290
B1-160	1775-1780	SM	Patelke, 1994	21,1	40500	14200	370	30	390
B1-160	1780-1785	SM	Patelke, 1994	17,7	31500	12400	21	5	300
B1-160	1785-1790	SM	Patelke, 1994	26,2	27500	15500	110	30	150
B1-160	1790-1796	SM	Patelke, 1994	18,3	66000	9300	340	30	360
B1-160	1796-1801	S-TROC	Patelke, 1994	0,33	3300	500	10	5	14
B1-163	1325	S-ÉGP	Severson et Hauck, 1997	1,27	6300	1500	57	155	519
B1-163	1335	S-ÉGP	Severson et Hauck, 1997	1,46	8100	1900	72	173	670
B1-421	1755-1762	S-TROC	Patelke, 1994	1,22	5300	600	21	10	55
B1-421	1762-1775	S-TROC	Patelke, 1994	7,26	22300	4700	120	10	270
B1-421	1775-1785	S-TROC	Patelke, 1994	8,95	27300	4000	42	10	230
B1-421	1785-1795	S-TROC	Patelke, 1994	3,14	11000	1700	55	90	140
B1-421	1795-1805	S-TROC	Patelke, 1994	6,91	12800	3900	18	10	82
B1-421	1805-1815	S-TROC	Patelke, 1994	3,15	10600	1800	28	20	99
B1-421	1815-1825	S-TROC	Patelke, 1994	2,39	8100	1400	24	10	89

LOCAL BOY - ROCHE TOTALE

No. forage	Profondeur (pieds)	Type de roche	Références	S(%)	Cu(ppm)	Ni(ppm)	Au(ppb)	Pt(ppb)	Pd(ppb)
B1-421	1825-1835	S-TROC	Patelke, 1994	3,30	8500	1800	14	10	63
B1-421	1835-1845	S-TROC	Patelke, 1994	1,06	2100	400	13	10	26
Moyenne	S-ÉGP	n=7		1,11	6614	1471	114	260	804
Moyenne	S-TROC	n=113		3,17	12212	2169	73	61	185
Moyenne	SM	n=48		19,8	62683	13113	118	107	484
Moyenne	TOTAL	n=168		7,84	26399	5266	87	83	296

LOCAL BOY - 100% SULFURES

No. forage	Profondeur (pieds)	Type de roche	Références	S(%)	Cu(%)	Ni(%)	Au(ppb)	Pt(ppb)	Pd(ppb)
B1-105	1624-1667	S-TROC	Patelke, 1994	36,0	15,4	3,57	2488	2382	13235
B1-105	1768-1778	S-TROC	Patelke, 1994	36,0	19,5	2,11	1952	304	4143
B1-105	1778-1783	SM	Patelke, 1994	36,0	19,4	1,86	98	301	778
B1-105	1783-1788	SM	Patelke, 1994	36,0	9,27	3,05	56	89	444
B1-105	1788-1793	S-TROC	Patelke, 1994	36,0	8,43	2,93	67	61	306
B1-105	1793-1798	S-TROC	Patelke, 1994	36,0	8,90	2,48	207	414	724
B1-105	1798-1803	S-TROC	Patelke, 1994	36,0	10,7	1,64	329	164	707
B1-105	1803-1808	S-TROC	Patelke, 1994	36,0	11,0	1,99	243	221	1016
B1-105	1808-1830	S-TROC	Patelke, 1994	36,0	13,1	1,85	711	541	1931
B1-105	1830-1834	S-TROC	Patelke, 1994	36,0	25,1	3,40	679	2717	1970
B1-105	1834-1842	S-TROC	Patelke, 1994	36,0	15,9	3,28	640	301	1393
B1-105	1842-1849	SM	Patelke, 1994	36,0	11,8	2,19	103	2428	931
B1-105	1849-1855	SM	Patelke, 1994	36,0	8,81	2,72	40	85	482
B1-116	1650-1655	S-TROC	Patelke, 1994	36,0	26,0	2,50	1251	1155	3658
B1-116	1655-1660	S-TROC	Patelke, 1994	36,0	63,9	5,88	1102	735	1837
B1-116	1660-1665	S-TROC	Patelke, 1994	36,0	51,2	2,47	5482	2010	8223
B1-116	1665-1670	SM	Patelke, 1994	36,0	32,1	0,98	967	295	1251
B1-116	1670-1675	SM	Patelke, 1994	36,0	32,5	1,11	89	813	346
B1-116	1675-1680	S-TROC	Patelke, 1994	36,0	18,3	5,53	511	383	2213
B1-116	1680-1685	SM	Patelke, 1994	36,0	31,1	1,08	666	460	2219
B1-116	1685-1690	SM	Patelke, 1994	36,0	17,9	3,15	511	96	1758
B1-116	1690-1695	SM	Patelke, 1994	36,0	21,2	3,47	38	632	1015
B1-116	1695-1698	SM	Patelke, 1994	36,0	19,8	2,87	2	107	226
B1-116	1698-1705	S-TROC	Patelke, 1994	36,0	15,8	3,24	121	404	1294
B1-116	1705-1709	S-TROC	Patelke, 1994	36,0	11,4	4,74	189	947	1137
B1-116	1709-1712	SM	Patelke, 1994	36,0	12,2	4,12	54	345	1524
B1-116	1712-1715	S-TROC	Patelke, 1994	36,0	15,5	4,09	900	409	1636
B1-120	1305-1315	S-ÉGP	Severson et Hauck, 1997	36,0	25,7	5,70	8590	29834	61592
B1-120	1325-1335	S-ÉGP	Severson et Hauck, 1997	36,0	23,2	4,56	2370	8977	28162
B1-124	1754-1824	S-TROC	Patelke, 1994	36,0	18,9	2,97	1485	961	4107
B1-124	1824-1829	S-TROC	Patelke, 1994	36,0	17,5	1,97	722	219	1532
B1-124	1829-1834	S-TROC	Patelke, 1994	36,0	19,4	2,29	614	241	1806
B1-124	1834-1838	S-TROC	Patelke, 1994	36,0	20,9	1,72	925	1321	1453
B1-129	1751-1757	S-TROC	Patelke, 1994	36,0	1,96	0,44	153	109	480
B1-129	1757-1775	S-TROC	Patelke, 1994	36,0	15,4	1,29	309	771	823
B1-130	1665-1668	S-TROC	Patelke, 1994	36,0	20,2	2,38	2160	166	2271
B1-130	1668-1686	S-TROC	Patelke, 1994	36,0	14,3	2,12	1376	2382	3706
B1-130	1686-1689	SM	Patelke, 1994	36,0	3,87	1,01	28	44	133
B1-130	1704-1710	SM	Patelke, 1994	36,0	12,3	2,51	269	154	998
B1-130	1710-1717	SM	Patelke, 1994	36,0	7,56	2,70	50	59	763
B1-133	985	S-ÉGP	Severson et Hauck, 1997	36,0	18,9	4,80	990	2700	15270
B1-134	1146	S-ÉGP	Severson et Hauck, 1997	36,0	22,3	4,46	1012	2648	14013
B1-134	1156-1166	S-TROC	Patelke, 1994	36,0	21,5	4,11	1674	3158	11368
B1-134	1216-1226	S-TROC	Patelke, 1994	36,0	19,5	4,00	2750	2500	12000
B1-134	1256-1266	S-TROC	Patelke, 1994	36,0	22,4	4,66	2075	2541	13553
B1-134	1706-1716	S-TROC	Patelke, 1994	36,0	28,0	5,33	3156	6222	22222
B1-135	1625-1655	S-TROC	Patelke, 1994	36,0	35,4	1,72	9080	5257	8920
B1-135	1657-1685	S-TROC	Patelke, 1994	36,0	16,9	2,14	340	186	1953
B1-135	1685-1702	SM	Patelke, 1994	36,0	9,77	2,68	45	79	1029
B1-135	1702-1708	S-TROC	Patelke, 1994	36,0	27,6	2,38	193	643	900
B1-136	1034	S-TROC	Ripley, 1990	36,0	15,7	8,11	548	1240	12397
B1-136	1108	S-TROC	Ripley, 1990	36,0	30,8	3,19	273	1071	4352
B1-136	1218	S-TROC	Ripley, 1990	36,0	19,0	4,39	251	1701	4209
B1-136	1504	S-TROC	Ripley, 1990	36,0	11,5	3,90	172	86	770
B1-136	1568	SM	Ripley, 1990	36,0	3,16	2,22	4	4	108

LOCAL BOY - 100% SULFURES

No. forage	Profondeur (pieds)	Type de roche	Références	S(%)	Cu(%)	Ni(%)	Au(ppb)	Pt(ppb)	Pd(ppb)
B1-136	1635-1645	S-TROC	Patelke, 1994	36,0	12,0	3,48	600	387	1142
B1-136	1645-1653	S-TROC	Patelke, 1994	36,0	8,63	2,32	253	211	874
B1-136	1653-1659	S-TROC	Patelke, 1994	36,0	7,96	2,61	198	42	1347
B1-136	1725-1729	S-TROC	Patelke, 1994	36,0	9,67	3,76	645	269	1290
B1-136	1729-1735	SM	Patelke, 1994	36,0	18,4	1,36	1786	74	6140
B1-136	1735-1741	SM	Patelke, 1994	36,0	9,21	1,67	170	43	595
B1-136	1741-1747	SM	Patelke, 1994	36,0	16,5	1,63	261	15	537
B1-136		S-TROC	Patelke, 1994	36,0	23,5	1,40	672	280	2101
B1-136	1755-1758	S-TROC	Patelke, 1994	36,0	10,1	1,92	142	23	178
B1-136	1758-1765	S-TROC	Patelke, 1994	36,0	15,5	2,10	656	124	1732
B1-136	1765-1770	S-TROC	Patelke, 1994	36,0	7,41	4,24	1376	529	1165
B1-136	1784-1793	S-TROC	Patelke, 1994	36,0	28,7	2,04	472	638	1404
B1-137	1154-1164	S-ÉGP	Severson et Hauck, 1997	36,0	24,3	5,02	12935	11679	46674
B1-138	1645-1725	S-TROC	Patelke, 1994	36,0	18,4	3,25	698	1348	3013
B1-138	1725-1730	S-TROC	Patelke, 1994	36,0	31,9	6,75	113	188	675
B1-138	1730-1735	S-TROC	Patelke, 1994	36,0	5,51	1,32	107	82	329
B1-138	1735-1743	S-TROC	Patelke, 1994	36,0	4,72	1,25	72	24	439
B1-138	1761-1766	S-TROC	Patelke, 1994	36,0	9,39	3,13	783	783	2191
B1-138	1766-1774	S-TROC	Patelke, 1994	36,0	16,9	1,64	10456	8465	4382
B1-138	1774-1779	S-TROC	Patelke, 1994	36,0	21,9	3,86	1414	1286	3729
B1-139	1651-1655	S-TROC	Patelke, 1994	36,0	18,0	1,47	953	220	2126
B1-139	1655-1665	S-TROC	Patelke, 1994	36,0	16,9	4,15	305	277	3323
B1-139	1665-1669	S-TROC	Patelke, 1994	36,0	29,3	2,03	1292	871	1452
B1-139	1669-1676	S-TROC	Patelke, 1994	36,0	18,2	2,71	426	387	735
B1-139	1676-1685	S-TROC	Patelke, 1994	36,0	17,3	3,74	795	468	1917
B1-139	1685-1693	S-TROC	Patelke, 1994	36,0	30,4	1,44	223	1656	648
B1-139	1693-1699	S-TROC	Patelke, 1994	36,0	19,0	5,00	900	1000	1900
B1-139	1699-1705	S-TROC	Patelke, 1994	36,0	24,5	3,15	652	597	12489
B1-139	1705-1710	S-TROC	Patelke, 1994	36,0	26,4	3,27	455	727	1455
B1-139	1710-1715	SM	Patelke, 1994	36,0	24,4	2,40	1149	360	8232
B1-139	1715-1719	SM	Patelke, 1994	36,0	20,2	4,05	59	348	429
B1-139	1719-1721	S-TROC	Patelke, 1994	36,0	39,4	6,00	1371	2571	2829
B1-139	1721-1725	SM	Patelke, 1994	36,0	18,0	4,37	390	406	961
B1-139	1725-1730	SM	Patelke, 1994	36,0	7,19	4,08	28	44	504
B1-139	1730-1735	SM	Patelke, 1994	36,0	6,10	3,84	192	96	1179
B1-139	1735-1740	SM	Patelke, 1994	36,0	12,9	4,08	249	128	488
B1-139	1740-1747	SM	Patelke, 1994	36,0	8,47	4,40	50	24	781
B1-140	1899-1914	S-TROC	Patelke, 1994	36,0	12,2	3,29	255	170	1077
B1-140	1914-1917	SM	Patelke, 1994	36,0	15,7	3,16	111	1614	916
B1-142	1665-1667	S-TROC	Patelke, 1994	36,0	2,87	1,97	51	56	501
B1-142	1667-1675	S-TROC	Patelke, 1994	36,0	5,29	2,12	1271	1059	635
B1-142	1675-1679	S-TROC	Patelke, 1994	36,0	8,39	2,07	57	94	188
B1-142	1679-1681	SM	Patelke, 1994	36,0	3,57	1,71	11	11	22
B1-142	1681-1690	S-TROC	Patelke, 1994	36,0	9,95	1,77	599	211	1096
B1-142	1690-1695	S-TROC	Patelke, 1994	36,0	4,35	1,90	42	46	167
B1-146	1628	S-TROC	Ripley, 1990	36,0	24,3	3,63	698	781	3405
B1-146	1658	SM	Ripley, 1990	36,0	7,15	2,24	5	5	54
B1-146	1751-1775	S-TROC	Patelke, 1994	36,0	13,8	2,61	1096	457	2022
B1-146	1782	SM	Ripley, 1990	36,0	3,83	0,81	6	6	153
B1-146	1775-1785	S-TROC	Patelke, 1994	36,0	10,4	2,61	1045	341	1249
B1-146	1785-1790	S-TROC	Patelke, 1994	36,0	13,7	3,19	1657	637	3504
B1-146	1790-1798	SM	Patelke, 1994	36,0	2,93	2,53	54	42	335
B1-146	1798-1799	S-TROC	Patelke, 1994	36,0	10,9	2,06	813	3806	2057
B1-146	1799-1809	S-TROC	Patelke, 1994	36,0	13,2	3,37	337	306	1363
B1-146	1809-1819	S-TROC	Patelke, 1994	36,0	27,9	5,10	457	269	1800

LOCAL BOY - 100% SULFURES

No. forage	Profondeur (pieds)	Type de roche	Références	S(%)	Cu(%)	Ni(%)	Au(ppb)	Pt(ppb)	Pd(ppb)
B1-146	1819-1829	S-TROC	Patelke, 1994	36,0	13,9	2,85	677	535	2139
B1-146	1829-1839	S-TROC	Patelke, 1994	36,0	11,0	2,55	1650	300	1335
B1-146	1839-1849	S-TROC	Patelke, 1994	36,0	15,3	2,76	950	460	2298
B1-146	1849-1855	S-TROC	Patelke, 1994	36,0	15,3	2,77	831	369	1532
B1-146	1855-1860	SM	Patelke, 1994	36,0	5,83	2,36	93	13	371
B1-146	1860-1865	SM	Patelke, 1994	36,0	3,17	2,29	8	6	91
B1-146	1865-1880	SM	Patelke, 1994	36,0	6,74	2,68	61	15	426
B1-146	1880-1897	S-TROC	Patelke, 1994	36,0	12,6	2,06	482	129	680
B1-153	1135	S-TROC	Severson et Hauck, 1997	36,0	20,2	5,83	1954	6000	11657
B1-154	1755-1757	SM	Patelke, 1994	36,0	2,72	1,71	24	10	285
B1-154	1765-1768	SM	Patelke, 1994	36,0	4,34	1,44	41	24	118
B1-154	1813-1815	S-TROC	Patelke, 1994	36,0	4,95	1,65	147	59	589
B1-154	1815-1825	S-TROC	Patelke, 1994	36,0	11,3	1,67	361	278	1181
B1-154	1825-1831	S-TROC	Patelke, 1994	36,0	7,18	1,44	164	205	615
B1-154	1860-1862	S-TROC	Patelke, 1994	36,0	12,3	3,00	2750	500	2750
B1-154	1862-1866	SM	Patelke, 1994	36,0	8,31	4,42	404	71	997
B1-154	1866-1875	S-TROC	Patelke, 1994	36,0	12,3	2,40	540	600	1260
B1-154	1875-1879	S-TROC	Patelke, 1994	36,0	7,96	1,59	350	159	1752
B1-154	1879-1883	SM	Patelke, 1994	36,0	4,15	2,13	38	28	282
B1-154	1883-1884	S-TROC	Patelke, 1994	36,0	10,7	2,42	553	234	2805
B1-156	1739-1740	SM	Patelke, 1994	36,0	3,09	1,18	9	16	85
B1-159	1740-1807	S-TROC	Patelke, 1994	36,0	18,6	3,52	1076	3522	5185
B1-159	1807-1815	S-TROC	Patelke, 1994	36,0	10,0	2,04	462	1778	1067
B1-159	1815-1820	S-TROC	Patelke, 1994	36,0	9,23	1,78	158	612	561
B1-159	1820-1825	SM	Patelke, 1994	36,0	6,88	2,10	35	270	243
B1-159	1825-1830	S-TROC	Patelke, 1994	36,0	9,77	1,54	143	439	955
B1-159	1830-1835	S-TROC	Patelke, 1994	36,0	15,0	2,34	234	468	1730
B1-159	1835-1839	S-TROC	Patelke, 1994	36,0	3,54	1,66	57	29	331
B1-159	1839-1843	S-TROC	Patelke, 1994	36,0	6,77	1,62	128	527	1806
B1-159	1843-1850	S-TROC	Patelke, 1994	36,0	16,4	2,20	540	400	1480
B1-159	1850-1855	S-TROC	Patelke, 1994	36,0	15,8	2,47	641	740	1899
B1-159	1855-1870	S-TROC	Patelke, 1994	36,0	12,5	2,03	1989	338	7105
B1-159	1870-1903	S-TROC	Patelke, 1994	36,0	14,6	2,06	446	514	1543
B1-159	1903-1904	SM	Patelke, 1994	36,0	10,8	0,97	35	59	354
B1-160	1745-1749	S-TROC	Patelke, 1994	36,0	6,23	1,46	58	292	467
B1-160	1749-1755	S-TROC	Patelke, 1994	36,0	10,6	2,93	243	221	995
B1-160	1755-1760	SM	Patelke, 1994	36,0	11,6	2,34	96	56	798
B1-160	1760-1765	SM	Patelke, 1994	36,0	10,2	1,97	328	22	416
B1-160	1765-1769	S-TROC	Patelke, 1994	36,0	26,5	3,18	1447	1765	3318
B1-160	1769-1775	SM	Patelke, 1994	36,0	18,5	1,65	88	77	748
B1-160	1775-1780	SM	Patelke, 1994	36,0	6,92	2,43	632	51	666
B1-160	1780-1785	SM	Patelke, 1994	36,0	6,39	2,52	43	10	609
B1-160	1785-1790	SM	Patelke, 1994	36,0	3,78	2,13	151	41	206
B1-160	1790-1796	SM	Patelke, 1994	36,0	13,0	1,83	671	59	710
B1-160	1796-1801	S-TROC	Patelke, 1994	36,0	36,0	5,45	1091	545	1527
B1-163	1325	S-ÉGP	Severson et Hauck, 1997	36,0	17,9	4,25	1616	4394	14712
B1-163	1335	S-ÉGP	Severson et Hauck, 1997	36,0	20,0	4,68	1775	4266	16521
B1-421	1755-1762	S-TROC	Patelke, 1994	36,0	15,6	1,77	620	295	1623
B1-421	1762-1775	S-TROC	Patelke, 1994	36,0	11,1	2,33	595	50	1339
B1-421	1775-1785	S-TROC	Patelke, 1994	36,0	11,0	1,61	169	40	925
B1-421	1785-1795	S-TROC	Patelke, 1994	36,0	12,6	1,95	631	1032	1605
B1-421	1795-1805	S-TROC	Patelke, 1994	36,0	6,67	2,03	94	52	427
B1-421	1805-1815	S-TROC	Patelke, 1994	36,0	12,1	2,06	320	229	1131
B1-421	1815-1825	S-TROC	Patelke, 1994	36,0	12,2	2,11	362	151	1341
B1-421	1825-1835	S-TROC	Patelke, 1994	36,0	9,27	1,96	153	109	687
B1-421	1835-1845	S-TROC	Patelke, 1994	36,0	7,13	1,36	442	340	883

LOCAL BOY - 100% SULFURES

No. forage	Profondeur (pieds)	Type de roche	Références	S(%)	Cu(%)	Ni(%)	Au(ppb)	Pt(ppb)	Pd(ppb)
Moyenne	S-ÉGP	n=7		36,0	21,7	4,78	4184	9214	28135
Moyenne	S-TROC	n=112		36,0	16,2	2,83	923	905	2683
Moyenne	SM	n=48		36,0	11,5	2,42	215	209	890
Moyenne	TOTAL	n=167		36,0	15,1	2,79	856	1053	3235

ANNEXE 5

DESCRIPTION PÉTROGRAPHIQUE DES ROCHES MINÉRALISÉES EN SULFURES DU GISEMENT DE DUNKA ROAD

NORITE MINÉRALISÉE

Minéralogie - silicates

Minéral	%	Description
Plagioclase	25-50	cristaux hypidiomorphes (localement xénomorphes); grain fin-moyen (0,5-3 mm);
	(moy= 37)	en partie recristallisé; généralement cumulus
Orthopyroxène	20-40	cristaux hypidiomorphes (localement xénomorphes); grain fin-moyen (0,5-3 mm);
	(moy= 30)	partiellement altéré en orthoamphibole; cumulus à intercumulus
Clinopyroxène	5-15	cristaux hypidiomorphes (localement xénomorphes); grain fin-moyen (0,5-2 mm);
	(moy= 6)	cumulus à intercumulus
Olivine	0-10	cristaux xénomorphes (parfois poécilitiques); grain moyen-grossier (3-10 mm);
	(moy= 6)	intercumulus (localement petits grains cumulus)
Biotite	1-10	cristaux hypidiomorphes; grain fin-moyen; généralement associée à
	(moy= 3)	l'orthopyroxène, l'ilménite et les sulfures
Cordiérite	0-30	porphyroblastes xénomorphes; grain fin-grossier (0,3-8 mm); abondant
	(moy= 5)	dans quelques lames minces (près d'enclaves)
Apatite	0-2	cristaux hypidiomorphes à idiomorphes; grain fin (0,2-1,0 mm); associée
	(moy= 0,5)	à la biotite (+/- ilménite)

Minéralogie - opaques

Minéral	%	Description
Ilménite	3-15	cristaux xénomorphes (localement hypidiomorphes); grain fin (0,5-1,5 mm);
	(moy= 7)	généralement intercumulus; associée aux sulfures et la biotite
Hercynite	0-1	observé localement au contact avec les enclaves
	(moy= 0,3)	
Magnétite	0-trace	observé localement
Pyrrhotite	1-10	généralement à grain fin (<0,5 mm); forme également des plages
	(moy= 4)	interstitielles (amas semi-massifs); associée à l'ilménite
Chalcopyrite	trace-3	petits grains généralement en bordure de la pyrrhotite; forme également
	(moy= 0,5)	des grains isolés (rares veinules)
Cubanite	trace-0,5	généralement sous forme de lamelles d'exsolution dans la chalcopyrite;
	(moy= 0,1)	rarement sous forme de petits grains autour de la pyrrhotite
Pentlandite	trace-0,5	petits grains à l'intérieur ou en bordure de la pyrrhotite
	(moy= 0,1)	
Mackinawite	0-trace	
Maucherite	trace	petits grains à l'intérieur de la pyrrhotite; associée à la chalcopyrite
Niccolite	0-trace	petits grains à l'intérieur de la pyrrhotite; associée à la chalcopyrite

TROCTOLITE MINÉRALISÉE (RELATIVEMENT APPAUVRIE EN ÉGP)

Minéralogie - silicates		
Minéral	**%**	**Description**
Plagioclase	60-70	cristaux hypidiomorphes à idiomorphes; grain moyen-grossier (2-6 mm);
	(moy= 63)	en partie recristallisé; cumulus (localement intercumulus)
Olivine	15-30	cristaux poécilitiques intercumulus (3-15 mm) et grains xénomorphes
	(moy= 20)	cumulus (1-2 mm); faiblement altérée en serpentine
Clinopyroxène	3-15	cristaux poécilitiques intercumulus (3-15 mm); phase silicatée la plus
	(moy= 8)	tardive
Orthopyroxène	2-10	sous forme de couronne autour de l'olivine (texture coronitique); forme
	(moy= 5)	localement des cristaux intercumulus (3-5 mm)
Biotite	1-3	cristaux hypidiomorphes; grain fin-moyen; généralement associée à
	(moy= 2)	l'ilménite et les sulfures
Apatite	trace-1	cristaux hypidiomorphes à idiomorphes; grain fin (0,2-1,0 mm); associée
	(moy= 0,3)	à la biotite (+/- ilménite et sulfures)

Minéralogie - opaques		
Minéral	**%**	**Description**
Ilménite	1-2	cristaux xénomorphes; grain fin (0,5-2,0 mm); intercumulus; associée aux
	(moy= 1)	sulfures et la biotite
Chromite	trace	associée à l'ilménite
Pyrrhotite	0,5-2,5	généralement sous forme de plages interstitielles (<3 mm); associée à
	(moy= 1,5)	l'ilménite
Chalcopyrite	0,5-2,0	petits grains généralement associés à la pyrrhotite et la pentlandite; forme
	(moy= 1,0)	également des grains isolés
Cubanite	trace-1,5	généralement sous forme de lamelles d'exsolution dans la chalcopyrite;
	(moy= 0,5)	également sous forme de petits grains dans la pyrrhotite (+/- pentlandite)
Pentlandite	trace-1,0	petits grains à l'intérieur ou en bordure de la pyrrhotite
	(moy= 0,5)	
Mackinawite	trace	petits grains (souvent en flammes) à l'intérieur de la pentlandite et la
		chalcopyrite
Bornite	trace	associée à la chalcopyrite
Maucherite	trace	quelques rares petits grains retrouvés en bordure de la pyrrhotite

TROCTOLITE MINÉRALISÉE (HORIZONS ENRICHIS EN ÉGP)

Minéralogie - silicates		
Minéral	**%**	**Description**
Plagioclase	55-70	cristaux hypidiomorphes à idiomorphes; grain moyen-grossier (2-5 mm);
	(moy= 63)	en partie recristallisé; cumulus (localement intercumulus)
Olivine	25-30	cristaux xénomorphes généralement poécilitiques (2-6 mm); intercumulus;
	(moy= 27)	*localement sous forme de petits cristaux cumulus (1-2 mm)*
Clinopyroxène	6-8	cristaux poécilitiques intercumulus (5-20 mm); phase silicatée la plus
	(moy= 7)	tardive
Orthopyroxène	1-3	sous forme de couronne autour de l'olivine (texture coronitique)
	(moy= 2)	
Biotite	0,5-3	cristaux hypidiomorphes (0,5-3,0 mm); généralement associée à
	(moy= 1,5)	l'ilménite et les sulfures
Apatite	trace	

Minéralogie - opaques		
Minéral	**%**	**Description**
Ilménite	*1-2*	*cristaux xénomorphes intercumulus; associée aux sulfures et à la biotite*
	(moy= 1,5)	
Chalcopyrite	1,0-3,5	petits grains associés à la pentlandite; forme également des plages
	(moy= 2)	interstitielles
Pentlandite	0,5-1,5	larges plages interstitielles (3-5 mm); localement bordée par de la
	(moy= 1)	chalcopyrite
Cubanite	0,2-0,5	sous forme de lamelles d'exsolution à l'intérieur de la chalcopyrite
	(moy= 0,3)	
Pyrrhotite	trace-0,5	petits grains en bordure de la pentlandite
	(moy= 0,2)	
Mackinawite	trace	flammes d'exsolution à l'intérieur de la chalcopyrite
Bornite	*trace*	*associée à la chalcopyrite*

SULFURES MASSIFS À SEMI-MASSIFS

Minéralogie - silicates		
Minéral	**%**	**Description**
Plagioclase	0-20	cristaux hypidiomorphes; grain fin-grossier (1-8 mm); en partie
	(moy= 10)	recristallisé; généralement cumulus
Orthopyroxène	0-6	petits cristaux hypidiomorphes (0,5-3,0 mm) ou sous forme de couronne
	(moy= 3)	autour de l'olivine (texture coronitique); partiellement altéré en orthoamphibole
Olivine	0-6	cristaux poécilitiques; grain moyen-grossier (5-10 mm); intercumulus;
	(moy= 3)	fortement altérée en talc et iddingsite
Clinopyroxène	0-5	cristaux hypidiomorphes (localement xénomorphes); grain fin (0,5 mm);
	(moy= 2)	cumulus à intercumulus
Biotite	0-2	cristaux hypidiomorphes; grain fin
	(moy= 1)	
Apatite	0-1	cristaux hypidiomorphes à idiomorphes; grain fin (0,2-0,5 mm); retrouvée
	(moy= 0,5)	en bordure des sulfures massifs

Minéralogie - opaques		
Minéral	**%**	**Description**
Ilménite	trace-5	cristaux xénomorphes; grain fin (0,3-1,0 mm); surtout en bordure et à
	(moy= 2)	l'intérieur des sulfures; en partie altérée en rutile
Hercynite	trace	très petits cristaux hypidiomorphes en bordure des sulfures massifs
Pyrrhotite	50-90	forme des veines (1-5 cm) de sulfures massifs; contient de fines exsolutions
	(moy= 70)	de troilite (pyrrhotite hexagonale) et des flammes de pentlandite
Chalcopyrite	2-10	masses de grains retrouvées en bordure des veines de sulfures massifs;
	(moy= 5)	contient des exsolutions de cubanite et de mackinawite
Pentlandite	3-8	petits grains hypidiomorphes à xénomorphes en bordure des veines; forme
	(moy= 5)	également des flammes d'exsolution dans la pyrrhotite
Cubanite	trace-0,5	généralement sous forme de lamelles d'exsolution dans la chalcopyrite
Mackinawite	trace	flammes d'exsolution à l'intérieur de la chalcopyrite
Maucherite	trace	petits grains arrondis (jusqu'à 0,5 mm) à l'intérieur de la pyrrhotite
Niccolite	0-trace	petits cristaux idiomorphes (0,1-0,2 mm) à l'intérieur de la pyrrhotite;
		associée à la chalcopyrite

SULFURES ENRICHIS EN CUIVRE

Minéralogie - silicates		
Minéral	**%**	**Description**
Plagioclase	40-60	cristaux hypidiomorphes; grain moyen-grossier (2-8 mm);
	(moy= 50)	en partie recristallisé; généralement cumulus
Orthopyroxène	12-18	petits cristaux hypidiomorphes (0,5-2,0 mm); partiellement altéré en
	(moy= 15)	orthoamphibole; origine secondaire (cristallisation métamorphique)
Clinopyroxène	0-20	cristaux xénomorphes intercumulus; grain moyen (2-4 mm);
	(moy= 10)	partiellement altéré en hornblende et actinolite
Quartz	2-15	plages interstitielles (3-10 mm); semble associé aux sulfures et à la
	(moy= 8)	biotite
Olivine	0-3	cristaux poécilitiques; grain moyen-grossier (6-10 mm); intercumulus;
	(moy= 1,5)	faiblement altérée en iddingsite
Biotite	3-5	cristaux hypidiomorphes; grain fin-moyen (1-4 mm); associée à l'ilménite
	(moy= 4)	et le quartz
Apatite	0,5-1,0	cristaux hypidiomorphes à idiomorphes; grain fin-moyen (0,2-2,0 mm);
	(moy= 0,7)	souvent à l'intérieur de la biotite
Minéralogie - opaques		
Minéral	**%**	**Description**
Ilménite	4-6	masses de grains (1-5 mm) associées aux sulfures et la biotite; aussi sous
	(moy= 5)	forme de petits cristaux idiomorphes (0,5 mm); en partie altérée en rutile
Chalcopyrite	3-4	masses de grains (4-6 mm) interstitielles aux silicates; associée à la biotite;
	(moy= 3,5)	contient des exsolutions de cubanite et de mackinawite
Pyrrhotite	1-3	masses irrégulières à l'intérieur de la chalcopyrite; associée à la pentlandite
	(moy= 2)	
Cubanite	0,2-0,8	lamelles d'exsolution dans la chalcopyrite
	(moy= 0,5)	
Pentlandite	0,1-0,3	petits grains hypidiomorphes; associée à la pyrrhotite
	(moy= 0,2)	
Mackinawite	trace	flammes d'exsolution à l'intérieur de la chalcopyrite
Froodite	0-trace	très petits cristaux idiomorphes à l'intérieur de la chalcopyrite; associée
		à la pentlandite